Development of novel chemically modified antisense oligonucleotides for tackling type 2 diabetes and Duchenne muscular dystrophy

Murdoch
UNIVERSITY

Suxiang Chen

Bachelor of Plant Protection in Microbiology

This thesis is presented for the Doctor of Philosophy at Murdoch University

School of Veterinary and Life Sciences

Molecular and Medical Sciences

2020

Thesis Declaration

I, Suxiang Chen, declare that this thesis is my own account of my research and contains as its main content work that has not previously been submitted for a degree at any tertiary educational institution.

This thesis does not contain any material previously published or written by another person, except where due reference has been made in the text.

This work (s) is not in any way a violation or infringement of any copyright, trademark, patent or other rights whatsoever of any person.

Scholarships supporting the candidate during the undertaking of this work were kindly provided by Perron Institute Top-Up Scholarship and International Tuition Fee Scholarship scheme from Murdoch University.

This thesis contains published work, some of which has been co-authored.

Signature: Suxiang Chen

Date: 4 May 2020

Abstract

Therapeutic nucleic acids such as antisense oligonucleotides (AOs) can specifically bind to target RNA and manipulate gene expression through different mechanism of actions, including RNase H mediated RNA degradation, splice modulation, and translational repression. So far, the United States Food and Drug Administration has approved seven AO drugs for the therapies of different human diseases. Among them, four drugs (eteplirsen, golodirsen, nusinersen, milasen) modulate splicing, and rescue the production of functional essential proteins by restoring ruined open reading frames due to mutations within genes.

This thesis explores the potential of novel chemically-modified splice-modulating AOs in tackling type 2 diabetes (T2D) and Duchenne muscular dystrophy (DMD). Chapter one provides an introduction of different types of therapeutic nucleic acids. Chapter two focused on developing AOs targeting protein tyrosine phosphatase 1B (PTP1B), a validated therapeutic target of T2D. An AO candidate, PTPN1 1E2A (+5+29), was identified to efficiently skip exon-2 of *PTPN1* RNA inducing premature termination codons in exon-3, thereby reducing the production of full-length, functional PTP1B proteins. Chapter three presents the work on design, synthesis and evaluation of splice-modulating chimeric AOs containing novel nucleotide analogues for exon skipping in H2K *mdx* myoblast, using DMD as a disease model. Morpholino nucleic acid modified 2'-O-Methyl (2'-OMe) AO mixmer exhibited comparable exon skipping ability as uniformly modified 2'-OMe AO. Locked nucleic acid (LNA) modified 2'-Fluoro (2'-F) AOs showed improved drug-like properties than 2'-OMe modified 2'-F AOs. In summary, the thesis expands the applicability of AOs in the therapy of T2D through downregulating PTP1B protein expression by splice modulation; the thesis also expands the scope of utilizing nucleotide analogues in splice modulation application by constructing AO chimeras, demonstrating the feasibility of using these analogues for optimizing AOs in terms of improved drug-like properties.

Table of Contents

Acknowledgements

There are many people who have supported me during my PhD journey since March, 2016. First and foremost, I would like to express my deepest gratitude to my principal supervisor, Assoc. Prof. Rakesh Veedu and my co-supervisors Prof. Steve Wilton and Prof. Sue Fletcher, who have supported me throughout the past four years. Rakesh, you have been my supervisor since 2013 in the University of Queensland. You are an inspiring mentor that is always there for exciting discussions and troubleshooting. Steve and Sue, you are always my motivation. The story of your DMD research has been an inspiration for my research career.

I am so grateful to have good colleagues with me along the way. Bao and Madhuri, thank you for all the discussions, chats, lunches, and dinners that we have been together. I could not come to this stage without your friendship. Special thanks are also given to the rest of RNV group, Tao, Milena, Tamer, Prithi, Akila, Leon, Kamal, Hadi, Lanmei, Nabbi, Michelle for your feedbacks and cooperation. I will remember all the time that we shared together. A big thank you especially to Jodie, Abbie, May, Kristin, Oliver, Russ, Fern, Janya, Kane, Khine, Loren, Jess, Di, Bal, Ianthe, Craig from MTL. The time you have taken out of your own busy schedules to help me, give me advice, and troubleshoot has been invaluable.

And finally, mum and dad, please accept my best thanks. My parents have financially supported me as a self-funded student for the first two years during my PhD journey before I got the scholarship in the year three. Words are powerless to express my gratitude for your unconditional love. Thanks for everything.

Authorship Declaration: Co-Authored Publications

Chapter three of this thesis contains some work that has been published. In addition, content from chapter one and chapter two are currently in manuscript preparation and are being developed to be published.

Chapter 3:

Title: Synthesis of a morpholino nucleic acid (MNA)-uridine phosphoramidite, and exon skipping using MNA/2'-O-methyl mixmer antisense oligonucleotide

DOI: 10.3390/molecules21111582

Name	Design	Data Collection	Data Analysis	Interpretation	Manuscript Development
Suxiang Chen	0%	70%	60%	50%	30%
Bao T. Le	0%	10%	15%	20%	25%
Kamal Rahimizadeh	0%	5%	5%	10%	10%
Khalil Shaikh	0%	10%	5%	10%	10%
Narinder Mohal	0%	5%	5%	10%	5%
Rakesh N. Veedu (Supervisor and Corresponding author)	100%	0%	10%	10%	20%

Confirmation of contribution

As a contributor to this Chapter, I confirm that the level of contribution attributed to me is correct.

Suxiang Chen 20/04/2020

Bao T. Le 22/04/2020

Kamal Rahimizadeh 22/04/2020

Khalil Shaikh: Not available

Narinder Mohal 22/04/2020

Rakesh N. Veedu 22/04/2020

Chapter 3:

Title: Systematic evaluation of 2'-Fluoro modified chimeric antisense oligonucleotide-mediated exon skipping *in vitro*

DOI: 10.1038/s41598-019-42523-0

Name	Design	Data Collection	Data Analysis	Interpretation	Manuscript Development
Suxiang Chen	0%	70%	70%	60%	80%
Bao T. Le	0%	5%	15%	10%	5%
Madhuri Chakravarthy	0%	20%	10%	10%	5%
Tamer R. Kosbar	0%	5%	5%	10%	5%
Rakesh N. Veedu (Supervisor and Corresponding author)	100%	0%	0%	10%	5%

Confirmation of contribution

As a contributor to this Chapter, I confirm that the level of contribution attributed to me is correct.

Suxiang Chen 20/04/2020

Bao T. Le 22/04/2020

Madhuri Chakravarthy 25/04/2020

Tamer R. Kosbar 22/04/2020

Rakesh N. Veedu 22/04/2020

Chapter 3:

Title: Author Correction: Systematic evaluation of 2′-Fluoro modified chimeric antisense oligonucleotide-mediated exon skipping *in vitro*

DOI: 10.1038/s41598-020-63706-0

Name	Manuscript Correction
Suxiang Chen	90%
Bao T. Le	0%
Madhuri Chakravarthy	0%
Tamer R. Kosbar	0%
Rakesh N. Veedu (Supervisor and Corresponding author)	10%

Confirmation of contribution

As a contributor to this Chapter, I confirm that the level of contribution attributed to me is correct.

Suxiang Chen 20/04/2020

Bao T. Le 22/04/2020

Madhuri Chakravarthy 25/04/2020

Tamer R. Kosbar 22/04/2020

Rakesh N. Veedu 22/04/2020

Abbreviations

DNA	deoxyribonucleic acid
RNA	ribonucleic acid
dsRNA	double stranded RNA
A	adenine
G	guanine
C	cytosine
T	thymine
U	uracil
PCR	polymerase chain reaction
tRNA	transfer RNA
pre-tRNA	precursor tRNA
rRNA	ribosomal RNA
mRNA	messenger RNA
pre-mRNA	precursor mRNA
gRNA	guide RNA
AO	antisense oligonucleotide
miRNA	microRNA
pre-miRNA	precursor miRNA
pri-miRNA	primary miRNA
RNAi	RNA interference
siRNA	small interfering RNA
AAV	adeno-associated virus
UTR	untranslated region
ORF	open reading frame

CRISPR	clustered regularly interspaced short palindromic repeats
Cas	CRISPR-associated system
crRNA	CRISPR RNA
tracrRNA	trans-activating CRISPR RNA
TFO	triplex forming oligodeoxynucleotide
exp5	exportin-5
GTP	guanosine-5'-triphosphate
RISC	RNA-induced silencing complex
RNA Pol II	RNA polymerase II
PAMP	pathogen-associated molecular pattern
TLR	Toll-like receptor
SELEX	Systematic Evolution of Ligands by EXponential enrichment
VEGF	vascular endothelial growth factor
PS	phosphorothioate
2′-OMe	2′-O-methyl
2′-OMOE	2′-O-methoxyethyl
PNA	peptide nucleic acid
PMO	phosphorodiamidate morpholino
MNA	morpholino nucleic acid
2′-NH_2	2′-amino
2′-F	2′-fluoro
FANA	fluoroarabinonucleotide
LNA	locked nucleic acid
TNA	threose nucleic acid
HNA	hexitol nucleic acid
CeNA	cyclohexenyl nucleic acid
ANA	anhydrohexitol nucleic acid
CMV	cytomegalovirus
ApoB	apolipoprotein B

LDL-C	low-density lipoprotein cholesterol
TTR	transthyretin
PTC	premature termination codon
FDA	Food and Drug Administration
DMD	Duchenne muscular dystrophy
SMN2	survival of motor neuron 2
SMA	spinal muscular atrophy
MFSD8	major facilitator superfamily domain containing 8
CLN7	ceroid lipofuscinosis type 7
T2D	type 2 diabetes
FFA	free fatty acid
PKC	protein kinase C
IκK	IκB-kinase
NFκB	nuclear factor κB
TNFα	tumor necrosis factor-α
IL6	interleukin 6
JNK1	Jun N-terminal kinase-1
SOCS3	suppressor of cytokine signaling-3
IR	insulin receptor
IRS	insulin receptor substrate
PI3K	phosphatidylinositol 3-kinase
Akt	protein kinase B
GLUT4	glucose transporter type 4
TCA	tricarboxylic acid
ROS	reactive oxygen species
AGE	advanced glycation end product
SGLT2	sodium glucose cotransporter-2
DPP4	dipeptidyl peptidase-4
GLP1	glucagon-like peptide-1
PTP1B	tyrosine phosphatase-1B

GCGR	glucagon receptor
GCCR	glucocorticoid receptor
ACC	acetyl-CoA carboxylase
DGAT2	diacylglycerol acyltransferase-2
PEP	phosphoenolpyruvate
PEPCK-M	mitochondrial phosphoenolpyruvate carboxykinase
G6PT1	glucose 6-phosphate transporter-1
CREB	cAMP response element binding protein
CRTC2	CREB-regulated transcription coactivator-2
FOXO1	forkhead box O1
DEP1	density-enhanced phosphatase-1
RBP4	retinol binding protein 4
TRIB3	tribbles homolog 3
IκKβ	IκB-kinase β
SCI	subcutaneous injection
IPI	intraperitoneal injection
LMW	low molecular weight
NAFLD	nonalcoholic fatty liver disease
GOT1	glutamic-oxaloacetictransaminase 1
PPARγ	peroxisome proliferator-activated receptor γ
ACO	acyl-CoA oxidase
C/EBPα	CCAAT/enhancer binding protein α

Chapter 1

Introduction to therapeutic nucleic acids

1.Therapeutic nucleic acids: an overview

1.1 Discovery of nucleic acid

In 1869, Friedrich Miescher isolated deoxyribonucleic acid (DNA) from cell nuclei, and named it “nuclein”. He was the first to identify nucleic acid as a distinct molecule [1, 2]. Extensive efforts have since been invested into the exploration of nucleic acid in an attempt to elucidate the structure and function of these molecules. In 1944, Oswald Avery and colleagues proved DNA to be a carrier of genetic information [3]. In 1953, the double-helix structure of DNA was determined by Francis Crick and James Watson, and the “Central Dogma” (simplified description is DNA makes ribonucleic acid (RNA) and RNA makes protein) was proposed by Francis Crick in 1958. Consequently, these breakthroughs opened the way for comprehensive research and applications of nucleic acid [4-7].

1.2 Composition of nucleic acid

According to the current knowledge, natural nucleic acids can be classified into two categories: DNA and RNA, both of which are composed of subunits called deoxyribonucleotides and ribonucleotides, respectively. Each nucleotide monomer consists of a sugar ring (deoxyribose or ribose), a nitrogenous base (nucleobase), and a phosphate group (**Figure 1.2**). In a nucleotide, the sugar ring is linked through a glycosidic bond to the base. Naturally occurring nucleobases include purines (adenine, A; guanine, G) and pyrimidines (cytosine, C; thymine, T; uracil, U). While A, G, and C can be components in both types of nucleotides, T only exists in deoxyribonucleotide and is represented by U in ribonucleotide (**Figure 1.2**). Nucleotides containing A, G, C, T or U connect to each other in a sequential manner, constructing a DNA or RNA molecule that genetic information is stored within.

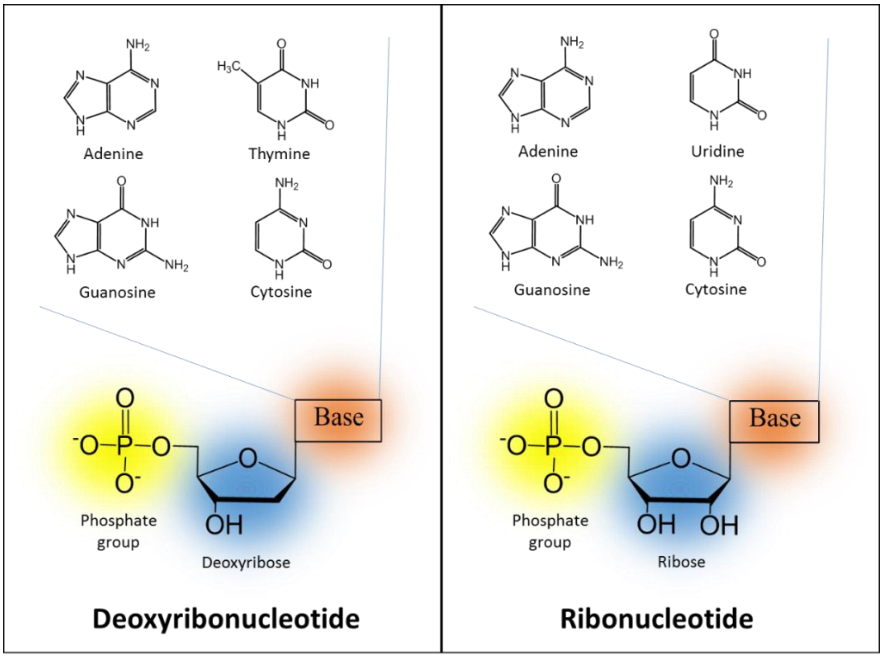

Figure 1.2 Structure of nucleotides.

1.3 Synthesis of nucleic acid

Rapid progression in the field of nucleic acid study required substantial quantities of these molecules, most commonly achieved by non-cellular artificial synthesis of DNA/RNA and cellular gene expression system that produces messenger RNA (mRNA). The great demand of artificial nucleic acid synthesis was met by the invention of the polymerase chain reaction (PCR) and solid phase oligonucleotide synthesis technologies for long and short nucleic acid production, respectively. As the power of PCR technology is indubitable, the capability of short nucleic acid synthesis is also of vital importance, as it enables the research and development of therapeutic oligonucleotides for the treatment of different human diseases.

While phosphorylase-based enzymatic reaction was introduced to the method of polynucleotide synthesis in the 1950s [8], the real breakthrough for this technology occurred when Khorana and colleagues demonstrated chemical synthesis of a sequence-defined oligonucleotide in 1958, widely regarded as the birth of nucleic acid synthesis technology [9]. Nevertheless, this process was still far from ideal as it produced oligonucleotides at low yield,

with intensive labor. The next leap was achieved by Caruthers and coworkers in 1981, with the invention of solid-phase oligonucleotide synthesis using phosphoramidite chemistry. This approach has become the most widely used method for the manufacture of oligonucleotides nowadays (**Figure 1.3**) [10,11]. A comprehensive review of the history of synthetic oligonucleotide technology can be found elsewhere [12].

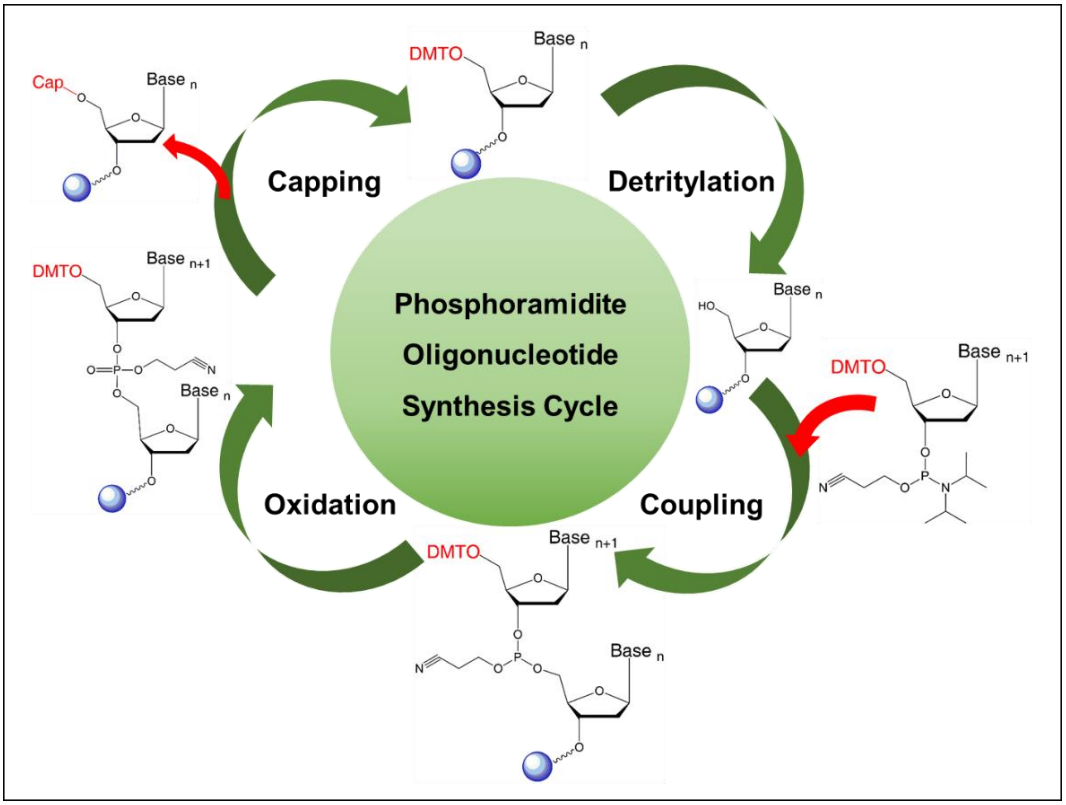

Figure 1.3 Cycle of phosphoramidite-based oligonucleotide synthesis.

1.4 Nucleic acid as therapeutics

Along with the technological advances in nucleic acid biology and chemistry, astounding progress has been made in the identification of genes responsible for many human diseases [13]. While conventional small molecule drugs predominantly target a disease-causing gene at the protein level, nucleic acid intervention can provide a comprehensive therapeutic strategies to overcome the effects of disease causing genes at all levels of gene expression (DNA, RNA, protein, and molecules derived as a result of protein-mediated enzymatic processes) [14]. To date, according to structural features and mechanisms of action, the

family of therapeutic nucleic acids is comprised of eleven categories, including transgene, synthetic mRNA, synthetic guide RNA (gRNA) for CRISPR/Cas, antigene, antisense oligonucleotide (AO), catalytic oligonucleotide, microRNA (miRNA)-related oligonucleotide, small interfering RNA (siRNA), immune-stimulatory oligonucleotide, decoy oligonucleotide, and aptamer. An introduction to these therapeutic nucleic acids is provided in the next section (section 2: therapeutic nucleic acids of different mechanisms of action) with an emphasis on their distinct mechanisms of action.

2.Therapeutic nucleic acids: mechanisms of action

2.1 Transgenes

Transgenes exhibit direct or indirect therapeutic effects in different ways, for example, replacement of a functionally defective gene (direct therapeutic effect) [13, 15, 16], or expression of antigenic proteins that are then presented to the host immune system to initiate immunoreaction that provides protection against infections (indirect therapeutic effect) [17-19]. Both effects are based on biosynthesis of therapeutic proteins, harnessing the intracellular transcription and translation apparatus by transgenes. Transgenes encoding antigens are often referred to as DNA vaccines [17]. A transgene expression cassette is composed of three elements: promoter, gene of interest, and terminator. Transcription of the desired gene is driven by the promotor sequence through binding with transcription factors, and ended by the terminator sequence [20]. The transgene expression cassette is delivered to the host cells with the aid of viral or non-viral vectors, which usually include retroviruses, adeno-associated virus (AAV), and plasmid [21-24] (**Figure 2.1**). Depending upon the nature of vectors in which expression cassettes are incorporated, transgenes can be structurally single stranded RNA (retrovirus vector), single stranded DNA (AAV vector), or double stranded DNA (plasmid vector) (**Figure 2.1**). All vectors are engineered so that they cannot replicate in the host. Transgenes incorporated in retroviral vectors that commonly originate

from γ-retrovirus, lentivirus, and spumavirus are able to integrate into the host chromosome through homologous recombination, while AAV and plasmid vectors are predominantly non-integrating upon transfer to host cells, and are stabilized extrachromosomally as episomes [21, 22] (**Figure 2.1**). Chromosome integration allows transgenes to be passed to daughter cells, therefore retroviral vectors are an appropriate choice for stem cell or precursor cell transformation. By contrast, non-integrating vectors (AAV, plasmid) are used in the transfection of long-lived post-mitotic cells, since loss or dilution of transgenes due to cell division is largely avoided.

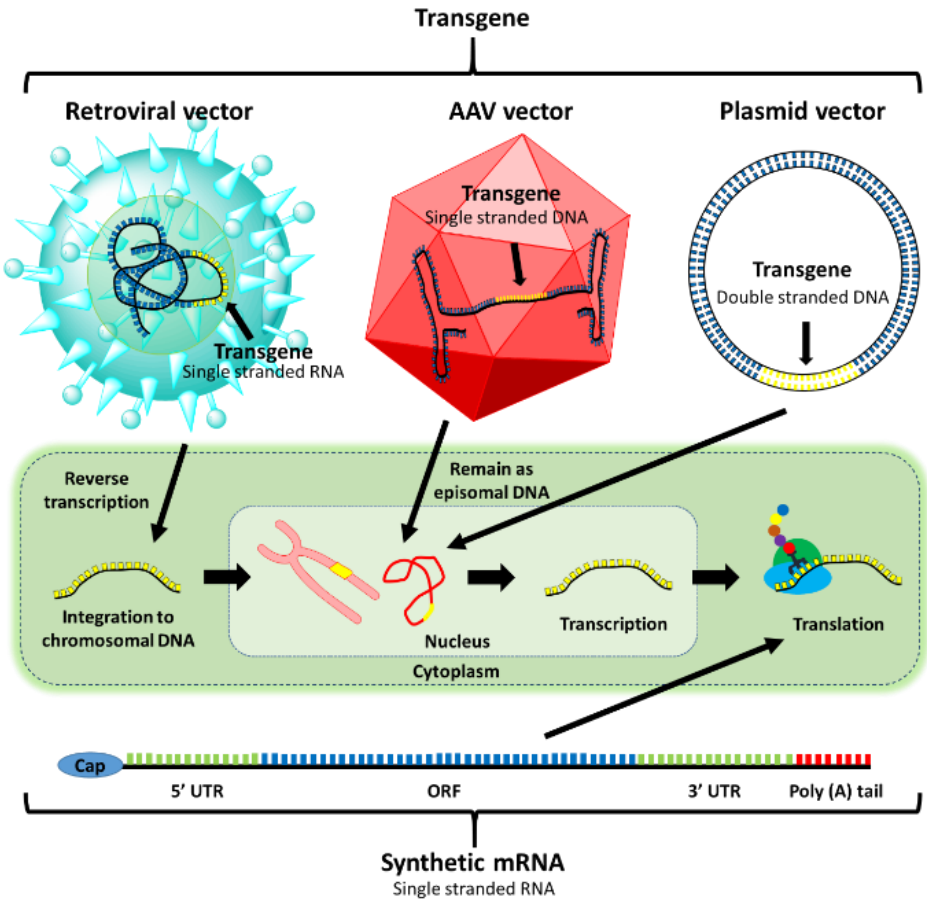

Figure 2.1 Mechanisms of transgene and synthetic mRNA-based therapeutics. AAV: adeno-associated virus, UTR: untranslated region, ORF: open reading frame.

2.2 Synthetic mRNA

Similar to transgenes, synthetic mRNA enables the host cell to express exogenous genes of interest to produce therapeutic proteins [25] (**Figure 2.1**). Synthetic mRNA encoding

antigen-coding sequences that activate the host immune responses upon expression are termed mRNA vaccines [26]. Synthetic mRNAs mainly possess two features that distinguish them from the transgenes: firstly, synthesis of protein encoded by synthetic mRNA is rapid and transient, while transgenes usually lead to longer term protein expression [27, 28]; secondly, unlike transgenes that are incorporated in viral or plasmid vectors containing other exogenous genes that are not of interest, synthetic mRNA is relatively simple and "clean" in terms of structure, as only the desired gene is involved, suggesting a safety profile advantage over transgenes [28, 29].

2.3 Synthetic guide RNA for CRISPR/Cas

Clustered regularly interspaced short palindromic repeats/CRISPR-associated system (CRISPR/Cas) is a prokaryotic adaptive immune system that protects bacteria and archeobacteria from foreign genetic material, such as phages, transposons and plasmids [13, 30, 31]. The CRISPR/Cas system enables a prokaryote to 'memorize' previous infections by storing foreign nucleic acid fragments from invaders (termed spacers) incorporated into its own genome. These spacers are interspaced with short repetitive sequences (termed repeats) that together form a CRISPR array (**Figure 2.3**) that is flanked by genes encoding nucleases, such as Cas9 [32-35]. When cells encounter reoccurring invaders, transcripts are produced from the CRISPR array and processed to produce CRISPR RNAs (crRNAs), each bearing a certain sequence transcribed from a spacer (termed protospacer) and part of its neighboring repeat sequence. Afterwards, each crRNA partially hybridizes with a trans-activating CRISPR RNA (tracrRNA) via Watson-Crick base pairing [36] and, upon recognition of the target invading DNA by its complementary protospacer in crRNA through hybridization, the Cas nuclease is directed to the target leading to its cleavage [37] (**Figure 2.3**). To date, CRISPR/Cas systems can be classified into two classes, and, more specifically, six types (type I, II, III, IV, V, and VI) [38-40]. The type II system (from Streptococcus pyogenes) that

uses Cas9 endonuclease has been extensively investigated and is currently the most commonly used system. In engineered type II CRISPR/Cas systems, a single synthetic gRNA combining a crRNA and a fixed tracrRNA is often used, while the naturally occurring system employs separate RNAs [34]. The first 20 nucleotides from the 5' end of gRNA (corresponding to the protospacer in crRNA) guides Cas9 to cleave the target genomic DNA through hybridization to its complementary portion in the target [31, 37] (**Figure 2.3**). The resultant cut genomic DNA allows researchers to add or delete sequences, to or from the genome, or replace an existing sequence with a foreign one using the host cell's own DNA repair machinery. Moreover, due to the amenability of the 20nt portion of gRNA, in theory any genomic DNA can be targeted, which presents the CRISPR/Cas system as a versatile platform for the development of therapeutics.

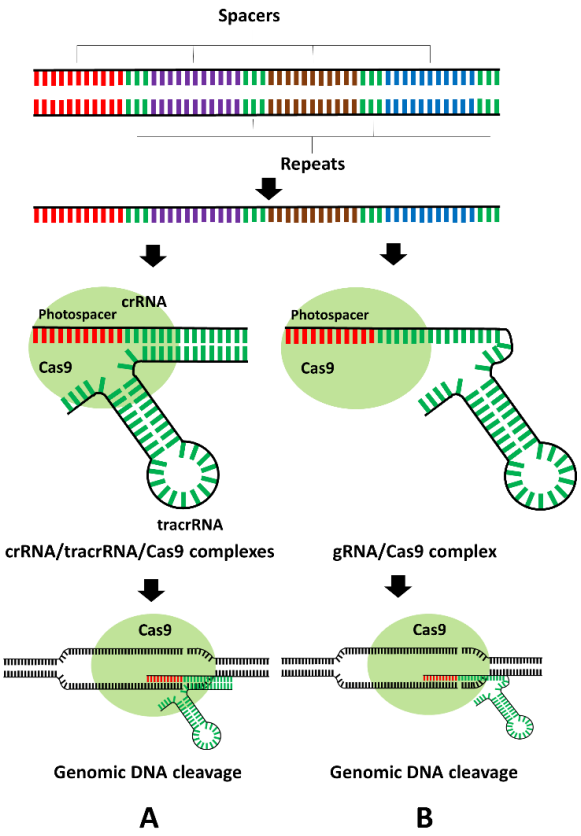

Figure 2.3 Type II CRISPR-Cas systems. (A) Naturally occurring type II CRISPR-Cas system employing crRNA and tracrRNA. (B) Engineered type II CRISPR-Cas system employing synthetic gRNA. crRNA: CRISPR RNAs, tracrRNA: trans-activating CRISPR RNA, gRNA: guide RNA.

2.4 Antigene

A group of single stranded, oligodeoxynucleotides that exhibit antigene effects by forming triplexes, composed of the oligodeoxynucleotide and the target double stranded genomic DNA, and it is thereby referred to as the triplex forming oligodeoxynucleotide (TFO). Although triplex formation was first demonstrated in 1957 [41], the basis of this phenomenon, an alternative form of hybridization to Watson-Crick base pairing was discovered by Karst Hoogsteen in 1963, and was subsequently named after him [42-44].

Upon hybridization to genomic DNA, TFO antigene agents inhibit transcription of the target gene either by blocking transcription factor binding to the promotor sequence and thus preventing initiation of transcription; or precluding unwinding of the DNA duplex and thereby inhibiting elongation of mRNA [13, 45-48]. Apart from inhibition of transcription, TFOs are also used to induce targeted mutagenesis and other genome-level therapeutic effects [49]. Moreover, a direct advantage of TFO antigenes over RNA-targeting agents (eg. AO, siRNA, catalytic oligonucleotides) is that only two copies of genomic DNA containing a target gene are present in a diploid cell, whilst hundreds to thousands of mRNAs are transcribed from the corresponding target gene within the cell [46, 50]. This suggests that a relatedly small dosage of antigene agent may be required for downregulation of the target gene, compared to using RNA-targeting therapeutic nucleic acid agents for the same purpose [46].

TFO antigene agents usually bind to the major groove [51, 52] and can only bind to a purine stretch in the target strand of the DNA duplex [53]. There exist two binding motifs that allow TFOs to form a triplex structure with its target: pyrimidine motif and purine rich motif. A pyrimidine motif containing TFO binds to its target purine stretch in parallel by forming Hoogsteen base pairs between thymine (T) in the TFO and adenine (A) of the A:T pair in the target, and protonated cytosine (C^+) in the TFO and guanine (G) of the G:C pair in the target

stretch (**Table 2.4**). On the other hand, purine rich motif containing TFOs bind to the target purine stretch in a antiparallel mode by forming reverse Hoogsteen base pairs between A or T in the TFO and A from the target A:T pair, and G in the TFO and G from the target G:C pair (**Table 2.4**) [52, 54]. There are four major drawbacks of TFO antigenes: firstly triplex formation of C^+:G-C requires an acidic environment (pH: 4.5-6) for protonation of the C in the TFO, which constrains *in vivo* utility of TFOs as the physiological pH is 7.35 to 7.45 [13, 52]. Secondly, G-rich TFOs tend to self-associate into G-quartets at physiologic potassium concentrations and thus affects the triplex formation [13, 52]. Third, limitations in the range of sequences for targeting (purine stretch only) restrict the design of TFOs. Finally, it is obvious that TFOs cannot be used to target those DNA regions entangled in highly packed forms such as nucleosomes. To date, efforts to introduce chemical modifications to TFOs have to some extent resolved these problems.

TFO binding motifs		
Motif	**Base pairing**	**Example**
Pyrimidine	T•A C+•G	3′-CTCTCTTTCCTCTCCTCCTTCTCCCTCTCTTTCTCCTC-5′ 5′-GAGAGAAAGGAGAGGAGGAAGAGGGAGAGAAAGAGGAG-3′ 5′-TTTC+C+TC+TC+C+TC+C+TTT-3′ Hoogsteen (parallel)
Purine rich	T•A T•A C•G	3′-CTCTCTTTCCTCTCCTCCTTCTCCCTCTCTTTCTCCTC-5′ 5′-GAGAGAAAGGAGAGGAGGAAGAGGGAGAGAAAGAGGAG-3′ 3′-AAAGGTGAGGAGGAA-5′ Reverse Hoogsteen (antiparallel)

Table 2.4. TFO pyrimidine and purine rich binding motifs. TFO: triplex forming oligodeoxynucleotide.

2.5 Antisense oligonucleotide (AO)

Antisense oligonucleotides (AOs) are single stranded oligonucleotides that can be designed to deliver therapeutic benefit through by modulating specific RNAs. The first demonstration of antisense potential was offered by Zamecnik and Stephenson in 1978, when a 13nt AO was synthesized and used to inhibit Rous sarcoma virus replication by targeting viral 35S RNA [55, 56]. Since then, AOs have been developed as a versatile platform that upon binding to its

target RNA through Watson-Crick base pairing, mainly function via three mechanisms, dependent on the chemistry and sequence: RNase H mediated mRNA degradation, splice modulation, translational blockage and altered stability [14, 21, 57].

Upon formation of a heteroduplex with the target mRNA, AOs composed of deoxyribonucleotides can induce degradation of the annealed mRNA and/or precursor mRNA (pre-mRNA) via recruitment of a ubiquitous endonuclease, RNase H that exists both in cytoplasm and the nucleus, and hydrolyzes the RNA component of the heteroduplex while leaving the AO intact (**Figure 2.5**) [13, 52, 58, 59]. Compared to RNase H recruitment, the other two mechanisms are somewhat more straightforward: steric blockade is created when the AO/RNA duplex is formed, it prevents interaction between the bound pre-mRNA and splicing factors, the bound mRNA and translational machinery [45, 57-60]. While the first leads to splice modulation, the latter result in translational arrest or altered stability (**Figure 2.5**).

The two mechanisms: degradation of mRNA by RNase H and inhibition of translation are used to downregulate the expression of disease-causing genes, whereas the AOs capable of modulate splicing events can be applied to switch the production of non-functional transcripts of an essential gene carrying mutations, to a functional transcript variant, thereby restoring the synthesis of functional protein encoded by the gene [61]. However, splicing modulation can be used to disrupt expression of a gene transcript as well, through disturbing the reading frame.

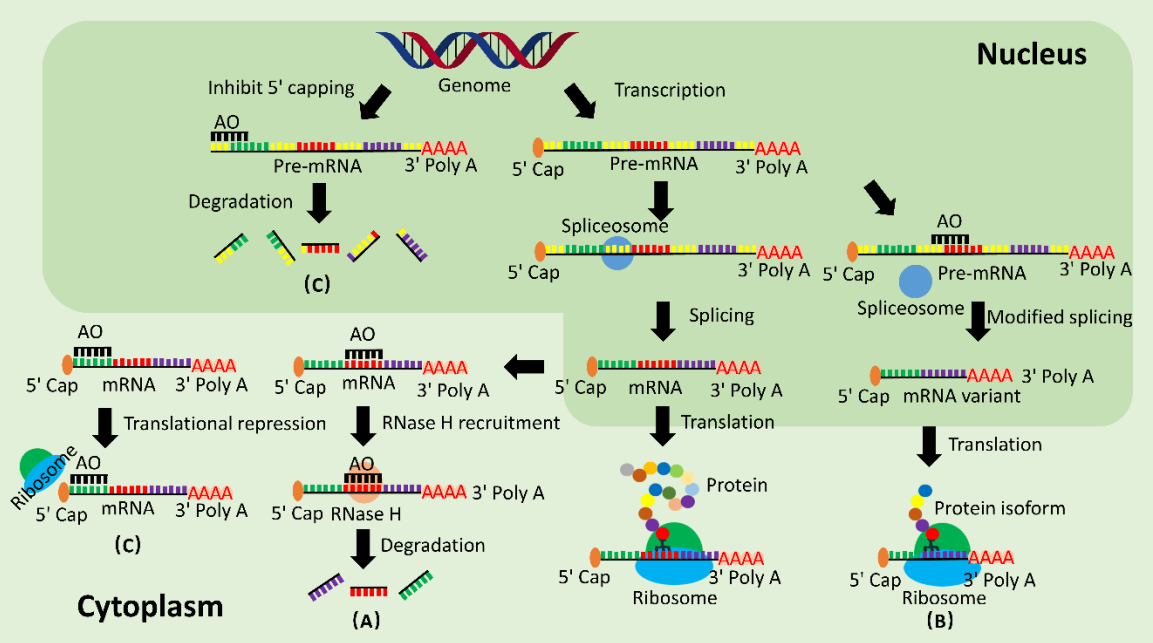

Figure 2.5 AO mechanisms. (A) Degradation of target RNA by RNase H; (B) induction of alternative splicing; (C) induction of translational repression. AO: antisense oligonucleotide, mRNA: messenger RNA, pre-mRNA: precursor messenger RNA.

2.6 Catalytic oligonucleotides

Catalytic oligonucleotides include ribozymes and DNAzymes. Ribozyme was originally discovered from nature in the early 1980s when Cech's team found that an intron contained in *Tetrahymena thermophilia's* precursor ribosomal RNA (rRNA) possesses self-splicing activity [62-65]. Later, Altman's group found that the RNA portion of RNase P endoribonuclease plays a role in the maturation of *Escherichia coli* transfer RNA (tRNA), through excising the 5' end from its precursor [66]. In contrast, DNAzymes are solely exploited in laboratories [67], first isolated by Breaker and Joyce in 1994 through *in vitro* selection [67]. DNAzymes can be considered analogs of ribozymes, in that the RNA backbone of ribozymes is replaced by DNA that confers improved biological stability [68].

Both ribozymes and DNAzymes utilize other nucleic acids as substrates, the catalytic reaction leads to substrate cleavage, ligation, or phosphorylation [69-73]. So far, RNA-cleaving oligonucleotides have been extensively investigated and developed. Among these, hammerhead ribozymes, hairpin ribozymes, 8-17 DNAzymes, and 10-23 DNAzymes are the most widely used, mainly due to their structural simplicity and small size (less than 150nt)

[24, 72, 74, 75], compared to the large naturally occurring ribozymes, such as self-splicing introns and the RNA portion of RNase P that may contain up to 3000 nucleotides [73]. All catalytic oligonucleotides exhibit enzymatic activity independent of any protein co-factors and external energy source, however, involvement of non-metal or metal positive charges are required for the catalysis effected by the ribozyme or DNAzyme, respectively [24, 76-79]. Structurally, all RNA-cleaving oligonucleotides contain two types of domains: a catalytic domain and flanking or adjacent sequences called substrate binding arms (**Figure 2.6**). The antisense nature of the binding arm sequences directs the specific binding of the catalytic oligonucleotide to the complementary stretch within its target RNA and thereby allows cleavage of the target by the catalytic domain [21, 80]. The sequence contained in the catalytic domain is completely or partly conserved, whereas the sequences comprising the binding arms are amendable, enabling design of catalytic oligonucleotides capable of recognizing a specific target. Different types of RNA cleaving oligonucleotides result in cleavage of their substrate RNAs at distinct sites: for example, hammerhead ribozyme cleaves 5'-NUH*-3' (N represents any nucleotide of A, U, G, C; H represents A, U, C; * represents cleavage site) [59, 65], hairpin ribozymes cut 5'-*GUC-3' [65, 67, 97, 82], 8-17 DNAzymes cleave 5'-A*G-3' [83, 84], and 10-23 DNAzyme sever 5'-R*Y-3' (R represents A, G; Y represents U, C) [83, 85, 87] (**Figure 2.6**). However, the *in vivo* applications of DNAzyme are limited due to the difficulty of balancing its catalytic activity and turnover kinetics. This is mainly due to the fact that, development of DNAzymes that are able to form stable complex with their substrates leads to higher catalytic activity but might result in reduced turnover efficacy at the same time [86].

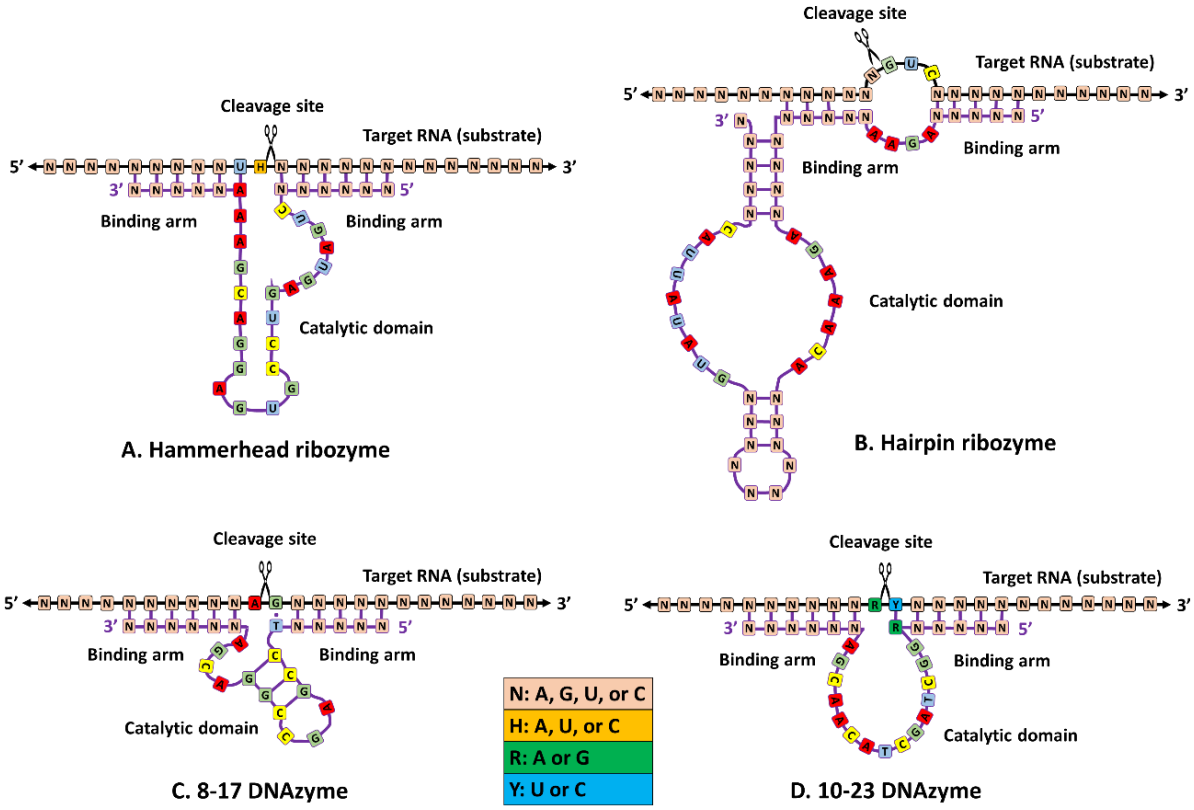

Figure 2.6 Schematic representations of commonly used RNA-cleaving catalytic oligonucleotides. (A) Hammerhead ribozyme; (B) hairpin ribozyme; (C) 8-17 DNAzyme; (D) 10-23 DNAzyme.

2.7 Micro RNA-related oligonucleotides

First discovered in 1993 [88, 89], miRNAs are naturally occurring, single stranded, 21-25nt long, non-coding RNAs that downregulate gene expression at the post-transcriptional level after partial Watson-Crick hybridization to target mRNAs [15, 45, 90]. The biogenesis and mechanism of miRNA is shown in **Figure 2.7**. Initially, primary miRNA (pri-miRNA) is transcribed from the genome by RNA polymerase II, followed by cleavage of the hairpin structures contained in pri-miRNA by the microprocessor complex consisting of Drosha (a nuclear RNase III endonuclease) and DGCR8 (cofactor for Drosha) [91-94] (**Figure 2.7**). These released hairpins are called precursor miRNA (pre-miRNA) and they are transported from the nucleus to the cytoplasm by exportin-5 (exp5) complex that contains exp5, Ran and guanosine-5'-triphosphate (GTP) [95, 96] (**Figure 2.7**). The pre-miRNA is then cleaved by Dicer (a cytoplasmic RNase III endonuclease) leaving the miRNA-miRNA* duplex [97-100]

(**Figure 2.7**). Subsequent binding of the RNA-induced silencing complex (RISC) to the duplex lead to removal of miRNA* (passenger strand) and loading of the mature miRNA into RISC [101]. Dependent upon the degree of homology of miRNA and its target mRNAs, the miRNA containing RISC induces degradation of target mRNA (caused by near perfect complementarity) or translational repression due to steric blockade of translational machinery by RISC (caused by imperfect complementarity) [90, 101, 102] (**Figure 2.7**), both lead to down-regulation of target genes. The advantage of partial complementarity is that a single miRNA is able to regulate multiple genes [45, 103].

Enlightened by the natural miRNA's mechanism of gene knockdown, therapeutic oligonucleotides can be designed [15]. For example, miRNAs can function as oncogene inhibitors (tumor suppressor miRNAs), as well as miRNAs that inhibit expression of tumor suppressor genes (onco-miRNAs) [90], miRNA mimics of tumor suppressor miRNAs and anti-miRNAs (also known as antagomirs) that are reverse complements of onco-miRNAs can be designed. The former, miRNA mimics can imitate the function of tumor suppressor miRNAs in an attempt to inhibit tumor development [104-106], while the latter, anti-miRNAs are used to bind to onco-miRNAs in order to deactivate their function through a steric blockage mechanism [90, 107-109].

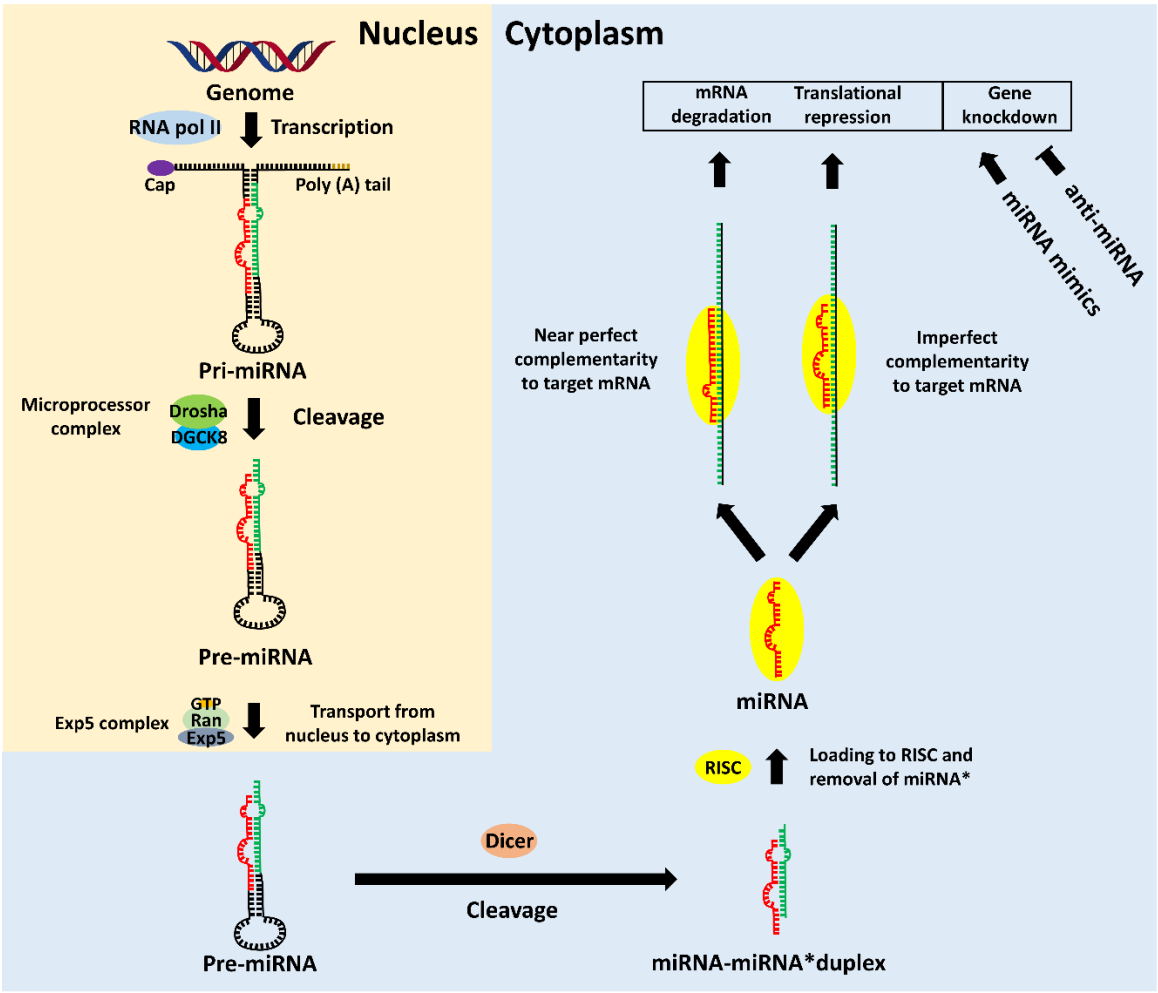

Figure 2.7 Biogenesis and mechanism of miRNA. RNA Pol II: RNA polymerase II, miRNA: microRNA, pri-miRNA: primary microRNA, pre-miRNA: precursor microRNA, exp5: exportin-5, GTP: guanosine-5'-triphosphate, RISC: RNA-induced silencing complex.

2.8 Small interfering RNA (siRNA)

The RNA interference (RNAi) pathway was first described by Fire et al. in 1998 when they introduced double stranded RNAs (dsRNA) into *Caenorhabditis elegans*, triggering specific degradation of homologous mRNAs [110]. The mechanism of RNAi is shown in **Figure 2.8**. The pathway is initiated by Dicer-mediated cleavage of long non-coding dsRNAs, leading to formation of double stranded siRNAs of 21-23bp in length with symmetrical overhangs of 2-3nt at the 3' end of each strand (antisense or guide strand, and sense or passenger strand) (**Figure 2.8**) [14, 15, 59, 90, 100, 111, 112]. Subsequent binding of RISC to siRNA results in removal of the sense strand and loading of the antisense strand into RISC, forming a catalytic complex that can induce cleavage and degradation of target mRNAs upon Watson-Crick

hybridization of the antisense strand to the target mRNA (**Figure 2.8**) [21, 59, 61, 90, 113-118].

It is worth mentioning that the pathways of RNAi and the afore-described miRNA (section 2.7) share similarities. For instance, they both require involvement of Dicer for long precursor RNAs to be cleaved into shorter forms, and RISC for antisense strands to be loaded into RISC, that eventually causes gene knockdown. On the other hand, RNAi is distinguished from miRNA in two respects: first, the two strands of siRNA are completely complementary to each other (**Figure 2.8**) while the hybridization within a miRNA-miRNA* duplex is incomplete (**Figure 2.7**) [119]; second, the antisense strand of siRNA binds to target mRNA through perfect complementarity, leading to RISC-induced target degradation (**Figure 2.8**), whereas the miRNA-target mRNA hybridization is imperfect in that the RISC complex may merely act as a steric blocker (**Figure 2.7**) [120].

In practice, the introduction of long dsRNA (>30bp) into mammalian cells stimulates the innate immune system, initiating an antiviral interferon response that usually causes cell death, and thereby hampers the application of RNAi [59, 121]. This problem was solved by Elbashir et al. and Caplen et al. who reported that an siRNA duplex with strands of 21-22bp in length can efficiently induce gene silencing in mammalian cells [115, 122, 123]. The use of siRNA instead of long dsRNA not only evades unwanted immunoreaction [45, 124], but also circumvents the Dicer pathway [21], and thus is the recognized strategy to exploit the RNAi pathway. The major risk of siRNA application is the potential of inducing off-target effects through binding to and then degrading non-target mRNAs as a result of partial sequence homology [15], due to the fact that as few as seven contiguous complementary base pairs may be sufficient to direct RNAi gene silencing [125].

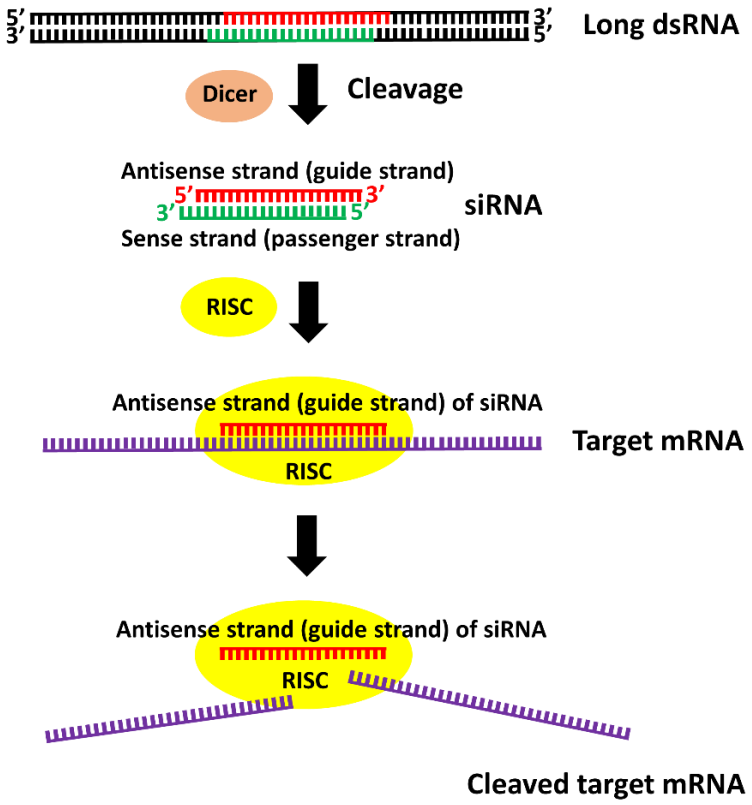

Figure 2.8 RNA interference mechanism for siRNA. dsRNA: double stranded RNA, siRNA: small interfering RNA, RISC: RNA-induced silencing complex.

2.9 Immune-stimulatory oligonucleotide

Immune-stimulatory oligonucleotides are a group of short, single-stranded oligodeoxynucleotides that contain CpG dinucleotides, in 5' to 3' direction (**Figure 2.9**), mimicking a distinct feature of bacterial genomic DNA: abundance of unmethylated CpG motifs [126-127]. In contrast, the frequency of CpG motifs is much lower in vertebrate genomes, and, CpG motifs are considered pathogen-associated molecular patterns (PAMPs) that upon binding and recognition by Toll-like receptor 9 (TLR9), these motifs are identified as invading microorganisms, leading to activation of the innate immune response. The TLR9-mediated signal transduction, followed by activation of essential downstream transcription factors such as NF-κB and AP-1 further induce the expression of inflammatory cytokines, such as TNF-α and IL-6 that modulate components of the innate immune system (**Figure 2.9**)

[128, 129]. Hence, synthetic oligodeoxynucleotides that contain CpG motifs can act as immunostimulants and have been developed as immune adjuvants [130-132].

It is notable that unlike the interactions between nucleic acids that are based on sequential base pairing, the interactions between CpG-containing oligodeoxynucleotides and its protein target, TLR-9, rely on a variety of structural features [133-138].

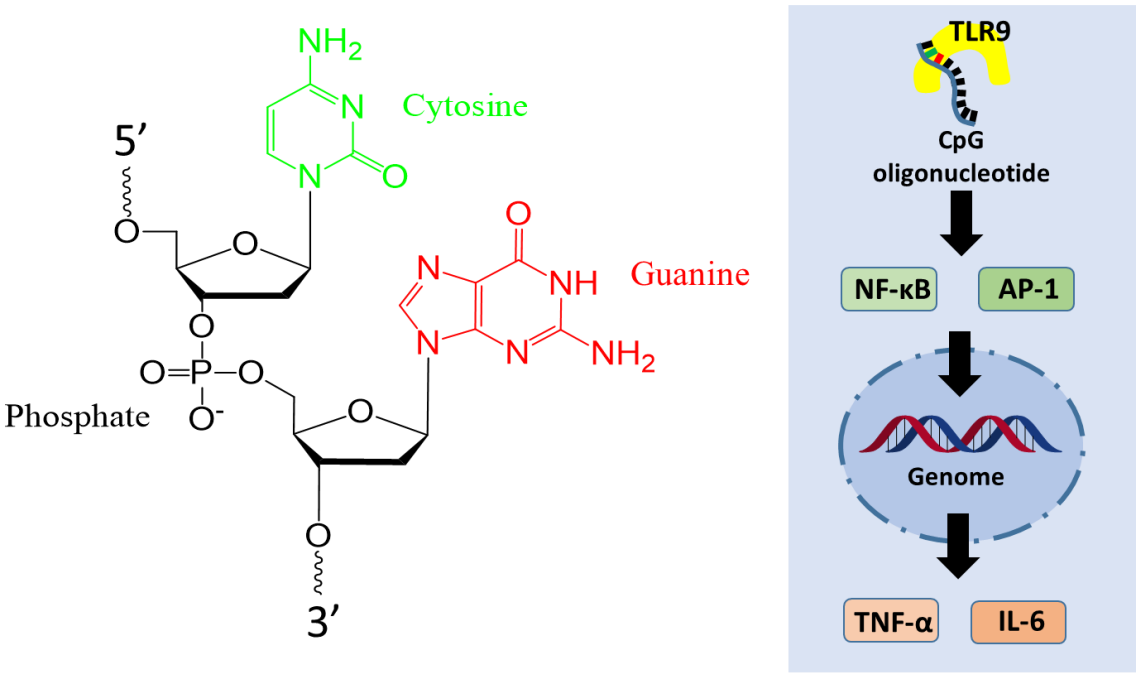

Figure 2.9 Schematic structure of a CpG motif (left) and simplified immune-stimulatory mechanism for CpG containing oligonucleotide (right).

2.10 Decoy oligonucleotides

Transcription factor proteins regulate gene expression by initiating gene transcription [139], through specific binding to multiple consensus sequences (6-10 bp in length) existing in the promotor region of target genes (**Figure 2.10**) [44]. Decoy oligonucleotides are double stranded oligodeoxynucleotides that contain stretches of the consensus sequences, mimicking the binding site for transcription factors, and thereby competing with the gene promotor region for transcription factor binding (**Figure 2.10**) [140-142]. By flooding cells with decoy oligonucleotides, large numbers of transcription factors are sequestered by decoys, diminishing the binding of transcription factors to the target promoter regions, thus the

function of the transcription factor, that is promoting target gene expression, is attenuated (**Figure 2.10**) [44, 140]. Accordingly, decoy oligodeoxynucleotides have therapeutic potential as they can also silence disease-related genes by preventing their transcription, as do other classes of gene silencing therapeutic nucleic acids, described earlier.

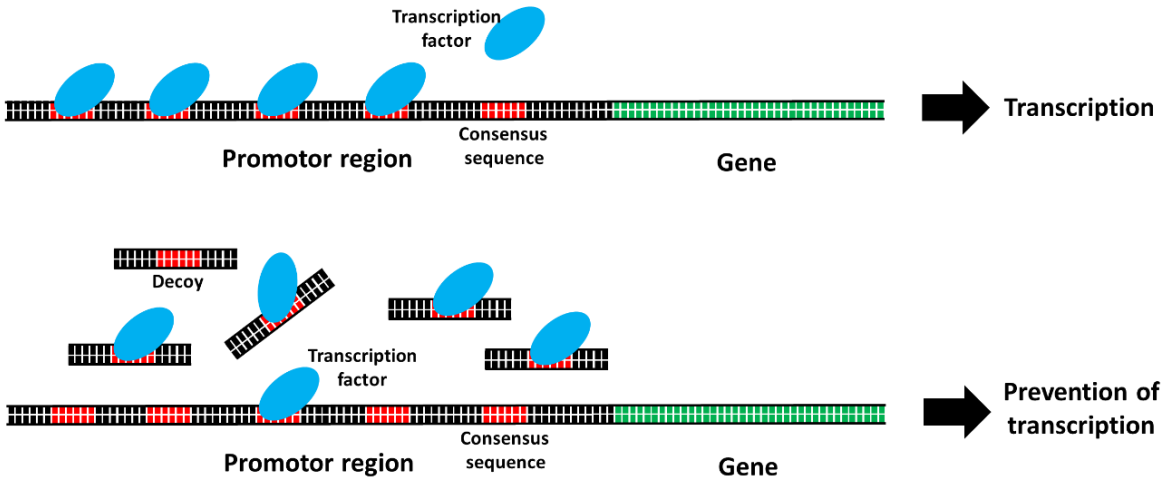

Figure 2.10 Mechanism of decoys. In the absence of decoys, transcription factors bind to consensus sequences within the promotor and initiate transcription (upper panel), decoys compete with the promotor region for transcription factor binding and thus prevent transcription (lower panel).

2.11 Aptamers

Aptamers are single stranded DNA or RNA oligonucleotides that are able to fold into unique 3D shapes that lay the foundation for their biological function: binding to and interfering with their target molecules through specific 3D structure recognition, instead of sequence recognition [45, 130, 143, 144]. This feature distinguishes aptamers from other oligomeric therapeutic nucleic acids that exhibit functions that depend on nucleotide sequence recognition by their targets.

Aptamers are isolated in laboratories from a large combinatorial pool of synthetic oligonucleotides (10^{14} to 10^{15} random sequences) by an iterative Darwinian selection process called SELEX (Systematic Evolution of Ligands by EXponential enrichment) [145-153], which mainly involves three steps: binding, elution, and amplification (**Figure 2.11**). In the binding step, the oligonucleotide candidate pool is incubated with target molecules, allowing

the association of the candidates with the target (**Figure 2.11**) [154, 155]. This is followed by a washing step that removes unbound candidates while the bound ones are retained and are amplified in the third step (**Figure 2.11**). The selection cycle is repeated multiple times in order to select candidates of the highest target binding affinity [154, 155]. Cloning and sequencing are performed at the end to characterize the sequence of the champion candidates: aptamers [155].

There are three major advantages of aptamers over other therapeutic nucleic acids. Firstly, aptamers can bind to extracellular molecules [20, 156], while other therapeutic nucleic acids can only strictly recognize intracellular nucleic acids or proteins. Hence, aptamers can reach target molecules that are inaccessible to other classes of therapeutic nucleic acid. For example, the first-in-class FDA-approved aptamer Macugen® specifically recognizes and blocks extracellular vascular endothelial growth factor (VEGF), thus preventing VEGF from binding to its receptor located on the cell surface, [157, 158] leading to inhibition of its downstream intracellular signaling process. Secondly, the 3D shape recognition mode enables aptamers to bind to nearly any type of target molecules or objects [20, 90, 159-162], thus greatly expanding the applicability of aptamers. Finally, optimization of aptamer sequences for better performance is unlimited, as aptamers do not have to contain or mimic any sequence with genetic information, while other therapeutic nucleic acids are restricted during optimization due to the necessity to possess specific sequence complementary to target nucleic acids or to be recognized by certain proteins. An inherent limitation of aptamer technology is, unlike amino acids, only four letters are available in the alphabetic table to evolve aptamers, severely compromising the potential in optimizing their abilities to recognize target molecules.

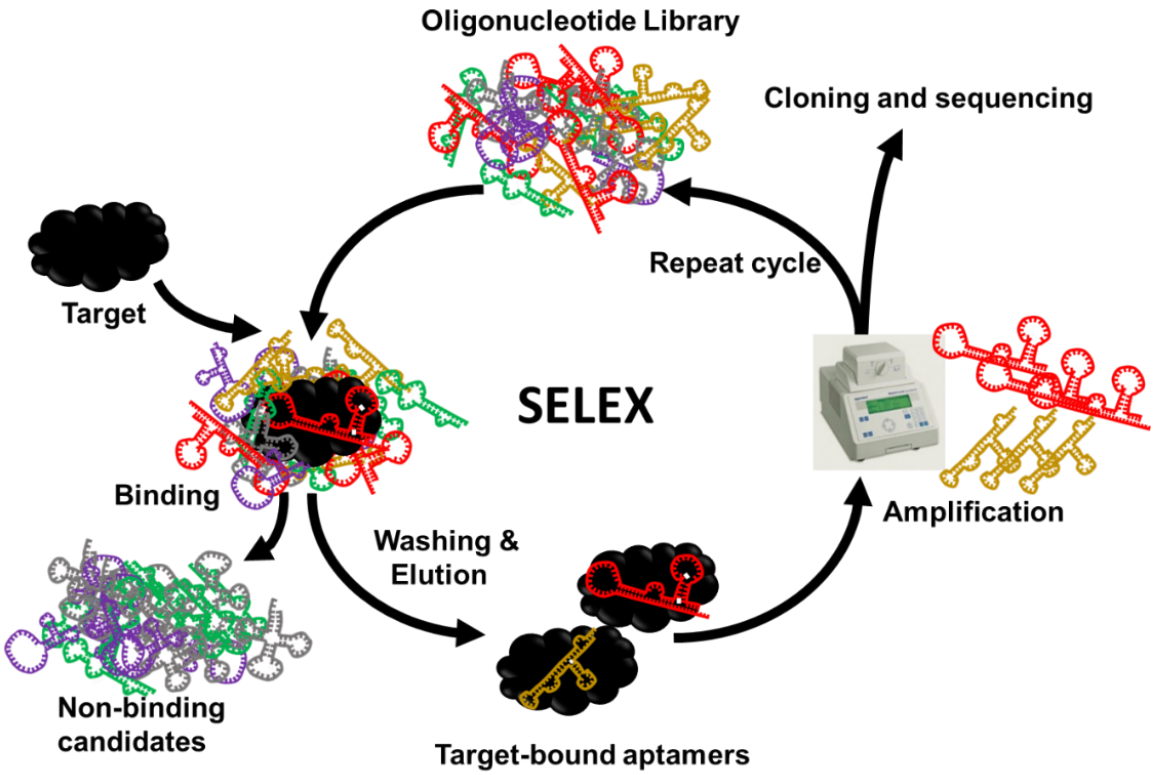

Figure 2.11 Schematic illustration of SELEX process.

The advantages and disadvantages of each type of therapeutic nucleic acids is summarized in **table 2.**

Type of therapeutic nucleic acids	Advantages	Disadvantages
Transgenes	**Long-lasting therapeutic effect.**	**Transgenes are incorporated in viral or plasmid vectors that contain other exogenous genes which are not of interest. This leads to potential safety issues.**
Synthetic mRNA	**Rapid expression of therapeutic proteins.**	**The therapeutic effect is transient.**
Synthetic guide RNA for CRISPR/Cas	**In theory any genomic DNA can be targeted.**	**Off-target effect.**
Antigene	**As a target gene only contains two copies of genomic DNA in a cell, whilst hundreds to thousands of mRNAs are transcribed from the corresponding target gene. This suggests that a relatedly small dosage of antigene agent may be required for downregulation of the target gene, compared to using RNA-targeting therapeutic nucleic acid agents for the same purpose.**	**Firstly, triplex formation of C^+:G-C requires an acidic environment (pH: 4.5-6) for protonation of the C in the antigene, which constrains *in vivo* utility of antigene. Secondly, G-rich antigene tends to self-associate into G-quartets at physiologic potassium concentrations and thus affects the triplex formation. Third, limitations in the range of sequences for targeting (purine stretch only) restricts the design of antigenes. Finally, it is obvious that antigene cannot be used to target those DNA regions entangled in highly packed forms such as nucleosomes.**
Antisense oligonucleotide	**Diverse mechanism of actions allow downregulation of disease-causing genes through RNase H recruitment, as well as restoration of essential functional genes by splice modulation.**	**Inefficient cellular delivery *in vivo* is the major obstacle.**
Catalytic oligonucleotide	**Simple and direct mechanism of action. All catalytic oligonucleotides exhibit enzymatic activity independent of any protein co-factors and external energy source.**	**Involvement of non-metal or metal positive charges are required for the catalysis.**
microRNA related oligonucleotide	**A single miRNA is able to regulate multiple genes.**	**Potential toxicity due to off-target effects.**
Small interfering RNA	**Efficient silencing of target gene**	**Off-target effect.**
Immune-stimulatory oligonucleotide	**It acts as immunostimulants and can be developed as immune adjuvants.**	**Excessive immune reaction.**
Decoy oligonucleotide	**Gene silencing by preventing transcription**	**Lack of efficiency.**
Aptamer	**Firstly, aptamers can bind to extracellular molecules, while other therapeutic nucleic acids can only strictly recognize intracellular nucleic acids or proteins. Secondly, the 3D shape recognition mode enables aptamers to bind to nearly any type of target molecules or objects, thus greatly expanding the applicability of aptamers. Finally, optimization of aptamer sequences for better performance is unlimited, as aptamers do not have to contain or mimic any sequence with genetic information, while other therapeutic nucleic acids are restricted during optimization due to the necessity to possess specific sequence complementary to target nucleic acids or to be recognized by certain proteins.**	**An inherent limitation of aptamer technology is, unlike amino acids, only four letters are available in the alphabetic table to evolve aptamers, severely compromising the potential in optimizing their abilities to recognize target molecules.**

Table 2. Advantages and disadvantages of each type of therapeutic nucleic acids.

3. Improving the utility of therapeutic nucleic acids

Therapeutic nucleic acids composed of natural DNA or RNA monomers are rapidly degraded *in vitro* and *in vivo* by nucleases, and are therefore generally unsuitable for therapeutics development. In order to overcome this issue, one strategy is to incorporate therapeutic nucleic acid sequences into viral or plasmid vectors for continuous cellular delivery. Vector-aided delivery has been widely adopted for the transportation of transgenes into target cells for exogenous gene expression [22-24, 163], while non-viral vectors, mainly lipid nanoparticles, have been extensively applied to the delivery of both synthetic mRNA and oligomeric therapeutic nucleic acids [164-167]. Another strategy for improving the therapeutic potential of nucleic acids is the introduction of chemical modifications [58, 168, 169]. Structure-modified nucleotide analogues have been used in oligomeric therapeutic nucleic acids synthesis that helps to increase their resistance to nuclease, enhance target binding specificity and affinity, and improve cellular uptake [14]. The inter-nucleotide linkages (phosphate groups) and sugar moieties of nucleotides are the hot-spots for modification, a number of analogues have been reported with changes to these moieties. The phosphorothioate (PS) backbone represents the first generation of chemical modification, whereby the non-bridging oxygen atom in the diester bond is replaced by a sulphur [170-172]. The second generation modifications include nucleotide analogues containing a modified sugar moiety, such as 2′-O-methyl (2′-OMe) and 2′-O-methoxyethyl (2′-O-MOE). Third generation modifications include analogues in which the backbone (both phosphate groups and sugar moieties) is completely replaced by alternative structures. Representatives of this generation are peptide nucleic acid (PNA) and phosphorodiamidate morpholino oligomers (PMO). Examples of chemical modifications are presented in **Figure 3.1**. In addition, it is noteworthy that nucleotide analogues are merely used in constructing oligomeric nucleic acids, i.e., synthetic gRNA for CRISPR/Cas, antigene, AO, catalytic oligonucleotide,

miRNA-related oligonucleotide, siRNA, immune-stimulatory oligonucleotide, decoy oligonucleotide, and aptamer, but not the long nucleic acids (transgene and synthetic mRNA) that encode intact genetic information.

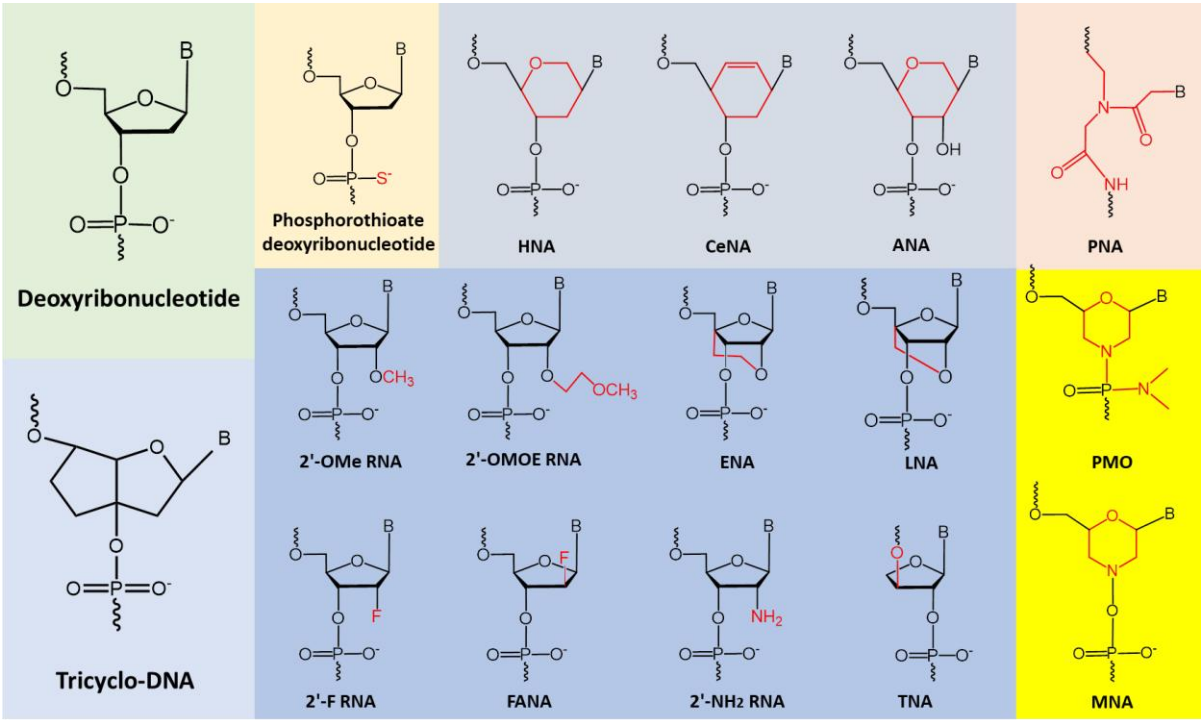

Figure 3.1 Examples of chemically-modified nucleotide analogues. 2'-OMe: 2'-O-methyl, 2'-OMOE: 2'-O-methoxyethyl, ENA: 2'-O, 4'-C-ethylene-bridged nucleic acid, LNA: locked nucleic acid, 2'-F: 2'-fluoro, 2'-FANA: 2'-fluroarabino nucleic acid, 2'-NH2: 2'-amino, TNA: threose nucleic acid, HNA: 1,5-anhydro hexitol nucleic acid, CeNA: cyclohexenyl nucleic acid, ANA: altritol nucleic acid, PNA: peptide nucleic acid, PMO: phosphorodiamidate morpholino oligomer, MNA: morpholino nucleic acid.

Importantly, apart from merely improving the drug-like properties of therapeutic nucleic acids, chemical modification can also lead to variations to their mechanism of actions. The best example is the fully modified AOs used for splice modulation. AOs were originally designed as oligodeoxynucleotides that induce RNase H-mediated target mRNA degradation. However, a number of modifications (2′-OMe, 2′-O-MOE, PMO) enable AOs to modulate alternative splicing by inducing exon skipping or exon inclusion, while at the same time compromising their ability to induce RNase H. In order to retain the RNase H activation function while confering sufficient protection from nucleases, gapmer-like AOs are designed:

a DNA core sequence is left unmodified (or with PS) to induce RNase H, flanked by modified sequences at both ends to provide protection from nucleases [173, 174] (**Figure 3.2**).

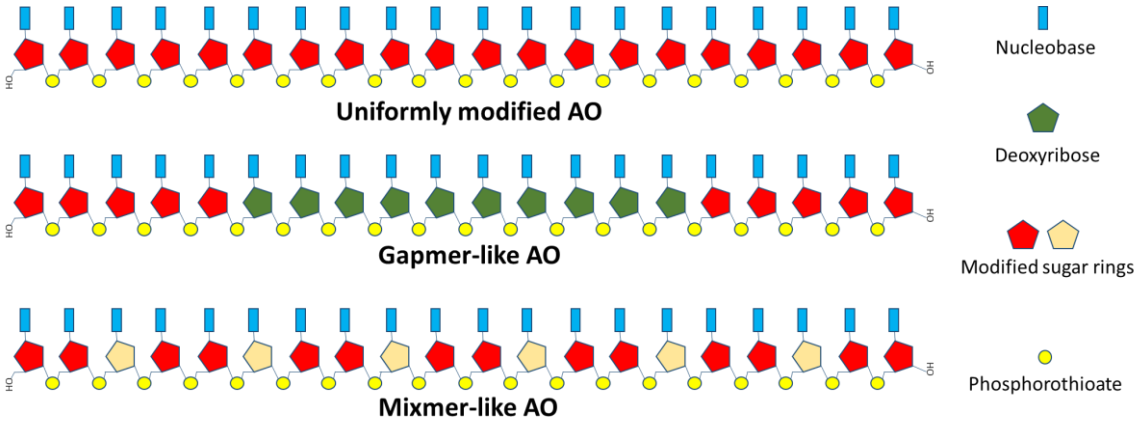

Figure 3.2 Schematic showing AOs with uniformly modified analogues and AOs composed of nucleotides of different chemistries (chimeric AO: gapmer and mixmer).

4. Project Aims:

In this thesis, we report the evaluation of chemically modified, splice modulating antisense oligonucleotides (AOs) for the therapy of type 2 diabetes (T2D) and Duchenne muscular dystrophy (DMD) (**Figure 4**). Specifically, novel AO sequences were developed to downregulate the expression of protein tyrosine phosphatase 1B (PTP1B), an enzyme involved in the pathogenesis of T2D through insulin dysregulation. In addition, novel chemical modifications to AOs in terms of new nucleotide analogue and new chimeric sequence design were explored towards improving the drug-like properties of AO sequences, using DMD as a disease model.

Specific Aims:

1. Development of novel splice modulating AOs to downregulate PTP1B expression towards targeting T2D.

a. Design and screening of 2′-O-methyl-phosphorothioate (2′-OMePS) AO sequences targeting different exons of the *PTPN1* pre-mRNA.

b. Validation of the best performing AO sequence from aim 1a.

c. Identification of the 'champion' AO sequence through a micro-walk AO design strategy (based on the sequence of the best performing AO from aim 1b).

d. Validation of the champion AO sequence.

e. Improvement of the champion AO sequence by constructing phosphorodiamidate morpholino oligomers (PMO) of the sequence and evaluation of its ability to inhibit PTP1B protein expression.

f. Development of 'mouse version' of the champion AO sequence for future *in vivo* animal studies.

2. Exploration of novel chemical modifications of splice modulating AOs towards optimizing their drug-like properties, using DMD as a disease model.

a. Exploration of a morpholino nucleic acid (MNA) modified 2′-OMePS mixmer AO in terms of its thermal stability, cytotoxicity, and ability to inducing *DMD* exon skipping.

b. Exploration of 2′-OMe modified 2′-fluoro (2′-F)-PS gapmer and mixmers, and locked nucleic acid (LNA) modified 2′-F-PS gapmer and mixmers in terms of their nuclease stability, cytotoxicity, and induced exon skipping.

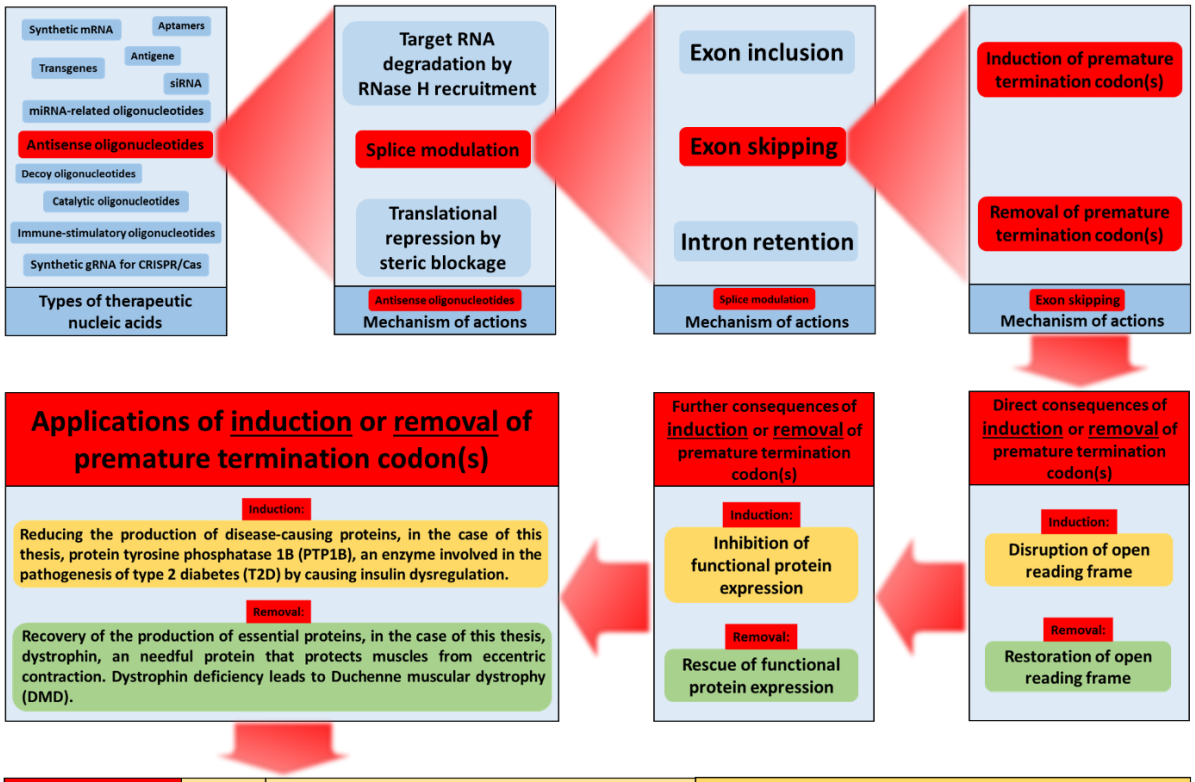

Project aims	**Aim 1**	To develop novel antisense oligonucleotide sequences that downregulate the expression of functional PTP1B towards targeting T2D.	**Major achievement** Identification of an antisense oligonucleotide sequence, PTPN1 1E2A (+5+29) that efficiently downregulate PTP1B expression.
	Aim 2	To explore novel chemical modification of antisense oligonucleotides towards improving their drug-like properties using DMD as a disease model.	**Major achievement** Expansion of the scope of using chimeric antisense oligonucleotides in splice modulation applications.

Figure 4 Schematic illustration of the aims and outcomes of the thesis.

Chapter one references

1. Dahm, R. Discovering DNA: Friedrich Miescher and the early years of nucleic acid research. *Hum Genet* 122, 565-581 (2008).
2. Dahm, R. Friedrich Miescher and the discovery of DNA. *Dev Biol* 278, 274-288 (2005).
3. Avery, O.T., Macleod, C.M., McCarty, M. Studies on the chemical nature of the substance inducing transformation of pneumococcal types: induction of transformation by a deoxyribonucleic acid fraction isolated from Pneumococcus type III. *J Exp Med* 79, 137-158 (1944).
4. Watson, J.D., Crick, F.H. Molecular structure of nucleic acids: a structure for deoxyribose nucleic acid. *Nature* 171, 737-738 (1953).
5. Crick, F.H. On protein synthesis *Symp Soc Exp Bio* 12, 138-163 (1958).
6. Crick, F.H. Central dogma of molecular biology. *Nature* 227, 561–563 (1970).
7. Cobb, M. 60 years ago, Francis Crick changed the logic of biology. *PLoS Biol* 15, e2003243 (2017).
8. Grunberg-Manago, M., Ortiz, P.J., Ochoa, S. Enzymic synthesis of polynucleotides. I. Polynucleotide phosphorylase of azotobacter vinelandii. *Biochim Biophys Acta* 20, 269-285 (1956).
9. Khorana, H.G. Synthesis in the study of nucleic acids. The Fourth Jubilee Lecture. *Biochem J* 109, 709-725 (1968).
10. Beaucage, S.L., Caruthers, M.H. Deoxynucleoside phosphoramidites—a new class of key intermediates for deoxypolynucleotide synthesis. *Tetrahedron Lett* 22, 1859-1862 (1981).
11. Matteucci, M.D., Caruthers, M.H. Synthesis of deoxyoligonucleotides on a polymer support. *J Am Chem Soc* 103, 3185-3191 (1981).
12. Brown, D.M. A brief history of oligonucleotide synthesis. *Methods Mol Biol* 20, 1-17 (1993).

13. Gewirtz, A.M., Sokol, D.L., Ratajczak, M.Z. Nucleic acid therapeutics: state of art and future prospects. *Blood* 92, 712-736 (1998).
14. Smith, C.I.E., Zain, R. Therapeutic oligonucleitides: state of the art. *Annu Rev Pharmacol Toxicol* 59, 605-630 (2019).
15. Sridharan, K., Gogtay, N.J. Therapeutic nucleic acids: current clinical status. *Br J Clin Pharmacol* 82, 659-672 (2016).
16. Verma, I.M., Naldini, L., Kafti, T., et al. Gene therapy: promises, problems, and prospects. In: Boulyjenkov, V., Berg, K., Christen, Y., editors. Genes and resistances to disease. Berlin, Heidelberg: Springer; 147-157 (2000).
17. Alarcon, J.B., Waine, G.W., McManus, D.P. DNA vaccines: technology and application as anti-parasite and anti-microbial agents. *Adv Parasitol* 42, 343-410 (1999).
18. Robinson, H.L., Pertmer, T.M. DNA vaccines for viral infections: basic studies and applications. *Adv Virus Res* 55, 1-74 (2000).
19. Johnston, S.A., Talaat, A.M., McGuire, M.J. Genetic immunization: what's in a name? *Arch Med Res* 33, 325-329 (2002).
20. Papadakis, E.D., Nicklin, S.A., Baker, A.H., White, S.J. Promoters and control elements: designing expression cassettes for gene therapy. *Curr Gene Ther* 4, 89-113 (2004).
21. Alvarez-Salas, L.M. Nucleic acids as therapeutic agents. *Curr Top Med Chem* 8, 1379-1404 (2008).
22. Dunbar, C.E., High, K.A., Joung, J.K., Kohn, D.B., Ozawa, K., Sadelain, M. Gene therapy comes of age. *Science* 359, eaan4672 (2018).
23. Steffin, D.H.M., Hsieh, E.M., Rouce, R.H. Gene Therapy: current applications and future possibilities. *Adv Pediatr* 66, 37-54 (2019).
24. Wirth, T., Parker, N., Ylä-Herttuala, S. History of gene therapy. *Gene* 525, 162-169 (2013).

25. Sahin, U., Karikó, K., Türeci, Ö. mRNA-based therapeutics-developing a new class of drugs. *Nat Rev Drug Discov* 13, 759-780 (2014).
26. Pardi, N., Hogan, M.J., Porter, F.W., Weissman, D. mRNA vaccines - a new era in vaccinology. *Nat Rev Drug Discov* 17, 261-279 (2018).
27. Zhong, Z., Cafferty, S.M., Combes, F., et al. mRNA therapeutics deliver a hopeful message. *Nano Today* 23, 16–39 (2018).
28. Islam, M.A., Reesor, E.K., Xu, Y., Zope, H.R., Zetter, B.R., Shi, J. Biomaterials for mRNA delivery. *Biomater Sci* 3, 1519-1533 (2015).
29. Lentacker, I., Vandenbroucke, R.E., Lucas, B., Demeester, J., De Smedt, S.C., Sanders, N.N. New strategies for nucleic acid delivery to conquer cellular and nuclear membranes. *J Control Release* 132, 279-288 (2008).
30. Hille, F., Charpentier, E. CRISPR-Cas: biology, mechanisms and relevance. *Philos Trans R Soc Lond B Biol Sci* 371, 20150496 (2016).
31. Sander, J.D., Joung, J.K. CRISPR-Cas systems for editing, regulating and targeting genomes. *Nat Biotechnol* 32, 347-355 (2014).
32. Haft, D.H., Selengut, J., Mongodin, E.F., Nelson, K.E. A guild of 45 CRISPR-associated (Cas) protein families and multiple CRISPR/Cas subtypes exist in prokaryotic genomes. *PLoS Comput Biol* 1, e60 (2005).
33. Makarova, K.S., Grishin, N.V., Shabalina, S.A., Wolf, Y.I., Koonin, E.V. A putative RNA-interference-based immune system in prokaryotes: computational analysis of the predicted enzymatic machinery, functional analogies with eukaryotic RNAi, and hypothetical mechanisms of action. *Biol Direct* 1, 7 (2006).
34. Mojica, F.J., Diez-Villasenor, C., Garcia-Martinez, J., Soria, E. Intervening sequences of regularly spaced prokaryotic repeats derive from foreign genetic elements. *J Mol Evol* 60, 174–182 (2005).

35. Barrangou, R., Fremaux, C., Deveau, H., Richards, M., Boyaval, P., Moineau, S., Romero, D.A., Horvath, P. CRISPR provides acquired resistance against viruses in prokaryotes. *Science* 315, 1709–1712 (2007).

36. Deltcheva, E., Chylinski, K., Sharma, C.M., Gonzales, K., Chao, Y., Pirzada, Z.A., Eckert, M.R., Vogel, J., Charpentier, E. CRISPR RNA maturation by trans-encoded small RNA and host factor RNase III. *Nature* 471, 602-607 (2011).

37. Jinek, M., Chylinski, K., Fonfara, I., Hauer, M., Doudna, J.A., Charpentier, E. A programmable dual-RNA-guided DNA endonuclease in adaptive bacterial immunity. *Science* 337, 816-821 (2012).

38. Makarova, K.S., Wolf, Y.I., Alkhnbashi, O.S., Costa, F., Shah, S.A., Saunders, S.J., Barrangou, R., Brouns, S.J., Charpentier, E., Haft, D.H., Horvath, P., Moineau, S., Mojica, F.J., Terns, R.M., Terns, M.P., White, M.F., Yakunin, A.F., Garrett, R.A., van der Oost, J., Backofen, R., Koonin, E.V. An updated evolutionary classification of CRISPR–Cas systems. *Nat Rev Microbiol* 13, 722–736 (2015).

39. Makarova, K.S., Haft, D.H., Barrangou, R., Brouns, S.J., Charpentier, E., Horvath, P., Moineau, S., Mojica, F.J., Wolf, Y.I., Yakunin, A.F., van der Oost, J., Koonin, E.V. Evolution and classification of the CRISPR-Cas systems. *Nat Rev Microbiol* 9, 467–477 (2011).

40. Shmakov, S., Abudayyeh, O.O., Makarova, K.S., Wolf, Y.I., Gootenberg, J.S., Semenova, E., Minakhin, L., Joung, J., Konermann, S., Severinov, K., Zhang, F., Koonin, E.V. Discovery and functional characterization of diverse class 2 CRISPR-Cas systems. *Mol Cell* 60, 385–397 (2015).

41. Felsenfeld, G., Rich, A. Studies on the formation of two- and three-stranded polyribonucleotides. *Biochim Biophys Acta* 26, 457-468 (1957).

42. Hoogsteen, K. The crystal and molecular structure of a hydrogen-bonded complex between 1-methylthymine and 9-methyladenine. *Acta Cryst* 16, 907–916 (1963).
43. Le Doan, T., Perrouault, L., Praseuth, D., Habhoub, N., Decout, J.L., et al. Sequence-specific recognition, photocrosslinking and cleavage of the DNA double helix by an oligo-[α]-thymidylate covalently linked to an azidoproflavine derivative. *Nucleic Acids Res* 15, 7749–7760 (1987).
44. Moser, H.E., Dervan, P.B. Sequence-specific cleavage of double helical DNA by triple helix formation. *Science* 238, 645–650 (1987).
45. Sharma, V.K., Rungtaa, P., Prasad, A.K. Nucleic acid therapeutics: basic concepts and recent developments. *RSC Adv* 4, 16618 (2014).
46. Buchini, S., Leumann, C.J. Recent improvements in antigene technology. *Curr Opin Chem Biol* 7, 717-726 (2003).
47. Ebbinghaus, S.W., Fortinberry, H., Gamper, H.B.J. Inhibition of transcription elongation in the HER-2/neu coding sequence by triplex-directed covalent modification of the template strand. *Biochemistry* 38, 619-628 (1999).
48. Carbone, G.M., McGuffie, E.M., Collier, A., Catapano, C.V. Selective inhibition of transcription of the Ets2 gene in prostate cancer cells by a triplex-forming oligonucleotide. *Nucleic Acids Res* 31, 833-843 (2003).
49. Armitage, B.A. Antigene leaps forward through an open door. *Nat Chem Biol* 1, 185-186 (2005).
50. Vasquez, K.M., Glazer, P.M. Triplex-forming oligonucleotides: principles and applications. *Q Rev Biophys* 35, 89-107 (2002).
51. Moser, H.E., Dervan, P.B. Sequence-specific cleavage of double helical DNA by triple helix formation. *Science* 238, 645-650 (1987).

52. Dagle, J.M., Weeks, D.L. Oligonucleotide-based strategies to reduce gene expression. *Differentiation* 69, 75-82 (2001).
53. Letai, A.G., Palladino, M.A., Fromm, E., Rizzo, V., Fresco, J.R. Specificity in formation of triple-stranded nucleic acid helical complexes: studies with agarose-linked polyribonucleotide affinity columns. *Biochemistry* 27, 9108-9112 (1988).
54. Beal, P.A., Dervan, P.B. Second structural motif for recognition of DNA by oligonucleotide-directed triple-helix formation. *Science* 251, 1360-1363 (1991).
55. Zamecnik, P.C., Stephenson, M.L. Inhibition of Rous sarcoma virus replication and cell transformation by a specific oligodeoxynucleotide. *Proc Natl Acad Sci USA* 75, 280–284 (1978).
56. Stephenson, M.L., Zamecnik, P.C. Inhibition of Rous sarcoma viral RNA translation by a specific oligodeoxyribonucleotide. *Proc Natl Acad Sci USA* 75: 285–288 (1978).
57. Dias, N., Stein, C.A. Antisense oligonucleotides: basic concepts and mechanisms. *Mol Cancer Ther* 1, 347-355 (2002).
58. Chan, J.H., Lim, S., Wong, W.S. Antisense oligonucleotides: from design to therapeutic application. *Clin Exp Pharmacol Physiol* 33, 533-540 (2006).
59. Kurreck, J. Antisense technologies. Improvement through novel chemical modifications. *Eur J Biochem* 270, 1628-1644 (2003).
60. Braasch, D.A., Corey, D.R. Novel antisense and peptide nucleic acid strategies for controlling gene expression. *Biochemistry* 41, 4503-4510 (2002).
61. Kole, R., Krainer, A.R., Altman, S. RNA therapeutics: beyond RNA interference and antisense oligonucleotides. *Nat Rev Drug Discov* 11, 125-140 (2012).
62. Cech, T.R., Zaug, A.J., Grabowski, P.J. In vitro splicing of the ribosomal RNA precursor of Tetrahymena: involvement of a guanosine nucleotide in the excision of the intervening sequence. *Cell* 27, 487-296 (1981).

63. Kruger, K., Grabowski, P.J., Zaug, A.J., Sands, J., Gottschling, D.E., Cech, T.R. Self-splicing RNA: autoexcision and autocyclization of the ribosomal RNA intervening sequence of Tetrahymena. *Cell* 31, 147-157 (1982).

64. Cech, T.R. Self-splicing of group I introns. *Annu Rev Biochem* 59, 543-568 (1990).

65. Abera, G., Wondie, G.B., Mogus, A.T. Ribozymes: nucleic acid enzymes with potential pharmaceutical applications - a review. *Pharmacophore* 3, 164-178 (2012).

66. Guerrier-Takada, C., Gardiner, K., Marsh, T., Pace, N., Altman, S. The RNA moiety of ribonuclease P is the catalytic subunit of the enzyme. *Cell* 35, 849-857 (1983).

67. Breaker, R.R., Joyce, G.F. A DNA enzyme that cleaves RNA. *Chem Biol* 1, 223-229 (1994).

68. Akhtar, S., Hughes, M.D., Khan, A. The delivery of antisense therapeutics. *Adv Drug Deliv Rev* 44, 3–21 (2000).

69. Haseloff, J., Gerlach, W.L. Simple RNA enzymes with new and highly specific endoribonuclease activities. *Nature* 334, 585-591 (1988).

70. Rossi, J.J. Ribozymes. *Curr Opin Biotechnol* 3, 3-7 (1992).

71. Eckstein, F., Kore, A.R., Nakamaye, K.L. In vitro selection of hammerhead ribozyme sequence variants. *Chembiochem* 2, 629-635 (2001).

72. Silverman, S.K. Catalytic DNA: scope, applications, and biochemistry of deoxyribozymes. *Trends Biochem Sci* 41, 595–609 (2016).

73. Hwang, K., Hosseinzade,h P., Lu, Y. Biochemical and biophysical understanding of metal ion selectivity of DNAzymes. *Inorganica Chim Acta* 452, 12-24 (2016).

74. Mueller, D., Stahl, U., Meyer, V. Application of hammerhead ribozymes in filamentous fungi. *J Microbiol Methods* 65, 585-595 (2006).

75. Lu, Y., Liu, J. Functional DNA nanotechnology: emerging applications of DNAzymes and aptamers. *Curr Opin Biotechnol* 17, 580-588 (2006).

76. Scott, W.G., Horan, L.H., Martick, M. The hammerhead ribozyme: structure, catalysis, and gene regulation. *Prog Mol Biol Transl Sci* 120, 1-23 (2013).
77. Murray, J.B., Seyhan, A.A., Walter, N.G., et al. The hammerhead, hairpin and VS ribozymes are catalytically proficient in monovalent cations alone. *Chem Biol* 5, 587–595 (1998).
78. Murray, J.B., Terwey, D.P., Maloney, L., et al. The structural basis of hammerhead ribozyme selfcleavage. *Cell* 92, 665–673 (1998).
79. Schubert, S., Kurreck, J. Ribozyme and deoxyribozyme-strategies for medical applications. *Curr Drug Targets* 5, 667-681 (2004).
80. Zhou, W., Ding, J., Liu, J. Theranostic DNAzymes. *Theranostics* 7, 1010-1025 (2017).
81. Burke, J.M. Hairpin ribozyme: current status and future prospects. *Biochem Soc Trans* 24, 608–615 (1996).
82. Usman, N., Beigelman, L., McSwiggen, J.A. Hammerhead ribozyme engineering. *Curr Opin Struct Biol* 1, 527–533 (1996).
83. Santoro, S.W., Joyce, G.F. A general purpose RNA-cleaving DNA enzyme. *Proc Natl Acad Sci USA* 94, 4262–4266 (1997).
84. Li, J., Zheng, W., Kwon, A.H., Lu, Y. In vitro selection and characterization of a highly efficient Zn(II)-dependent RNA-cleaving deoxyribozyme. *Nucleic Acids Res* 28, 481–488 (2000).
85. Santoro, S.W., Joyce, G.F. Mechanism and utility of an RNA-cleaving DNA enzyme. *Biochemistry* 37, 13330–13342 (1998).
86. Höbartner, C., Silverman, S.K. Recent advances in DNA catalysis. *Biopolymers* 87, 279-292 (2007).
87. Lee, R.C., Feinbaum, R.L., Ambros, V. The C. elegans heterochronic gene lin-4 encodes small RNAs with antisense complementarity to lin-14. *Cell* 75, 843–854 (1993).

88. Wightman, B., Ha, I., Ruvkun, G. Posttranscriptional regulation of the heterochronic gene lin-14 by lin-4 mediates temporal pattern formation in C. elegans. *Cell* 75, 855–862 (1993).

89. Lundin, K.E., Gissberg, O., Smith, C.I. Oligonucleotide therapies: the past and the present. *Hum Gene Ther* 26, 475-485 (2015).

90. Lee, Y., Kim, M., Han, J., Yeom, K.H., Lee, S., Baek, S.H., Kim, V.N. MicroRNA genes are transcribed by RNA polymerase II. *EMBO J* 23, 4051-4060 (2004).

91. Lee, Y., Ahn, C., Han, J., Choi, H., Kim, J., Yim, J., Lee, J., Provost, P., Rådmark, O., Kim, S., Kim, V.N. The nuclear RNase III Drosha initiates microRNA processing. *Nature* 425, 415-419 (2003).

92. Han, J., Lee, Y., Yeom, K.H., et al. The Drosha-DGCR8 complex in primary microRNA processing. *Genes Dev* 18, 3016–3027 (2004).

93. Denli, A.M., Tops, B.B.J., Plasterk, R.H.A., et al. Processing of primary microRNAs by the microprocessor complex. *Nature* 432, 231–235 (2004).

94. Lund, E., Güttinger, S., Calado, A., Dahlberg, J.E., Kutay, U. Nuclear export of microRNA precursors. *Science* 303, 95-98 (2004).

95. Yi, R., Qin, Y., Macara, I.G., Cullen, B.R. Exportin-5 mediates the nuclear export of pre-microRNAs and short hairpin RNAs. *Genes Dev* 17, 3011–3016 (2003).

96. Grishok, A., Pasquinelli, A.E., Conte, D., Li, N., Parrish, S., Ha, I., Baillie, D.L., Fire, A., Ruvkun, G., Mello, C.C. Genes and mechanisms related to RNA interference regulate expression of the small temporal RNAs that control C. elegans developmental timing. *Cell* 106, 23-34 (2001).

97. Hutvágner, G., McLachlan, J., Pasquinelli, A.E., Bálint, E., Tuschl, T., Zamore, P.D. A cellular function for the RNA-interference enzyme Dicer in the maturation of the let-7 small temporal RNA. *Science* 293, 834-838 (2001).

98. Ketting, R.F., Fischer, S.E., Bernstein, E., Sijen, T., Hannon, G.J., Plasterk, R.H. Dicer functions in RNA interference and in synthesis of small RNA involved in developmental timing in C. elegans. *Genes Dev* 15, 2654-2659 (2001).

99. Bernstein, E., Caudy, A.A., Hammond, S.M., Hannon, G.J. Role for a bidentate ribonuclease in the initiation step of RNA interference. *Nature* 409, 363-366 (2001).

100. He, L., Hannon, G.J. MicroRNAs: small RNAs with a big role in gene regulation. *Nat Rev Genet* 5, 522-531 (2004).

101. Eichhorn, S.W., Guo, H., McGeary, S.E., Rodriguez-Mias, R.A., Shin, C., et al. mRNA destabilization is the dominant effect of mammalian microRNAs by the time substantial repression ensues. *Mol Cell* 56, 104–115 (2014).

102. Lorio, M.V., Croce, C.M. MicroRNA dysregulation in cancer: diagnostics, monitoring and therapeutics. A comprehensive review. *EMBO Mol Med* 4, 143–159 (2012).

103. Beg, M.S., Brenner, A.J., Sachdev, J., Borad, M., Kang, Y.K., et al. Phase I study of MRX34, a liposomal miR-34a mimic, administered twice weekly in patients with advanced solid tumors. *Investig New Drugs* 35, 180–188 (2017).

104. van Zandwijk, N., Pavlakis, N., Kao, S.C., Linton, A., Boyer, M.J., et al. Safety and activity of microRNA loaded minicells in patients with recurrent malignant pleural mesothelioma: a first-in-man, phase 1, open-label, dose-escalation study. *Lancet Oncol* 18, 1386–1896 (2017).

105. Ling, H., Fabbri, M., Calin, G.A. MicroRNAs and other non-coding RNAs as targets for anticancer drug development. *Nat Rev Drug Discov* 12, 847-865 (2013).

106. Piva, R., Spandidos, D.A., Gambari, R. From microRNA functions to microRNA therapeutics: novel targets and novel drugs in breast cancer research and treatment (Review). *Int J Oncol* 43, 985-994 (2013).

107. Poltronieri, P., D'Urso, P.I., Mezzolla, V., D'Urso, O.F. Potential of anti-cancer therapy based on anti-miR-155 oligonucleotides in glioma and brain tumours. *Chem Biol Drug Des* 81, 79-84 (2013).

108. Lennox, K.A., Behlke, M.A. Chemical modification and design of anti-miRNA oligonucleotides. *Gene Ther* 18, 1111-1120 (2011).

109. Fire, A., Xu, S.Q., Montgomery, M.K., Kostas, S.A., Driver, S.E., Mello, C.C. Potent and specific genetic interference by double-stranded RNA in Caenorhabditis elegans. *Nature* 391, 806–811 (1998).

110. Tuschl, T., Zamore, P.D., Lehmann, R., Bartel, D.P., Sharp, P.A. Targeted mRNA degradation by double-stranded RNA in vitro. *Genes Dev* 13, 3191-3197 (1999).

111. Hamilton, A.J., Baulcombe, D.C. A species of small antisense RNA in posttranscriptional gene silencing in plants. *Science* 286, 950–952 (1999).

112. Rand, T.A., Ginalski, K., Grishin, N.V., Wang, X. Biochemical identification of Argonaute 2 as the sole protein required for RNA-induced silencing complex activity. *Proc Natl Acad Sci U S A* 101, 14385-14389 (2004).

113. Matranga, C., Tomari, Y., Shin, C., Bartel, D.P., Zamore, P.D. Passenger-strand cleavage facilitates assembly of siRNA into Ago2-containing RNAi enzyme complexes. *Cell* 123, 607-620 (2005).

114. Elbashir, S.M., Harborth, J., Lendeckel, W., Yalcin, A., Weber, K., Tuschl, T. Duplexes of 21-nucleotide RNAs mediate RNA interference in cultured mammalian cells. *Nature* 411, 494–498 (2001).

115. Bertrand, J.R., Pottier, M., Vekris, A., Opolon, P., Maksimenko, A., Malvy, C. Comparison of antisense oligonucleotides and siRNAs in cell culture and in vivo. *Biochem Biophys Res Commun* 296, 1000-1004 (2002).

116. McManus, M.T., Sharp, P.A. Gene silencing in mammals by small interfering RNAs. *Nat Rev Genet* 3, 737-747 (2002).

117. Scherr, M., Morgan, M.A., Eder, M. Gene silencing mediated by small interfering RNAs in mammalian cells. *Curr Med Chem* 10, 245-256 (2003).

118. Tomari, Y., Zamore, P.D. Perspective: machines for RNAi. *Genes Dev* 19, 517-529 (2005).

119. He, L., Hannon, G.J. MicroRNAs: small RNAs with a big role in gene regulation. *Nat Rev Genet* 5, 522-531 (2004).

120. Stark, G.R., Kerr, I.M., Williams, B.R., Silverman, R.H., Schreiber, R.D. How cells respond to interferons. *Annu Rev Biochem* 67, 227-264 (1998).

121. Elbashir, S.M., Lendeckel, W., Tuschl, T. RNA interference is mediated by 21- and 22-nucleotide RNAs. *Genes Dev* 15, 188-200 (2001).

122. Caplen, N.J., Parrish, S., Imani, F., Fire, A., Morgan, R.A. Specific inhibition of gene expression by small double-stranded RNAs in invertebrate and vertebrate systems. *Proc Natl Acad Sci U S A* 98, 9742-9747 (2001).

123. Grimm, D., Streetz, K.L., Jopling, C.L., Storm, T.A., Pandey, K., Davis, C.R., Marion, P., Salazar, F., Kay, M.A. Fatality in mice due to oversaturation of cellular microRNA/short hairpin RNA pathways. *Nature* 441, 537-541 (2006).

124. Jackson, A.L., Linsley, P.S. Noise amidst the silence: off-target effects of siRNAs? *Trends Genet* 20, 521–524 (2004).

125. Krieg, A.M., Yi, A.K., Matson, S., et al. CpG motifs in bacterial DNA trigger direct B cell activation. *Nature* 374, 546-549 (1995).

126. Klinman, D.M. CpG DNA as a vaccine adjuvant. *Expert Rev Vaccines* 2, 305-315 (2003).

127. Krieg, A.M. Therapeutic potential of Toll-like receptor 9 activation. *Nat Rev Drug Discov* 5, 471-484 (2006).

128. Lee, M., Kim, Y.J. Signaling pathways downstream of pattern recognition receptors and their cross talk. *Annu Rev Biochem* 76, 447-480 (2007).

129. Yamakawa, K., Nakano-Narusawa, Y., Hashimoto, N., Yokohira, M., Matsuda, Y. Development and clinical trials of nucleic acid medicines for pancreatic cancer treatment *Int J Mol Sci* 20, 4224 (2019).

130. Barton, G.M., Medzhitov, R. Toll-Like receptors and their ligands. *Curr Top Microbiol Immunol* 270, 81–92 (2002).

131. Jin, M.S., Lee, J.O. Structures of TLR-ligand complexes. *Curr Opin Immunol* 20, 414–419 (2008).

132. Leaman, D.W. Recent progress in oligonucleotide therapeutics: antisense to aptamers. *Expert Opin Drug Discov* 3, 997-1009 (2008).

133. Krieg, A.M. CpG still rocks! Update on an accidental drug. *Nucleic Acid Ther* 2, 77–89 (2012).

134. Shirota, H., Tross, D., Klinman, D.M. CpG oligonucleotides as cancer vaccine adjuvants. *Vaccines* 3, 390–407 (2015).

135. Zhao, Q., Temsamani, J., Iadarola, P.L., Jiang, Z., Agrawal, S. Effect of different chemically modified oligodeoxynucleotides on immune stimulation. *Biochem Pharmacol* 51, 173-182 (1996).

136. Kandimalla, E.R., Yu, D., Zhao, Q., Agrawal, S. Effect of chemical modifications of cytosine and guanine in a CpG-motif of oligonucleotides: structure-immunostimulatory activity relationships. *Bioorg Med Chem* 9, 807-813 (2001).

137. Zhao, Q., Yu, D., Agrawal, S. Immunostimulatory activity of CpG containing phosphorothioate oligodeoxynucleotide is modulated by modification of a single deoxynucleoside. *Bioorg Med Chem Lett* 10, 1051-1054 (2000).

138. Yu, D., Kandimalla, E.R., Zhao, Q., Bhagat, L., Cong, Y., Agrawal, S. Requirement of nucleobase proximal to CpG dinucleotide for immunostimulatory activity of synthetic CpG DNA. *Bioorg Med Chem* 11, 459-464 (2003).

139. Kandimalla, E.R., Bhagat, L., Yu, D., Cong, Y., Tang, J., Agrawal, S. Conjugation of ligands at the 5'-end of CpG DNA affects immunostimulatory activity. *Bioconjug Chem* 13, 966-974 (2002).

140. Kandimalla, E.R., Bhagat, L., Zhu, F.G., Yu, D., Cong, Y.P., Wang, D., Tang, J.X., Tang, J.Y., Knetter, C.F., Lien, E., Agrawal, S. A dinucleotide motif in oligonucleotides shows potent immunomodulatory activity and overrides species-specific recognition observed with CpG motif. *Proc Natl Acad Sci U S A* 100, 14303-14308 (2003).

141. Morschhäuser, J., Barker, K.S., Liu, T.T., BlaB-Warmuth. J., Homayouni, R., Rogers, P.D. The transcription factor Mrr1p controls expression of the MDR1 efflux pump and mediates multidrug resistance in Candida albicans. *PLoS Pathog* 3, e164 (2007).

142. Hecker, M., Wagner, A.H. Transcription factor decoy technology: a therapeutic update. *Biochem Pharmacol* 144, 29–34 (2017).

143. Deng, C., Zheng, J., Wan, W., Zhang, S., Ding, Z., Mao, G., Yang, S. Suppression of cell proliferation and collagen production in cultured human hypertrophic scar fibroblasts by Sp1 decoy oligodeoxynucleotide. *Mol Med Rep* 7, 785-790 (2013).

144. Yuan, H.F., Huang, H., Li, X.Y., Guo, W., Xing, W., Sun, Z.Y., Liang, H.P., Yu, J., Chen, D.F., Wang, Z.G., Hao, J., Xu, X. A dual AP-1 and SMAD decoy ODN suppresses tissue fibrosis and scarring in mice. *J Invest Dermatol* 133, 1080-1087 (2013).

145. Kaur, G., Roy, I. Therapeutic applications of aptamers. *Expert Opin Investig Drugs* 17, 43–60 (2008).

146. Wang, T., Chen, C., Larcher, L.M., Barrero, R.A., Veedu, R.N. Three decades of nucleic acid aptamer technologies: lessons learned, progress and opportunities on aptamer development. *Biotechnol Adv* 37, 28-50 (2019).

147. Tuerk, C., Gold, L. Systematic evolution of ligands by exponential enrichment: RNA ligands to bacteriophage T4 DNA polymerase. *Science* 249, 505-510 (1990).

148. Ohuchi, S. Cell-SELEX Technology. *Biores Open Access* 1, 265-272 (2012).

149. Dwivedi, H.P., Smiley, R.D., Jaykus, L.A. Selection of DNA aptamers for capture and detection of Salmonella Typhimurium using a whole-cell SELEX approach in conjunction with cell sorting. *Appl Microbiol Biotechnol* 97, 3677-3686 (2013).

150. Avci-Adali, M., Wilhelm, N., Perle, N., Stoll, H., Schlensak, C., Wendel, H.P. Absolute quantification of cell-bound DNA aptamers during SELEX. *Nucleic Acid Ther* 23, 125-130 (2013).

151. Ninomiya, K., Kaneda, K., Kawashima, S., Miyachi, Y., Ogino, C., Shimizu, N. Cell-SELEX based selection and characterization of DNA aptamer recognizing human hepatocarcinoma. *Bioorg Med Chem Lett* 23, 1797-1802 (2013).

152. Brody, E.N., Gold, L. Aptamers as therapeutic and diagnostic agents. *J Biotechnol* 74, 5-13 (2000).

153. Nimjee, S.M., White, R.R., Becker, R.C., Sullenger, B.A. Aptamers as therapeutics. *Annu Rev Pharmacol Toxicol* 57, 61–79 (2017).

154. Zhou, J., Rossi, J. Aptamers as targeted therapeutics: current potential and challenges. *Nat Rev Drug Discov* 16, 181–202 (2017).

155. Blind, M., Blank, M. Aptamer selection technology and recent advances. *Mol Ther Nucleic Acids* 4, e223 (2015).

156. James, W. Aptamers in the virologists' toolkit. *J Gen Virol* 88, 351-364 (2007).

157. Bouchard, P.R., Hutabarat, R.M., Thompson, K.M. Discovery and development of therapeutic aptamers. *Annu Rev Pharmacol Toxicol* 50: 237-257 (2010).

158. Germer, K., Leonard, M., Zhang, X. RNA aptamers and their therapeutic and diagnostic applications. *Int J Biochem Mol Biol* 4, 27–40 (2013).

159. Ruckman, J., Green, L.S., Beeson, J., et al. 2′-Fluoropyrimidine RNA-based aptamers to the 165-amino acid form of vascular endothelial growth factor (VEGF165). Inhibition of receptor binding and VEGF-induced vascular permeability through interactions requiring the exon 7-encoded domain. *J Biol Chem* 273, 20556–20567 (1998).

160. Ng, E.W., Shima, D.T., Calias, P., et al. Pegaptanib, a targeted anti-VEGF aptamer for ocular vascular disease. *Nat Rev Drug Discov* 5, 123–132 (2006).

161. Hori, S.I., Herrera, A., Rossi, J.J., Zhou, J. Current advances in aptamers for cancer diagnosis and therapy. *Cancers (Basel)* 10, 9 (2018).

162. Williams, B.A., Lin, L., Lindsay, S.M., Chaput, J.C. Evolution of a histoneH4-K16 acetyl-specificDNA aptamer. *J Am Chem Soc* 131, 6330–6331 (2009).

163. Zhang, A., Chang, D., Zhang, Z., Li, F., Li, W., et al. In vitro selection of DNA aptamers that binds geniposide. *Molecules* 22, 383 (2017).

164. Jaffrey, S.R. RNA-based fluorescent biosensors for detecting metabolites in vitro and in living cells. *Adv Pharmacol* 82, 187–203 (2018).

165. Goswami, R., Subramanian, G., Silayeva, L., Newkirk, I., Doctor, D., Chawla, K., Chattopadhyay, S., Chandra, D., Chilukuri, N., Betapudi, V. Gene Therapy Leaves a Vicious Cycle. *Front Oncol* 9, 297 (2019).

166. Zhang, C., Maruggi, G., Shan, H., Li, J. Advances in mRNA vaccines for infectious diseases. *Front Immunol* 10, 594 (2019).

167. Hecker, J.G. Non-viral, lipid-mediated DNA and mRNA gene therapy of the central nervous system (CNS): chemical-based transfection. *Methods Mol Biol* 1382, 307-324 (2016).

168. Kowalski, P.S., Rudra, A., Miao, L., Anderson, D.G. Delivering the messenger: advances in technologies for therapeutic mRNA delivery. *Mol Ther* 27, 710-728 (2019).

169. Juliano, R.L. The delivery of therapeutic oligonucleotides. *Nucleic Acids Res* 44, 6518-6548 (2016).

170. De Mesmaeker, A., Haener, R., Martin, P., Moser, H.E. Antisense oligonucleotides. *Acc Chem Res* 28, 366–374 (1995).

171. Lipi, F., Chen, S., Chakravarthy, M., Rakesh, S., Veedu, R.N. In vitro evolution of chemically-modified nucleic acid aptamers: pros and cons, and comprehensive selection strategies. *RNA Biol* 13, 1232-1245 (2016).

172. Eckstein, F. Phosphorothioates, essential components of therapeutic oligonucleotides. *Nucleic Acid Ther* 24, 374–387 (2014).

173. Monia, B.P., Lesnik, E.A., Gonzalez, C., Lima, W.F., McGee, D., Guinosso, C.J., Kawasaki, A.M., Cook, P.D., Freier, S.M. Evaluation of 2'-modified oligonucleotides containing 2'-deoxy gaps as antisense inhibitors of gene expression. *J Biol Chem* 268, 14514-14522 (1993).

174. Shen, X., Corey, D.R. Chemistry, mechanism and clinical status of antisense oligonucleotides and duplex RNAs. *Nucleic Acids Res* 46, 1584-1600 (2018).

Chapter 2

Development of chemically modified, splice modulating antisense oligonucleotides towards tackling type 2 diabetes

1. Introduction

Antisense oligonucleotides (AOs) are synthetic nucleic acid molecules that are capable of manipulating gene expression through binding to RNA targets [1-4]. Since the publication of seminal AO papers by Paterson, Zamecnik, Stephenson and co-workers in the late 1970s [5-7], the therapeutic potential of AOs has been extensively explored. To date, seven AOs and two siRNAs have been recognized by the US Food and Drug Administration (FDA) and granted approval as therapies for infectious and genetic disorders, as shown in **Table 1** [8-29]. These successful clinical translations have been inspiring researchers and pharmaceutical companies to develop AO-based therapeutics targeting different human maladies, by either knocking down the expression of disease-causing genes or rescuing/upregulating the expression of essential or defective genes.

No.	Drug	Year of approval	Type of oligonucleotide	Indication
1	Fomivirsen (Vitravene®)	1998	AO	Cytomegalovirus (CMV) retinitis
2	Mipomersen (Kynamro®)	2013	AO	Familial hypercholesterolemia (FH)
3	Eteplirsen (Exondys 51®)	2016	AO	Duchenne muscular dystrophy (DMD)
4	Nusinersen (Spinraza®)	2016	AO	Spinal muscular atrophy (SMA)
5	Inotersen (Tegsedi®)	2018	AO	Hereditary transthyretin amyloidosis (hATTR)
6	Patisaran (Onpattro®)	2018	siRNA	hATTR
7	Givosiran (Givlaari®)	2019	siRNA	Porphyria
8	Milasen	2019	AO	Batten disease
9	Golodirsen (Vyondys 53®)	2019	AO	DMD

Table 1 AOs and siRNAs approved by the US FDA for clinical applications. Milasen is a customized AO drug for one person.

AOs are single stranded nucleic acids that contain 15-30 nucleotides. AOs can be used to manipulate target gene expression through specifically binding to target RNAs by Watson-Crick base pairing [30]. Basically, there exist three distinct, potentially therapeutic AO mechanisms of action: 1) induction of RNase H-mediated degradation of messenger RNA (mRNA); 2) modulation of splicing by sterically blocking the binding of splicing factors to the precursor mRNA (pre-mRNA); 3) translational repression by either sterically blocking the 5' untranslated region (5'-UTR) in pre-mRNA to avoid 5' cap formation, or hindering the

association of translation machinery to mRNA [2, 31-35]. To date, a number of mRNA degrading AOs and splice modulating AOs have been used clinically.

RNase H recruitment to form an AO:mRNA duplex and the subsequent hydrolysis of mRNA is the most widely utilized mechanism for potent downregulation of target gene expression. To date, three AOs evoking this mechanism have reached the market: fomivirsen (Vitravene^{TM}), mipomersen (Kynamro^{TM}), and inotersen (Tegsedi^{TM}). Their specific mechanisms are described below:

1) Fomivirsen binds to and degrade the mRNAs encoding cytomegalovirus (CMV) immediate-early-2 protein (required for viral replication), thus providing therapeutic effects for CMV retinitis by inhibition of virus proliferation [8, 9].

2) Mipomersen binds to and degrade the mRNAs encoding apolipoprotein B (ApoB, a component of low-density lipoprotein cholesterol, LDL-C), thus providing therapeutic effects for familial hypercholesterolemia through reducing atherogenic LDL-C production [10, 11].

3) Inotersen binds to and degrade the mRNAs encoding transthyretin (TTR), thus providing therapeutic effects for hereditary TTR amyloidosis via knocking down the expression of mutant TTR that causes amyloid aggregates to deposit in organs [24, 25].

Splice modulation is mainly applied to remove or prevent premature termination codons (PTCs), caused by loss-of-function mutations, through exon skipping or exon inclusion, in an attempt to restore the open reading frame (ORF) and rescue or increase the production of functional essential proteins [32]. Alternatively, AO mediated exon skipping can also be used to induce a frameshift and elicit PTCs that lead to knockdown of target gene expression [36].

Four splice modulating AOs have been approved by FDA for the treatment of genetic diseases: eteplirsen (Exondys 51^{TM}), golodirsen (Vyondys 53^{TM}), nusinersen (Spinraza^{TM}), and milasen. Their specific mechanisms are described below:

1) Eteplirsen and golodirsen lead to skipping of exon 51 and 53, respectively, in the dystrophin mRNA and overcome PTCs resulting from frameshifting deletions, thus restoring the dystrophin ORF and allowing synthesis of truncated but partially functional dystrophin proteins that benefit patients with Duchenne muscular dystrophy (DMD) [12-15, 29].

2) Nusinersen retains exon 7 in the mRNA of survival of motor neuron 2 (SMN2) preventing loss of function resulting from natural skipping of exon 7, and increasing the production of full length, functional SMN protein that has shown clinical benefit in patients with spinal muscular atrophy (SMA) [16-23].

3) Milasen skips a transposon-activated cryptic exon located between exon 6 and 7 in major facilitator superfamily domain containing 8 (MFSD8) mRNA, thereby evading the PTC in the cryptic exon, and rescuing functional MFSD8 synthesis, providing a molecular therapy for ceroid lipofuscinosis type 7 (CLN7) related Batten disease [26-28].

AOs that induce RNase H mediated target mRNA degradation have been extensively utilized in the characterization of genes involved in type 2 diabetes (T2D) pathogenesis and the subsequent development of AO therapeutics, whereas so far none of the published reports has shown application of splice modulating AOs to T2D therapy. We developed novel, chemically modified, splice modulating AOs as potential therapeutics to treat T2D through knocking down the expression of protein tyrosine phosphatase-1B (PTP1B, encoded by *PTPN1*), a negative regulator of the insulin signal transduction pathway that largely contributes to the development of T2D, by skipping an exon to induce a frameshift that leads to PTCs.

Section 2 of this chapter provides an overview of T2D and its current treatment options. This is then followed by a review of AOs developed to suppress causative genes in T2D (section

3). The latter part (section 4) of this chapter describes my study on novel designs of chemically-modified, splice modulating AOs targeting *PTP1B* to treat T2D.

2. Type 2 Diabetes

2.1 Overview

Type 2 diabetes (T2D) is a chronic metabolic disorder characterized by persistent hyperglycemia as a result of insulin dysregulation, namely, inefficient signaling of insulin (usually referred to as insulin resistance or insulin insensitivity) in glucose recipient organs and tissues (muscle, adipose, liver, and brain) and insufficient production of insulin from pancreatic β cells [37-40]. Obesity is closely associated with the initiation of insulin resistance and T2D [41]. The level of circulating free fatty acid (FFA) is elevated in obese individuals and leads to excess uptake by muscle and liver cells, resulting in sequential activation of protein kinase C (PKC), IκB-kinase (IκK), and nuclear factor κB (NFκB) that stimulates the release of inflammatory chemokines, such as tumor necrosis factor-α (TNFα) and interleukin 6 (IL6), which further stimulate Jun N-terminal kinase-1 (JNK1) and suppressor of cytokine signaling-3 (SOCS3), respectively (**Figure 2.1**) [42-44]. Collectively, JNK1 and SOCS3 downregulate the proteins participating in the insulin signal transduction pathway, including insulin receptor substrate (IRS), phosphatidylinositol 3-kinase (PI3K), and protein kinase B (Akt), thus preventing the translocation of glucose transporter type 4 (GLUT4) from the cytoplasm to cell membrane that eventually inhibits the cellular uptake of glucose, leading to hyperglycemia (**Figure 2.1**) [38, 44]. On the other hand, FFAs enter the mitochondria, participate in the tricarboxylic acid (TCA) cycle, resulting in the generation of reactive oxygen species (ROS) that also triggers JNK1 (**Figure 2.1**) [45]. Furthermore, in chronic state of hyperglycemia, glucose also interacts with proteins through non-enzymatic glycation and oxidation processes, leading to the formation of advanced glycation end

products (AGEs) that in turn aggravate insulin resistance through triggering ROS generation and NFκB (**Figure 2.1**) [46]. Besides, glucotoxicity, lipotoxicity, and inflammation caused by hyperglycemia and high FFA concentration impair the pancreatic β cells and finally exhaust their capability to secrete insulin, as a result of cellular dysfunction and apoptosis [47-50].

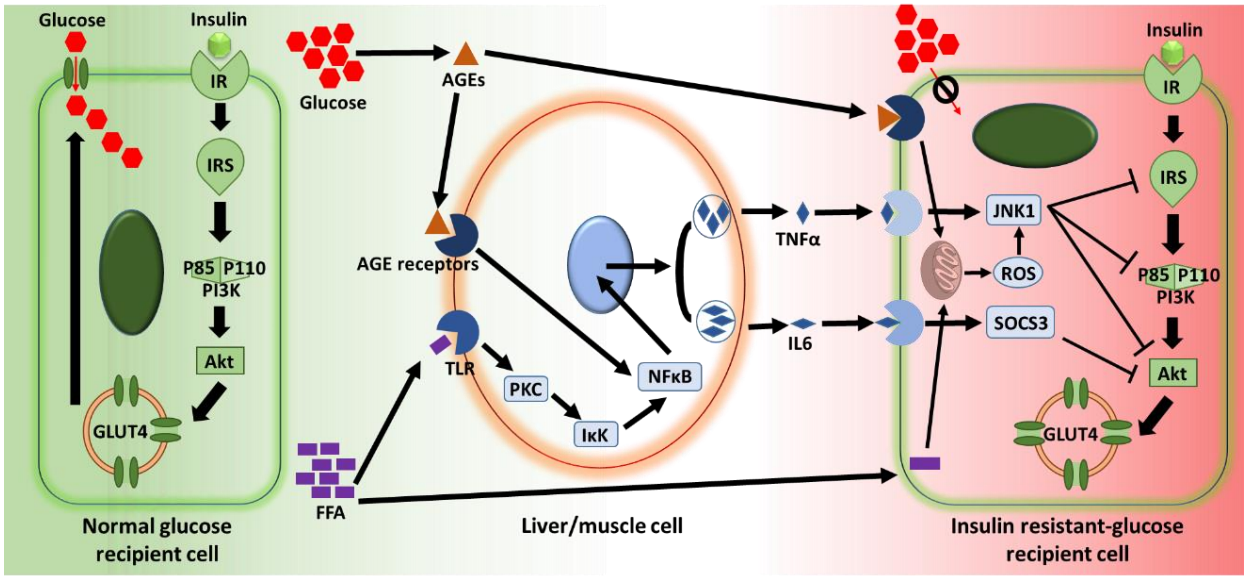

Figure 2.1 Mechanism of insulin resistance. IR: insulin receptor, IRS: insulin receptor substrate, PI3K: phosphatidylinositol 3-kinase, Akt: protein kinase B, GLUT4: glucose transporter type 4, FFA: free fatty acid, AGE: advanced glycation end product, PKC: protein kinase C, IκK: IκB-kinase, NFκB: nuclear factor κB, TNFα: tumor necrosis factor-α, IL6: interleukin 6, JNK1: Jun N-terminal kinase-1, ROS: reactive oxygen species, SOCS3: suppressor of cytokine signaling-3, glucose recipient cell represents cells from glucose recipient organs/tissues including muscle, fat, liver, and brain.

2.2 Current treatments

Currently prescribed small molecule-based antidiabetic drugs mainly aim at reducing blood glucose level by targeting key glycometabolic organs including the small intestine, pancreas, muscle, liver, fat, and kidney [51]. So far, several classes of oral hypoglycemic drugs have been used such as glitazones, meglitinides, biguanides, sulfonylureas, α-glucosidase inhibitors, sodium glucose cotransporter-2 (SGLT2) inhibitors, dipeptidyl peptidase-4 (DPP4) inhibitors, and glucagon-like peptide-1 (GLP1) receptor agonists [45-47]. However, these agents do not halt the progression of T2D due to two reasons: first, few of the agents target the underlying root cause of the disease: insulin resistance; second, as small molecule drugs,

they do not interfere with the transcription or translation processes of the disease causing genes, thus show lack of efficacy compared to RNA-targeting nucleic acid interventions, for example, AO and small interfering RNA (siRNA). In addition, oral hypoglycemic drugs induce adverse reactions, affecting patient compliance. Recently, Kokil et al. comprehensively reviewed the mechanisms and limitations of conventional hypoglycemic agents and elaborated the potential of siRNA as a novel therapy for T2D [38]. The following section outlines another option of RNA therapeutics: AO interventions to modify expression of genes implicated in the T2D pathogenesis.

3. AO-based intervention targeting T2D

3.1 Overview

Compared to the steric blocking AOs that either modulate splicing or repress translation, gapmer-like AOs that knock down gene expression via RNase H mechanisms are predominantly utilized in the modification of target gene expression involved in T2D pathogenesis and the development of AO-based therapeutics. In this section, we focus on chemically modified AOs that impede production of proteins involved in insulin resistance and hyperglycemia. These include: protein tyrosine phosphatase-1B (PTP1B, encoded by *PTPN1*), glucagon receptor (GCGR, encoded by *GCGR*), SGLT2 (encoded by *SLC5A2*), glucocorticoid receptor (GCCR, encoded by *NR3C1*), acetyl-CoA carboxylase 1 or 2 (ACC1 or ACC2, encoded by *ACACA* or *ACACB*), diacylglycerol acyltransferase-2 (DGAT2, encoded by *DGAT2*), mitochondrial phosphoenolpyruvate carboxykinase (PEPCK-M, encoded by *PCK2*), protein kinase C-ε (PKCε, encoded by *PRKCE*), glucose 6-phosphate transporter-1 (G6PT1, encoded by *SLC37A4*), cAMP response element binding protein (CREB, encoded by *CREB*), CREB-regulated transcription coactivator-2 (CRTC2, encoded by *CRTC2*), forkhead box O1 (FOXO1, encoded by *FOXO1*), density-enhanced phosphatase-

1 (DEP1, encoded by *PTPRJ*), retinol binding protein 4 (RBP4, encoded by *RBP4*), TTR (encoded by *TTR*), tribbles homolog 3 (TRIB3, encoded by *TRIB3*), IκB-kinase β (IκKβ, encoded by *IKBKB*), and toll-like receptor 2 (TLR2, encoded by *TLR2*).

3.2 AO interventions to treat T2D

3.2.1 Protein tyrosine phosphatase-1B (PTP1B)

PTP1B negatively regulates insulin signaling by dephosphorylating the upstream proteins in the insulin signal transduction pathway, including IR and IRS [52, 53]. The AO ISIS 113715, developed by Ionis Pharmaceuticals, is a 5-10-5 2'-O-methoxyethyl (2'-OMOE) gapmer AO on a phosphorothioate (PS) backbone that downregulates the expression of PTP1B protein [54]. ISIS 113715 is utilized in the characterization of PTP1B function, since the therapeutic potential of this AO for T2D has been investigated.

Zinker et al. reported that intraperitoneal injection (IPI) of ISIS 113715 into *ob/ob* and *db/db* mice resulted in significant reduction of PTP1B expression in both liver (*ob/ob* mice treated by 25mg/kg for 6 weeks: -50%; *db/db* mice treated by 50mg/kg for 4 weeks: -50%) and fat (*ob/ob* mice treated by 25mg/kg for 6 weeks: -60%), with reduced hyperinsulinemia (*ob/ob* mice treated by 25mg/kg for 6 weeks: -77%) and increased expression of proteins involved in the insulin signaling pathway, including IRS2, PI3K p50α and p55α isoforms [54]. On the other hand, the expression of p85α was decreased [54]. It is noteworthy that increased expression of p50α and p55α isoforms instead of p85α was reported to improve insulin sensitivity [55]. Besides, AO treatment also led to reduced expression of enzymes related to gluconeogenesis such as phosphoenolpyruvate carboxykinase (PEPCK) and fructose-1,6-bisphosphatase (FBP) [54]. Collectively, changes in protein expression levels as a result of ISIS 113715 treatment correlated with increased Akt phosphorylation in liver, improved insulin sensitivity, and normalization of hyperglycemia as plasma glucose, postprandial glucose excursion, and hemoglobin A1C (HbA_{1C}) were corrected to normal levels [54].

Rondinone et al. provided more evidence on the differential expression of PI3K isoforms induced by PTP1B reduction [56]. *Ob/ob* mice dosed with 50mg/kg ISIS 113715 for 3 weeks exhibited downregulation of p85α isoform and upregulation of p50α and p55α isoforms in both liver and fat [56]. Mouse hepatocytes treated with an AO targeting p85α (ISIS 131410) exhibited reduction in p85α expression and increased production of p50α and p55α that correlated with enhanced Akt phosphorylation, indicating an increase in insulin sensitivity [56].

Apart from modulating the expression levels of proteins involved in the insulin signaling pathway, Clampit et al. found that PTP1B reduction directly leads to improved insulin sensitivity by modulating key signal transduction events: tyrosine phosphorylation of those proteins [57]. In that *in vitro* study, up to 70% decrease of PTP1B expression in FAO rat hepatoma cells was achieved by transfecting the cells with ISIS 113715 at a very high level (20 μM) through electroporation. Subsequent insulin stimulation resulted in elevated tyrosine phosphorylation of IR, IRS, Akt and glycogen synthase kinase 3 (GSK3, substrate of Akt), indicating an ameliorated insulin signaling efficiency [57].

A report from Gum et al. illustrated that the reduction of PTP1B is sufficient to improve insulin sensitivity, at least in an animal model [58]. In their study, *ob/ob* mice were treated with ISIS 113715 at a dosage of 25 mg/kg for 6 weeks leading to 60% decrease of PTP1B protein in liver. Subsequent insulin stimulation resulted in elevated tyrosine phosphorylation of IR, IRS1, IRS2, PI3K, Akt, and GSK3 by three, four, three, three, seven, and more than two fold, respectively. Although the PTP1B level was not reduced in muscle, increased Akt phosphorylation was observed, demonstrating that insulin resistance is ameliorated by PTP1B targeting AO treatment in vital peripheral tissues [58].

Rondinone et al. demonstrated that PTP1B plays an important role in lipogenesis, fat storage, and the development of obesity [59], and thus contributes to insulin resistance and T2D. In their study, administration of ISIS 113715 into *ob/ob* mice at a dosage of 25 mg/kg for 6 weeks decreased the level of a number of proteins involved in lipogenesis, such as sterol regulatory element-binding protein 1 (SREBP1), fatty acid synthase (FAS), and spot14. Reduction of these proteins correlated with significant decrease of fat depot (-42%) and triglyceride content (-25%) in adipocytes compared to control group (saline treatment) [59]. In addition, AO treatment increased IRS2 and PI3K p50α isoforms, and also decreased p85α in fat [59], suggesting that insulin signal transduction was improved. Similarly, Waring et al. also studied the effect of PTP1B reduction on the expression of lipogenesis related genes by treating *ob/ob* mice with ISIS 113715 for 6 weeks [60]. They found that PTP1B reduction not only led to downregulation of lipogenetic genes in fat, but also in liver [60]. In addition, the expression of genes involved in adipocyte differentiation such as malic enzyme, adipsin, and retinol-binding protein were also downregulated as a result of PTP1B inhibition [60]. These findings provide further evidence that PTP1B plays an important role in enlargement of fat storage and the development of obesity.

Swarbrick et al. reported that the improvements of hyperglycemia and hyperinsulinemia resulting from PTP1B reduction correlated to the increase of adiponectin [61], a fat-derived hormone that strengthens insulin signaling mainly by activating IRS [62]. In a non-human primate study conducted by this group, obese, insulin-resistant rhesus monkeys were treated by ISIS 113715 with a dosage of 20 mg/kg for 4 weeks. Fasting concentrations of plasma glucose and insulin were reduced, insulin sensitivity was increased, and the monkeys receiving 4 weeks of treatment exhibited marked increase of adiponectin concentration by 70%, which was in proportion to the amelioration of insulin sensitivity [61].

Gum et al. discovered that ameliorated hyperglycemia and hyperinsulinemia resulting from PTP1B reduction correlates with inhibition of p38 mitogen-activated protein kinase (p38 MAPK) phosphorylation and the subsequent inhibition of its substrates: TNFα and CREB [63]. TNFα is associated with insulin resistance [43, 64, 65], and CREB contributes to hyperglycemia by promoting gluconeogenesis through induction of PEPCK transcription [66, 67]. In this study, *ob/ob* mice treated by 25 mg/kg of ISIS 113715 for 6 weeks led to significantly decreased phosphorylation of p38 MAPK and CREB by 70% and 80%, respectively in contrast to the mice treated with saline. ISIS 113715 treated mice also showed ~37% of reduction in TNFα expression [63].

In an attempt to optimize the efficacy of ISIS 113715, Koizumi et al. synthesized a 5-10-5 ENA gapmer named ENA-1 (chemical structure of ENA is shown in **Figure 3.1** of Chapter 1) with the identical nucleobase sequence to ISIS 113715 and compared the antidiabetic effect of these two AOs [68]. Their results showed that PTP1B expression in *db/db* mice was reduced more effectively when treated with ENA-1 than ISIS 113715 at a dosage of 60 mg/kg, either through subcutaneous injection (SCI) or IPI (they tried 45 mg/kg IPI at first but the difference of activity between two AOs was not apparent, so they shifted to 60 mg/kg for better comparison). Further, plasma glucose was decreased to a larger extent in ENA-1 treated mice compared to those treated by ISIS 113715 [68]. In addition, the melting temperature (T_m) of ENA-1 (77°C) was higher than ISIS 113715 (62.5°C), indicating that ENA-1 possesses higher binding affinity than ISIS 113715. The distribution of ENA-1 in both liver and fat, 72h after administration was also found to be at least twofold higher than that of ISIS 113715, which was probably due to the higher nuclease stability of ENA compared to the 2'-OMOE chemistry. Altogether, these results suggest that ENA modification may be a better option than 2'-OMOE in constructing gapmer AOs targeting PTP1B [68].

As the therapeutic effect of PTP1B reduction on obesity associated T2D has been widely explored, Pandey et al. investigated the role of low molecular weight PTP (LMW-PTP) in T2D through downregulating LMW-PTP expression by a specific AO, ISIS 288267 in diet-induced obese (DIO) mice and *ob/ob* mice [69]. AO induced LMW-PTP reduction led to increased phosphorylation of IR, PI3K, and Akt in mice treated with 25 mg/kg of ISIS 288267 for 4 weeks (twice a week). In addition, ~42% and 20% decreases of fed plasma insulin and glucose in DIO mice, and ~47% and 42% decreases of fasted plasma insulin and glucose in *ob/ob* mice were observed respectively, indicating an increased insulin sensitivity resulting from LMW-PTP reduction [69]. This research demonstrated that LMW-PTP plays a similar role to PTP1B in terms of insulin resistance and thus it is a potential target for T2D therapy.

3.2.2 Glucagon receptor (GCGR)

Glucagon is a hormone produced by pancreatic α cells that stimulates glucose production through two pathways: glycogenolysis mediated by cAMP-related signaling and gluconeogenesis through activation of multiple enzymes [70, 71]. Excess glucagon leads to hyperglycemia [72]. Liang et al. developed a 5-10-5 2'-OMOE-PS gapmer AO (ISIS 148359) that reduces the expression of glucagon receptor, GCGR in an attempt to block glucagon signal transduction and thus ameliorate hyperglycemia and T2D [73]. In this study, *db/db* mice treated with 25 mg/kg of ISIS 148359 through IPI for 3 weeks (twice a week) resulted in decreased GCGR expression and hepatic cAMP production stimulated by glucagon. This correlated with significant decreases of serum glucose (-24%), triglyceride (-62%), and FFA (-36%) [73]. Hypoglycemia was not identified in the mice receiving AO treatment, in support of the concept that GCGR could be a therapeutic target in controlling hyperglycemia caused by T2D [73].

In order to further characterize the mechanisms underlying amelioration of T2D mediated by GCGR reduction, Sloop et al. treated rodent models with GCGR-targeting AOs (ISIS 148359 and ISIS 180475), leading to decreased production of enzymes related to gluconeogenesis and glycogenolysis, normalized plasma glucose, increased GLP1 production (GLP1 promotes insulin secretion in a glucose-dependent manner [74]), and preserved insulin secretion [75]. Zucker diabetic fatty (*ZDF*) rats treated with 25 mg/kg ISIS 180475 for 4.5 weeks (SCI twice a week) exhibited reduced gluconeogenetic or glycogenetic enzyme levels, such as glucose-6-phosphatase catalytic subunit (G6P [cat]), PEPCK cytosolic isoform (PEPCK-C), and glycogen phosphorylase (GP) reduction by about 65%, 78%, and 45% respectively, decreased plasma glucose by ~66% compared to the saline control group. The amount of islet GLP1 and insulin in *db/db* mice treated by ISIS 180475 was 3.5 and 2 fold higher than in the saline-treated control group, respectively [75]. This study demonstrated that attenuation of glucagon action resulting from GCGR reduction improves hyperglycemia through decreasing glucose production and ameliorating pancreatic β cell function.

3.2.3 Sodium glucose cotransporter-2 (SGLT2)

SGLT2 plays a vital role in renal glucose reabsorption. SGLT2 inhibition increases urinary glucose excretion, decreases blood glucose levels, and thus presents a therapeutic option for hyperglycemia and T2D [76]. Zanardi et al. treated mice and cynomolgus monkeys with a SGLT2 targeting, short 2-8-2 2'-OMOE-PS gapmer AO (ISIS 388626) at various SCI doses (1, 3, 10, 30 mg/kg/week), and achieved decreased renal SGLT2 mRNA production, in a dose dependent manner, after 13 weeks of treatment (mice: 18%, 5%, 4%, 2%, monkey: 64%, 53%, 31%, 10%) compared to the saline controls [77]. Reduction of SGLT2 expression correlated with increased urine glucose elimination, although dose-dependent basophilic granule accumulation was identified in renal tubular epithelial cells due to AO accumulation but no functional kidney changes were observed [77]. These results indicated that ISIS

388626 may be an effective SGLT2 inhibitor with a satisfactory safety profile, and further investigation in clinical trials was recommended [77].

3.2.4 Glucocorticoid receptor (GCCR)

Glucocorticoids are steroid hormones that promote hepatic gluconeogenesis and antagonize the insulin response in skeletal muscle and white adipose tissue, thereby excess glucocorticoids contribute to hyperglycemia [78]. Inhibition of the action of glucocorticoid receptor (GCCR) could be a therapeutic approach for T2D. Watts et al. treated different rodents (*ob/ob* mice, *db/db* mice, *ZDF* rats, and high-fat diet-fed rats) with optimized GCCR targeting 2'-OMOE-PS gapmer AOs for 4 weeks (up to 25 mg/kg, SCI) resulting in significant decreases of GCCR expression in both liver and fat that were accompanied by ~30%, 40%, 40%, 70% decreases in fasted glucose levels in *ob/ob* mice, *db/db* mice, *ZDF* rats, and high-fat diet-fed rats respectively [79]. Furthermore, a 60% decrease in insulin levels and 35% decrease of TNFα was observed in *ob/ob* mice, and reduction of plasma triglycerides was observed in both *db/db* mice and *ZDF* rats [79]. This research indicated that glucocorticoid antagonism through AO mediated GCCR inhibition is a promising antidiabetic approach. At the same time, Liang et al, provided similar evidence that GCCR inhibition leads to alleviation of hyperglycemia in *ob/ob* and *db/db* mice through IPI administration of a mouse specific, GCCR targeting, 5-10-5 2'-OMOE-PS gapmer AO (ISIS 180272) at a dosage of 25 mg/kg for three weeks [80]. AO treatment lowered plasma glucose levels by 45% and 23% in *ob/ob* and *db/db* mice, respectively, and marked reduction in the activity of gluconeogenetic proteins such as PEPCK and G6P was identified [80].

3.2.5 Acetyl-CoA carboxylase (ACC)

Nonalcoholic fatty liver disease (NAFLD) caused by hepatic triglyceride accumulation is responsible for insulin resistance and elevated glucose production that are key elements of T2D [81-83]. Therefore, reducing lipid accumulation in liver could be a promising strategy

for T2D therapy. ACC catalyzes the synthesis of malonyl-CoA, a regulator of both synthesis and oxidation of fatty acid [84-87]. ACC has two isoforms: ACC1 and ACC2 [88]. In order to explore the impact of downregulating ACC1, ACC2, and both ACC1/2 on lipid levels and insulin sensitivity in liver, Savage et al. developed three 5-10-5 2'-OMOE-PS gapmer AOs targeting ACC1 (ISIS 338292), ACC2 (ISIS 189594), and both ACC1/2 (ISIS 362037), and treated rats with NAFLD with these AOs for ACC suppression [89]. Knockdown of either ACC1 or ACC2 with AOs promoted hepatic fat oxidation, while suppression of both ACC1/2 with ISIS 362037 increased fat oxidation to a significantly higher degree [89]. Interestingly, ACC1 reduction also resulted in inhibition of lipogenesis. Furthermore, ACC1/2 suppression by ISIS 362037 lowered the level of hepatic lipids such as diacylglycerol and triglycerides, and increased insulin sensitivity [89]. These results support ACC modulation as a novel approach to the treatment of insulin resistance and T2D.

3.2.6 Diacylglycerol acyltransferase-2 (DGAT2)

DGAT2 is an enzyme that participates in the synthesis of triglyceride [90]. In an attempt to investigate the role of DGAT2 in lipid metabolism, Yu et al. treated both DIO mice and *ob/ob* mice with an DGAT2 specific, 5-10-5 2'-OMOE-PS gapmer AO (ISIS 217376) at a dose of 25 mg/kg through SCI. ISIS 217376 treatment decreased DGAT2 mRNA levels by more than 75% in liver and fat, this was accompanied by decreased triglyceride synthesis and increased fatty acid oxidation in mouse hepatocytes, and a marked reduction of triglyceride (-37%), FFA (-50%), and diacylglycerol (-74%) in liver compared to mice treated by control AO [90]. Reduction in mRNA levels encoded by lipogenic genes, for example, ACC1, ACC2, and FAS were also observed [90], indicating that DGAT2 reduction negatively regulates lipogenesis in liver, thereby ameliorating hyperlipidemia and steatosis.

Later, Choi et al. studied the antidiabetic effect of DGAT2 reduction by administering another DGAT2 targeting gapmer AO, ISIS 369235 (50 mg/kg, IPI) to rats with diet-induced

NAFLD [91]. Similar to the report from Yu et al, AO treatment led to significant reduction in hepatic diacylglycerol, triglyceride, and decreased expression of lipogenic genes. In addition, increased expression of genes related to lipid oxidation was also identified [91]. Importantly, changes of gene expression and lipid content level were accompanied with increased activity of PI3K, Akt, and decreased hepatic glucose production, indicating a significantly improved insulin sensitivity [91]. Therefore, AO induced DGAT2 knockdown could be an antidiabetic strategy as it alleviates insulin resistance through lowering hepatic lipid content.

3.2.7 Mitochondrial phosphoenolpyruvate carboxykinase (PEPCK-M)

Gluconeogenesis generates glucose from non-carbohydrate carbon substrates such as pyruvate, lactate, alanine, glutamine, and glycerol. Conversion of oxaloacetate to phosphoenolpyruvate (PEP) is required for gluconeogenesis from pyruvate, which is catalyzed by PEPCK [92]. Generally, this reaction is attributed to the PEPCK-C [93]. Stark et al. hypothesized that PEPCK-M also contributes importantly to gluconeogenesis [94]. In this research, they silenced the expression of PEPCK-M in rats by administration of a PEPCK-M specific, 5-10-5 2'-OMOE-PS gapmer AO (ISIS 421062) through IPI at a dosage of 25 mg/kg (twice weekly) for 4 weeks [94]. As a result, lowered plasma glucose, insulin, triglycerides, and reduced white adipose tissue were observed. No hypoglycemia was identified and was accompanied with a switch of gluconeogenic substrate preference to glycerol, bypassing the PEPCK reaction [94]. Besides, normal mitochondrial function was maintained in PEPCK-M-deficient hepatocytes compared to PEPCK-C knockout that led to mitochondrial deficiency. This research pointed out the significance of the role of PEPCK-M in rodent gluconeogenesis, and suggests that perhaps PEPCK-M, instead of PEPCK-C could be a therapeutic target for T2D in humans [94], however, target verification is definitely required in future experiments.

3.2.8 Protein kinase C-ε (PKCε)

In order to investigate the role of PKCε in linking fat accumulation and insulin resistance in liver, Samuel et al. treated rats with high-fat diet induced hepatic insulin resistance by a PKCε specific, 5-10-5 2'-OMOE-PS gapmer AO (ISIS 232697) with a IPI dosage of 75 mg/kg per week for 4 weeks [95]. It was found that PKCε, rather than other isoforms of PKC was activated in insulin resistant rats and PKCε knockdown by ISIS 232697 increased the hepatic insulin sensitivity [95]. The AO treatment led to markedly raised IRS2 tyrosine phosphorylation (~300% above basal) that was accompanied by ~350% increase of Akt2 activity when compared to the saline control. Significantly elevated Akt2 activity was also identified in adipose tissue in AO treated rats (221%) compared to saline control (32%). Furthermore, it was found that PKCε impairs IR kinase activity both *in vivo* and *in vitro* [95]. Altogether, this research reveals the critical role of PKCε in fat-induced insulin resistance, therefore, PKCε inhibition could be a therapeutic strategy for NAFLD and T2D.

3.2.9 Glucose 6-phosphate transporter-1 (G6PT1)

Glucose 6-phosphate hydrolization and the subsequent glucose formation is catalyzed by G6P as the final step of gluconeogenesis, therefore G6P plays a pivotal role in glucose homeostasis [96]. Sloop et al. hypothesized that inhibition of G6P transporter-1 (G6PT1) may provide a therapeutic effect on hyperglycemia and T2D. They treated *ob/ob* mice with a G6PT1 targeting, 5-10-5 2'-OMOE-PS gapmer AO (ISIS 149008) with a SCI dosage of 25 mg/kg (twice a week) for 6 weeks [97]. The hepatic G6PT1 mRNA was decreased by 85% and the activity of G6P transport was reduced by 75%, compared to the control group. Inhibition of G6PT1 was correlated with blunted hepatic glucose production, reduced plasma glucose level, and improved hyperglycemia in mice [97]. In addition, hypoglycemia and other adverse metabolic effects were not identified [97]. According to these findings, AO induced G6PT1 inhibition could lead to effective glucose control in T2D, without adverse effects on metabolism.

3.2.10 cAMP response element binding protein (CREB)

CREB promotes glucose production by directly activating the transcription of key gluconeogenic genes such as PEPCK, G6P, and FBP due to the presence of a cAMP response element (CRE) at the promotor of these genes [98]. Erion et al. hypothesized that reduction of CREB expression could improve hyperglycemia resulting from insulin resistance [99]. In this study, rats with high fat diet (HFD) induced insulin resistance were treated by a CREB specific, 2'-OMOE-PS gapmer AO that improved insulin sensitivity. This was seen in a series of changes: 43%, 55%, and 54% reductions in the mRNA expression of the gluconeogenic proteins, PEPCK-C, PEPCK-M, and PGC1α, respectively; suppression of glucose production in liver by 45%; fasting plasma insulin level was reduced by 66%; hepatic and plasma triglycerides were decreased by 57% and 24% respectively; and diacylglycerols in liver were lowered, accompanied by reduced PKCε membrane translocation [99]. This study demonstrates that AO induced CREB reduction prevents hepatic steatosis and insulin resistance, and therefore CREB is an attractive therapeutic target for T2D.

3.2.11 CREB-regulated transcription coactivator-2 (CRTC2)

CRTC2 is a coactivator of CREB that regulates transcription of gluconeogenic genes by enhancing binding of CREB to the target CRE within the specified cAMP responsive genes [100, 101]. Erion et al. investigated the effect of CRTC2 reduction on the control of glucose homeostasis by treating rats with T2D with a CRTC2 targeting, 5-10-5 2'-OMOE-PS gapmer AO (ISIS 384680) at an IPI dose of 37.5 mg/kg (twice a week) for 4 weeks [102]. Surprisingly, little change in glucose synthesis was identified in the rats treated by AO alone, and it was accompanied by elevated glucagon levels and an 80% reduction in glucagon clearance. However, this phenomenon was prevented when the rats received somatostatin or glucagon-neutralizing antibody, together with the AO. The combined treatments led to significantly decreased glucose production [102]. In addition, AO induced CRTC2 reduction also resulted in decreased expression of enzymes participating in the conversion of amino

acids to gluconeogenic intermediates (pyruvate and oxaloacetate), such as pyruvate carboxylase, glutamic-oxaloacetictransaminase 1 (GOT1), and serine dehydratase [102]. This research suggests that CRTC2 reduction could lead to improved hyperglycemia if combined with glucagon inhibition.

Dullea et al. presented a chemically modified AO development process using CRTC2 as a model [103]. They designed and synthesized around 400 CRTC2 specific, 3-8-3 LNA-PS gapmers and performed a three-step screening process: first, transfection of AOs into both human (Hep3B) and mouse (Hepa1-6) cell lines was conducted to select candidates inducing efficient CRTC2 mRNA knockdown; second, 41 AO "finalists" were then evaluated *in vivo* in mice to determine both hepatic CRTC2 mRNA reduction and safety profile; third, the "champion" and "runner-up" AOs were examined in DIO mice and human primary hepatocytes for subchronic efficacy studies [103]. This research confirmed the beneficial effect of CRTC2 knockdown towards ameliorating glucose control and provides an example of development of target-specific gapmer AO through a step-by-step selection process.

3.2.12 Forkhead box O1 (FOXO1)

Fasting hyperglycemia is mainly due to raised gluconeogenesis. FOXO1 is a primary transcription factor involved in gluconeogenesis that promotes the expression of PEPCK and G6P [104, 105]. Reduction of FOXO1 in nucleus decreases the production of PEPCK and G6P thereby attenuates gluconeogenesis [106]. Samuel et al. proved that AO induced FOXO1 reduction improves glucose control [107]. In that study, a FOXO1 specific, 5-10-5 2'-OMOE-PS gapmer (ISIS 188764) was utilized to transfect mouse primary hepatocytes with an AO concentration of 100nM, and DIO mice was administered with this AO at a dose of 50 mg/kg/week for 4 weeks [107]. Markedly decreased PEPCK (-48%) and G6P (-64%) in hepatocytes were observed, compared to the untreated group. In DIO mice, AO treatment led to significant reduction of fed plasma glucose level (-34%) and insulin concentration (-87%),

indicating an improved insulin action. In addition, ameliorated insulin resistance was also identified in both liver and fat that correlated with decreased hepatic triglyceride and diacylglycerol content, and suppression of lipolysis in adipocytes [107]. This research suggests that AO induced FOXO1 reduction could be a potential therapy for insulin resistance and T2D.

3.2.13 Density-enhanced phosphatase-1 (DEP1)

The activity of IR kinase determined by phosphorylation status is regulated by protein-tyrosine-phosphatases (PTPs), including PTP1B [108]. PTP1B also directly deactivates IR other than IR kinase by dephosphorylating its tyrosine residues [109, 110]. Comparable to PTP1B, DEP1, as a phosphatase may interfere with insulin signaling through also dephosphorylating IR. In order to examine the role of DEP1 in the insulin signal transduction pathway, Krüger et al. treated mice with high-fat diet-induced insulin resistance with a DEP1 specific, 5-10-5 2'-OMOE-PS gapmer AO (ISIS 285564) by IPI at a dosage of 25 mg/kg (twice a week) for 6 weeks [111]. AO treatment resulted in significant body weight loss, involving reduced epididymal and perirenal fat weight. Importantly, AO induced DEP1 suppression improved insulin sensitivity that was reflected by significant decreases in baseline glucose level and fasting insulin concentration, accompanied by hepatic hyperphosphorylation of insulin signaling intermediates, including IR and Akt [111]. This study revealed the role of DEP1 as an endogenous antagonist of insulin signaling elements, especially IR. Therefore, reduction of DEP1 represents a novel therapeutic strategy for insulin resistance and T2D.

3.2.14 Retinol binding protein 4 (RBP4)

RBP4 is an adipocytokine associated with hepatic steatosis and insulin resistance [112-116]. Increased serum RBP4 level causes insulin resistance by activation of proinflammatory pathways in fat tissues [117-119]. In fact, the level of circulating RBP4 is positively

correlated with the magnitude of insulin resistance in obese T2D patients [120-122]. In an attempt to investigate the role of overexpressed RBP4 in the development of T2D, Tan et al. treated HFD-fed mice with a RBP4 targeting, 2'-O-methyl (2'-OMe) modified, 18mer AO (25 mg/kg, IPI, once every two days) for 4 weeks [123]. Mice fed by HFD showed markedly increased weight of visceral fat, elevated levels of circulating triglyceride, FFA, glucose, and insulin, reduced GLUT4 expression, and increased PEPCK expression, suggesting an induced insulin resistant state, whereas anti-RBP4 AO treatment avoided these changes. In addition, histological observation revealed that HFD-induced fat infiltrations and hepatic steatosis were prevented by anti-RBP4 AO treatment [123]. This study indicated the association of RBP4 with NAFLD and T2D, and reduced expression of RBP4 by AO treatment could be efficacious for T2D.

3.2.15 Transthyretin (TTR)

TTR is a transport protein of RBP4 and thyroxine [124]. TTR binding to RBP4 decreases the glomerular filtration rate of RBP4, thereby retaining it in the blood [125]. Therefore, reduction of TTR lowers RBP4 levels by increasing renal clearance, and subsequently ameliorates insulin resistance. In order to determine whether reduction of TTR by AOs improves glucose homeostasis and insulin signaling, Zemany et al. administered a TTR specific, 5-10-5 2'-OMOE-PS gapmer AOs to *ob/ob* mice (ISIS 401723, 12.5 mg/kg IPI) and DIO mice (ISIS 401724, 25 mg/kg SCI) twice a week, respectively [126]. Two weeks of AO treatment led to dramatic reductions in circulating RBP4 levels in *ob/ob* mice and DIO mice by ~80% and ~95%, respectively, which was associated with 45-60% increase in muscle glucose uptake, decreased glucose production in liver, and reduced fat inflammation. These changes corelated with a marked increase of insulin signal transduction in muscle by twofold, and 30-60% reduction in insulin levels that were sustained for 9 weeks, suggesting increased insulin sensitivity [126]. The study revealed that AO induced TTR reduction could be a

potential therapeutic strategy for the treatment of insulin resistance and T2D through lowering RBP4.

3.2.16 Tribbles homolog 3 (TRIB3)

Overexpressed TRIB3 is associated with insulin resistance and T2D as TRIB3 negatively regulates Akt in the insulin signaling pathway [127, 128]. On the other hand, TRIB3 inhibits the activity of peroxisome proliferator-activated receptor γ (PPARγ), and thus suppresses adipocyte differentiation [129]. Activation of PPARγ is associated with improved insulin signal transduction that leads to increased insulin sensitivity [130]. Weismann et al. explored the role of TRIB3 reduction in improving insulin resistance by administering HFD-fed rats with a TRIB3 specific, 5-10-5 2'-OMOE-PS gapmer (ISIS 391274) at an IPI dose of 75 mg/kg weekly for 4 weeks [131]. AO treatment led to ∼50% increase in the rate of whole-body glucose uptake under euglycaemic-hyperinsulinaemic condition that was mainly attributed to the raised muscle glucose uptake. Moreover, ISIS 391274 treatment relieved the inhibitory effect of TRIB3 on PPARγ and its downstream enzymes /transcription factors, such as acyl-CoA oxidase (ACO) and CCAAT/enhancer binding protein α (C/EBPα), leading to increased level of these proteins, raised adiponectin levels, and expanded white fat tissue mass by ∼70% [131]. It is noteworthy that when PPARγ was inhibited by an antagonist, the aforementioned changes resulting from AO treatment were prevented, suggesting that the improved insulin resistance resulting from TRIB3 reduction is PPARγ dependent [131]. Based on this study, inhibition of TRIB3 might be beneficial for the therapy of insulin resistance and T2D.

3.2.17 IκB-kinase β (IκKβ)

Chronic inflammation associated with obesity is a major contributor to T2D [132, 133]. Over-nutrition results in IκKβ activation [134-136], which subsequently activates NFκB, a transcription factor that regulates inflammatory pathways contributing to insulin resistance

[137, 138]. Therefore, IκKβ could be a potential target for the therapy of obesity associated T2D. To this end, Helsley et al. explored AO based IκKβ inhibitor as a pharmacological approach to insulin resistance and obesity by treating DIO mice with a IκKβ targeting, 5-10-5 2'-OMOE-PS gapmer at a biweekly IPI dosage of 25 mg/kg for eight weeks [139]. AO treatment led to reduced levels of fasting plasma glucose and insulin, and increased Akt phosphorylation and glucose uptake in fat, suggesting improved insulin sensitivity [139]. Furthermore, the IκKβ targeting AO significantly decreased adiposity and weight gain, with a 45% reduction in fat mass that correlated with decreased hepatic triglyceride content, diminished adipocyte differentiation from adipose stromal vascular cells, and the fact that lipid accumulation and hepatic steatosis was avoided in DIO mice [139]. These findings establish IκKβ as a vital regulator of adipogenesis, and reduction of IκKβ by AO represents a potential therapeutic approach to combat insulin resistance and obesity.

3.2.18 Toll-like receptor 2 (TLR2)

Toll-like receptors (TLRs) are associated with upregulation of inflammatory cytokines through activation of NFκB [140, 141]. Inflammation mediated by cytokines such as TNFα and IL6 eventually leads to insulin resistance [42-44]. Senn et al. showed that activation of TLR2 inhibited insulin signaling pathway in differentiated C2C12 myotubes [142]. In order to investigate the effect of TLR2 reduction by AO treatment in high-fat diet induced insulin resistance, Caricilli et al. used a TLR2 targeting, 18mer AO to treat DIO mice at an IPI dose of 25 mg/kg (mice were killed 4 days after single AO injection) [143]. It is known that activation of IκKβ and JNK1 induces insulin resistance through IRS1 inhibition [144], and TLR2 AO treatment led to decreased phosphorylation of IκKβ and JNK1 in both muscle and fat, suggesting an improvement to insulin resistance [143]. Furthermore, increased phosphorylation of IRS1 and Akt was also identified in muscle and fat, indicating increased IRS1 and Akt activation and ameliorated insulin signal transduction [143]. This study

revealed that AO induced reduction of TLR2 improved insulin resistance in peripheral tissues [143], thereby highlighting the potential of TLR2 as a target for T2D therapy.

3.3 Clinical trials

To date, none of the AOs developed as inhibitors of genes involved in the T2D pathogenesis has been approved for clinical application, in contrast, a number of small molecule inhibitors have been approved and commercialized as T2D therapeutics (**Table 3.3**). However, some investigational AO candidates have entered clinical trials and they are detailed in **Table 3.3**.

Number	Drug/trade name	Molecular target	Development stage	Drug type	Reference
Approved drugs					
1	Dapagliflozin/ Farxiga™	SGLT2	Approved drug	Small molecule	145
2	Canagliflozin/ Invokana™	SGLT2	Approved drug	Small molecule	146
3	Empagliflozin/ Jardiance™	SGLT2	Approved drug	Small molecule	147
4	Ertugliflozin/ Steglatro™	SGLT2	Approved drug	Small molecule	148
5	Sotagliflozin/ Zynquista™	SGLT2	Approved drug	Small molecule	149
6	Acarbose/ Glucobay™	α-glucosidase	Approved drug	Small molecule	150
7	Miglitol/Glyset™	α-glucosidase	Approved drug	Small molecule	151
8	Sitagliptin/Januvia™	DPP4	Approved drug	Small molecule	152
9	Vildagliptin/Galvus™	DPP4	Approved drug	Small molecule	153
10	Saxagliptin/Onglyza™	DPP4	Approved drug	Small molecule	154
11	Linagliptin/Tradjenta™	DPP4	Approved drug	Small molecule	155
12	Alogliptin/Nesina™	DPP4	Approved drug	Small molecule	156
Investigational antisense-based drugs					
13	ISIS 113715	PTP1B	Phase I trial	AO	157
14	IONIS-PTP-1B$_{RX}$ (ISIS 404173)	PTP1B	Phase II trial	AO	158
15	ISIS 325568	GCGR	Phase I trial	AO	159
16	IONIS-GCGR$_{RX}$ (ISIS 449884)	GCGR	Phase I trial	AO	160
17	IONIS-GCGR$_{RX}$ (ISIS 449884)	GCGR	Phase II trial	AO	160, 161
18	ISIS 388626	SGLT2	Phase I trial	AO	162, 163
19	IONIS-GCCR$_{RX}$ (ISIS 426115)	GCCR	Phase I trial	AO	164
20	IONIS-GCCR$_{RX}$ (ISIS 426115)	GCCR	Phase II trial	AO	165
21	IONIS-DGAT2$_{RX}$ (ISIS 484137)	DGAT2	Phase I trial	AO	166
22	Volanesorsen (ISIS 308401)	Apolipoprotein C-III (APOC3)	Phase I trial	AO	167
23	Volanesorsen (ISIS 308401)	APOC3	Phase II trial	AO	168
24	AKCEA-ANGPTL3-L$_{RX}$ (ISIS 703802)	Angiopoietin-like protein 3 (ANGPTL3)	Phase II trial	AO	169

Table 3.3 Approved small molecule drugs and investigational AOs in clinical trials targeting insulin resistance and/or hyperglycemia in T2D.

4. Exploration of novel splice modulating AOs targeting PTP1B as potential therapeutic molecules for T2D

4.1 Introduction

Insulin and leptin are hormones responsible for glucose uptake and energy expenditure, respectively [170-174]. In the insulin signaling pathway, binding of insulin to its receptor, IR sequentially activates IRS, PI3K, and Akt, leading to translocation of GLUT4 to the cell membrane that allows cellular uptake of glucose [170-172]. In the leptin signaling pathway, binding of leptin to its receptor (ObR) leads to activation of Janus kinase 2 (JAK2), signal transducer and activator of transcription 3 (STAT3) and conceivably the PI3K pathway as well. Subsequent translocation of STAT3 to the nucleus results in reduced production of ACC, thereby inhibiting fatty acid synthesis, while increasing its oxidation [173, 174].

PTP1B negatively regulates both the insulin and leptin signaling by tyrosine dephosphorylation [170-174] (**Figure 4.1**). Insulin resistance and leptin resistance resulting from overexpression of PTP1B are the hallmarks for T2D and obesity, respectively. Thus, PTP1B is a therapeutic target for both the diseases and inhibition of PTP1B is expected to actuate the action of insulin and leptin, hence, development of PTP1B inhibitors can be beneficial for the treatment of T2D and obesity.

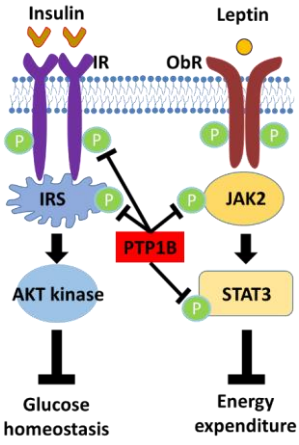

Figure 4.1 Mechanism of PTP1B induced inhibition of insulin and leptin signaling pathways. IR: insulin receptor, IRS: insulin receptor substrate, Akt: protein kinase B, ObR: leptin receptor, JAK2: Janus kinase 2, STAT3: signal transducer and activator of transcription 3, PTP1B: protein tyrosine phosphatase 1B.

Although efforts have been made in the development of small molecule PTP1B inhibitors [175-178], none of the candidates have been approved for clinical application. On the other hand, gapmer-like AO-based PTP1B inhibitors, ISIS 113715 and ISIS 404173, developed by Ionis Pharmaceuticals have entered clinical trials [157, 158]. Although application of uniformly modified, splice modulating AOs has been extensively studied for the treatment of DMD, there are no reports of utilizing splice modulating AOs for T2D therapy. In this research, we envisioned an approach to develop *PTPN1* specific, uniformly modified, splice modulating AOs to inhibit the expression of functional PTP1B proteins through exon skipping to disrupt the open reading frame and induce PTCs that lead to the generation of largely truncated, non-functional protein isoforms and possibly nonsense mediated decay of *PTPN1* mRNA.

4.1.1 Experimental design

The aim of the study is to develop splice modulating AOs that efficiently downregulate the expression of PTP1B, thereby providing an novel PTP1B inhibitor for the therapy of T2D. The mRNA encoded by the human *PTPN1* gene contains ten exons, while the mouse *Ptpn1* has nine (**Figure 4.1.1.1**). The AO development process can be divided into three phases: 1) *in vitro* screening of AOs targeting exons of human *PTPN1* pre-mRNA in order to recognize the best performing AO candidate (**Figure 4.1.1.2**), 2) identification of the champion candidate through designing and testing AOs that are very similar to the best performing candidate identified in the previous step by a 'micro-walking' AO design strategy (**Figure 4.1.1.2**), 3) design and testing of the 'mouse version' of the champion AO that targets mouse *Ptpn1* pre-mRNA *in vitro* for the preparation of future *in vivo* mouse studies (**Figure 4.1.1.2**).

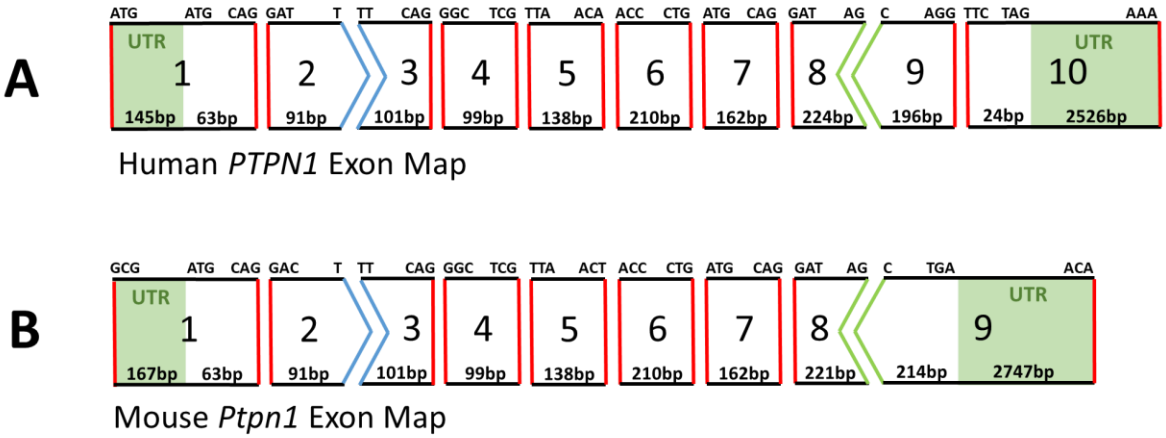

Figure 4.1.1.1 Exon map of human *PTPN1* (A) and mouse *Ptpn1* (B).

In general, thirty uniformly modified 2'-OMePS 25mer AOs (AO1-30) were initially designed and synthesized targeting exons 2-9 in human *PTPN1* pre-mRNA. These AOs were examined *in vitro* for their ability to knock down full length *PTPN1* transcript after transfection of AOs into Huh-7 hepatocarcinoma cells. AO1 that induces exon-2 skipping was found to be the best performing candidate. Next, the champion candidate, AO32 was identified through a micro-walking AO design strategy based on the nucleobase sequence of AO1, and subsequent *in vitro* screening in multiple human hepatic cell lines including Huh-7, HepG2, and IHH. Furthermore, mouse *Ptpn1* exon-2 targeting AOs were also designed and evaluated in a mouse hepatic cell line, AML-12 for the preparation of future animal studies *in vivo*.

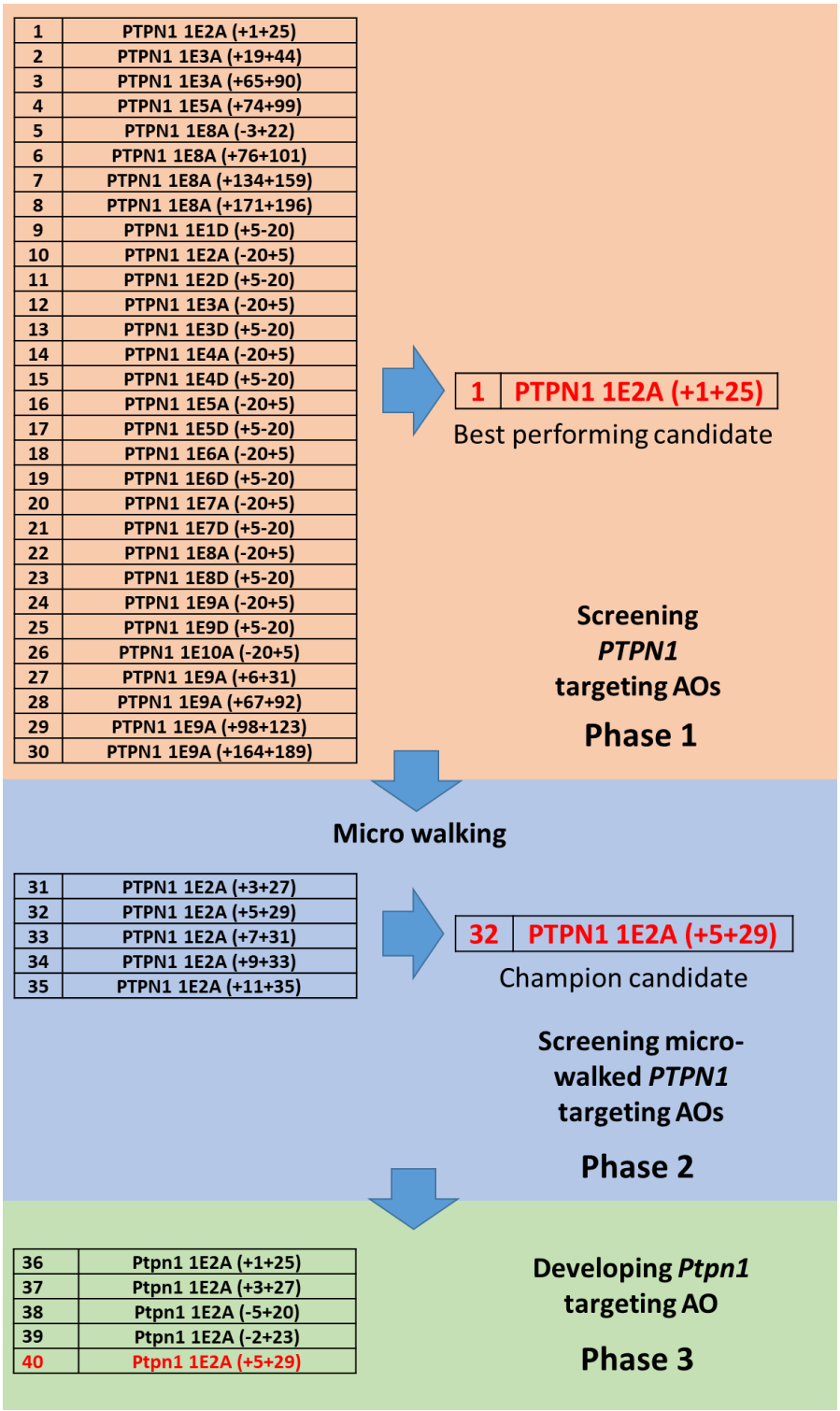

Figure 4.1.1.2 The AO development process in this study.

4.2 General protocols for exon skipping AO experiments

4.2.1 Design and synthesis of chemically-modified AOs

2'-OMePS AOs (**Figure 4.1.1.2**) were designed and synthesised in-house on an ABI Expedite® 8909 Nucleic Acid Synthesis System (Applied Biosystems) or GE AKTA

Oligopilot 10 synthesizer (GE Healthcare Life Sciene) using standard phosphoramidite chemistry at the 1 μmol scale using solid-phase thioate synthesis protocol. The synthesised AOs were deprotected and cleaved from the solid support by treatment with 1 mL ammonium hydroxide (NH_4OH) (Sigma Aldrich) at 55℃ for 8 hours. The crude/cleaved AOs were then desalted on Illustra NAP-10 columns (GE Healthcare) in sterile water. Purified oligonucleotides were then verified by polyacrylamide gel electrophoresis. AO solution stocks are stored at -20℃.

4.2.2 Cell culture and transfection

The human liver cancer cell line Huh-7 was obtained from American Type Culture Collection (ATCC); the other human hepatocarcinoma cell line, HepG2 was obtained from the European Collection of Authenticated Cell Cultures (ECACC). Huh-7 cells were cultured in 10% fetal bovine serum (FBS), Dulbecco's Modified Eagle's Medium (DMEM) (Thermo Fisher Scientific) and HepG2 cells was cultured in 10% FBS Eagle's Minimum Essential Medium (ATCC). Both IHH and AML-12 cell lines were cultured in 10% FBS, 1% ITS (Insulin-transferrin-sodium) liquid media supplement (Thermo Fisher Scientific), and 40 ng/mL dexamethasone (Sigma). All of the liver cell lines were cultured in a humidified atmosphere at 37°C, 5% CO_2. Cells were cultured until 70-90% confluent, followed by harvesting and seeding at a density of 5.0×10^4 (cells/mL) into 24-well plates (Thermo Fisher Scientific) 24 hours prior to transfection. The next day, AOs were transfected at 400 nM concentration using RNAiMAX reagent, following the manufacturer's protocol. Twenty-four hours after transfection, the cells were collected for RNA extraction.

4.2.3 RNA extraction and RT-PCR

Total RNA was extracted from transfected cells using Direct-zol™ RNA MinPrep Plus with TRI reagent (Zymo Research) as per the manufacturer's instructions. The human *PTPN1* exon-2 skipping products (product size: 639 bp), full-length products (product size: 730 bp),

and mouse *Ptpn1* exon-2 skipped products (product size: 493 bp) and full-length products (product size: 584 bp) were amplified using SuperScript® III one-step RT-PCR kit (Thermo Fisher Scientific) with human *PTPN1* primer pair (PTP1B_Ex1F: 5'-GTG ATG CGT AGT TCC GGC TG-3'; PTP1B_Ex6R: 5'-CAG GGA CTC CAA AGT CAG GC-3') or mouse *Ptpn1* primer pair (Ptpn1_B_Ex1F: 5'-AGA TCG ACA AGG CTG GGA AC-3'; Ptpn1_B_Ex6R: 5'-TGA GCC TGA CTC TCG GAC TT-3'). Briefly, the conditions were 55°C, 30 minutes; 94°C, 2 minutes followed by 33 cycles of 94°C, 30 seconds, 60°C, 1 minute and 68°C, 2 minutes. The PCR products were then separated on a 2% agarose gel in Tris-acetate-EDTA buffer and visualized with a Fusion Fx gel documentation system. Densitometry was performed using ImageJ software.

4.2.4 Sequencing

Bandstab technique was performed following the guidelines from Anthony and James [179]. The bandstab samples were then amplified with the same primer set mentioned above using AmpliTaq Gold® DNA Polymerase kit (Thermo Fisher Scientific). Briefly, the conditions were 94°C, 6 minutes followed by 32 cycles of 94°C, 30 seconds, 55°C, 1 minute and 72°C, 2 minutes. PCR products were confirmed by 2% agarose gel and sent to AGRF (Australian Genome Research Facility) for Sanger sequencing using both the forward primer and reverse primer mentioned above.

4.2.5 Western blot

Western blotting was performed to evaluate the effects of the 2'-OMe-PS and PMO analogues of PTPN1 1E2A (+5+29) (AO32) on inhibition of PTP1B protein, in comparison to the untreated sample. Seventy-two hours after transfection, IHH cells were harvested and stored at -80°C. Frozen transfected IHH cell pellets were thawed and homogenized in SDS lysis buffer (0.5 M Tris-HCl pH 6.8, 3% SDS (w/v) and 10% glycerol (v/v)) containing protease inhibitor (Sigma). The homogenates were then centrifuged at 14 000 g for 3 minutes, after which the supernatant was removed, and the protein concentration of the supernatant was

estimated using Pierce™ BCA Protein Assay kit (Thermo Fisher Scientific). Protein from the samples was then resolved on 10% polyacrylamide gel in Tris-glycine-SDS buffer, and transferred to nitrocellulose membrane (Biorad) in Tris-glycine-methanol buffer. The membrane was incubated with primary anti-PTP1B antibody (1:1000) (Cat. 5311S, Cell Signaling Technology) in 5% skim milk in TBS-T overnight at 4°C, with shaking. The membrane was then washed in TBS-T on a shaker at room temperature for 1 hour. After washing, the membrane was incubated with secondary anti-rabbit HRP antibody (1:10000) (Cat. 31460, Thermo Fisher Scientific) with shaking at room temperature for 1 hour, followed by washing in TBS-T. The protein bands were visualized by chemiluminescence using the Clarity Western ECL detection kit according to the manufacturer's instructions (Biorad).

4.3 Results

4.3.1 Initial screening of AOs targeting human *PTPN1*

Thirty 2'-OMePS modified 25mer AOs (AO1-30) targeting exons 2-9 in the *PTPN1* pre-mRNA were designed, synthesized in-house, and transfected into Huh7 liver cancer cells at 400 nM concentration with RNAiMAX transfection reagent, followed by RT-PCR and agarose gel analysis. AOs exhibited diverse *PTPN1* exon skipping efficiencies (**Supplementary figure 4.3.1.1-4.3.1.3**). An exon-2 targeting candidate, PTPN1 1E2A (+1+25) (AO1) induced highly efficient exon-2 skipping (**Supplementary figure 4.3.1.1**). Dose dependent assays of this candidate were then performed by transfecting HepG2 liver cancer cells with AO1 at various concentrations (400, 200, 100, 50, 25, 12.5, 6.3, 3.1 nM) and results showed a clear decrease in exon-2 skipping efficiency as the AO1 concentration decreased. This implies that the exon-2 skipping effect induced by AO1 is dose dependent, thereby obviating the possibility of a non-specific effect (**Figure 4.3.1.1**). Furthermore, Sanger sequencing was performed on both the exon-2 skipped and full-length RT-PCR products. Sequencing clearly showed direct joining of exon 1 to exon 3 in the shortened

PTPN1 transcript, thus confirmed the capability of AO1 to induce *PTPN1* exon 2 skipping (**Figure 4.3.1.2**).

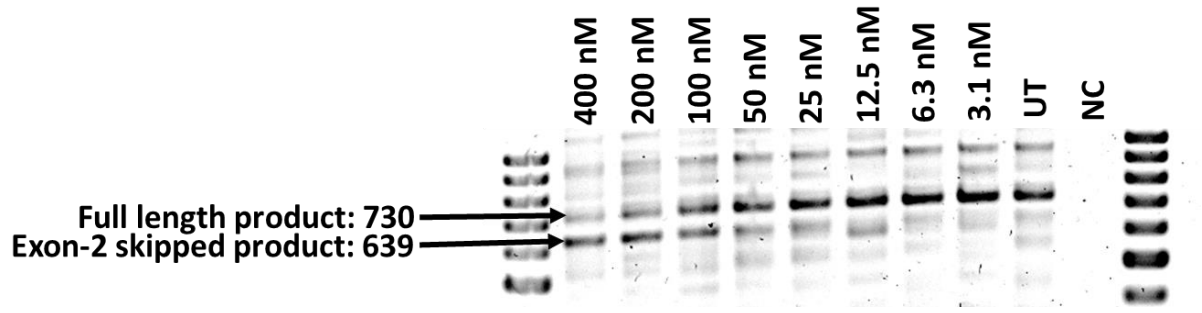

Figure 4.3.1.1 Dose dependent assay of AO1 induced exon-2 skipping in *PTPN1* transcript. UT: untreated, NC: negative control.

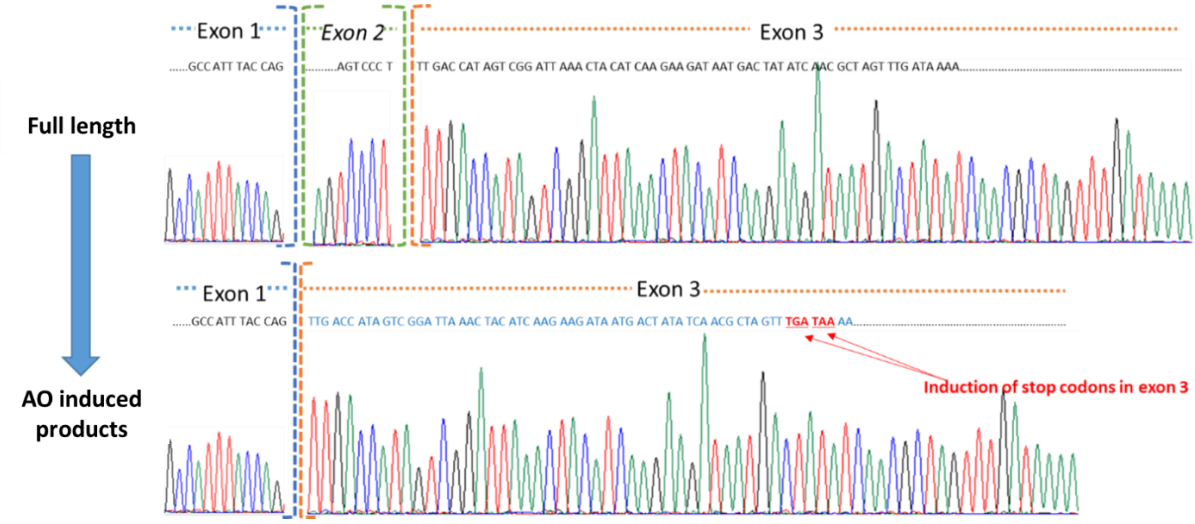

Figure 4.3.1.2 Sanger sequencing result confirmed that AO1 induces exon-2 skipping during the transcription process of the gene *PTPN1*.

4.3.2 Screening micro-walked AOs targeting exon-2 of human *PTPN1*

In an attempt to optimize the exon-2 skipping efficacy of AO1, AO31-35 were designed through a micro-walking strategy based on the sequence of AO1 (**Figure 4.3.2.1**).

Figure 4.3.2.1 Micro-walking strategy used for the design of AO31-35.

Thereafter, AO1, AO31-35, and ISIS107773 (a *PTPN1* targeting AO sequence designed by Ionis Pharmaceuticals) of both uniformly modified 2'-OMePS form and 5-10-5 2'-OMOE-PS gapmer form were transfected into different hepatic cell lines, including two carcinoma cell lines (Huh7 and HepG2) and a normal cell line (IHH) at 400 nM (**Figure 4.3.2.2**). Subsequent RT-PCR and agarose gel electrophoresis was performed and the gel images were analyzed by densitometry through ImageJ software. Results showed that PTPN1 1E2A (+5+29) (AO32) was the champion candidate compared to other exon-2 targeting AOs in terms of both the efficiencies of exon-2 skipping and knockdown of the full-length mRNA product (**Figure 4.3.2.2**). In addition, a dose response assay was conducted and results indicated that the exon-2 skipping effect induced by AO32 is dependent on dosage, obviating the possibility of a non-specific effect (**Figure 4.3.2.3**). Furthermore, a PMO form of AO32 was purchased and tested for induced exon-2 skipping and downregulation of PTP1B protein through RT-PCR and western blotting analysis, respectively. The PMO AO32 efficiently induced exon-2 skipping in IHH liver cells in a dose dependent manner (**Figure 4.3.2.4**), and markedly reduced the expression of PTP1B protein in IHH cells (**Figure 4.3.2.5**). Specifically, 7.5 μM and 15 μM of PMO AO32 led to 20% and 50% of PTP1B protein reduction, respectively (**Figure 4.3.2.5**).

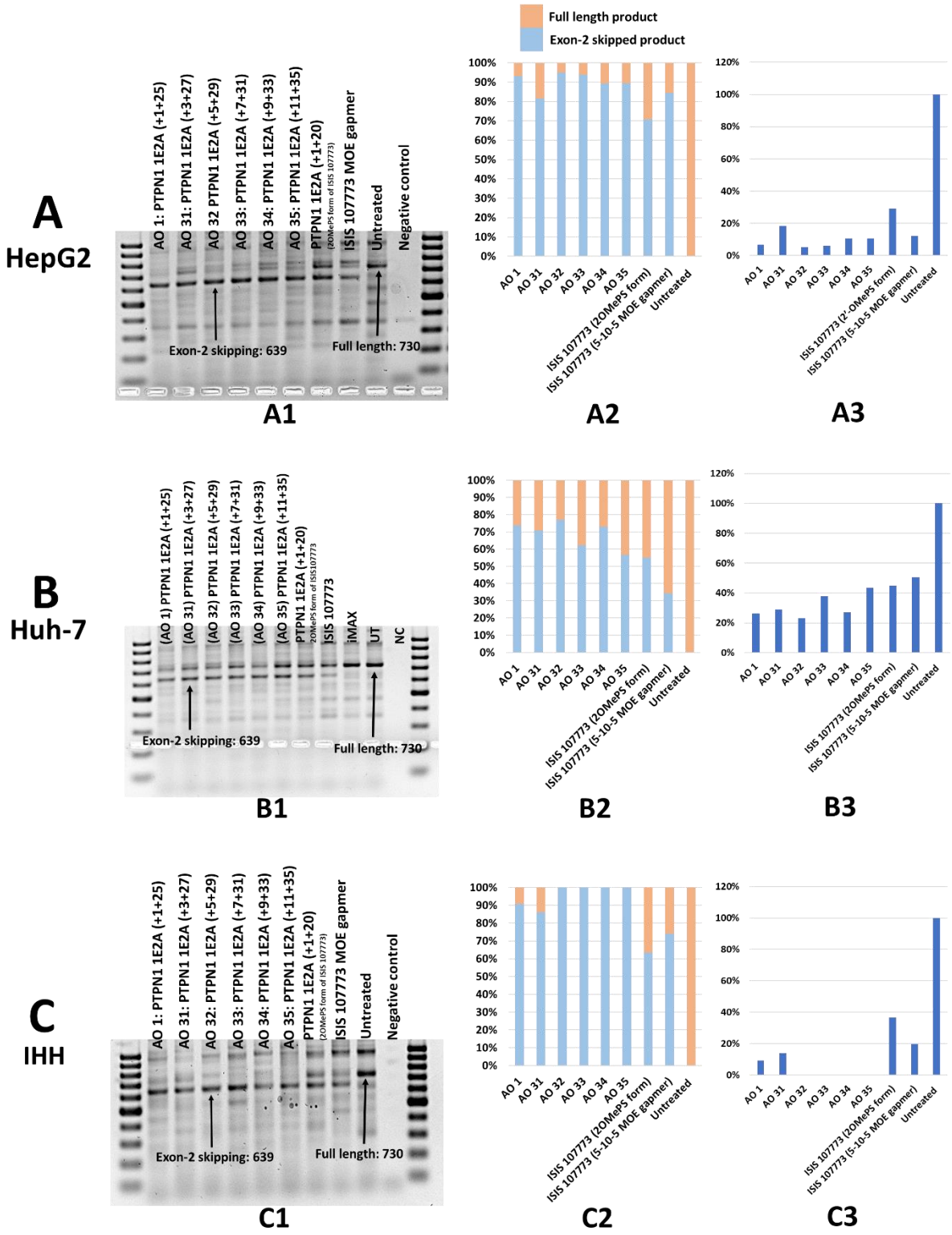

Figure 4.3.2.2 Screening of AO31-35 in different human liver cell lines using RNAiMAX transfection reagent at 400 nM concentration. A. HepG2; B. Huh-7; C. IHH; 1: agarose gel images, 2: densitometric analysis of exon-2 skipping efficiency, 3: densitometric analysis of full-length transcript knockdown efficiency.

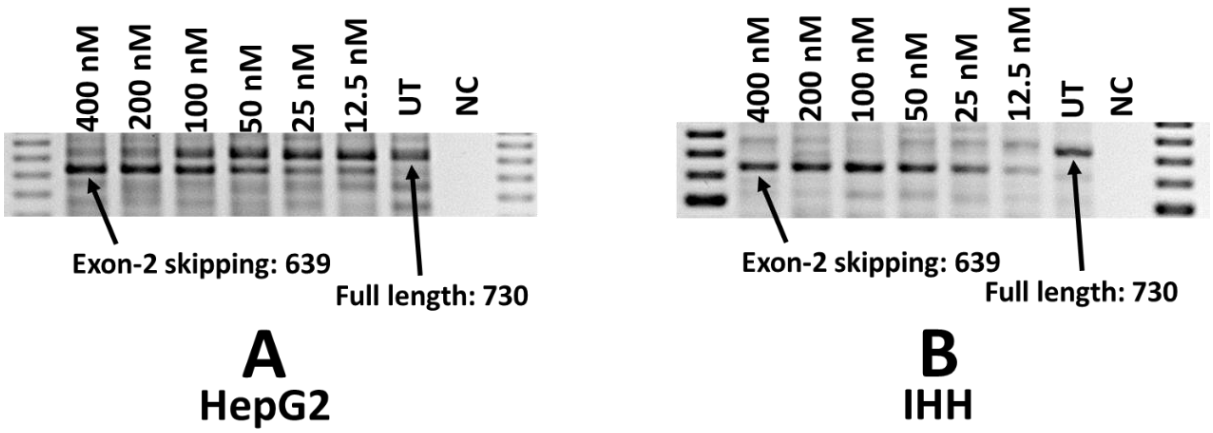

Figure 4.3.2.3 Dose dependency assay of 2'-OMePS modified AO32 induced exon-2 skipping in *PTPN1* transcript. A. HepG2; B. IHH.

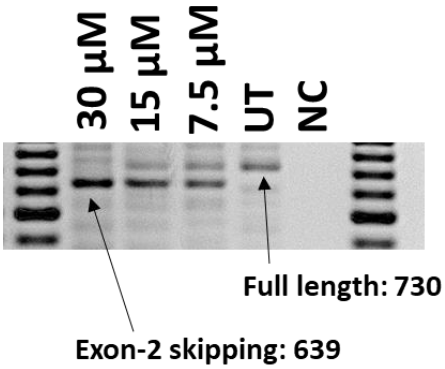

Figure 4.3.2.4 Dose dependency assay of the PMO form of AO32 to induce exon 2 skipping in the *PTPN1* transcript in IHH liver cells.

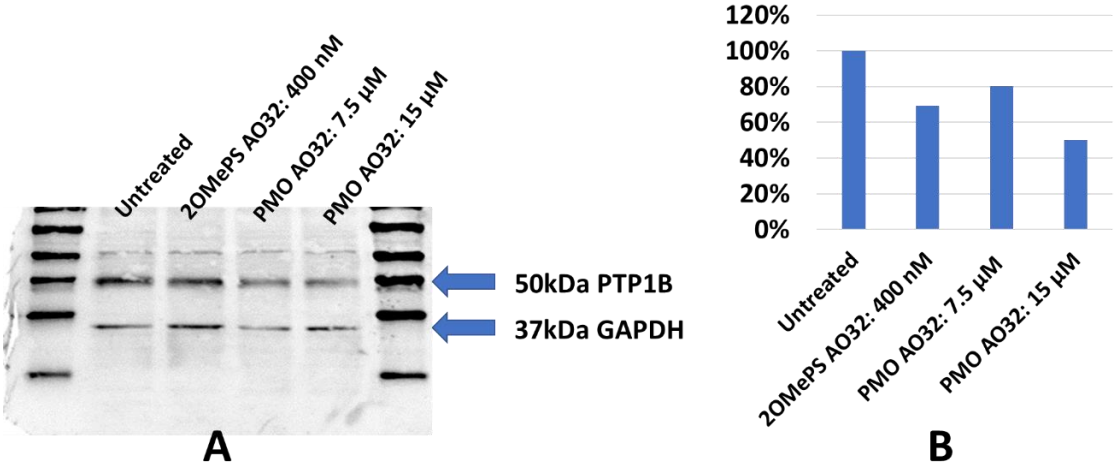

Figure 4.3.2.5 Western blotting of both 2'-OMePS and PMO forms of AO32 in IHH cells. A. Representative image of western blotting, B. densitometry analysis of PTP1B protein knockdown.

4.3.3 Development of mouse *Ptpn1* exon 2 targeting AOs

Animal studies are a necessary and integral part of drug development. In preparation for future *in vivo* evaluation of the selected PTP1B inhibiting AOs in murine models, AOs targeting mouse *Ptpn1* exon-2 were designed and synthesized (**Phase 3 in figure 4.1.1.2**). Among these, Ptpn1 1E2A (+1+25) (AO36), Ptpn1 1E2A (+3+27) (AO37), and Ptpn1 1E2A (+5+29) (AO40) are the 'mouse equivalents' of PTPN1 1E2A (+1+25) (AO1), PTPN1 1E2A (+3+27) (AO31), and PTPN1 1E2A (+5+29) (AO32), respectively. Due to differences between species, mismatches exist between human specific AOs and mouse specific AOs (**Figure 4.3.3.1**).

AO1: PTPN1 1E2A (+1+25)	AGU CAC UGG CUU CAU GUC GGA UAU C
AO36: Ptpn1 1E2A (+1+25)	AGU CGC UGG CUU CAU GUC GAA UGU C
AO31: PTPN1 1E2A (+3+27)	GAA GUC ACU GGC UUC AUG UCG GAU A
AO37: Ptpn1 1E2A (+3+27)	GAA GUC GCU GGC UUC AUG UCG AAU G
AO32: PTPN1 1E2A (+5+29)	GGG AAG UCA CUG GCU UCA UGU CGG A
AO40: Ptpn1 1E2A (+5+29)	GGG AAG UCG CUG GCU UCA UGU CGA A

Figure 4.3.3.1 Mismatches between AOs targeting human *PTPN1* exon 2 and AOs targeting mouse *Ptpn1* exon 2.

In order to screen out the best performing *Ptpn1* exon-2 targeting AO candidate and also evaluate the effect of the mismatches, mouse *Ptpn1* exon-2 targeting AOs (AO36-40) and human *PTPN1* exon-2 targeting AOs (AO1, AO31, AO32) were transfected into a mouse liver cell line, AML-12 with RNAiMAX reagent at 400 nM concentration. RT-PCR and agarose gel electrophoresis were subsequently conducted. Results clearly showed that AO40 was the best performing candidate in inducing exon 2 skipping (**Figure 4.3.3.2, supplementary figure 4.3.3.1**). Not surprisingly, human *PTPN1* exon-2 targeting AOs did not induce efficient exon-2 skipping in mouse cells as a result of the mismatches (**Figure 4.3.3.2, supplementary figure 4.3.3.1**). Conversely, mouse *Ptpn1* exon 2 targeting AOs

(AO36-40) were also transfected into the human liver cancer cell line, HepG2 at 400 nM concentration. Interestingly, AO40 induced highly efficient exon 2 skipping, despite two mismatches between the AO and target pre-mRNA (**Figure 4.3.3.3**). Moreover, a dose response assay was performed for the champion candidate, AO40 and results indicated that the exon 2 skipping effect induced by this candidate was dose dependent, thereby obviating the possibility of non-specific effect (**Figure 4.3.3.4**).

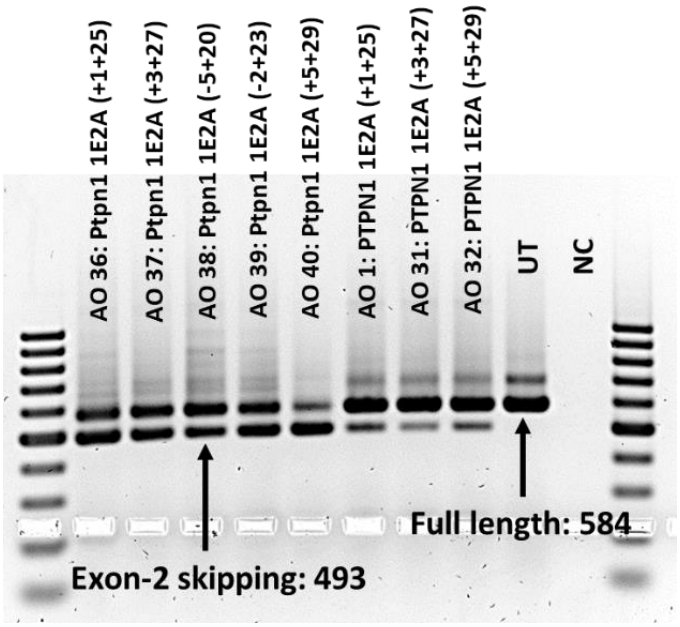

Figure 4.3.3.2 Screening of AO36-40 in mouse AML-12 cells using RNAiMAX transfection reagent at 400 nM concentration. UT: untreated, NC: negative control.

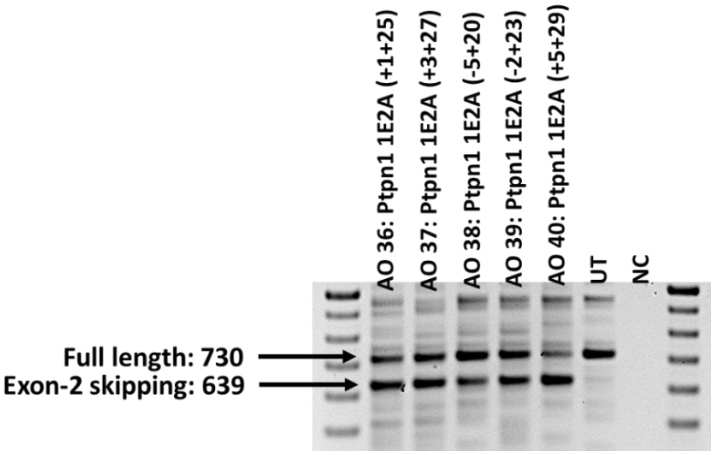

Figure 4.3.3.3 Screening of AO36-40 in human HepG2 cells using RNAiMAX transfection reagent at 400 nM concentration. UT: untreated, NC: negative control.

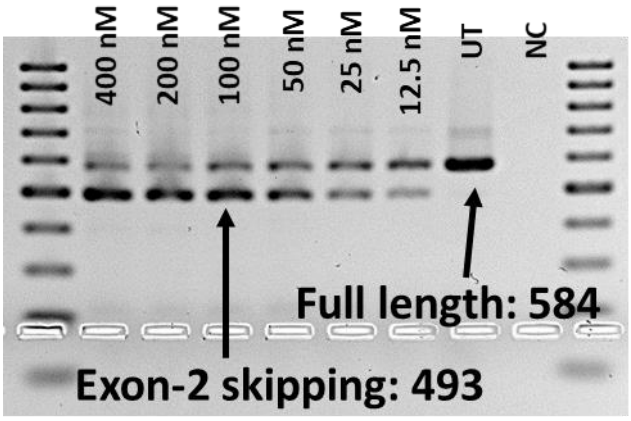

Figure 4.3.3.4 Dose dependency assay of AO41 induced exon-2 skipping in *Ptpn1* transcript in mouse AML-12 cells. RNAiMAX transfection reagent was used.

4.4 Discussion

RNA degradation mediated by RNase H, and splice modulation resulting from steric blockage are the two mechanisms of action widely used in AO-based drug development towards tackling different human maladies. So far, seven AO drugs have been approved by the US FDA for clinical applications [8-29]. Among these, three AOs (fomivirsen, mipomersen, inotersen) degrade the mRNA of disease-causing genes through RNase H recruitment [8-11, 24, 25], while the other four antisense molecules (eteplirsen, golodirsen, nusinersen, and milasen) modulate splicing (by either exon skipping or inclusion) to repair the ORF of essential genes, thereby rescuing the production of functional proteins interrupted by mutations [12-23, 26-29]. As reviewed in detail in section 3 of this chapter, gapmer AOs that recruit RNase H have been extensively applied in the development of therapeutics targeting T2D through reducing the expression of genes involved in T2D pathogenesis, including *PTPN1*. Some of these gapmer candidates have entered different phases of clinical trials [157-169], although so far none have been approved for market. To this end, we have explored a novel strategy for developing *PTPN1* targeting AOs aiming at reducing PTP1B expression, that is development of splice modulating AOs capable of skipping exons in

PTPN1 pre-mRNA during splicing that leads to decreased full-length *PTPN1* transcript, thus downregulating the expression of intact, functional PTP1B protein.

Initially, thirty fully modified 2'-OMePS AOs (AO1-30) targeting different *PTPN1* exons were designed and evaluated *in vitro* in liver cancer Huh-7 cells. PTPN1 1E2A (+1+25) (AO1) was identified as the best performing candidate for the following reasons:

1) AO1 was one of the candidates that induced the most efficient exon skipping.

2) *PTPN1* contains 10 exons, however only skipping of exons 2, 3, 8, or 9 causes a frame-shift that leads to PTCs in the downstream exon (**Figure 4.1.1.1**). AO1 treatment induced exon 2 skipping, resulting in PTCs in exon 3 (**Figure 4.3.1.2**), thus causing either the synthesis of prematurely truncated, non-functional PTP1B isoform encoded by only one exon, with presumed induction nonsense mediated decay of the induced *PTPN1* mRNA. Both the possible scenarios upon exon-2 skipping lead to a common consequence: reduction of functional PTP1B protein expression.

In order to maximize the efficiency of AO-induced exon 2 skipping, micro-walked AO sequences (AO31-35) were designed, based on the sequence of AO1 (**Figure 4.3.2.1**). Results of *in vitro* investigation of these candidates in multiple human liver cell lines (Huh-7, HepG2, IHH) showed that PTPN1 1E2A (+5+29) (AO32) induced exon 2 skipping and reduced the expression of full-length *PTPN1* mRNA most efficiently compared to other exon 2 targeting AO counterparts (**Figure 4.3.2.2**). This is probably due to the fact that AO32 targets the most amenable splice motifs. Therefore, AO32 was considered the champion candidate and was selected for further improvement in terms of pharmacokinetics through PMO modification. The preliminary results obtained from 2'-OMePS form of AOs can indeed be extended to their PMO counterparts, this has been recently proven by Li et al [180].

Indeed, clinical translation of antisense drug molecules constructed by modified nucleotides (nucleotide analogues) has clearly demonstrated the importance of chemical modification in improving the pharmacokinetics of AO therapeutics [181], in particular, DNA PS, 2'-OMOE, and PMO are so far the only three chemistries used for constructing AO drugs approved by the FDA. However, chemically modified AOs need to meet the balance between efficacy and safety [182]. One example highlighting the importance of this safety-efficacy balance is the competition between 2'-OMePS and PMO in the development of AO drugs to treat DMD: drisapersen (BioMarin Pharmaceutical), a 2'-OMe-PS candidate was rejected, while eteplirsen and golodirsen (Sarepta Therapeutics), two PMO drugs were approved by the FDA recently. The PMO chemistry showed excellent safety data in DMD trials [182, 183], while life-threatening toxicity and severe injection site reactions resulted from treatment by 2'-OMe-PS AOs [184]. Therefore, the PMO chemistry is preferable for AO modification, compared to 2'-OMe-PS in terms of the *in vivo* safety profile. In consideration of this, the PMO form of the champion candidate AO32 will be recommended for clinical evaluation in the future. The reason that 2'-OMe-PS AOs were used for initial and secondary screening in this study is due to its advantages in terms of convenience of synthesis (2'-OMe-PS AOs can be synthesized in-house by oligonucleotide synthesizer but not to clinical grade at the moment) and relatively low cost. In contrast, PMO production is costly due to complex and distinctive synthesis procedures, compared to standard phosphoramidite chemistry synthesis. In line with the 2'-OMe-PS form of AO32, the PMO form of this sequence efficiently induced exon 2 skipping in a dose dependent manner (**Figure 4.3.2.4**), and moreover led to significantly lowered expression of PTP1B protein in IHH cells (**Figure 4.3.2.5**). Hence, PMO AO32 is appropriate for future *in vivo* studies in humans.

Prior to clinical trials in drug development, *in vivo* mouse studies are an integral procedure. However, due to the mismatches between human *PTPN1* and the mouse *Ptpn1* gene, AOs

developed for exon skipping in *PTPN1* did not induce exon 2 skipping in mouse liver cells as efficiently as in human cells, therefore, 'mouse versions' of exon 2 skipping AOs were designed and evaluated in AML-12 mouse liver cells. Results confirmed that Ptpn1 1E2A (+5+29) (AO40), the mouse version of the champion molecule (AO32) is also the best performing candidate for targeting mouse *Ptpn1*. Surprisingly, despite the presence of two mismatches (**Figure 4.3.3.3**), AO40 also induced highly efficient exon 2 skipping in human cells (HepG2). This is probably due to the lower number of mismatches (2 mismatches) between AO32 and AO40 compared to the higher number of mismatches (3 mismatches) between AO1 and AO36, AO31 and AO37 (**Figure 4.3.3.1**). Thereby, this further demonstrates that AO40 is the most suitable candidate for *in vivo* mouse studies in the future.

4.5 Conclusion

PTP1B is a negative regulator of insulin and leptin signaling. Overexpression of PTP1B is responsible for insulin resistance and leptin resistance, leading to T2D. Thus, PTP1B is a therapeutic target for T2D. This chapter presents the design and evaluation of uniformly modified, splice modulating AOs in reducing the expression of PTP1B protein through exon skipping induced PTCs, thereby providing a novel AO PTP1B inhibitor for the therapy of T2D. The champion candidate, PTPN1 1E2A (+5+29) (AO32) that induces efficient human *PTPN1* exon 2 skipping was developed through initial screening (thirty AO candidates) and secondary screening (five micro-walked AO candidates). In an attempt to improve the safety profile of AO32 for future clinical applications, PMO modification was introduced and evaluated. In addition, Ptpn1 1E2A (+5+29) (AO40) was developed for the future *in vivo* studies in mouse. In conclusion, this study provides a novel antisense therapy for PTP1B related conditions, in particular, T2D.

Chapter two references

1. Alama, A., Barbieri, F., Cagnoli, M., Schettini, G. Antisense oligonucleotides as therapeutic agents. *Pharmacol Res* 36, 171-178 (1997).

2. Dias, N., Stein, C.A. Antisense oligonucleotides: basic concepts and mechanisms. *Mol Cancer Ther* 1, 347-355 (2002).

3. Chan, J.H., Lim, S., Wong, W.S. Antisense oligonucleotides: from design to therapeutic application. *Clin Exp Pharmacol Physiol* 33, 533-540 (2006).

4. Smith, C.I.E., Zain, R. Therapeutic oligonucleotides: state of the art. *Annu Rev Pharmacol Toxicol* 59, 605-630 (2019).

5. Paterson, B.M., Roberts, B.E., Kuff, E.L. Structural gene identification and mapping by DNA-mRNA hybrid-arrested cell-free translation. *Proc Natl Acad Sci U S A* 74, 4370-4374 (1977).

6. Zamecnik, P.C., Stephenson, M.L. Inhibition of Rous sarcoma virus replication and cell transformation by a specific oligodeoxynucleotide. *Proc Natl Acad Sci U S A* 75, 280-284 (1978).

7. Stephenson, M.L., Zamecnik, P.C. Inhibition of Rous sarcoma viral RNA translation by a specific oligodeoxyribonucleotide. *Proc Natl Acad Sci U S A* 75, 285-288 (1978).

8. Roehr, B. Fomivirsen approved for CMV retinitis. *J Int Assoc Physicians AIDS Care* 4, 14-16 (1998).

9. De Smet, M.D., Meenken, C.J., Van den Horn, G.J. Fomivirsen-a phosphorothioate oligonucleotide for the treatment of CMV retinitis. *Ocul Immunol Inflamm* 7, 189-198 (1999).

10. Hair, P., Cameron, F., McKeage, K. Mipomersen sodium: first global approval. *Drugs* 73, 487-493 (2013).

11. Wong, E., Goldberg, T. Mipomersen (Kynamro): a novel antisense oligonucleotide inhibitor for the management of homozygous familial hypercholesterolemia. *P T* 39, 119-122 (2014).

12. Syed, Y.Y. Eteplirsen: first global approval. *Drugs* 76, 1699-1704 (2016).

13. Lim, K.R.Q., Maruyama, R., Yokota, T. Eteplirsen in the treatment of Duchenne muscular dystrophy. *Drug Des Devel Ther* 11, 533-545 (2017).

14. Baker, D.E. Eteplirsen. *Hosp Pharm* 52, 302-305 (2017).

15. Charleston, J.S., Schnell, F.J., Dworzak, J. Eteplirsen treatment for Duchenne muscular dystrophy: exon skipping and dystrophin production. *Neurology* 90, e2146-e2154 (2018).

16. Hoy, S.M. Nusinersen: first global approval. *Drugs* 77, 473-479 (2017).

17. Corey, D.R. Nusinersen, an antisense oligonucleotide drug for spinal muscular atrophy. *Nat Neurosi* 20, 497-499 (2017).

18. Goodkey, K., Aslesh, T., Maruyama, R., Yokota, T. Nusinersen in the treatment of spinal muscular atrophy. *Methods Mol Biol* 1828, 69-76 (2018).

19. Neil, E.E., Bisaccia, E.K. Nusinersen: a novel antisense oligonucleotide for the treatment of spinal muscular atrophy. *J Pediatr Pharmacol Ther* 24, 194-203 (2019).

20. Wurster, C.D., Ludolph, A.C. Nusinersen for spinal muscular atrophy. *Ther Adv Neurol Disord* 11, 1756285618754459 (2018).

21. Gidaro, T., Servais, L. Nusinersen treatment of spinal muscular atrophy: current knowledge and existing gaps. *Dev Med Child Neurol* 61, 19-24 (2019).

22. Chiriboga, C.A. Nusinersen for the treatment of spinal muscular atrophy. *Expert Rev Neurother* 17, 955-962 (2017).

23. Claborn, M.K., Stevens, D.L., Walker, C.K., Gildon, B.L. Nusinersen: a treatment for spinal muscular atrophy. *Ann Pharmacother* 53, 61-69 (2019).

24. Keam, S.J. Inotersen: first global approval. *Drugs* 78, 1371-1376 (2018).

25. Gales, L. Tegsedi (inotersen): an antisense oligonucleotide approved for the treatment of adult patients with hereditary transthyretin amyloidosis. *Pharmaceuticals* 12, 78 (2019).

26. Aartsma-Rus, A., Watts, J.K. The Munich meeting: medical maturation, more mechanisms, and milasen. *Nucleic Acid Ther* 29, 302-304 (2019).

27. Kim, J., Hu, C., Moufawad El Achkar, C., et al. Patient-customized oligonucleotide therapy for a rare genetic Disease. *N Engl J Med* 381, 1644-1652 (2019).

28. Fyfe, I. Oligonucleotide designed for ultimate personalized treatment. *Nat Rev Neurol* 15, 687 (2019).

29. Heo, Y. Golodirsen: first approval. *Drugs* 80, 329-333 (2020).

30. Goyal, N., Narayanaswami, P. Making sense of antisense oligonucleotides: a narrative review. *Muscle Nerve* 57, 356-370 (2018).

31. Crooke, S.T. Molecular mechanisms of antisense oligonucleotides. *Nucleic Acid Ther* 27, 70-77 (2017).

32. Havens, M.A., Hastings, M.L. Splice-switching antisense oligonucleotides as therapeutic drugs. *Nucleic Acids Res* 44, 6549-6563 (2016).

33. Good, L. Translation repression by antisense sequences. *Cell Mol Life Sci* 60, 854-861 (2003).

34. Kole, R., Krainer, A.R., Altman, S. RNA therapeutics: beyond RNA interference and antisense oligonucleotides. *Nat Rev Drug Discov* 11, 125-140 (2012).

35. Scoles, D.R., Minikel, E.V., Pulst, S.M. Antisense oligonucleotides: a primer. *Neurol Genet* 5, e323 (2019).

36. Sud, R., Geller, E.T., Schellenberg, G.D. Antisense-mediated exon skipping decreases tau protein expression: a potential therapy for tauopathies. *Mol Ther Nucleic Acids* 3, e180 (2014).

37. Cerf, M.E. Beta cell dysfunction and insulin resistance. *Front Endocrinol (Lausanne)* 4, 37 (2013).

38. Kokil, G.R., Veedu, R.N., Ramm, G.A., Prins, J.B., Parekh, H.S. Type 2 diabetes mellitus: limitations of conventional therapies and intervention with nucleic acid-based therapeutics. *Chem Rev* 115, 4719-4743 (2015).

39. Vollenweider, P., Ménard, B., Nicod, P. Insulin resistance, defective insulin receptor substrate 2—associated phosphatidylinositol-3′ kinase activation, and impaired atypical protein kinase C (ζ/λ) activation in myotubes from obese patients with impaired glucose tolerance. *Diabetes* 51, 1052-1059 (2002).

40. Kokil, G.R., Rewatkar, P.V., Verma, A., Thareja, S., Naik, S.R. Pharmacology and chemistry of diabetes mellitus and antidiabetic drugs: a critical review. *Curr Med Chem* 17, 4405-4423 (2010).

41. Al-Goblan, A.S., Al-Alfi, M.A., Khan, M.Z. Mechanism linking diabetes mellitus and obesity. *Diabetes Metab Syndr Obes* 7, 587-591 (2014).

42. Erion, D.M., Shulman, G.I. Diacylglycerol-mediated insulin resistance. *Nat Med* 16, 400-402 (2010).

43. Yang, J., Park, Y., Zhang, H., Gao, X., Wilson, E., Zimmer, W., Abbott, L., Zhang, C. Role of MCP-1 in tumor necrosis factor-α-induced endothelial dysfunction in type 2 diabetic mice. *Am J Physiol Heart Circ Physiol* 297, H1208-H1216 (2009).

44. Rieusset, J., Bouzakri, K., Chevillotte, E., Ricard, N., Jacquet, D., Bastard, J.P., Laville, M., Vidal, H. Suppressor of cytokine signaling 3 expression and insulin resistance in skeletal muscle of obese and type 2 diabetic patients. *Diabetes* 53, 2232-2241 (2004).

45. Ji, C., Kaplowitz, N., Lau, M.Y., Kao, E., Petrovic, L.M., Lee, A.S. Liver-specific loss of glucose-regulated protein 78 perturbs the unfolded protein response and exacerbates a spectrum of liver diseases in mice. *Hepatology* 54, 229-239 (2011).

46. Unoki, H., Yamagishi, S. Advanced glycation end products and insulin resistance. *Curr Pharm Des* 14, 987-989 (2008).

47. Poitout, V., Robertson, R.P. Glucolipotoxicity: fuel excess and beta-cell dysfunction. *Endocr Rev* 29, 351-366 (2008).

48. Cnop, M., Ladrière, L., Igoillo-Esteve, M., Moura, R.F., Cunha, D.A. Causes and cures for endoplasmic reticulum stress in lipotoxic β-cell dysfunction. *Diabetes Obes Metab* 12, 76-82 (2010).

49. Wang, C., Guan, Y., Yang, J. Cytokines in the Progression of Pancreatic β-Cell Dysfunction. *Int J Endocrinol* 2010, 515136 (2010).

50. Marrif, H.I., Al-Sunousi, S.I. Pancreatic β cell mass death. *Front Pharmacol* 7, 83 (2016).

51. Nathan, D.M., Buse, J.B., Davidson, M.B., Heine, R.J., Holman, R.R., Sherwin, R., Zinman, B. Management of hyperglycemia in type 2 diabetes: a consensus algorithm for the initiation and adjustment of therapy. *Diabetes Care* 29, 1963-1972 (2006).

52. Kenner, K.A., Anyanwu, E., Olefsky, J.M., Kusari, J. Protein-tyrosine phosphatase 1B is a negative regulator of insulin- and insulin-like growth factor-I-stimulated signaling. *J Biol Chem* 271, 19810-19819 (1996).

53. Goldstein, B.J., Bittner-Kowalczyk, A., White, M.F., Harbeck, M. Tyrosine dephosphorylation and deactivation of insulin receptor substrate-1 by protein-tyrosine phosphatase 1B. Possible facilitation by the formation of a ternary complex with the Grb2 adaptor protein. *J Biol Chem* 275, 4283-4289 (2000).

54. Zinker, B.A., Rondinone, C.M., Trevillyan, J.M., Gum, R.J., et al. PTP1B antisense oligonucleotide lowers PTP1B protein, normalizes blood glucose, and improves insulin sensitivity in diabetic mice. *Proc Natl Acad Sci U S A* 99, 11357-11362 (2002).

55. Terauchi, Y., Tsuji, Y., Satoh, S., Minoura, H., et al. Increased insulin sensitivity and hypoglycaemia in mice lacking the p85 alpha subunit of phosphoinositide 3-kinase. *Nat Genet* 21, 230-235 (1999).

56. Rondinone, C.M., Clampit, J., Gum, R.J., Zinker, B.A., et al. Reduction of PTP1B induces differential expression of PI3-kinase (p85alpha) isoforms. *Biochem Biophys Res Commun* 323, 652-659 (2004).

57. Clampit, J.E., Meuth, J.L., Smith, H.T., Reilly, R.M., et al. Reduction of protein-tyrosine phosphatase-1B increases insulin signaling in FAO hepatoma cells. *Biochem Biophys Res Commun* 300, 261-267 (2003).

58. Gum, R.J., Gaede, L.L., Koterski, S.L., Heindel, M., et al. Reduction of protein tyrosine phosphatase 1B increases insulin-dependent signaling in ob/ob mice. *Diabetes* 52, 21-28 (2003).

59. Rondinone, C.M., Trevillyan, J.M., Clampit, J., Gum, R.J., et al. Protein Tyrosine Phosphatase 1B Reduction Regulates Adiposity and Expression of Genes Involved in Lipogenesis. *Diabetes* 51, 2405-2411 (2002).

60. Waring, J.F., Ciurlionis, R., Clampit, J.E., Morgan, S., et al. PTP1B antisense-treated mice show regulation of genes involved in lipogenesis in liver and fat. *Mol Cell Endocrinol* 203, 155-168 (2003).

61. Swarbrick, M.M., Havel, P.J., Levin, A.A., Bremer, A.A. Inhibition of protein tyrosine phosphatase-1B with antisense oligonucleotides improves insulin sensitivity and increases adiponectin concentrations in monkeys. *Endocrinology* 150, 1670-1679 (2009).

62. Achari, A.E., Jain, S.K. Adiponectin, a therapeutic target for obesity, diabetes, and endothelial dysfunction. *Int J Mol Sci* 18, 1321 (2017).

63. Gum, R.J., Gaede, L.L., Heindel, M.A., Waring, J.F., et al. Antisense protein tyrosine phosphatase 1B reverses activation of p38 mitogen-activated protein kinase in liver of ob/ob mice. *Mol Endocrinol* 17, 1131-1143 (2003).

64. Hotamisligil, G.S. The role of TNF alpha and TNF receptors in obesity and insulin resistance. *J Intern Med* 245, 621-625 (1999).

65. Cheung, A.T., Ree, D., Kolls, J.K., Fuselier, J., et al. An *in vivo* model for elucidation of the mechanism of tumor necrosis factor-alpha (TNF-alpha)-induced insulin resistance: evidence for differential regulation of insulin signaling by TNF-alpha. *Endocrinology* 139, 4928-4935 (1998).

66. Xing, L., Quinn, P.G. Involvement of 3',5'-cyclic adenosine monophosphate regulatory element binding protein (CREB) in both basal and hormone-mediated expression of the phosphoenolpyruvate carboxykinase (PEPCK) gene. *Mol Endocrinol* 7, 1484-1494 (1993).

67. Quinn, P.G. Inhibition by insulin of protein kinase A-induced transcription of the phosphoenolpyruvate carboxykinase gene. Mediation by the activation domain of cAMP eesponse element-binding protein (CREB) and factors bound to the TATA box. *J Biol Chem* 269, 14375-14378 (1994).

68. Koizumi, M., Takagi-Sato, M., Okuyama, R., Araki, K., et al. Direct comparison of in vivo antisense activity of ENA oligonucleotides targeting PTP1B mRNA with that of 2'-O-(2-methoxy) ethyl-modified oligonucleotides. *Oligonucleotides* 16, 253-262 (2006).

69. Pandey, S.K., Yu, X.X., Watts, L.M., Michael, M.D., et al. Reduction of low molecular weight protein-tyrosine phosphatase expression improves hyperglycemia and insulin sensitivity in obese mice. *J Biol Chem* 282, 14291-14299 (2007).

70. Boden, G., Tappy, L., Jadali, F., Hoeldtke, R.D., Rezvani, I., Owen, O.E. Role of glucagon in disposal of an amino acid load. *Am J Physiol* 259, E225-E232 (1990).

71. Pilkis, S.J., Granner, D.K. Molecular physiology of the regulation of hepatic gluconeogenesis and glycolysis. *Annu Rev Physiol* 54, 885-909 (1992).

72. Dobbs, R., Sakurai, H., Sasaki, H., Faloona, G., et al. Glucagon: role in the hyperglycemia of diabetes mellitus. *Science* 187, 544-547 (1975).

73. Liang, Y., Osborne, M.C., Monia, B.P., Bhanot, S., et al. Reduction in glucagon receptor expression by an antisense oligonucleotide ameliorates diabetic syndrome in db/db mice. *Diabetes* 53, 410-417 (2004).

74. Holst, J.J. The physiology of glucagon-like peptide 1. *Physiol Rev* 87, 1409-1439 (2007).

75. Sloop, K.W., Cao, J.X., Siesky, A.M., Zhang, H.Y., et al. Hepatic and glucagon-like peptide-1–mediated reversal of diabetes by glucagon receptor antisense oligonucleotide inhibitors. *J Clin Invest* 113, 1571-1581 (2004).

76. Bailey, C.J. Renal glucose reabsorption inhibitors to treat diabetes. *Trends Pharmacol Sci* 32, 63-71 (2011).

77. Zanardi, T.A., Han, S., Jeong, E.J., Rime, S., et al. Pharmacodynamics and Subchronic Toxicity in Mice and Monkeys of ISIS 388626, a Second-Generation Antisense Oligonucleotide That Targets Human Sodium Glucose Cotransporter 2. *J Pharmacol Exp Ther* 343, 489-496 (2012).

78. Kuo, T., McQueen, A., Chen, T., Wang, J.C., et al. Regulation of Glucose Homeostasis by Glucocorticoids. *Adv Exp Med Biol* 872, 99-126 (2015).

79. Watts, L.M., Manchem, V.P., Leedom, T.A., Rivard, A.L., et al. Reduction of hepatic and adipose tissue glucocorticoid receptor expression with antisense oligonucleotides improves hyperglycemia and hyperlipidemia in diabetic rodents without causing systemic glucocorticoid antagonism. *Diabetes* 54, 1846-1853 (2015).

80. Liang, Y., Osborne, M.C., Monia, B.P., Bhanot, S., et al. Antisense Oligonucleotides Targeted Against Glucocorticoid Receptor Reduce Hepatic Glucose Production and Ameliorate Hyperglycemia in Diabetic Mice. *Metabolism* 54, 848-855 (2005).

81. Kim, J.K., Fillmore, J.J., Chen, Y., Yu, C., et al. Tissue-specific overexpression of lipoprotein lipase causes tissue-specific insulin resistance. *Proc Natl Acad Sci U S A* 98, 7522-7527 (2001).

82. Samuel, V.T., Liu, Z., Qu, X., Elder, B.D., et al. Mechanism of hepatic insulin resistance in non-alcoholic fatty liver disease. *J Biol Chem* 279, 32345-32353 (2004).

83. Petersen, K.F., Dufour, S., Befroy, D., Lehrke, M., et al. Reversal of nonalcoholic hepatic steatosis, hepatic insulin resistance, and hyperglycemia by moderate weight reduction in patients with type 2 diabetes. *Diabetes* 54, 603-608 (2005).

84. Munday, M.R., Hemingway, C.J. The regulation of acetyl-CoA carboxylase-a potential target for the action of hypolipidemic agents. *Adv Enzyme Regul* 39, 205-234 (1999).

85. Munday, M.R. Regulation of mammalian acetyl-CoA carboxylase. *Biochem Soc Trans* 30, 1059-1064 (2002).

86. Wakil, S.J., Stoops, J.K., Joshi, V.C. Fatty acid synthesis and its regulation. *Annu Rev Biochem* 52, 537-579 (1983).

87. McGarry, J.D., Brown, N.F. The mitochondrial carnitine palmitoyltransferase system. From concept to molecular analysis. *Eur J Biochem* 244, 1-14 (1997).

88. Abu-Elheiga, L., Matzuk, M.M., Abo-Hashema, K.A., Wakil, S.J. Continuous fatty acid oxidation and reduced fat storage in mice lacking acetyl-CoA carboxylase 2. *Science* 291, 2613-2616 (2001).

89. Savage, D.B., Choi, C.S., Samuel, V.T., Liu, Z.X., et al. Reversal of diet-induced hepatic steatosis and hepatic insulin resistance by antisense oligonucleotide inhibitors of acetyl-CoA carboxylases 1 and 2. *J Clin Invest* 116, 817-824 (2006).

90. Yu, X.X., Murray, S.F., Pandey, S.K., Booten, S.L., et al. Antisense oligonucleotide reduction of DGAT2 expression improves hepatic steatosis and hyperlipidemia in obese mice. *Hepatology* 42, 362-371 (2005).

91. Choi, C.S., Savage, D.B., Kulkarni, A., Yu, X.X., et al. Suppression of diacylglycerol acyltransferase-2 (DGAT2), but not DGAT1, with antisense oligonucleotides reverses diet-induced hepatic steatosis and insulin resistance. *J Biol Chem* 282, 22678-22688 (2007).

92. Holyoak, T., Sullivan, S.M., Nowak, T. Structural insights into the mechanism of PEPCK catalysis. *Biochemistry* 45, 8254-8263 (2006).

93. Hanson, R.W. Thematic minireview series: a perspective on the biology of phosphoenolpyruvate carboxykinase 55 years after its discovery. *J Biol Chem* 284, 27021-27023 (2009).

94. Stark, R., Guebre-Egziabher, F., Zhao, X., Feriod, C., et al. A role for mitochondrial phosphoenolpyruvate carboxykinase (PEPCK-M) in the regulation of hepatic gluconeogenesis. *J Biol Chem* 289, 7257-7263 (2014).

95. Samuel, V.T., Liu, Z., Wang, A., Beddow, S.A., et al. Inhibition of protein kinase cepsilon prevents hepatic insulin resistance in nonalcoholic fatty liver disease. *J Clin Invest* 117, 739-745 (2007).

96. Ghosh, A., Shieh, J.J., Pan, C.J., Sun, M.S., Chou, J.Y. The catalytic center of glucose-6-phosphatase. HIS176 is the nucleophile forming the phosphohistidine-enzyme intermediate during catalysis. *J Biol Chem* 277, 32837-32842 (2002).

97. Sloop, K.W., Showalter, A.D., Cox, A.L., Cao, J.X.C., et al. Specific reduction of hepatic glucose 6-phosphate transporter-1 ameliorates diabetes while avoiding complications of glycogen storage disease. *J Biol Chem* 282, 19113-19121 (2007).

98. Hanson, R.W., Reshef, L. Regulation of phosphoenolpyruvate carboxykinase (GTP) gene expression. *Annu Rev Biochem* 66, 581-611 (1997).

99. Erion, D.M., Ignatova, I.D., Yonemitsu, S., Nagai, Y., et al. Prevention of hepatic steatosis and hepatic insulin resistance by knockdown of cAMP response element-binding protein. *Cell Metab* 10, 499-506 (2009).

100. Koo, S.H., Flechner, L., Qi, L., Zhang, X., et al. The CREB coactivator TORC2 is a key regulator of fasting glucose metabolism. *Nature* 437, 1109-1111 (2005).

101. Ravnskjaer, K., Kester, H., Liu, Y., Zhang, X., et al. Cooperative interactions between CBP and TORC2 confer selectivity to CREB target gene expression. *EMBO J* 26, 2880-2889 (2007).

102. Erion, D.M., Kotas, M.E., McGlashon, J., Yonemitsu, S., et al. cAMP-responsive element-binding protein (CREB)-regulated transcription coactivator 2 (CRTC2) promotes glucagon clearance and hepatic amino acid catabolism to regulate glucose homeostasis. *J Biol Chem* 288, 16167-16176 (2013).

103. Dullea, R., Salatto, C., Sciabola, S., Chen, T., et al. Study of CRTC2 pharmacology using antisense oligonuceotides. *Nucleic Acid Ther* 24, 127-138 (2014).

104. Haeusler, R.A., Kaestner, K.H., Accili, D. FoxOs function synergistically to promote glucose production. *J Biol Chem* 285, 35245-35248 (2010).

105. Matsumoto, M., Pocai, A., Rossetti, L., Depinho, R.A., Accili, D. Impaired regulation of hepatic glucose production in mice lacking the forkhead transcription factor Foxo1 in liver. *Cell Metab* 6, 208-216 (2007).

106. Altomonte, J., Richter, A., Harbaran, S., Suriawinata, J., et al. Inhibition of Foxo1 function is associated with improved fasting glycemia in diabetic mice. *Am J Physiol Endocrinol Metab* 285, E718-E728 (2003).

107. Samuel, V.T., Choi, C.S., Phillips, T.G., Romanelli, A.J., et al. Targeting foxo1 in mice using antisense oligonucleotide improves hepatic and peripheral insulin action. *Diabetes* 55, 2042-2050 (2006).

108. Stull, A.J., Wang, Z.Q., Zhang, X.H., Yu, Y., et al. Skeletal muscle protein tyrosine phosphatase 1B regulates insulin sensitivity in African Americans. *Diabetes* 61, 1415-1422 (2012).

109. lchebly, M., Payette, P., Michaliszyn, E., Cromlish, W., et al. Increased insulin sensitivity and obesity resistance in mice lacking the protein tyrosinephosphatase-1B gene. *Science* 283, 1544-1548 (1999).

110. Bandyopadhyay, D., Kusari, A., Kenner, K.A., Liu, F., et al. Protein-tyrosine phosphatase 1B complexes with the insulin receptor in vivo and is tyrosine-phosphorylated in the presence of insulin. *J Biol Chem* 272, 1639-1645 (1997).

111. Krüger, J., Trappiel, M., Dagnell, M., Stawowy, P., et al. Targeting density-enhanced phosphatase-1 (DEP-1) with antisense oligonucleotides improves the metabolic phenotype in high-fat diet-fed mice. *Cell Commun Signal* 11, 49 (2013).

112. Takashima, N., Tomoike, H., Iwai, N. Retinol-binding protein 4 and insulin resistance. *N Engl J Med* 355, 1392-1395 (2006).

113. Eynatten, M.V., Humpert, P.M. Retinol-binding protein-4 in experimental and clinical metabolic disease. *Expert Rev Mol Diagn* 8, 289-299 (2008).

114. Nobili, V., Alkhouri, N., Alibi, A., Ottino, S., et al. Retinol binding protein 4: a promising circulating marker of liver damage in pediatric nonalcoholic fatty liver disease. *Clin Gastroenterol Hepatol* 7, 575-579 (2009).

115. Stefan, N., Hennige, A.M., Staiger, H., Machann, J., et al. High circulating retinol-binding protein 4 is associated with elevated liver fat but not with total, subcutaneous, visceral, or intramyocellular fat in humans. *Diabetes Care* 30, 1173-1178 (2007).

116. Wu, H., Jia, W., Bao, Y., Lu, J., et al. Serum retinol binding protein 4 and nonalcoholic fatty liver disease in patients with type 2 diabetes mellitus. *Diabetes Res Clin Pract* 79, 185-190 (2008).

117. Yang, Q., Graham, T.E., Mody, N., Preitner, F., et al. Serum retinol binding protein 4 contributes to insulin resistance in obesity and type 2 diabetes. *Nature* 436, 356-362 (2005).

118. Moraes-Vieira, P.M., Yore, M.M., Dwyer, P.M., Syed, I., et al. RBP4 activates antigen-presenting cells, leading to adipose tissue inflammation and systemic insulin resistance. *Cell Metab* 19, 512-526 (2014).

119. Norseen, J., Hosooka, T., Hammarstedt, A., et al. Retinol-binding protein 4 inhibits insulin signaling in adipocytes by inducing proinflammatory cytokines in macro-phages through a c-Jun N-terminal kinase- and toll-like receptor 4-dependent and retinol-independent mechanism. *Mol Cell Biol* 32, 2010-2019 (2012).

120. Graham, T.E., Yang, Q., Blüher, M., Hammarstedt, A., et al. Retinol-binding protein 4 and insulin resistance in lean, obese and diabetic subjects. *N Engl J Med* 354, 2552-2563 (2006).

121. Cho, Y.M., Youn, B.S., Lee, H., Lee, N., et al. Plasma retinol-binding protein-4 concentrations are elevated in human subjects with impaired glucose tolerance and type 2 diabetes. *Diabetes Care* 29, 2457-2461 (2006).

122. Broch, M., Vendrell, J., Ricart, W., Richart, C., et al. Circulating retinol-binding protein-4, insulin sensitivity, insulin secretion, and insulin disposition index in obese and nonobese subjects. *Diabetes Care* 30, 1802-1806 (2007).

123. Tan, Y., Sun, L.Q., Kamal, M.A., Wang, X., et al. Suppression of retinol-binding protein 4 with RNA oligonucleotide prevents high-fat diet-induced metabolic syndrome and non-alcoholic fatty liver disease in mice. *Biochim Biophys Acta* 1811, 1045-1053 (2011).

124. Zanotti, G., Berni, R. Plasma retinol-binding protein: structure and interactions with retinol, retinoids, and transthyretin. *Vitam Horm* 69, 271-295 (2004).

125. Van Bennekum ,A.M., Wei, S., Gamble, M.V., Vogel, S., et al. Biochemical basis for de-pressed serum retinol levels in transthyretin-deficient mice. *J Biol Chem* 276, 1107-1113 (2001).

126. Zemany, L., Bhanot, S., Peroni, O.D., Murray, S.F., et al. Transthyretin antisense oligonucleotides lower circulating RBP4 levels and improve insulin sensitivity in obese mice. *Diabetes* 64, 1603-1614 (2015).

127. Du, K., Herzig, S., Kulkarni, R.N., Montminy, M. TRB3: a tribbles homolog that inhibits Akt/PKB activation by insulin in liver. *Science* 300, 1574-1577 (2003).

128. Prudente, S., Hribal, M.L., Flex, E., Turchi, F., et al. The functional Q84R polymorphism of mammalian Tribbles homolog TRB3 is associated with insulin resistance and related cardiovascular risk in Caucasians from Italy. *Diabetes* 54, 2807-2811 (2005).

129. Takahashi, Y., Ohoka, N., Hayashi, H., Sato, R. TRB3 suppresses adipocyte differentiation by negatively regulating PPAR gamma transcriptional activity. *J Lipid Res* 49, 880-892 (2008).

130. Leonardini, A., Laviola, L., Perrini, S., Natalicchio, A., Giorgino, F. Cross-talk between PPARγ and insulin signaling and modulation of insulin sensitivity. *PPAR Res* 2009, 818945 (2009).

131. Weismann, D., Erion, D.M., Ignatova-Todorava, I., Nagai, Y., et al. Knockdown of the gene encoding Drosophila tribbles homologue 3 (Trib3) improves insulin sensitivity through peroxisome proliferator-activated receptor-γ (PPAR)-γ activation in a rat model of insulin resistance. *Diabetologia* 54, 935-944 (2011).

132. Kahn, S.E., Hull, R.L., Utzschneider, K.M. Mechanisms linking obesity to insulin resistance and type 2 diabetes. *Nature* 444, 840-846 (2006).

133. Gregor, M.F., Hotamisligil, G.S. Inflammatory mechanisms in obesity. *Annu Rev Immunol* 29, 415-445 (2011).

134. Jiao, P., Ma, J., Feng, B., Zhang, H., et al. FFA-induced adipocyte inflammation and insulin resistance: involvement of ER stress and IKKβ pathways. *Obesity (Silver Spring)* 19, 483-491 (2011).

135. Nguyen, M.T., Satoh, H., Favelyukis, S., Babendure, J.L., et al. JNK and tumor necrosis factor-alpha mediate free fatty acid-induced insulin resistance in 3T3-L1 adipocytes. *J Biol Chem* 280, 35361-35371 (2005).

136. Hotamisligil, G.S., Erbay, E. Nutrient sensing and inflammation in metabolic diseases. *Nat Rev Immunol* 8, 923-934 (2008).

137. Hayden, M.S., Ghosh, S. Shared principles in NF-kappaB signaling. *Cell* 132, 344-362 (2008).

138. Cai, D., Yuan, M., Frantz, D.F., Melendez, P.A., et al. Local and systemic insulin resistance resulting from hepatic activation of IKK-beta and NF-kappa B. *Nat Med* 11, 183-190 (2005).

139. Helsley, R.N., Sui, Y., Park, S., Liu, Z., et al. Targeting IκB kinase β in adipocyte lineage cells for treatment of obesity and metabolic dysfunctions. *Stem Cells* 34, 1883-1895 (2016).

140. Aderem, A., Ulevitch, R.J. Toll-like receptors in the induction of the innate immune response. *Nature* 406, 782-787 (2000).

141. Heldwein, K.A., Fenton, M.J. The role of Toll-like receptors in immunity against mycobacterial infection. *Microbes Infect* 4, 937-944 (2002).

142. Senn, J.J. Toll-like receptor-2 is essential for the development of palmitate-induced insulin resistance in myotubes. *J Biol Chem* 285, 14842 (2006).

143. Caricilli, A.M., Nascimento, P.H., Pauli, J.R., Tsukumo, D.M.L., et al. Inhibition of toll-like receptor 2 expression improves insulin sensitivity and signaling in muscle and white adipose tissue of mice fed a high-fat diet. *J Endocrinol* 199, 399-406 (2008).

144. Hirosumi, J., Tuncman, G., Chang, L., Gorgun, C.Z., et al. A central role for JNK in obesity and insulin resistance. *Nature* 420, 333-336 (2002).

145. Liakos, A., Karagiannis, T., Bekiari, E., Boura, P., Tsapas, A. Update on long-term efficacy and safety of dapagliflozin in patients with type 2 diabetes mellitus. *Ther Adv Endocrinol Metab* 6, 61-67 (2015).

146. Jakher, H., Chang, T.I., Tan, M., Mahaffey, K.W. Canagliflozin review – safety and efficacy profile in patients with T2DM. *Diabetes Metab Syndr Obes* 12, 209-215 (2019).

147. Frampton, J.E. Empagliflozin: a review in type 2 diabetes. *Drugs* 78, 1037-1048 (2018).

148. Kovacich, N., Chavez, B. Ertugliflozin (steglatro): a new option for SGLT2 inhibition. *P T* 43, 736-742 (2018).

149. Markham, A., Keam, S.J. Sotagliflozin: first global approval. *Drugs* 79, 1023-1029 (2019).

150. Hanefeld, M., Schaper, F. Acarbose: oral anti-diabetes drug with additional cardiovascular benefits. *Expert Rev Cardiovasc Ther* 6, 153-163 (2008).

151. Sugimoto, S., Nakajima, H., Kosaka, K., Hosoi, H. Review: miglitol has potential as a therapeutic drug against obesity. *Nutr Metab (Lond)* 12, 51 (2015).

152. Scott, L.J. Sitagliptin: a review in type 2 diabetes. *Drugs* 77, 209-224 (2017).

153. Keating, G.M. Vildagliptin: a review of its use in type 2 diabetes mellitus. *Drugs* 74, 587-610 (2014).

154. Dave, D.J. Saxagliptin: a dipeptidyl peptidase-4 inhibitor in the treatment of type 2 diabetes mellitus. *J Pharmacol Pharmacother* 2, 230-235 (2011).

155. McKeage, K. Linagliptin: an update of its use in patients with type 2 diabetes mellitus. *Drugs* 74, 1927-1946 (2014).

156. Jarvis, C.I., Cabrera, A., Charron, D. Alogliptin: a new dipeptidyl peptidase-4 inhibitor for type 2 diabetes mellitus. *Ann Pharmacother* 47, 1532-1539 (2013).

157. Geary, R.S., Bradley, J.D., Watanabe, T., Kwon, Y., et al. Lack of pharmacokinetic interaction for ISIS 113715, a 2'-O-methoxyethyl modified antisense oligonucleotide targeting protein tyrosine phosphatase 1B messenger RNA, with oral antidiabetic compounds metformin, glipizide or rosiglitazone. *Clin Pharmacokinet* 45, 789-801 (2006).

158. Digenio, A., Pham, N.C., Watts, L.M., Morgan, E.S., et al. Antisense inhibition of protein tyrosine phosphatase 1B with IONIS-PTP-1BRx improves insulin sensitivity and reduces weight in overweight patients with type 2 diabetes. *Diabetes Care* 41, 807-814 (2018).

159. Van Dongen, M.G.J., Geerts, B.F., Morgan, E.S., Brandt, T.A., et al. First proof of pharmacology in humans of a novel glucagon receptor antisense drug. *J Clin Pharmacol* 55, 298-306 (2015).

160. Luu, K.T., Morgan, E.S., Bhanot, S., Geary, R., et al. Population pharmacokinetics and pharmacodynamics of IONIS-GCGRRx, an antisense oligonucleotide for type 2 diabetes mellitus: a red blood cell lifespan model. *J Pharmacokinet Pharmacodyn* 44, 179-191 (2017).

161. Morgan, E.S., Tai, L., Pham, N.C., Overman, J.K., et al. Antisense inhibition of glucagon receptor by IONIS-GCGRRx improves type 2 diabetes without increase in hepatic glycogen content in patients with type 2 diabetes on stable metformin therapy. *Diabetes Care* 42, 585-593 (2019).

162. Van Meer, L., Moerland, M., Van Dongen, M., Goulouze, B., et al. Renal effects of antisense-mediated inhibition of SGLT2. *J Pharmacol Exp Ther* 359, 280-289 (2016).

163. Van Meer, L., Van Dongen, M., Moerland, M., De Kam, M., et al. Novel SGLT2 inhibitor: first-in-man studies of antisense compound is associated with unexpected renal effects. *Pharmacol Res Perspect* 5, e00292 (2017).

164. Morgan, E., Bethune, C., Larouche, R., Xia, S., et al. ISIS-GCCRRX, a novel glucocorticoid receptor antisense drug reduces CHOL, TG, attenuates dexamethasone

induced hepatic IR without systemic GC antagonism in normal subjects. EASD Virtual Meeting. Barcelona 2013; Session: PS 048 Liver metabolism, Abstract # 698.

165. Chikara, G., Sharma, P.K., Dwivedi, P., Charan, J., et al. A narrative review of potential future antidiabetic drugs: should we expect more? *Indian J Clin Biochem* 33, 121-131 (2018).

166. Loomba, R., Morgan, E., Fung, M., Watts, L., et al. An international, randomized, placebo-controlled phase 2 trial demonstrates novel effects of DGAT2 antisense inhibition in reducing steatosis without causing hypertriglyceridemia in T2DM patients. *J Hepatol* 70, PS-106 (2019).

167. Graham, M.J., Lee, R.G., Bell, T.A., Fu, W., et al. Antisense oligonucleotide inhibition of apolipoprotein C-III reduces plasma triglycerides in rodents, nonhuman primates, and humans. *Circ Res* 112, 1479-1490 (2013).

168. Digenio, A., Dunbar, R.L., Alexander, V.J., Hompesch, M., et al. Antisense-mediated lowering of plasma apolipoprotein C-III by volanesorsen improves dyslipidemia and insulin sensitivity in type 2 diabetes. *Diabetes Care* 39, 1408-1415 (2016).

169. Clinical Trials [Internet]. Bethesda, M.D.: U.S. National Library of Medicine; c2018. Study of ISIS 703802 in Subjects With Hypertriglyceridemia, Type 2 Diabetes Mellitus, and Nonalcoholic Fatty Liver Disease; 2018 Sep 26 [cited 2020 Apr 6]. https://clinicaltrials.gov/ct2/show/NCT03371355.

170. Yip, S.C., Saha, S., Chernoff, J. PTP1B: a double agent in metabolism and oncogenesis. *Trends Biochem Sci* 35, 442-449 (2010).

171. Kennedy, B.P. Role of protein tyrosine phosphatase-1B in diabetes and obesity. *Biomed Pharmacother* 53, 466-470 (1999).

172. Goldstein, B.J. Protein-tyrosine phosphatase 1B (PTP1B): a novel therapeutic target for type 2 diabetes mellitus, obesity and related states of insulin resistance. *Curr Drug Targets Immune Endocr Metabol Disord* 1: 265-275 (2001).

173. Zabolotny, J.M., Bence-Hanulec, K.K., Stricker-Krongrad, A., Haj, F., et al. PTP1B regulates leptin signal transduction *in vivo*. *Dev Cell* 2, 489-495 (2002).

174. Morris, D.L., Rui, L. Recent advances in understanding leptin signaling and leptin resistance. *Am J Physiol Endocrinol & Metab* 297, E1247-E1259 (2009).

175. Liu, G. Recent advances in protein-tyrosine-phosphatase PTP1B inhibitors for treatment of type 2 diabetes and obesity. *Drugs Fut* 29, 1245 (2004).

176. Zhang, Z.Y., Lee, S.Y. PTP1B inhibitors as potential therapeutics in the treatment of type 2 diabetes and obesity. *Expert Opin Inv Drug* 12, 145-153 (2003).

177. Panzhinskiy, E., Ren, J., Nair, S. Pharmacological inhibition of protein tyrosine phosphatase 1B: a promising strategy for the treatment of obesity and type 2 diabetes mellitus. *Curr Med Chem* 20, 2609-2625 (2013).

178. Johnson, T.O., Ermolieff, J., Jirousek, M.R. Protein tyrosine phosphatase 1B inhibitors for diabetes. *Nat Rev Drug Discov* 1, 696-709 (2002).

179. Bjourson, A.J., Cooper, J.E. Band-stab PCR: a simple technique for the purification of individual PCR products. *Nucleic Acids Res* 20, 4675 (1992).

180. Li, D., Aung-Htyt, M., Ham, K.A., Fletcher, S., Wilton, S.D. A Splice intervention therapy for autosomal recessive juvenile Parkinson's disease arising from Parkin mutations. *Int J Mol Sci* 21, 7282 (2020).

181. Stein, C.A., Castanotto, D. FDA-approved oligonucleotide therapies in 2017. *Mol Ther* 25, 1069-1075 (2017).

182. Le, B.T., Raguraman, P., Kosbar, T.R., Fletcher, S., et al. Antisense oligonucleotides targeting angiogenic factors as potential cancer therapeutics. *Mol Ther Nucleic Acids* 14, 142-157 (2019).

183. Saoud, J., Mendell, J., Rodino-Klapac, L, et al. Safety profile and pharmacokinetic properties of eteplirsen in the treatment of boys with Duchenne muscular dystrophy. *Neurology* 82 (10 Suppl), S6.001 (2014).

184. GSK and Prosensa Announce Primary Endpoint Not Met in Phase III Study of Drisapersen in Patients With Duchenne Muscular Dystrophy. Available online, https://globenewswire.com/news-release/2013/09/20/574726/10049265/en/GSK-and-Prosensa-Announce-Primary-Endpoint-Not-Met-in-Phase-III-Study-of-Drisapersen-in-Patients-With-Duchenne-MuscularDystrophy.html (accessed on 28 April 2020).

Chapter 3

Exploring novel design of chemically modified splice-modulating antisense oligonucleotides towards tackling Duchenne muscular dystrophy

1. Introduction

Splice modulating antisense oligonucleotides (AO) were first reported in 1993 [1]. Since then, novel applications of these molecules have been reported for therapeutic application for different maladies. Some of the latest examples of their clinical translation include Exondy51 and Vyondys53 [2-4], these splice modulating AOs were approved by the US FDA in 2016 and 2019, respectively, as drugs for the treatment of Duchenne muscular dystrophy (DMD). These inspiring milestones of successful drug development present a great therapeutic potential for splice modulating AOs and encourage researchers with differentiated backgrounds and expertise to enter this field.

Development of splice modulating AO molecules can be divided into two stages. The first step is to confirm a best performing AO sequence (i.e. inducing splice modulation most efficiently) by screening a variety of AO candidates covering different regions of a target exon. This strategy has been utilized for selection of the lead candidate AO sequences inducing exon 2 skipping of the highest efficiency in the *PTPN1* transcript (see Chapter 2 of the thesis). The second stage of AO development is to optimize the known best performing compound in terms of efficacy (for more effective splice modulation), safety (for lower cytotoxicity), specificity, delivery and stability (for higher resistance to nuclease) through novel designs and chemical modification. In this chapter, DMD was chosen as a disease modal, and mouse *H-2K^{b}-tsA58 mdx* (*H2K*) myotubes were utilized as an *in vitro* cellular modal for the exploration of optimizing efficacy, cellular toxicity, and/or stability of *Dmd* exon 23 skipping AOs through novel designs of chemical modification.

The section 2 of this chapter provides an overview of DMD and its current treatment options. This is then followed by a review of development of splice modulation based molecular therapies targeting DMD (section 3). The latter part (section 4) of this chapter describes my

study of novel designs of chemically-modified AOs for splice modulation utilizing DMD as a model system.

2. Duchenne muscular dystrophy

2.1 Overview

Duchenne muscular dystrophy (DMD) is the most common and severe form of muscular dystrophy, a class of inherited muscle wasting conditions. DMD mainly affects boys with an approximate frequency of 1 in 5000 [5]. Affected children show no obvious signs at birth, then manifest onset of clinical symptoms by 3 years of age [6]. Early symptoms include muscle weakness and abnormal movement, such as waddling gait and difficulty in running and jumping. Relentless progression of muscle wasting leads to impaired ambulation normally before 12 years of age, in some cases, by seven [6-9]. Later, DMD teenagers develop cardiomyopathy and respiratory problems as a result of cardiac and respiratory muscle weakness, that eventually leads to pre-mature death in their early thirties due to heart and pulmonary failure [9, 10].

DMD and its milder allelic condition, Becker muscular dystrophy (BMD) are both caused by mutations in the *DMD* gene located on the X chromosome (Xp21.2). *DMD*, the huge human gene containing 79 exons (**figure 2.1**), encodes the cytoskeletal structural protein dystrophin [11, 12]. Dystrophin assembles other sarcolemma (muscle fibre cell membrane) associated proteins (dystroglycan, sarcoglycan, syntrophin, and dystrobrevin) forming the dystrophin associated complex (**figure 2.2**). The dystrophin complex acts as a bridge connecting the intracellular actin cytoskeleton and the extracellular matrix (**figure 2.2**), thereby protecting muscle fibers from damage by maintaining the integrity and stability of sarcolemma during muscle contraction [13]. The dystrophin complex also provides binding sites for neuronal nitric oxide synthase (nNOS) (**figure 2.2**), an enzyme that plays a vital role in myogenesis

and muscle repair following injury [14]. As proteins in the dystrophin complex are tightly connected, abnormalities affecting any one of the proteins due to mutations may disrupt the integrity of the complex, thereby leading to its dysfunction [15].

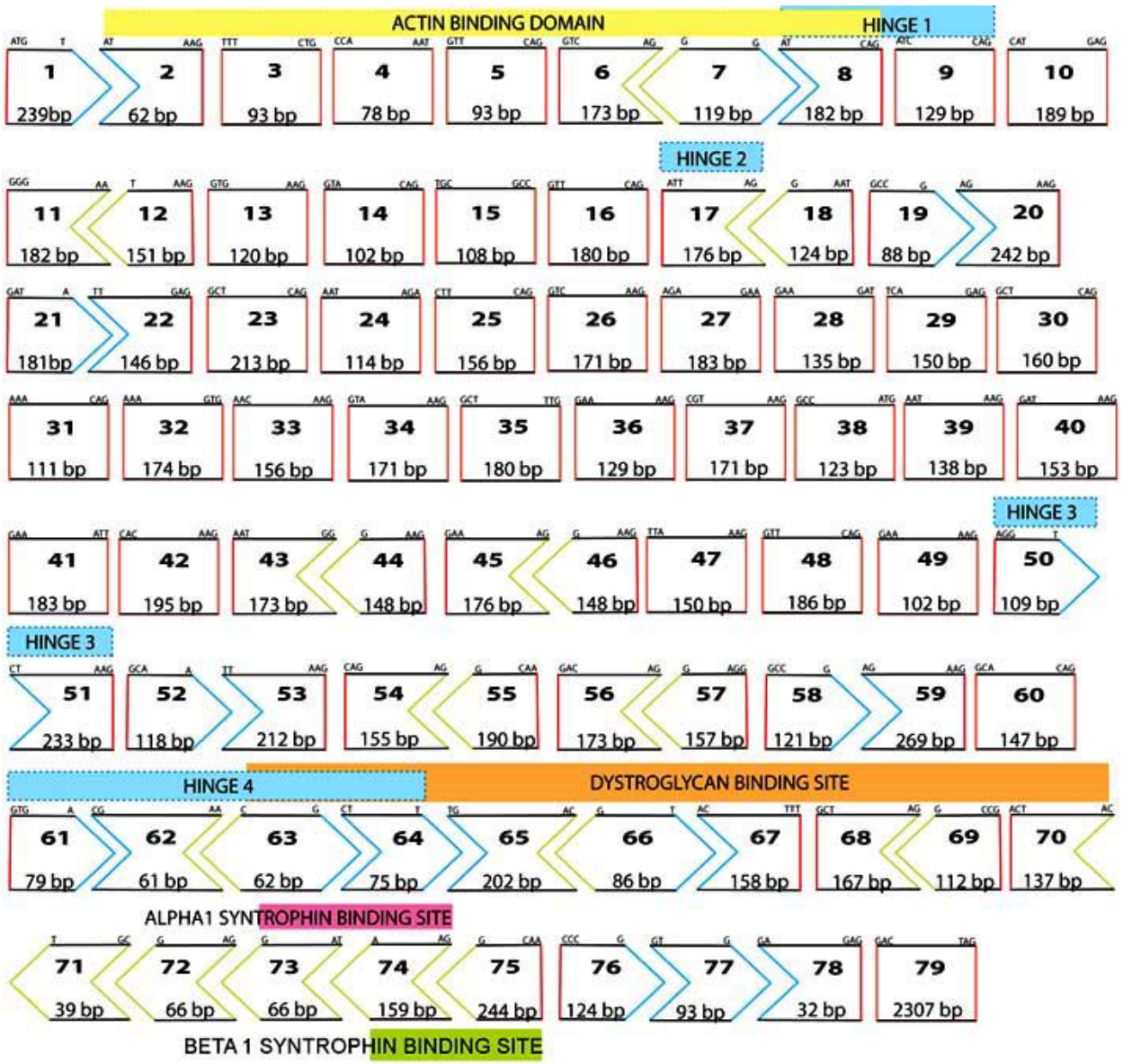

Figure 2.1 Structure of the dystrophin gene transcript. The structure indicates the reading frame and major functional domains of the dystrophin gene transcript. The dystrophin transcript contains 34 in-frame exons, represented as boxes whereas interlocking forward and reverse arrows and notches indicate codons spanning the exon:exon junction. Sequences of junction crossing codons are shown above the boxes, and base pair numbers of each exon are shown within each box underneath the exon number. Adapted from Mitrpant C, Fletcher S, and Wilton S, 2009 [12].

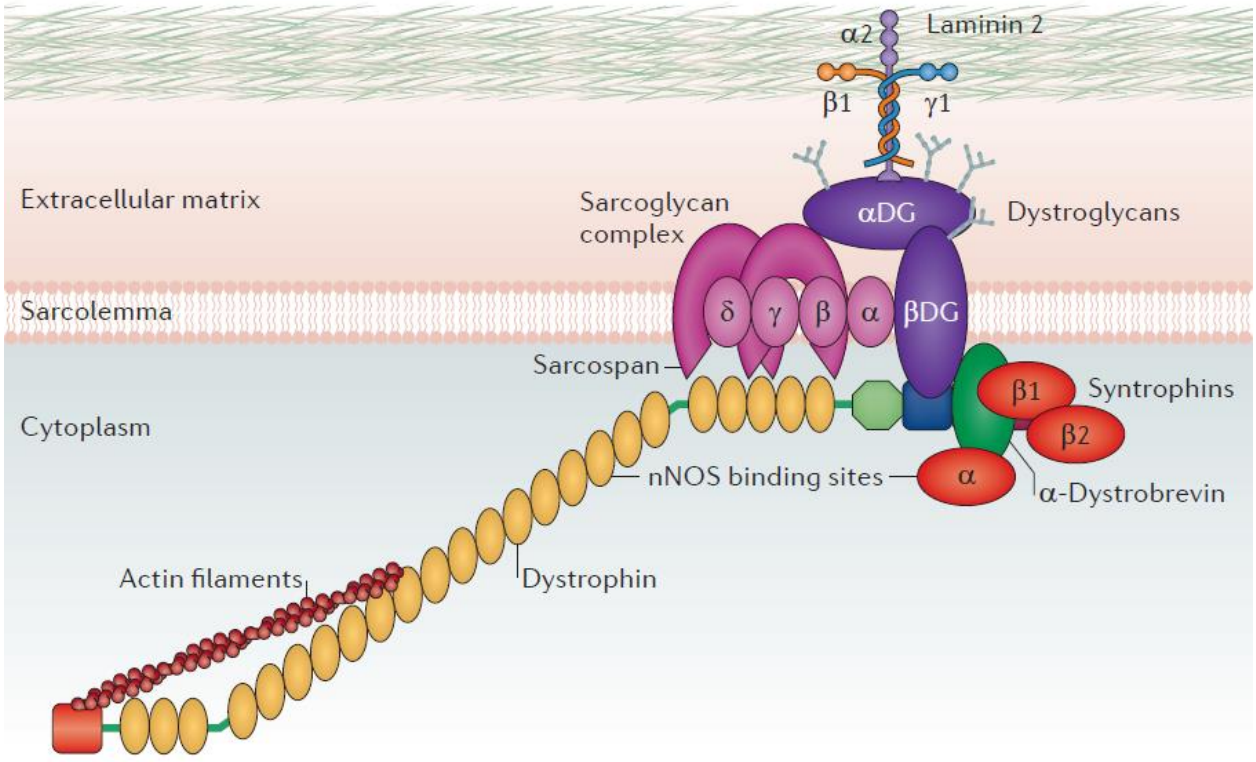

Figure 2.2 The dystrophin-associated proteins. Dystrophin assembles other sarcolemma associated proteins including dystroglycan subunits (αDG and βDG), sarcoglycan complex, syntrophins (α, β1, β2) and α-dystrobrevin forming dystrophin complex. The dystrophin complex acts as a bridge connecting intracellular the cytoskeleton (actin) and extracellular matrix. Neuronal nitric oxide synthase (nNOS) binds to α-syntrophin but also has a binding site in repeat 17 of the rod domain of dystrophin. Adapted from Fairclough RJ, Wood MJ, and Davies KE, 2013 [16].

More than 4700 causative mutations of DMD have been recognized in the dystrophin gene. Generally, these mutations can be classified as three types: deletions (65.8%), duplications (13.6%), and point mutations (20.6%) including nonsense, missense, splice site mutations, micro-deletions and -insertions [17], however, a small number of complex rearrangements have been reported (madden, Human mutation). Missense mutations are rare but have been reported in crucial functional domains. Typically, mutations that induce premature termination codons (out-of-frame mutations) disrupt the reading frame, and result in a lack of functional dystrophin production, thereby disabling the protective dystrophin complex and leading to sarcolemma damage and myofibre necrosis, and finally substitution of muscles by connective and scar tissues [18]. Nevertheless, DNA lesions that do not disrupt the *DMD* reading frame (in-frame mutations) normally cause BMD, as presence of these mutations allows synthesis of an internally truncated, partially functional dystrophins [10]. Symptoms

of BMD may vary from borderline DMD to asymptomatic, depending upon the quantity and quality of the dystrophin produced. In some cases, people with BMD may not be diagnosed until their later years in life, and live into their eighties with clinical presentations ranging from loss of ambulation to cardiomyopathy [16].

2.2 Current treatments

Currently there is no cure for DMD, and it is likely that there never will be a true "cure". The "gold standard" treatment options for the disease are corticosteroid therapy, physical rehabilitation, management of respiratory function, (prevention of respiratory tract infections) and nocturnal assisted ventilation. These interventions have significantly extended life expectancy of DMD patients by about one decade, otherwise in most cases they succumb to the disorder by 20 years of age. However, these therapies are limited to alleviating symptoms, reducing inflammation, and slowing muscle wasting [19-21]. None of these conventional interventions has halted the progression of DMD, i.e. addressed the root cause of the disease which is a deficiency of functional dystrophin protein synthesis and localization. Besides, long term administration of steroids (eg. prednisone, prednisolone, and deflazacort) leads to ineluctable side effects including bone demineralization, vertebral compression fractures, weight gain, hypertension and/or behavior disorders [22, 23].

Cell and/or gene replacement may be considered as logical therapeutic strategies for treating DMD. However, replacing patient tissues with cells producing or potentially producing functional dystrophins has to face several obstacles, such as ethical issues, limited availability of donor muscles, survival and proliferation of administered cells, and immune activation [24]. On the other hand, developing gene replacement approaches is challenging as the size of the *DMD* transcript (cDNA) coding for the full-length 427 kDa dystrophin is beyond the cargo capacity of currently used viral vectors [25]. Although recent advances in vector design have seen promising preclinical and clinical results with mini- and micro-dystrophin cassettes

introduced into animal models *in utero* using adeno-associated virus (AAV) vectors, the sufficiency and sustainability of dystrophin expression required for treating DMD, a chronic condition still poses challenges [26-29].

3. Splice modulating AO based intervention targeting DMD

3.1 Overview of AO-mediated exon-skipping

Since the first splice modulating AOs were developed in 1993 [1], interest in field increased, especially in 2016 when Eteplirsen, to treat a subset of DMD patients received 'first in class' accelerated approval from the US FDA. The successful clinical translations now include Exondy 51 and Vyondys 53 [2-4], approved by the US FDA in 2016 and 2019, respectively as therapeutic molecules for the treatment of DMD. Specifically, these splice modulating AO drugs (Exondy 51 and Vyondys 53) promote functional protein production by inducing *DMD* exon 51 and 53 skipping to restore of the open reading frame around amenable frame shifting deletions [30, 31].

AO-induced splice modulation, in particular, exon skipping has been developed as a therapeutic strategy to treat DMD [12, 32-36]. Exon skipping is achieved by administration of AOs designed to anneal to specific motifs of the target exon. By hybridization to a target region, AOs are assumed to obscure the exon from the splicing machinery so that it is excluded with the flanking introns [33]. As the out-of-frame mutations in the *DMD* gene disrupt the reading frame and abolish production of functional dystrophin, skipping of the mutation-flanking exons by AOs can restore the reading frame and allow the synthesis of partially functional dystrophin isoforms, similar to those found in BMD patients. A schematic illustration of healthy, DMD, and BMD dystrophin transcripts is shown in **figure 3.1**. More specifically, according to different types of mutations (duplications, deletions, point

mutations), skipping of duplicated exons, exons adjacent to deletions (both exon duplication and deletion may lead to frame-shift), and exons containing nonsense or missense point mutations, or indels can remove or avoid the early-onset termination signals, and thereby restore the reading frame and recover partially functional BMD-like dystrophin expression [33-36].

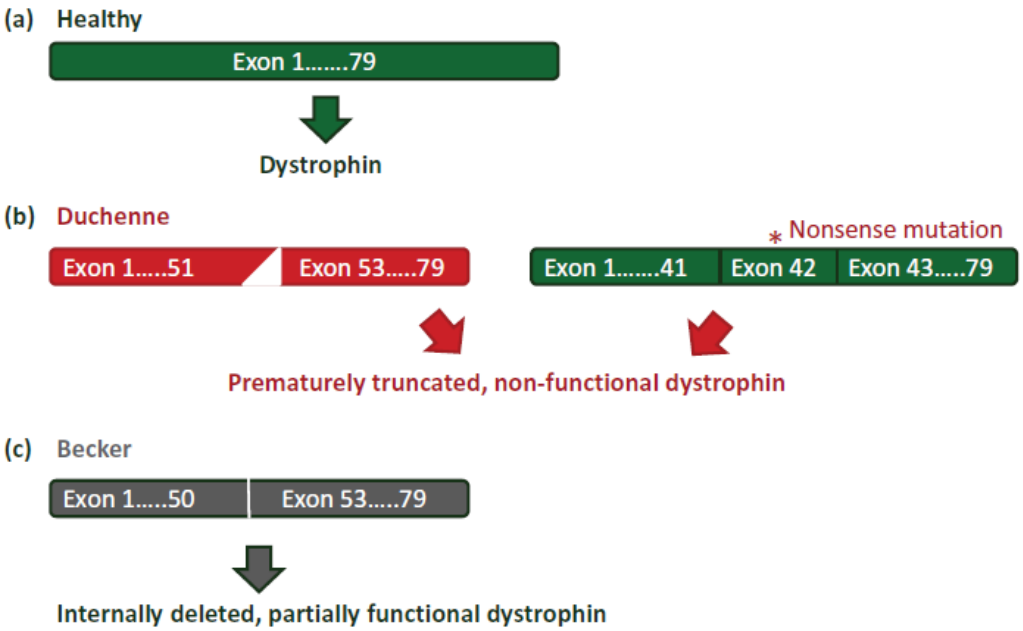

Figure 3.1 Schematic example of *DMD* gene expression in healthy (a), DMD (b), and BMD (c) indivduals (a) The healthy allele dystrophin mRNA transcript encodes full length, functional dystrophin protein. (b) In DMD patients, mutations disrupt the reading frame (e.g. a deletion of exon 52, left panel; nonsense mutation in exon 42, right panel), induce premature termination codons, and result in production of truncated, non-functional dystrophin protein. (c) In BMD patients, mutations maintain the reading frame, allow synthesis of internally truncated, but partially functional dystrophin protein. Adapted from Niks EH, Aartsma-Rus A, 2013 [33].

3.2 Exon skipping based intervention towards tackling DMD

The earliest endeavor to explore splice modulation as a research tool in the DMD field can date back to 1995 [37]. Since then, increasing numbers of researchers have entered this field, and substantive AO sequences inducing skipping of different exons have been reported, in an attempt to correct the disrupted dystrophin reading frame resulting from the protein truncating mutations. Two animal models, the *mdx* mouse bearing a nonsense mutation in exon 23, and a canine model that manifests with exon 7 exclusion, both resulting in out-of-frame *DMD* transcripts, have been utilized for the research into DMD. AOs developed to address mutations in animal models demonstrate that exon skipping strategies are feasible in

muscle cells both *in vitro* and *in vivo*, and thereby offer a prediction of the therapeutic potential of AOs in humans.

Apart from designing new AO sequences for exon skipping, a major focus of DMD research is also placed on optimizing known AO sequences, in terms of their efficacy (for more effective exon skipping), safety (for lower cytotoxicity), and stability (for higher resistance to nuclease) through introducing and evaluating novel chemical modifications. Herein, a brief review of exon-skipping AO development to treat DMD in the past two decades is given as follows, providing a picture of "co-evolution" of AO sequences and their chemistries.

3.2.1 Initial effort: human dystrophin exon 19 skipping

In 1995, Takeshima et al. designed a 31-mer AO to modulate dystrophin pre-mRNA splicing in an *in vitro* expression system, using Hela cell nuclear extracts and a partial dystrophin gene sequence construct [37]. This was the first report of AO-induced splice modulation of the dystrophin transcript: the AO of 31 nucleotides in length was 2′-O-Methyl (2′-OMe)-modified sequence targeting a splicing enhancer within exon 19, found to be deleted in a DMD patient. Subsequently, Pramono et al. reported *DMD* exon 19 skipping after transfection of the same 31-mer AO sequence, however in the form of DNA chemistry instead of 2′-OMe, into human lymphoblastoid cells [38]. This was the first report of inducing dystrophin exon skipping in living cells. In both publications, the 31-mer AOs were not phosphorothioate (PS) modified, but clearly induced some degree of exon-19 skipping *in vitro*. Although DNA AOs are typically used to induce mRNA degradation through RNase-H activation, Pramono and colleagues reported the DNA AO as a splice modulating oligonucleotide. According to this finding, DNA AOs could to some extent induce splice modulation. Nevertheless, the unequivocal demonstration of the induced transcripts with an exon deletion suggests that exon skipping occurred within the nucleus and that the resultant exon 19 deleted transcripts would no longer be susceptible to RNase-H degradation [38].

In 2001, Takeshima et al. again showed the efficacy of their previously reported 31-mer AO sequence, however, in the form of a DNA-PS AO, rather than 2′-OMe or natural DNA, to induce exon 19 skipping in muscle cells derived from a DMD patient carrying an exon 20 deletion [39]. Gebski et al. replicated exon 19 skipping in immortalized murine myogenic cells after transfection with the 31-mer DNA-PS oligonucleotide at 300 nM concentration, but the exon skipping was inefficient, less than 5% of transcripts were exon 19-deleted [40]. In comparison, the DNA/2′-OMe-PS mixmer of this sequence (contains 26 DNA nucleotides and 9 2′-OMe nucleotides) achieved greater exon 19 skipping at 300 nM, further, its fully modified 2′-OMe-PS counterpart resulted in 100% exon 19 skipping at an even lower AO concentration (100 nM). This clearly demonstrated that chemical modification is crucial for optimizing exon skipping efficacy after AO sequence design [40]. Gebski and co-workers' report indicates that the 2′-OMe-PS AOs are significantly more efficient than their DNA counterparts in inducing exon 19 skipping, at least when delivered into cells as cationic lipoplexes. Continuing the 31-mer AO story, Yagi et al. transfected primary muscle cells from a DMD patient with 2′-O, 4′-C-ethylene-bridge nucleic acid (ENA) modified chimeric AO of 5-21-5 ENA-2′-OMe-ENA gapmer design on a PS backbone. This AO achieved 40 times higher efficacy of exon 19 skipping in contrast to the conventional DNA-PS oligomer [41].

Instead of dedicating more efforts to optimizing the 31-mer exon 19 skipping sequence by testing new chemical modifications, Errington et al. developed a series of shorter AOs modified by full 2′-OMe-PS chemistry of varying lengths (12 to 20 nucleotides). These AOs targeted the exon 19 splicing enhancer region and the donor/acceptor splice sites [42]. They showed that short AO sequences complementary to the splice enhancer site achieved comparable exon 19 skipping efficacy to that induced by the original 31-mer AO, and with higher efficiency than their counterparts complementary to the donor or acceptor splice sites.

This indicated that AOs directed at the splicing enhancer region tended to be marginally more effective than those that targeted the splice sites, at least for this exon [42].

3.2.2 AO development targeting other exons in human dystrophin gene

Inspired by the pioneer proof-of-concept dystrophin exon 19 skipping of *DMD* gene by the "natural" deoxy and chemically modified AOs, subsequent efforts have expanded this strategy by developing AOs to skip other exons in the dystrophin gene transcript, for the correction of different out-of-frame mutations. Researchers have also learned lessons from the early exon 19 skipping reports, for example, AOs composed of modified analogues exhibit better exon skipping efficacy than the "naturally occurring" DNA oligomers, AOs of length shorter than 31-mer may be sufficient to induce efficient exon skipping, and the splicing enhancer sequences may not be the only suitable target for AO design.

Van Deutekom et al. developed a 20-mer dystrophin exon 46 skipping AO sequence through a two-step selection. They began with screening 12 partly overlapping 2′-OMe-PS AOs covering the polypurine-rich exon recognition region of mouse exon 46, using a gel mobility shift assay. Based on the result, five AO candidates were selected, and redesigned to target the human *DMD* sequence for further exon skipping validation in DMD patient primary myoblasts. Their best performing AO was reported to induce up to 15% of exon 46 skipping at 1 μM concentration [43].

Takagi et al. have screened ENA modified 2′-OMe-PS chimeric AOs of 15 to 18 nucleotides in length (each contained 10 ENA residues) targeting dystrophin exon 45 and 46, respectively. Two AO candidates, named AO85 and AO27, were found to induce strongest skipping for exon 45 and 46, respectively. Furthermore, they optimized AO27 by relocating the positions of ENA residues in the sequence and thereby AO92 was developed with much higher exon 46 skipping efficacy than AO27. This suggested that varied dispersion of chemical modification(s) in a given AO sequence may lead to varied exon skipping efficacy [44].

Aartsma-Rus et al. performed comparative analysis of fully modified 20-mer 2′-OMe-PS, 22-mer PMO, 14-mer locked nucleic acid (LNA), and 14-mer peptide nucleic acid (PNA) AOs in inducing dystrophin exon 46 skipping in primary myoblasts, derived from a DMD patient carrying exon 45 deletion [45]. Using the 2′-OMe-PS AO as a positive control, a fully LNA modified AO led to the highest yield of exon 46 skipped transcripts (up to 98%). In contrast, the 2′-OMe-PS control and a PMO AO achieved 75% and 5% exon 46 skipping, respectively. However, the PNA, tagged with four lysines to facilitate uptake, did not induce any exon skipping [45]. This study confirmed the feasibility of using 2′-OMe-PS as a first-line chemistry for developing exon skipping AOs, highlighted the potential application of LNAs in this field, and suggested that better conjugates may be required to aid PMO and PNA cellular delivery. Towards this end, the same group developed 2′-OMe-PS AOs inducing dystrophin exon 44, 49, 50, 51, and 53 skipping and evaluated their therapeutic potential in muscle cells from six DMD patents [46]. They also reported induction of multiexon skipping by administration of different cocktails of 2′-OMe-PS AOs that were designed to skip exon 43, 44, 45, and 51 [47].

Later, Wilton et al. tested over four hundred and seventy 2′-OMe-PS AOs in normal human myoblasts, targeting all exons in the *DMD* gene transcript, except for the first and last exons [48]. The length of these AOs varied from 20 to 31 nucleotides, and approximately two thirds of the AOs were able to induce specific exon skipping at varying levels. Importantly, a general trend was observed where AOs directed at the first half of a target exon sequence induced relatively higher skipping efficiencies. It is also noteworthy that in some cases an AO candidate could induce skipping of a target exon together with a flanking exon, while for other exons, a combination of AOs as a ‘cocktail’ was required to induce target exon skipping [48].

Fletcher et al. reported dystrophin exon 19, 20, 52, and 53 targeting peptide-conjugated PMO AOs that induced exon skipping *in vivo*, by administering these PMOs into C57BL/10ScSn mice (without mutations) at a dosage of 20 mg/kg per injection, in order to generate transient 'DMD' like and 'BMD' like mouse dystrophinopathy models [49]. Efficient single (exon 19, 20; exon 52, 53) or double (dual exon 19/20, dual exon 52/53) exon-skips were achieved by single or cocktail PMO administration, leading to disruption or maintenance of the dystrophin reading frame, respectively [49]. This study indicated that peptide conjugation can facilitate PMO AO delivery to cells *in vivo* and thereby greatly improve splice modulation efficacy. In addition, utilization of PMOs in the healthy mouse model to induce transient dystrophin silencing highlights the potential of antisense PMOs as a useful tool for gene functionalization.

Heemskerk et al. compared the 2′-OMe-PS and PMO AOs targeting exon 44, 45, 46, and 51 *in vivo* in *mdx* mice [50]. AOs were administered by injection for 2 consecutive days with 2.9 nmol (approximately 20 µg) in 50 µl physiologic saline. In terms of exon 44 skipping, no significant difference was observed between AOs of 2′-OMe-PS and PMO chemistries, however, PMOs were found to induce higher levels of exon 45, 46, and 51 skipping than their 2′-OMe-PS counterparts [50].

Shimo et al. investigated the scope of LNA modification in exon skipping as mixmer AO constructs [51]. A series of 15-mer LNA/DNA-PS chimeric AOs containing five LNA analogues in each sequence were designed and synthesized to target *DMD* exon 58. Two candidates targeting the 5' and 3' splice sites of the exon, respectively, were found to induce efficient exon 58 skipping. Further AO optimization by increasing the number of LNA modifications led to identification of the best-performing 15-mer AO candidate containing 8 LNA units. It is also worth noting that the proportion of LNA modification in a chimeric sequence and the melting temperature of the AO are important factors contributing to the

overall efficacy and specificity of exon skipping. In addition, this study suggested the minimum length of LNA modified AOs inducing exon 58 skipping was 7 nucleotides [51]. Inspired by Shimo's work, Pires et al. expanded the application of LNA modification to other exons by developing a 16-mer chimeric LNA modified AO inducing effective exon 51 skipping in DMD patient myoblasts. Importantly, LNA modification of this AO candidate accounted for 60% of the nucleotides [52].

Jirka et al. compared exon 45 and 53 targeting 2′-Fluoro (2′-F)-PS modified AOs and their 2′-OMe-PS counterparts for induced exon skipping in primary human myoblasts [53, 54]. They demonstrated that relatively higher exon skipping efficacy was achieved by the 2′-F-PS AOs than the 2′-OMe-PS controls. Further evaluation of the exon 53 targeting AOs in patient-derived myoblasts confirmed the relative advantage of 2′-F-PS modification in inducing exon skipping *in vitro* [54].

Watanabe et al. developed a PMO-based AO to induce efficient exon 53 skipping via a two-step screening process [55]. At first, they designed and evaluated thirty-eight 25-mer, overlapping 2′-OMe-PS AOs covering exon 53 completely, as a result, an intra-exon region of 35 nucleotides in length was found to be the best target region for exon skipping induction through AO binding. In the second stage, twenty-five PMO AOs (15 to 25-mer) targeting the identified region were designed and tested, resulting in the selection of a best-performing 21-mer candidate, named NS-065/NCNP-01. Western blot analysis demonstrated dystrophin production in DMD patient cells after administration of NS-065/NCNP-01 [55]. Recently, Lee et al. designed six 30-mer PMO AOs using a predictive software algorithm developed by their group targeting exon 45, 51, 52, 53, 54, and 55, respectively [56]. They transfected these PMOs as a cocktail into myotubes transdifferentiated from fibroblasts of a DMD patient bearing deletion of exon 46 to 50 and achieved efficient multi-exon skipping (exon 45 to 55), to restore the dystrophin reading frame and allowed partial functional dystrophin production.

3.2.3 *Mdx* mouse dystrophin exon 23 skipping AO development

In 1998, Dunckley et al. reported design and evaluation of three 2′-OMe modified AOs (12 to 14 nucleotides in length) targeting the *mdx* mouse *Dmd* exon 23 [57]. However, after transfecting these AOs into primary *mdx* myoblasts, only one candidate apparently induced very low level multi-exon skipping (exon 23 to 29). In 1999, Wilton et al. reported achievement of efficient and specific *Dmd* exon 23 skipping in primary *mdx* myoblasts by administration of a 20-mer 2′-OMe-PS AO complementary to the 5' splice site of intron 23 [58]. An 18-mer AO designed to target the 3' splice site of intron 22 did not induce any exon 23 skipping *in vitro* [58]. Next, Mann et al. evaluated exon skipping induction by AOs, for the first time, in *H-2K*^{b}*-tsA58* (*H2K*) *mdx* myoblasts [59]. In this study, as the previously reported 20-mer intron 23 5' splice site targeting AO did not entirely replicate the exon 23 skipping effect in *H2K* myoblasts, they extended the AO sequence to a 25-mer, leading to both exon 23 and exon 22/23 dual skipping. Furthermore, they demonstrated restoration of dystrophin expression *in vivo* by this 25-mer 2′-OMe-PS AO through intramuscular AO injections into *mdx* mice [59]. They then optimized exon 23 skipping 2′-OMe-PS AOs by screening six new sequences targeting the 5' donor splice site of exon 23 (i.e. 5' splice site of intron 23). The champion candidate, M23D (+02-18) achieved higher exon skipping efficiency at lower dosages, compared to other AOs tested [60]. In 2005, Lu et al. reported systemic delivery of the same 2′-OMe-PS M23D (+02-18) in *mdx* mice by intravenous administration of the AO (dissolved in saline with block co-polymer F127) at 250 µg/mL, through tail vein injection, thrice a week. Functional dystrophin expression was detected in skeletal muscles body wide, except for the cardiac muscles [61].

In order to enhance the exon skipping efficacy of PMO mediated exon 23 targeting AOs, Gebski et al. reported the use of leashes (DNA, RNA, or modified nucleic acid sequences, complementary to the PMO) to allow formation of lipoplexes (formation of PMO/leash

duplex complexing with a cationic liposome) for improved PMO cellular uptake [62]. The neutral charge of the PMO does not allow for direct complexing with a cationic liposome. The leash aided PMO delivery resulted in efficient exon 23 skipping both *in vitro* and *in vivo*, induced by an extended PMO sequence, M23D (+07-18). Slightly shortened but functional dystrophin was detected at the sarcolemma of muscle fibers 2 weeks after injection of the PMO into *mdx* mice [62]. Subsequently, Fletcher et al. compared the efficacy of PMO and 2′-OMe-PS forms of M23D (+07-18), and PNA AO sequences including M23D (-2-16) and (-2-18), in inducing exon 23 skipping and dystrophin restoration, by localized and systemic delivery of the AOs of different chemistries into *mdx* mice [63]. Their results demonstrated that PMO modification was preferred, as it achieved longer duration of AO effect and stronger dystrophin expression in contrast to the 2′-OMe-PS and PNA sequences [63]. Alter et al. also performed systemic administration of PMO M23D (+07-18) in 6-week-old *mdx* mice [64]. Recovery of functional dystrophin was detected body wide in skeletal muscles, with the highest expression levels in diaphragm, abdominal, and intercostal regions. However, like the 2′-OMe-PS AO [61], PMO treatment did not induce detectable dystrophin in the heart [64].

Yin et al. explored the PNA chemistry as an option for exon skipping AO construction by evaluating PNA modified M23D (+2-18) for induced dystrophin exon 23 skipping in the *mdx* mouse *in vitro* and *in vivo* [65]. Transfection of this PNA into *H2K mdx* myoblasts only led to weak *Dmd* exon 23 skipping, however, *in vivo* studies showed that intramuscular injection of a single dosage of 5 μg of the PNA into *mdx* mice, at two-month of age resulted in significant increases in dystrophin synthesis a fortnight after administration, in comparison with their age-matched control group [65]. Later, Gao et al. compared the efficacy of PNA and PMO forms of M23D (+2-18) in recovery of functional dystrophin production, via systemic administration of the AO candidates to *mdx* mice at a weekly dose of 50 mg/kg, for three

weeks [66]. Except for cardiac muscle, body wide dystrophin synthesis was achieved by both PNA and PMO AOs in a comparable manner. Specifically, both chemistries induced exon 23 skipping at a similar level in quadriceps, while the PNA achieved slightly higher skipping levels in gastrocnemius and triceps and the PMO resulted in better exon skipping efficiency in abdominal and diaphragm than the PNA [66]. In addition, this group explored optimizing the exon skipping efficacy of the PNA by rational design of longer sequences (25, 26, 28, and 30 nucleotides) and the 30-mer candidate, M23D (+14-16) was found to be more potent than its shorter counterparts [66]. On the other hand, Le et al. introduced serinol nucleic acid (SNA), a close mimic of PNA to AO construction for inducing splice modulation [67]. In this study, SNA, PNA, and 2′-OMe-PS forms of M23D (+2-18) were synthesized and transfected into myotubes differentiated from *H2K mdx* myoblasts by complexing with Lipofectin reagent. At 400 nM concentration, the 2′-OMe-PS AO achieved ~90% of exon 23 skipping compared to SNA (52%) and PNA (~10%) [67]. This indicated that SNA may be a promising alternative chemistry to PNA, however *in vivo* evaluation is required to gain more insights of SNA-modified AO potential.

Goyenvalle et al. reported *in vivo* comparisons between tricyclo-DNA (tcDNA) M23D (+2-13), 2′-OMe-PS M23D (+2-18), and PMO M23D (+7-18) in their ability to induce exon 23 skipping and functional correction of dystrophin in *mdx* mouse [68]. Different modified AOs were intravenously injected into *mdx* mice at 200 mg/kg/week for 12 weeks. The tcDNA treatment achieved up to six-fold higher levels of exon 23 skipping in muscles of various body regions compared to other chemistries [68]. It is notable that tcDNA treatment restored dystrophin production in heart while 2′-OMe-PS and PMO did not. Later, the same group also reported that a truncated tcDNA AO, M23D (-1-13) induced efficient exon 23 skipping and dystrophin restoration in *mdx* mice [69].

In 2016, Le et al. reported evaluation of anhydrohexitol nucleic acid (HNA), cyclohexenyl nucleic acid (CeNA), and D-altritol nucleic acid (ANA) for their potential as splice modulating AOs [70]. These modifications were introduced to the 2′-OMe-PS M23D (+2-18) sequence to generate mixmer AOs, while the fully modified 2′-OMe-PS sequence was used as a positive control. All AOs induced efficient *Dmd* exon 23 skipping in myotubes differentiated from *H2K mdx* myoblasts, however, the 2′-OMe-PS control demonstrated higher exon skipping efficiency than its mixmer counterparts. For example, the control AO achieved 40% of exon 23 skipping at 50 nM concentration while the mixmers induced 20-23% of skipping. However, HNA, CeNA, and ANA modified mixmers showed lower cellular toxicity and higher nuclease stability compared to the 2′-OMe-PS control according to the results of *in vitro* cytotoxicity and phosphodiesterase I-based enzyme resistance assays [70]. Later, this group reported exploration of a nucleobase modification, 5-(phenyltriazol)-2′-deoxyuridine in constructing AOs for inducing splice modulation [71]. Results of transfection experiments indicated that 2′-OMe-PS M23D (+2-18) containing 5-(phenyltriazol)-2′-deoxyuridine analogues achieved comparable exon 23 skipping efficiency to the fully modified 2′-OMe-PS control [71]. In 2017, the same group also reported that introduction of LNA modification to 2′-OMe-PS M23D (+2-18) allowed its truncated mixmer versions, i.e. LNA/2′-OMe-PS M23D (+1-17), (-1-16), (-2-15), and (-3-14) to retain their capability of inducing exon 23 skipping. In contrast, the corresponding truncated fully modified 2′-OMe-PS AOs failed to mediate exon 23 skipping as efficiently as the shortened LNA modified mixmers [72]. Although these observations were based on preliminary *in vitro* data, the potential of LNA analogues in constructing splice modulating AO is clearly highlighted.

3.2.4 Canine dystrophin Exon 6 and exon 8 skipping AO development

Although the *mdx* mouse bears a nonsense mutation in dystrophin exon 23, it superficially appears asymptomatic and lives a normal life span. In contrast, the golden retriever muscular

dystrophy (GRMD) affected dog with manifests with exon 7 exclusion as a consequence of an exon 7 acceptor splice site mutation suffers from DMD-like symptoms, and is therefore a more relevant animal modal for DMD phenotypic and preclinical studies [73].

In 2006, McClorey et al. reported design of AOs targeting dystrophin exon 6 and exon 8 in GRMD affected dog [74]. Administration of these AOs as a cocktail achieved exon 6/8/9 multi- skipping and thus correction of the dystrophin reading frame. Moreover, comparison of exon skipping efficacy was made between 2′-OMe-PS, PMO, and cell penetrating peptide-conjugated PMOs. The latter led to induction of exon 6/8/9 multi- skipping and resultant dystrophin restoration at the highest level [74]. In 2009, Yokota et al. reported *in vivo* administration of a PMO cocktail containing three AOs targeting exon 6 and exon 8 in the GRMD dog, via intravenous delivery at a dosage of 200 mg/kg, seven times per week [75]. PMO treatment resulted in a transcript with in-frame deletion of three exons (exon 6, 7, 8 and 9) and achieved body wide dystrophin restoration [75]. Later, Saito et al. reproduced the exon skipping effect of the 3 sequence-containing PMO cocktail in GRMD dog, further, they demonstrated the feasibility of direct translation of these PMOs from the dog model to human patients, by achieving human dystrophin exon 6/8/9 multi skipping and the resultant dystrophin restoration in DMD patient cells after transfection of these AOs [76].

3.3 Clinical trials

DMD patients possessing deletions of dystrophin exon 45 to 50, 47 to 50, 48 to 50, 50, 52, and 52 to 63 account for approximately 13% of the total DMD affected population, and it is therefore the largest sub-group of the disease [77]. As the disrupted dystrophin reading frame for all these deletions can be restored by further removal of exon 51, this exon was considered a preferential target for the development of exon skipping AO therapeutics for DMD. Two AO candidates of different chemistries have been developed for the induction of exon 51 skipping [78-81]. PRO051 (commercially named drisapersen) is a fully 2′-OMe-PS

modified candidate developed by a biotechnology company in Netherlands named Prosensa (later acquired firstly by GlaxoSmithKline and then by BioMarin Pharmaceuticals), while Eteplirsen (brand name Exondys 51) is a PMO based candidate developed in Australia (Wilton et al., 2006) and licensed to Sarepta Therapeutics (formerly known as AVI Biopharmaceuticals). Clinical trials were initiated in parallel for these two AOs following similar procedures: detection of dystrophin expression after an intramuscular injection, and subsequent demonstration of increased dystrophin restoration with correct localization by analyzing biopsies collected before and after AO treatment [82, 83].

In line with predictions made in the pre-clinical animal studies [84], both clinical trials demonstrated dystrophin expression near the injection site, indicating a proof of concept in restoration of dystrophin synthesis. Both candidates progressed to phase III clinical trials, however, investigation of drisapersen sponsored by GlaxoSmithKline was halted in 2013 due to the failure to meet primary and secondary end points. A detailed report of this study was published by Voit et al [85]. It was not surprising that drisapersen did not meet the end points in this study as no concomitant increase of dystrophin production was detected after extended periods of drisapersen treatment. Although Goemans et al. reported drisapersen achieved dystrophin restoration of up to 15% of healthy levels [86], a critical analysis of the data suggests that only a fractional increase from baseline dystrophin synthesis was induced by drisapersen treatment [87]. Further investigation is underway to understand if males of younger age are more responsive to drisapersen, and the latest data released suggest that this candidate might be useful in treating the less impaired DMD population [88]. However, in the light of unproven efficacy and severe adverse effects, including injection site reactions, drisapersen did not receive FDA approval.

In contrast, eteplirsen was offered accelerated approval by the US FDA in September 2016 as it induced a modest increase in functional dystrophin production after administration to DMD

patients, with an excellent safety profile. It was reported that 48 weeks after eteplirsen treatment, 10 out of 12 teenage participants achieved maintenance of ambulation capability. The functional benefits were supported by evidence at the mRNA and protein levels showing that synthesis of BMD-like partially functional dystrophin was restored in the DMD participants treated by eteplirsen [89]. Furthermore, phase II clinical trials of eteplirsen in boys 4–6 years old (NCT02420379) and older males aged 7–21 years (NCT02286947) are ongoing [81]. It is worth noting that most recently golodirsen (Vyondys 53) targeting *DMD* exon 53 has been granted accelerated approval by the US FDA.

In addition, clinical trials of three AO candidates: PRO044 (BMN044), PRO045 (BMN45) and PRO053 (BMN053) designed to target dystrophin exon 44, 45, and 53 for induced exon skipping respectively, were halted by BioMarin Pharmaceuticals. On the other hand, the PMO drug candidate developed by Sarepta Therapeutics: SRP-4045 for inducing exon 45 skipping is currently in phase III clinical trials (NCT02500381) and recruiting participants [81]. Another PMO candidate, NS-065/NCNP-01 (viltolarsen) targeting exon 53 developed by a Japanese pharmaceutical company, Nippon Shinyaku Co., Ltd has recently completed a phase II clinical trial (NCT02740972), and it is enrolling participants in an extension study (NCT03167255) at present. Wave Life Sciences has been performing a global Phase I clinical trial (NCT03508947) for safety and tolerability examination of a drug candidate named WVE-210201, targeting exon 51 of DMD [81], however, the trial has recently been withdrawn after no increases in dystrophin expression was detected in trial participants.

4. Exploration of novel chemical modification to improve therapeutic effects of splice modulating AOs in DMD

Splice modulating AO induced exon skipping has been widely explored and validated as a feasible alternative therapy for DMD [90]. The accelerated approval of Exondys 51 and

Vyondys 53 (PMO chemistry, Sarepta Therapeutics) and rejection of Drisapersen (2′-OMe-PS chemistry, Biomarin) by the US FDA highlights the importance of utilizing and optimizing chemical modification in therapeutic AO development, towards improving efficacy and reducing toxicity. More specifically, development and optimization of AOs incorporating nucleotide analogues aim at enhancing their target binding affinity, specificity, and nuclease stability, in contrast to the non-modified AOs (DNA/RNA).

To expand the scope of chemically modified nucleic acids in developing AO therapeutics, compounds composed of different modified nucleotide analogues targeting the *mdx* mouse *Dmd* exon 23 were designed, synthesized, and evaluated in this study. Briefly, based on an *in vitro* DMD cellular modal, modified AOs were transfected into cultured *mdx* mouse *H2K* myotubes, followed by semi-quantitative examination of their exon skipping efficacy by performing reverse transcriptase polymerase chain reaction (RT-PCR) and subsequent densitometry analysis. In addition, the modified AOs were also characterized by their cytotoxicity (cell viability assay), and/or target binding affinity (melting temperature assay), and/or nuclease stability (enzyme degradation assay).

4.1 General protocols for exon skipping AO experiments

4.1.1 Design and synthesis of chemically-modified AOs

All AOs were prepared in-house on either an ABI Expedite® 8909 (Applied Biosystems, Foster City, California, USA) or ÄKTA Oligopilot Plus 10 (GE Healthcare Life Sciences, Parramatta, NSW, Australia) oligonucleotide synthesizer using standard phosphoramidite chemistry at the 1 µmol scale. All synthesis reagents for ÄKTA and Expedite syntheses were purchased from Merck Millipore (Bayswater, VIC, Australia) and Sigma-Aldrich (Castle Hill, NSW, Australia). Synthesized AOs were deprotected and cleaved from the solid support by treatment with 1.0M NH_4OH (Merck Millipore) at 55^{o}C overnight, and the crude AOs were then purified by desalting through Illustra NAP-10 Columns (GE Healthcare Life Sciences).

4.1.2 Cell culture and transfection

H2K mdx myoblasts [91, 92] (provided by Prof. Sue Fletcher and Prof. Steve Wilton's laboratory, Murdoch University, Australia) were cultured and differentiated as described previously [93]. Briefly, when 60–80% confluent, myoblast cultures were treated with trypsin (Thermo Fisher Scientific, Scoresby, VIC, Australia) and seeded onto 24-well plates, pre-treated with 50 μg/mL poly-D-lysine (Merck Millipore, Bayswater, VIC, Australia), followed by 100 μg/mL Matrigel (Corning, supplied through In Vitro Technologies, Noble Park North, VIC, Australia) at a density of 2.5×10^4 cells/well. Cells were differentiated into myotubes in Dulbecco's Modified Eagle Medium (DMEM) (Thermo Fisher Scientific) containing 5% horse serum (Thermo Fisher Scientific) by incubating at 37°C, 5% CO_2 for 24 hours. AOs were complexed with Lipofectin transfection reagent (Thermo Fisher Scientific) at the ratio of 2:1 (w:w) (lipofectin:AO) and used in a final transfection volume of 500 μL/well in a 24-well plate, as per the manufacturer's instructions, except that the solution was not removed after 3 hours.

4.1.3 RNA extraction and RT-PCR

Total RNA was extracted from transfected cells using Direct-zol™ RNA MiniPrep Plus with TRI Reagent® (Zymo Research, supplied through Integrated Sciences, Chatswood, NSW, Australia) as per the manufacturer's instructions. The dystrophin transcripts were then analysed by nested-RT-PCR using SuperScript™ III Reverse Transcriptase III and AmpliTaq Gold® 360 DNA Polymerase (Thermo Fisher Scientific) across exons 20–26 as described previously [93]. PCR products were separated on 2% agarose gels in Tris–acetate–EDTA buffer and the images were captured on a Fusion Fx gel documentation system (Vilber Lourmat, Marne-la-Vallee, France). Densitometry was performed by Image J software [94]. To quantify the actual exon skipping efficacy induced by AOs, the amounts of full length (901bp), exon 23 skipped (688bp), and exon 22/23 dual skipping (542bp) products are expressed as percentages of total dystrophin transcript products.

4.1.4 Cell viability assay

Cells were seeded and transfected with the AOs as described previously. After 24 hours, cell viability assay was performed using a dye-based colorimetric assay using WST-1 reagent (2-(4-iodophenyl)-3-(4-nitro-phenyl)-5-(2,4-disulfophenyl)-2H-tetrazolium) (Sigma-Aldrich). Briefly, WST-1 solution was added at ratio 1:10 (v/v) per well and incubated for 4 hours at 37°C, 5% CO_2. The absorbance was then measured with a microplate reader (FLUOstar Omega, BMG Labtech, Germany) at a wavelength of 450 nm.

4.1.5 Melting temperature analysis of the AOs

The samples were prepared as duplexes by mixing equal volumes of the AO and the synthetic complementary RNA sequence at 2 μM concentration in a buffer solution containing 10 mM NaCl, 0.01 mM EDTA adjusted to pH 7.0 with 10 mM sodium phosphate buffer. Before loading into a quartz cuvette of 1 mm path-length, the duplexes were denatured at 95°C for 10 minutes followed by slow cooling to room temperature. The melting process was monitored in a Shimadzu UV-1800 Spectrophotometer (Shimadzu, Rydalmere, NSW, Australia) with the Peltier temperature controller over the range of 20–90°C at a ramp rate of 1.0°C min^{-1}. T_m values were then determined as the maxima of the first derivative plots of the melting curves.

4.1.6 Nuclease stability analysis of the AOs

Stability of AOs against 3′→5′ exonuclease degradation was investigated using phosphodiesterase I from *Crotalus adamanteus* venom (Sigma-Aldrich, Castle Hill, NSW, Australia). Briefly, 10 μM of the AOs were incubated with 0.08 units/mL phosphodiesterase in a buffer containing 10 mM Tris–HCl, 100 mM NaCl, and 15 mM $MgCl_2$ in a final volume of 60 μL. Samples were incubated at 37 °C and 10 μL samples were collected at 0, 10, 30, 60 and 120 minutes and quenched with an equal volume of 80% formamide containing bromophenol blue and xylene cyanol gel tracking dyes. The samples were then heated for 5 min at 95°C and analyzed by 20% denaturing polyacrylamide gel electrophoresis.

Quantitation and image capture was performed on a Fusion Fx gel documentation system (Vilber Lourmat, Marne-la-Vallee, France).

4.2 Evaluation of exon skipping by novel chemically modified AOs in DMD modal

4.2.1 Morpholino nucleic acid (MNA)-modified 2′-OMe AO

4.2.1.1 Introduction

Nucleic acid technologies have attracted significant interest in recent years as a means of targeting the molecular pathogenesis of various diseases [95]. AOs can efficiently regulate the expression of cellular RNAs by selectively cleaving, blocking, modifying or repairing pathogenic messenger RNAs [95]. AOs bind to complementary target RNA sequences through hydrogen bonding. High affinity RNA targeting, better mis-match recognition and a high degree of nuclease resistance are key factors in developing successful AO-based therapeutics. AOs composed of naturally occurring nucleotides show low target binding affinity and poor resistance to nucleases, and consequently are unsuitable for therapeutic application.

To overcome these limitations and improve their pharmacokinetic profile, chemically-modified nucleic acid analogues, mainly of sugar and phosphate backbone modifications, have been utilized in developing therapeutic oligonucleotides. So far, prominent chemical modifications that have been granted approval for clinical usage include PS [96], used in Vitravene, Kynamro, and Spinraza; 2'-OMe [53, 54, 97-99], used in Macugen and Onpattro; 2'-Fluoro (2'-F) [53, 54, 97-99], used in Macugen; 2'-O-methoxyethyl (2'-OMOE) [100], used in Kynamro and Spinraza; and PMO [101], used in Exondys 51 and Vyondys 53 [2-4]. Of these, 2'-OMe and PMO have been explored extensively for AO-mediated splice modulation. In addition, several other analogues such as LNA [72, 102, 103], unlocked nucleic acid (UNA) [104], PNA [105], SNA [67], tcDNA [106], TINA [107], HNA [70], CeNA [70], and ANA [70] have also been investigated in splice modulation. Recently, nucleobase-modified AOs

containing 2-thioribothymidine, and 5-(phenyltriazol)-2'-deoxyuridine nucleotides have been reported to induce exon skipping in DMD model systems [108].

AO-mediated exon skipping has been established as one of the most promising therapeutic strategies for treating DMD [16, 87, 89, 109-112]. Skipping the mutation-associated exons can restore the dystrophin reading frame and rescue the production of the internally truncated but partially functional dystrophin protein. PMO and 2'-OMe-PS-modified AOs have been investigated in phase-3 clinical trials for DMD [10, 16, 87, 89, 90, 110-113]. The PMO drugs (Exondys 51 and Vyondys 53) have been granted accelerated approval by the US FDA [2-4]. In contrast, the 2'-OMe-PS-based candidate (drisapersen) was rejected mainly due to safety issues and lack of efficacy [114]. Although PMO-modified oligonucleotides show an excellent safety profile, production is not compatible with standard oligonucleotide synthesis chemistries for generation as mixmers with other well-known nucleotide analogues, and large-scale production of PMOs is challenging due to distinctive synthesis procedures. Therefore, it is necessary to evaluate alternatively modified PMO analogues that can be used for AO drug development. Towards this goal, herein, we report the synthesis of morpholino nucleic acid (MNA) phosphoramidite (**Figure 4.2.1.1)** and the evaluation of MNA/2'-OMe-PS mixmer AOs for inducing exon 23 skipping in *mdx* mouse myogenic cells.

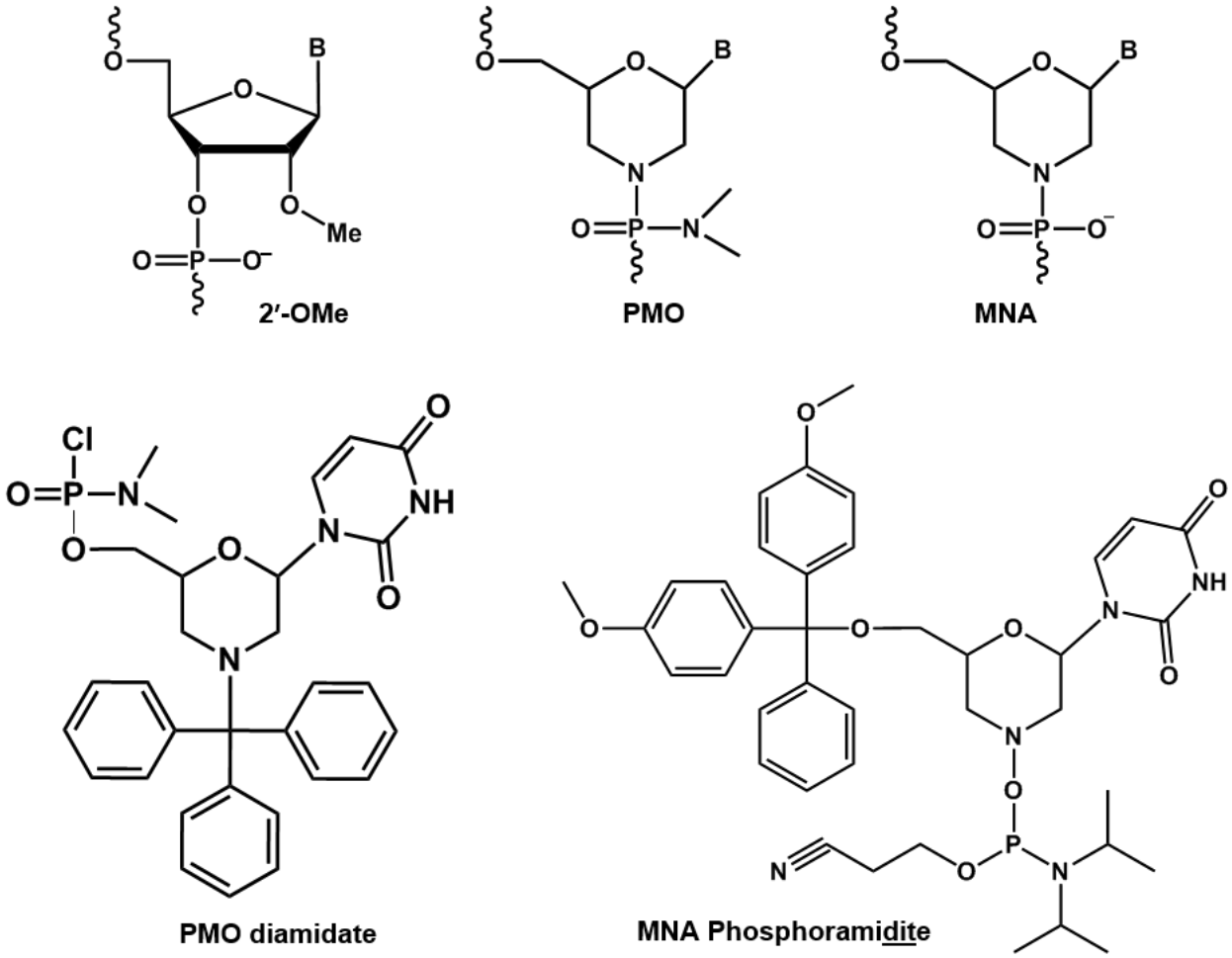

Figure 4.2.1.1 Structural representations of: 2'-OMe, PMO, MNA, PMO diamidate and MNA phosphoramidite monomer.

4.2.1.2 Results and discussion: evaluation of melting temperature, exon skipping, and cytotoxicity using MNA-modified 2'-OMe-PS AO

Inspired by the efficacy of PMO candidates to induce exon skipping in DMD and the recent clinical benefit of the PMO candidate eteplirsen (Exondys 51), we envisaged the construction of a mixmer AO candidate with a morpholino ring on a phosphodiester/phosphorothioate backbone (we name this as morpholino nucleic acid, MNA) via standard phosphoramidite chemistry. For this purpose, we have synthesized morpholino-urdine (MNA-U) phosphoramidite that is compatible with other nucleotide chemistries to synthesize a mixmer AO using an oligonucleotide synthesizer.

In our study, we used DMD as a well characterized model system to evaluate the potential of MNA-modified AOs. Two candidates, derived from a previously reported sequence, M23D

(+2-18) were synthesized at the one micromole scale: a fully modified 2'-OMe-PS AO control and a MNA-modified 2'-OMe-PS mixmer (**Table 4.2.1.2**) that were designed to target *Dmd* exon 23 carrying a nonsense mutation. The MNA/2'-OMe-PS AO synthesized in this preliminary study had one MNA nucleotide at position 10.

We performed thermal stability experiments for both AOs using the complementary target RNA (5'-rAG GUA AGC CGA GGU UUG GCC-3'). Notably, the MNA/2'-OMe-PS duplex was found to be less stable (55.4°C) compared to the control 2'-OMe-PS AO (59.8°C) (**Table 4.2.1.2**).

AO names	Sequence, 5'→ 3' direction	Tm, °C
2'-OMe-PS	GGCCAAACCUCGGCUUACCU	59.8
MNA/2'-OMe-PS	GGCCAAACC**U**$^{\mathbf{M}}$CGGCUUACCU	55.4
MNA nucleotide is represented in bold underlined with a superscript 'M'		

Table 4.2.1.2 AO sequences used in this study and their melting temperature.

To evaluate the efficacy of these AOs, *mdx* mice H2K myoblasts were propagated as previously described [115]. Cells were plated at confluent density and allowed to differentiate for 24 hours in low serum medium, prior to transfection. The 2'-OMe-PS and MNA/2'-OMe-PS AOs were then transfected into differentiated myotubes, complexed with Lipoectin transfection reagent at 400 nM concentration, in a 2:1 Lipofectin /AO ratio. Transfected cells were incubated for 24 h, cells were harvested and total RNA was extracted, followed by RT-PCR (SuperScript® III one-step RT-PCR kit and specific primer pair were used to amplify exon 20-26) and 2% agarose gel electrophoresis. The results clearly showed that both MNA/2'-OMe-PS and the fully modified 2'-OMe-PS AOs induced efficient skipping of exon 23 (full length band at 901 bp) at a 400 nM concentration by yielding the 688 bp deletion product (**Figure 4.2.1.2.1A**). Densitometry analysis of the gel images was performed to determine the percentage of skipped transcript (**Figure 4.2.1.2.1B**). Specifically, the 2'-OMe-

PS AO achieved a higher percentage of exon skipping compared with the MNA/2'-OMe-PS mixmer AO (**Figure 4.2.1.2.1**). However, under these conditions, the MNA/2'-OMe-PS mixmer AO induced the exon 23 deletion product of 688 bp at a similar yield at 400 nM (60%, **Figure 4.2.1.2.1**), compared to the 2'-OMe-PS AO (61%, **Figure 4.2.1.2.1**). Notably, both AOs showed an additional band at 542 bp, due to the undesired dual exon 22/23 skipping products (**Figure 4.2.1.2.1A**). This product was more evident in the case of the control 2'-OMe-PS AO (28%, **Figure 4.2.1.2.1**) compared with the MNA/2'-OMe-PS mixmer AO (25%, **Figure 4.2.1.2.1**). The efficacy of 2'-OMe-PS and the MNA/2'-OMe-PS AOs were analysed three times and it was observed that the conventional 2'-OMe-PS was slightly better at inducing exon skipping. Although these are very preliminary data, more systematic studies are currently underway.

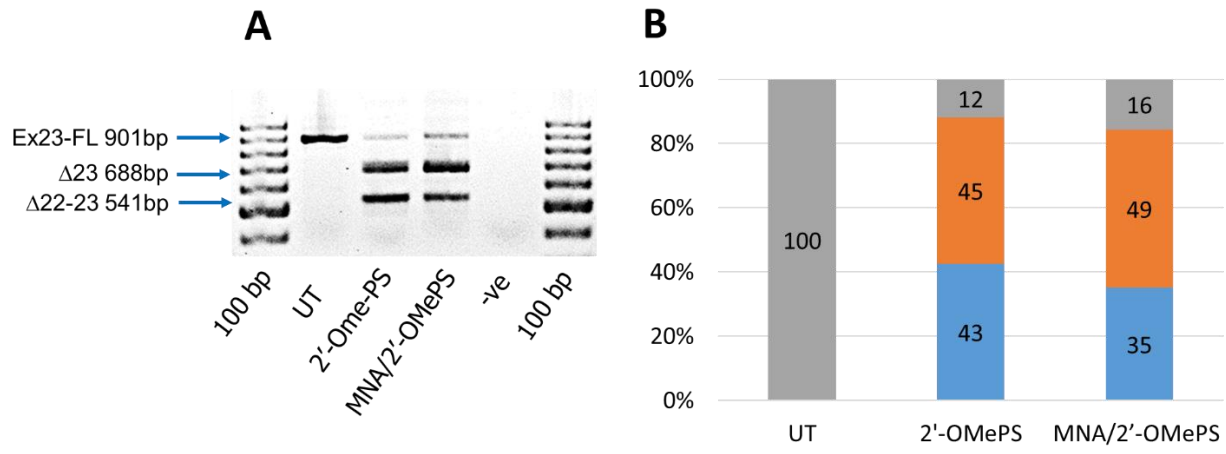

Figure 4.2.1.2.1 PCR analysis (A) and densitometry analysis (B) of exon 23 skipping in cultured *mdx* myotubes. Orange: percentage of exon 23 skipped product. Blue: percentage of dual exon 22/23 skipped product. Grey: percentage of full length product. UT: Untreated.

To evaluate the cytotoxicity of the AOs, we then conducted a cell viability assay using WST-1 reagent (Sigma, St. Louis, MO, USA). Briefly, the cells were seeded and transfected with the AOs (400 nM) as described previously. After 24 h incubation, cells were combined with a WST-1 reagent and incubated for 2 h at 37 C, 5% CO_2, and the absorbance was measured at 450 nm wavelength by a plate reader. In general, there was no difference between cells

treated with the 2'-OMe-PS AO and the MNA/2'-OMe-PS mixmer, which suggests that both AOs did not induce any cytotoxicity under the applied conditions (**Figure 4.2.1.2.2**).

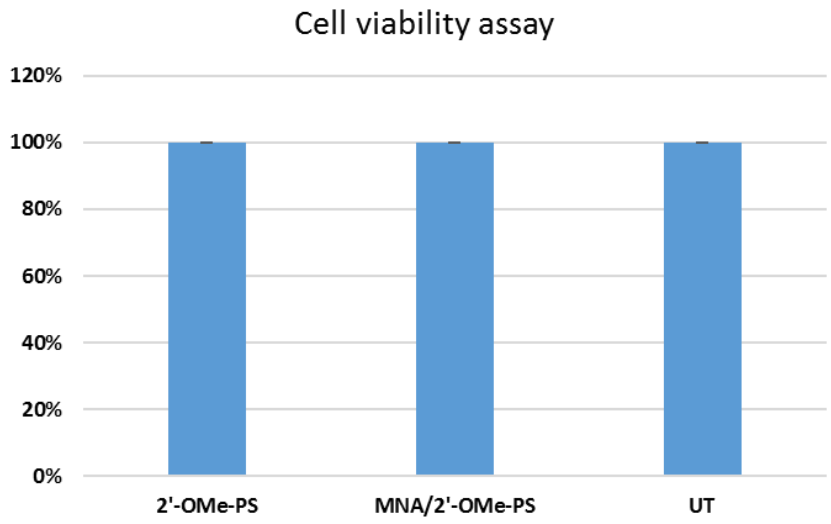

Figure 4.2.1.2.2 Cell viability assay after 24 h of transfection. UT: Untreated.

4.2.1.3 Conclusion

To summarise, we synthesized a morpholino nucleoside-uridine phosphoramidite and subsequently a 20-mer MNA-modified 2'-OMe mixmer AO was synthesized to investigate its potential in inducing exon 23 skipping in the *Dmd* gene transcript in mouse myotubes *in vitro*. We showed that the MNA-modified 2'-OMe-PS AO efficiently induced exon 23 skipping in parallel with the fully modified 2'-OMe-PS AO control. Although these are only preliminary studies, and more detailed investigations are essential for further verification. Based on the results to date, we believe that MNA-modified AOs could be used in constructing therapeutic antisense oligonucleotides for exon skipping and other antisense mechanisms.

4.2.2 *In vitro* comparison between LNA and 2′-OMe modified 2′-F-PS chimeric AOs

4.2.2.1 Introduction

Apart from new nucleotide analogue design, more practically, AO optimization is focused on exploring novel chimeric design of existing analogues. Towards this, Kawasaki et al. introduced 2'-F as an attractive ribonucleotide analogue for constructing AOs. In fact, 2'-F-PS

AOs showed higher target binding affinity, and nuclease stability [98]. Previous studies have also revealed its enhanced capability to induce exon skipping *in vitro* compared to 2'-OMe-PS (**Figure 4.2.2.1**) AOs [53, 54, 98, 99] that may be due to the recruitment of interleukin enhancer binding factors 2 and 3 (ILF2/3) by 2'-F AO/pre-mRNA duplex, resulting in improved steric block efficiency [53, 54, 99]. However, 2'-F-modified AOs did not reach clinical evaluation and the scope of 2'-F-modified AOs needs to be improved by novel design approaches. LNA (**Figure 4.2.2.1**) is another prominent RNA analogue that has been successfully investigated in recent studies to induce exon skipping in the dystrophin gene transcript [51, 72]. In this study, for the first time we report the design, synthesis and evaluation of LNA and 2′-OMe modified 2′-F-PS chimeric AOs based on a previously reported AO sequence, M23D (+1-17) to induce exon 23 skipping in DMD mouse myotubes *in vitro* [72].

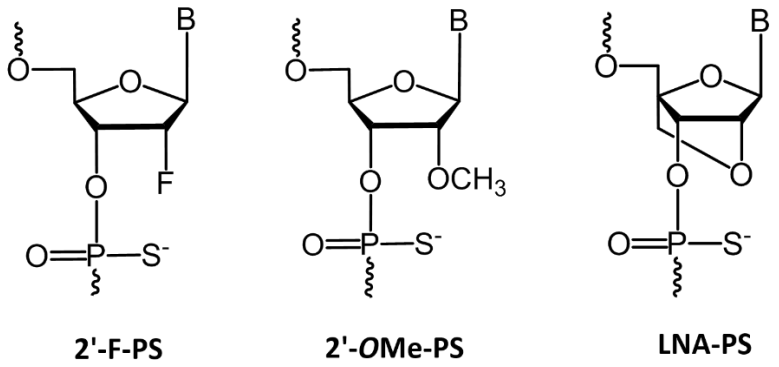

Figure 4.2.2.1 Structural representations of 2'-F, 2'-OMe, and LNA monomers on a PS backbone.

4.2.2.2 Results

In the present study, we used a previously reported fully modified 2'-OMe-PS 18-mer AO sequence, M23D (+1-17) that was designed to induce exon 23 skipping in mouse *Dmd* transcript [72], as a positive control (**Table 4.2.2.2**). Based on this AO, we systematically designed and synthesized a fully modified 2'-F AO on a PS backbone, three 2'-OMe/2'-F-PS chimeric AOs, and three LNA/2'-F-PS chimeric AOs that include a gapmer and two mixmers designs (**Table 4.2.2.2**). Two-step systematic evaluation was performed *in vitro* in mouse

myotubes differentiated from *H2K mdx* myoblasts. Initial evaluation was conducted for all AOs at 12.5 nM, 25 nM, and 50 nM concentrations while secondary evaluation was performed at lower concentrations (2.5 nM, 5 nM, and 12.5 nM) for the chimeric AOs. In general, *H2K mdx* myoblasts were plated on 24-well plates and incubated for 24 h for differentiation. The differentiated myotubes were then transfected with different concentrations of the above-mentioned AOs using Lipofectin transfection reagent. Twenty-four hours after transfection, cells were collected, followed by total cellular RNA extraction, and RT-PCR to amplify the dystrophin transcripts across exons 20 to 26, as reported previously [93]. The PCR products were separated by electrophoresis on 2% agarose gels, prior to image capture (Fusion FX gel documentation system) and densitometry analysis using Image J software. The percentages of full length (901bp), exon 23 skipped (688bp), and exon 22/23 dual skipped (542bp) products are presented relative to the total amount of the dystrophin transcripts. Systematic exon skipping evaluation was performed in duplicate.

AO name	Sequence, 5'→ 3' direction
Fully 2'-*O*Me-PS	**GCCAAACCUCGGCUUACC**
Fully 2'-F-PS	$G^FC^FC^FA^FA^FA^FC^FC^FU^FC^FG^FG^FC^FU^FU^FA^FC^FC^F$
2'-*O*Me/2'-F-PS gapmer	**GC**$C^FA^FA^FA^FC^FC^FU^FC^FG^FG^FC^FU^FU^FA^F$**CC**
2'-*O*Me/2'-F-PS mixmer 1	**G**$C^FC^FA^FA^FA^F$**C**$C^FU^FC^FG^F$**G**$C^FU^FU^FA^FC^F$**C**
2'-*O*Me/2'-F-PS mixmer 2	$G^FC^FC^FA^FA^FA^FC^FC^F$**U**C^FG^F**G**C^FU^F**U**A^FC^F**C**
LNA/2'-F-PS gapmer	**G^{L}C^L**$C^FA^FA^FA^FC^FC^FU^FC^FG^FG^FC^FU^FU^FA^F$**C^{L}C^L**
LNA/2'-F-PS mixmer 1	**G^L**$C^FC^FA^FA^FA^F$**C^L**$C^FU^FC^FG^F$**G^L**$C^FU^FU^FA^FC^F$**C^L**
LNA/2'-F-PS mixmer 2	$G^FC^FC^FA^FA^FA^FC^FC^F$**T^L**C^FG^F**G^L**C^FU^F**T^L**A^FC^F**C^L**

Table 4.2.2.2 List of AO names and sequences used in this study. 2'-OMe nucleotides are represented underlined, bold in blue; 2'-F nucleotides are represented as black characters with superscript F; LNA nucleotides are represented underlined and bold, in red with superscript L. All AOs pare on a PS backbone.

4.2.2.2.1 Evaluation of 2'-F modified AOs to induce exon skipping in dystrophin transcript in *H2K mdx* mouse myotubes *in vitro* at 12.5 nM, 25 nM, and 50 nM concentrations

Firstly, we evaluated the exon skipping efficiency of all AOs (**Table 4.2.2.2**) *in vitro* at three different concentrations (12.5 nM, 25 nM, and 50 nM). The results demonstrated that all AOs are capable of inducing variable, but efficient exon skipping (**Figures 4.2.2.2.1.1: agarose gel images and densitometries of each repetition; 4.2.2.2.1.2: averaged densitometry with error bars**). In line with a previous report [72], the 2'-OMe-PS control AO induced efficient exon 23 skipping, yielding the skipped product of 688 bp at all concentrations (43% at 12.5 nM, 47% at 25 nM, and 51% at 50 nM; **Figure 4.2.2.2.1.2A**). Interestingly, the fully modified 2'-F-PS AO showed higher exon 23 skipping at 12.5 nM (50%) compared to the control AO (43%), but the efficiency reduced to 44% at 25 nM and remained at 51% at 50 nM. However, the 2'-F-PS AOs showed the undesired exon 22/23 dual skipping product of 542 bp at a higher yield at 25 nM (35%) compared to 2'-OMe-PS AO (27%) (**Figure 4.2.2.2.1.2A**).

All mixmer and gapmer AOs achieved the highest exon 23 skipping at 25 nM or 50 nM, (**Figure 4.2.2.2.1.2B and C**). Notably, the LNA/2'-F-PS mixmer 2 yielded the highest level of exon 23 skipping (63%) (**Figure 4.2.2.2.1.2C**) compared to all other AOs (42-53%) at 50 nM concentration (**Figure 4.2.2.2.1.2**). Surprisingly, a significant drop in the exon 23 skipped product was observed after transfection with 12.5 nM of the 2'-OMe/2'-F-PS gapmer, which induced only 26% (**Figure 4.2.2.2.1.2B**) skipping while other AOs achieved 43-56% of skipping at this concentration (**Figure 4.2.2.2.1.2**). Direct comparison between the 2'-OMe/2'-F-PS and the corresponding LNA/2'-F-PS gapmer and mixmer AOs indicated that the LNA/2'-F-PS AOs achieved higher exon 23 skipping efficiency at various concentrations. For instance, at 25 nM concentration, exon 23 skipping induced by LNA/2'-F gapmer (58%) was higher than 2'-OMe/2'-F gapmer (42%), LNA/2'-F mixmer 1 (54%) was higher than 2'-

OMe/2'-F mixmer 1 (46%), and LNA/2'-F mixmer 2 (51%) was higher than 2'-OMe/2'-F mixmer 2 (50%). Furthermore, at all concentrations, each type of LNA/2'-F mixmers (mixmer 1: 31% at 12.5 nM, 35% at 25 nM; mixmer 2: 19% at 12.5 nM, 27% at 25 nM, 22% at 50 nM) induced the unwanted exon 22/23 dual skipping than its corresponding 2'-OMe/2'-F mixmers (mixmer 1: 39% at 12.5 nM, 37% at 25 nM; mixmer 2: 37% at 12.5 nM, 36% at 25 nM, 40% at 50 nM) except mixmer 1 AOs at 50 nM (LNA/2'-F mixmer 1: 46%; 2'-OMe/2'-F mixmer 1: 39%).

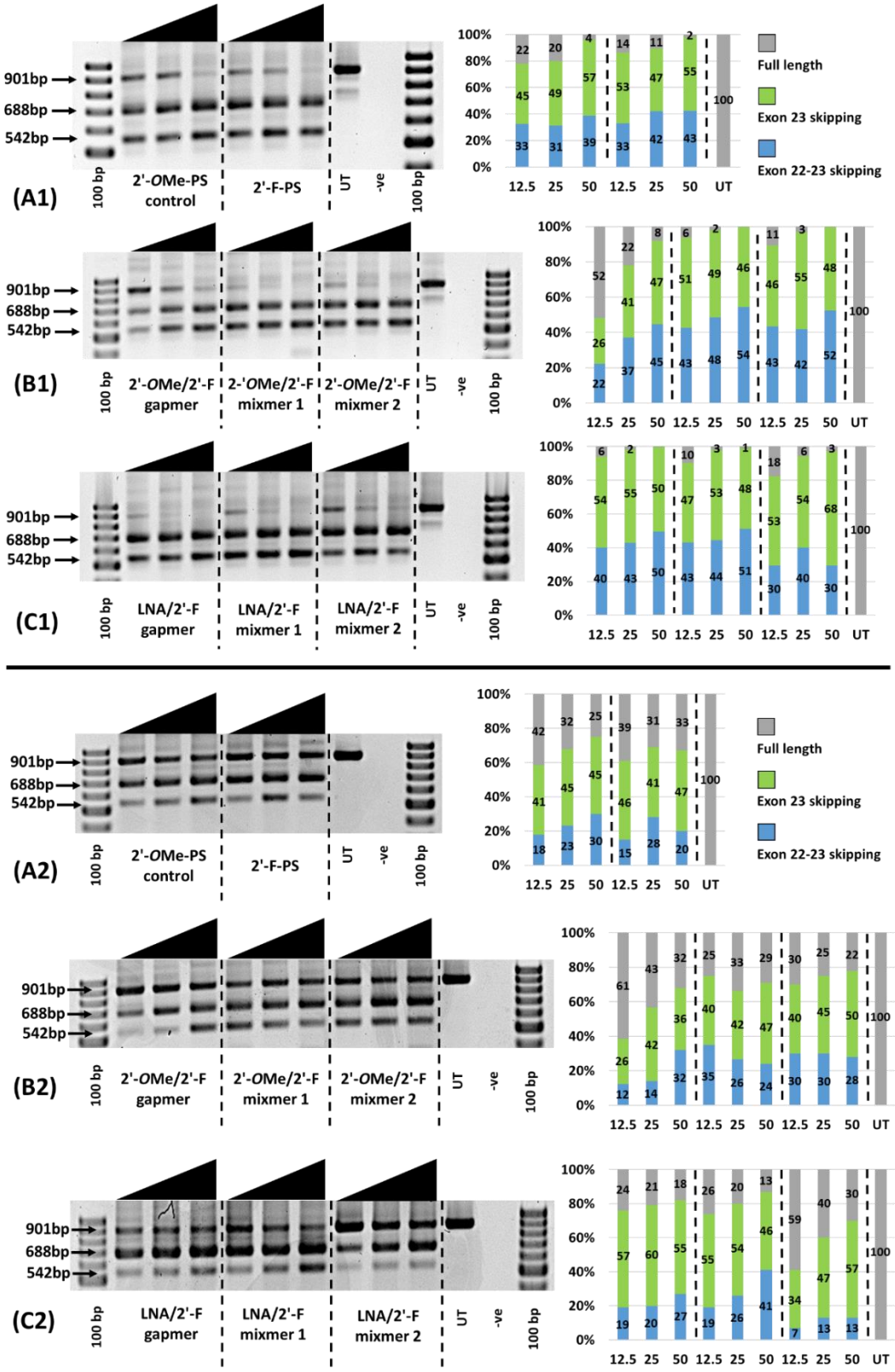

Figure 4.2.2.2.1.1 Agarose gel analysis of RT-PCR products (two repetitions) and corresponding densitometry analysis of each repetition showed exon 23 and exon 22/23 dual skipping in *mdx* mouse H2K myotubes *in vitro*. Concentrations of AOs used include 12.5 nM, 25 nM, and 50 nM. (A1, 2) Fully modified 2'-OMe-PS control AO and fully modified 2'-F-PS AO; (B1, 2) 2'-OMe modified 2'-F-PS AO chimeras including 2'-OMe/2'-F-PS gapmer, 2'-OMe/2'-F-PS mixmer 1, and 2'-OMe/2'-F-PS mixmer 2; (C1, 2) LNA modified 2'-F-PS AO chimeras including LNA/2'-F-PS gapmer, LNA/2'-F-PS mixmer 1, and LNA/2'-F-PS mixmer 2.

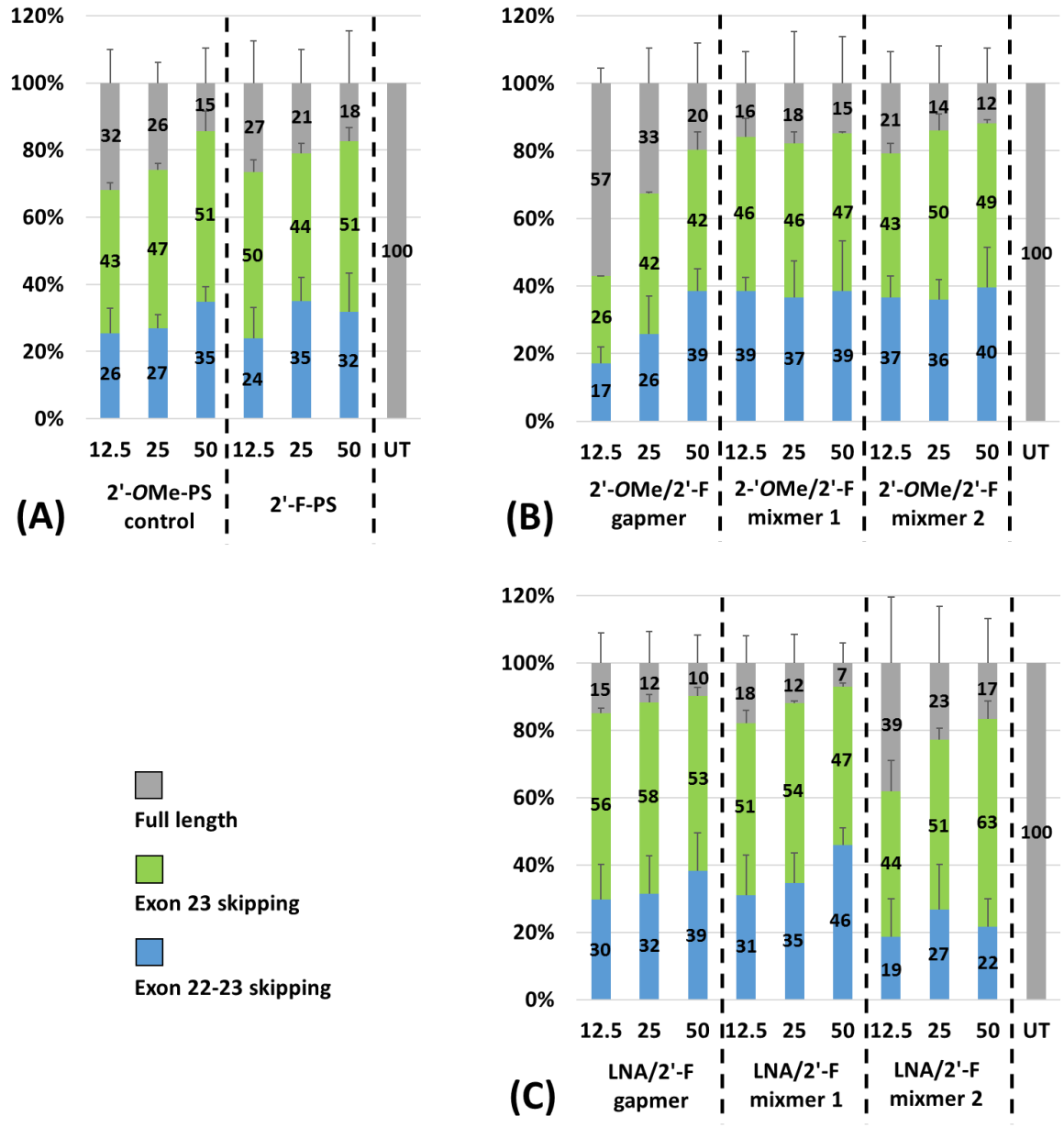

Figure 4.2.2.2.1.2 Densitometry analysis of RT-PCR products (in duplicate) showed exon 23 and exon 22/23 dual skipping in AO transfected (12.5 nM, 25 nM, and 50 nM) *mdx* mouse H2K myotubes *in vitro*. (A) Fully modified 2'-OMe-PS control AO and fully modified 2'-F-PS AO; (B) 2'-OMe modified 2'-F-PS AO chimeras including 2'-OMe/2'-F-PS gapmer, 2'-OMe/2'-F-PS mixmer 1, and 2'-OMe/2'-F-PS mixmer 2; (C) LNA modified 2'-F-PS AO chimeras including LNA/2'-F-PS gapmer, LNA/2'-F-PS mixmer 1, and LNA/2'-F-PS mixmer 2.

4.2.2.2.2 Evaluation of chimeric AOs to induce exon skipping in the dystrophin transcript in *H2K mdx* mouse myotubes *in vitro* at 2.5 nM, 5 nM, and 12.5 nM concentrations

To further explore the ability of the 2'-F modified chimeric AOs in inducing exon skipping, we transfected all chimeric AOs (2'-OMe/2'-F-PS chimeras and LNA/2'-F-PS chimeras) (**Table 4.2.2.2**) at lower concentrations (2.5 nM, 5 nM, and 12.5 nM) together with 2'-OMe-

PS control. In general, all AOs yielded efficient exon 23 skipped products in a dose-dependent manner, except the 2'-OMe/2'-F gapmer (**Figures 4.2.2.2.2.1: agarose gel images and densitometries of each repetition; 4.2.2.2.2.2: averaged densitometry with error bars**). Furthermore, all 2'-F modified chimeras achieved higher exon 23 skipping efficiency than the 2'-OMe-PS control at all concentrations except 2'-OMe/2'-F gapmer at 12.5 nM (2'-OMe/2'-F gapmer: 20%; 2'-OMe-PS control: 33%) (**Figure 4.2.2.2.2.2**). Notably, at 12.5 nM, LNA/2'-F-PS gapmer achieved the highest level of exon 23 skipping (51%) (**Figure 4.2.2.2.2.2C**) in comparison to all other chimeric AOs (20-48%) (**Figure 4.2.2.2.2.2B, C**). It was also noted that LNA/2'-F chimeric AOs achieved higher or comparable exon 23 skipping efficiency compared with the corresponding 2'-OMe/2'-F chimeric AO at all concentrations except LNA/2'-F mixmer 2 at 2.5 nM (LNA/2'-F mixmer 2: 18%; 2'-OMe/2'-F mixmer 2: 24%) (**Figure 4.2.2.2.2.2B, C**). The percentage of exon 23 skipping induced by LNA/2'-F gapmer (33% at 2.5 nM, 40% at 5 nM, 51% at 12.5 nM) was higher than 2'-OMe/2'-F gapmer (14% at 2.5 nM, 26% at 5 nM, 20% at 12.5 nM); LNA/2'-F mixmer 1 (33% at 2.5 nM, 40% at 5 nM, 48% at 12.5 nM) was higher than 2'-OMe/2'-F mixmer 1 (31% at 2.5 nM, 34% at 5 nM, 39% at 12.5 nM); and LNA/2'-F mixmer 2 (32% at 5 nM, 44% at 12.5 nM) was higher than or equivalent to 2'-OMe/2'-F mixmer 2 (32% at 5 nM, 41% at 12.5 nM). In addition, at all concentrations (2.5nM, 5nM, 12.5 nM), LNA/2'-F mixmers (mixmer 1: 15%, 18%, 27%; mixmer 2: 16%, 13%, 22%) induced less undesired exon 22/23 dual skipping than their corresponding 2'-OMe/2'-F mixmer (mixmer 1: 23%, 29%, 35%; mixmer 2: 29%, 33%, 34%) (**Figure 4.2.2.2.2.2B, C**). Interestingly, exon 22/23 dual skipping was not evident in the case of 2'-OMe/2'-F-PS gapmer at 2.5 nM and 5 nM (**Figures 4.2.2.2.2.1B, 4.2.2.2.2.2B**).

To further evaluate the optimal design of the AO, we compared the exon skipping efficiency between the gapmer and two mixmer chimeric AOs. The results demonstrated that at all concentrations (2.5 nM, 5 nM, 12.5 nM), the 2'-OMe/2'-F mixmer chimeras achieved higher

exon 23 skipping efficiency than the 2'-OMe/2'-F gapmer chimeras (**Figures 4.2.2.2.2.1B, 4.2.2.2.2.2B**), however, the LNA/2'-F gapmer induced higher or comparable exon 23 skipping compared with the LNA/2'-F mixmers. That is, exon 23 skipping induced by 2'-OMe/2'-F mixmers (mixmer 1: 31% at 2.5 nM, 34% at 5 nM, 39% at 12.5 nM; mixmer 2: 24% at 2.5 nM, 32% at 5 nM, 41% at 12.5 nM) was higher than 2'-OMe/2'-F gapmer (14% at 2.5 nM, 26% at 5 nM, 20% at 12.5 nM) (**Figure 4.2.2.2.2.2B**); while exon 23 skipping induced by LNA/2'-F gapmer (33% at 2.5 nM, 40% at 5 nM, 51% at 12.5 nM) was higher than or comparable to that induced by the LNA/2'-F mixmers (mixmer 1: 33% at 2.5 nM, 40% at 5 nM, 48% at 12.5 nM; mixmer 2: 18% at 2.5 nM, 32% at 5 nM, 44% at 12.5 nM) (**Figure 4.2.2.2.2.2C**). On the other hand, LNA/2'-F mixmers induced less of the unwanted exon 22/23 dual skipped product than LNA/2'-F gapmer. Therefore, exon 22/23 skipping induced by LNA/2'-F mixmers (mixmer 1: 15% at 2.5 nM, 18% at 5 nM, 27% at 12.5 nM; mixmer 2: 16% at 2.5 nM, 13% at 5 nM, 22% at 12.5 nM) was lower than LNA/2'-F gapmer (21% at 2.5 nM, 27% at 5 nM, 28% at 12.5 nM) (**Figure 4.2.2.2.2.2C**).

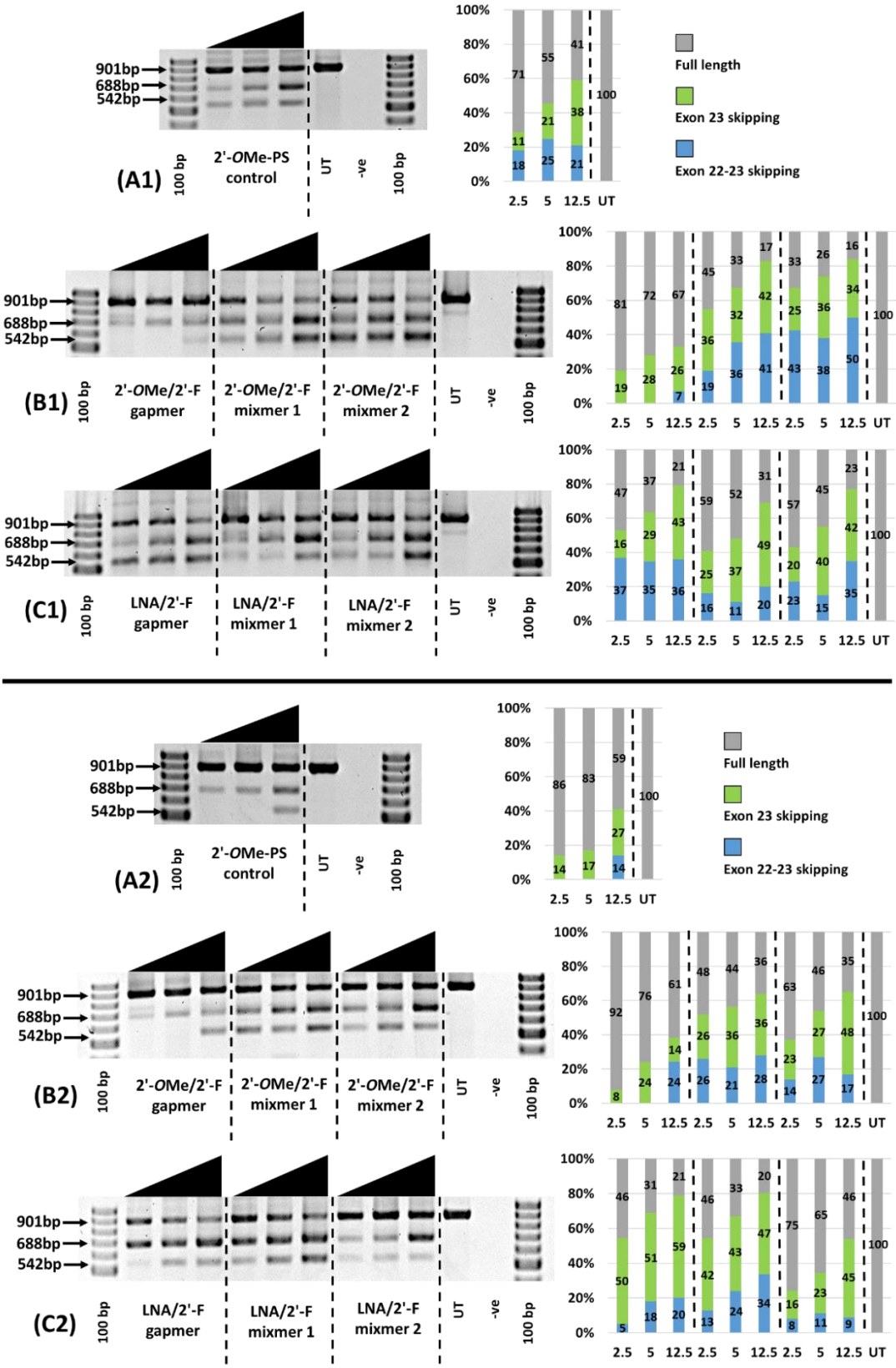

Figure 4.2.2.2.2.1 Agarose gel analysis of RT-PCR products (two repetitions) and corresponding densitometry of *Dmd* transcript products from AO treated *mdx* mouse myotubes *in vitro*. Concentrations of AOs used include 2.5 nM, 5 nM, and 12.5 nM. (A1, 2) Fully modified 2'-OMe-PS control AO; (B1, 2) 2'-OMe modified 2'-F-PS AO chimeras including 2'-OMe/2'-F-PS gapmer, 2'-OMe/2'-F-PS mixmer 1, and 2'-OMe/2'-F-PS mixmer 2; (C1, 2) LNA modified 2'-F-PS AO chimeras including LNA/2'-F-PS gapmer, LNA/2'-F-PS mixmer 1, and LNA/2'-F-PS mixmer 2.

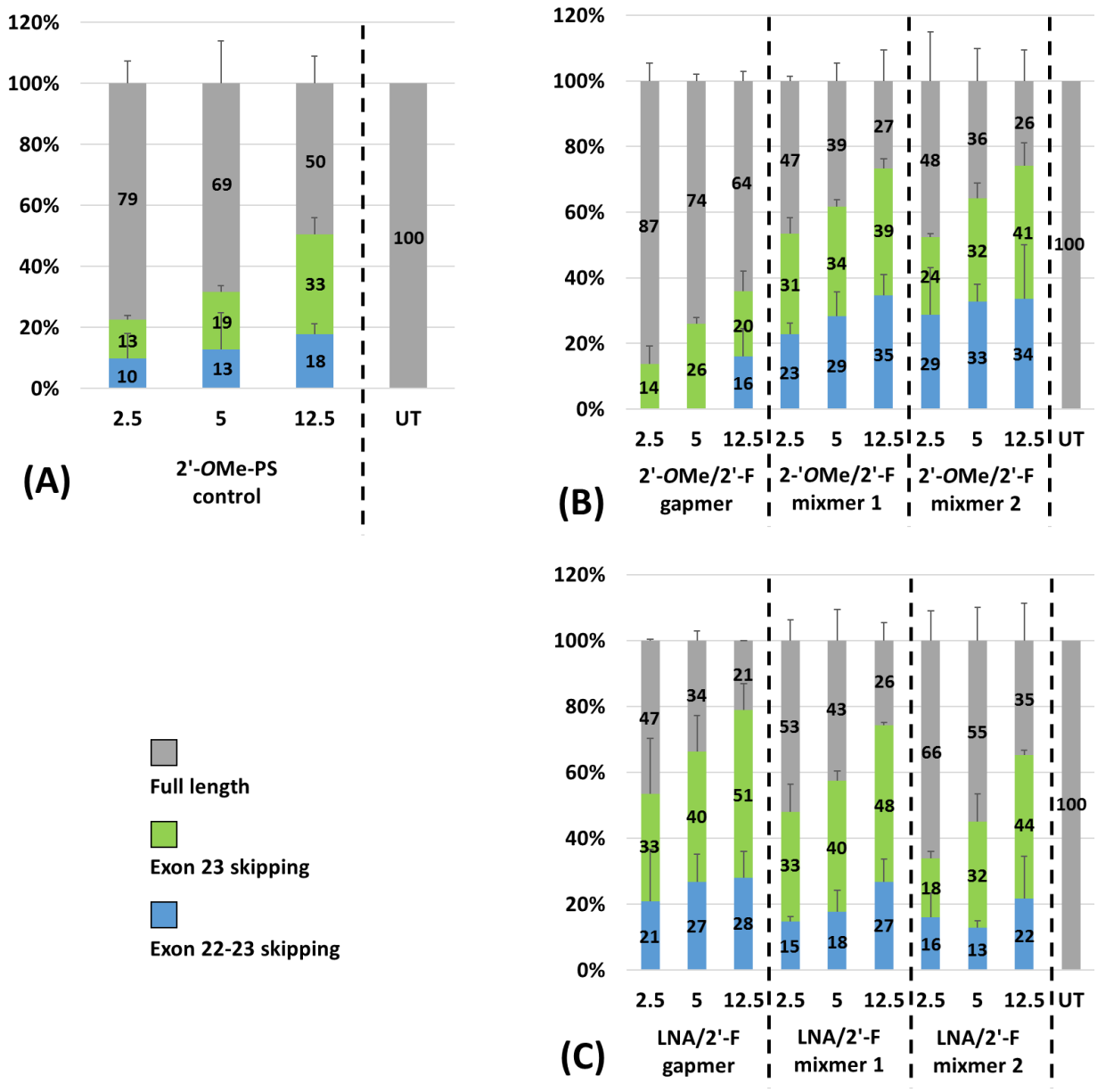

Figure 4.2.2.2.2.2 Densitometry analysis of the *Dmd* RT-PCR products (in duplicate) derived from AO transfected (2.5 nM, 5 nM, and 12.5 nM) *mdx* mouse myotubes *in vitro*. (A) Fully modified 2'-OMe-PS control AO; (B) 2'-OMe modified 2'-F-PS AO chimeras including 2'-OMe/2'-F-PS gapmer, 2'-OMe/2'-F-PS mixmer 1, and 2'-OMe/2'-F-PS mixmer 2; (C) LNA modified 2'-F-PS AO chimeras including LNA/2'-F-PS gapmer, LNA/2'-F-PS mixmer 1, and LNA/2'-F-PS mixmer 2.

4.2.2.2.3 Evaluation of *in vitro* cytotoxicity of the 2'-F modified AOs

Safety is crucial for any clinically relevant therapeutic drug. Therefore, we performed cytotoxicity evaluation for all 2'-F modified AOs by conducting WST-1 reagent-based cell viability assay. Briefly, mouse myoblasts were seeded and differentiated into myotubes, followed by transfecting with the AOs (50 nM and 12.5 nM). The untreated groups were not transfected with an AO but were incubated with only the Lipofectin reagent. The cells were

then incubated with WST-1 reagent at a ratio of 1:10 (v/v) at 37°C, 5% CO_2 for 4 h. Cytotoxicity was determined by measuring the absorbance at 450 nm wavelength. In general, all 2'-F modified AOs did not show any significant cytotoxicity in comparison to the fully 2'-OMe-PS control (**Figure 4.2.2.2.3**). Notably, at 12.5 nM, LNA modified 2'-F chimeras showed higher viability than 2'-OMe modified 2'-F chimeras. On the other hand, 2'-OMe/2'-F-PS mixmer 2 demonstrated lower viability than the other AOs at both concentrations, which may be due to the positioning of the 2'-OMe nucleotides, as the 2'-OMe/2'-F-PS mixmer 1 achieved higher cell viability at both concentrations (**Figure 4.2.2.2.3**).

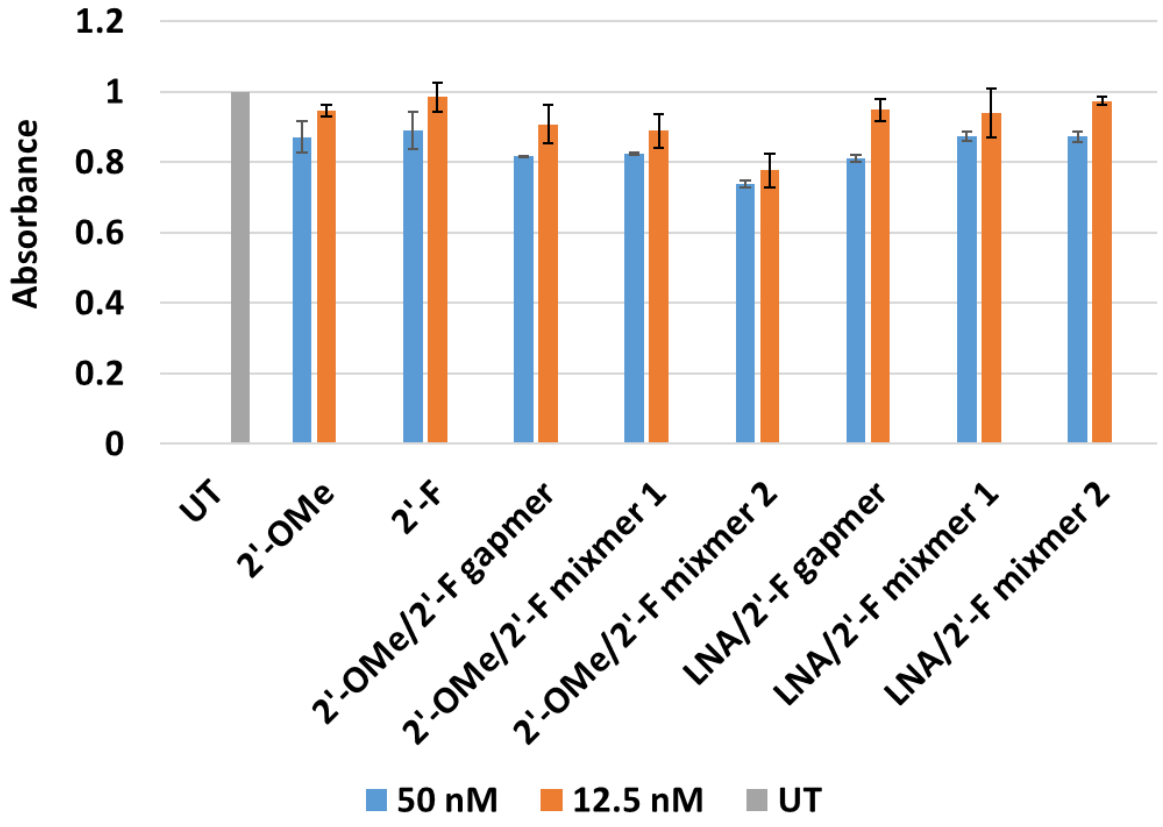

Figure 4.2.2.2.3 Cell viability assay (in duplicate) of 2'-F modified AOs.

4.2.2.2.4 Evaluation of *in vitro* nuclease stability of the 2'-F modified AOs

To gain greater insight into the AO stability, we then performed the nuclease degradation assay on all the 2'-F modified AOs in comparison to the fully 2'-OMe-PS control. In short, AOs were incubated with Phosphodiesterase I from *Crotalus adamanteus* venom that

possesses very high exonuclease activity at 37°C, for 0, 1, 2, 4, and 6 h. Samples were collected at the specified timepoints and quenched with formamide loading buffer, followed by denaturation at 95°C for 5 min. Next, 20% denaturing polyacrymide gel analysis was performed and the results were assessed by image capture (Fusion FX Gel documentation system) and analysis using ImageJ. All 2'-F modified AOs demonstrated high stability under the applied conditions, compared to the fully 2'-OMe-PS control (**Figure 4.2.2.2.4**). Not surprisingly, all the LNA/2'-F-PS chimeras showed higher nuclease resistance than the AOs without LNA modification (**Figure 4.2.2.2.4**). In addition, the gapmer chimeras showed higher stability than the mixmer chimeras.

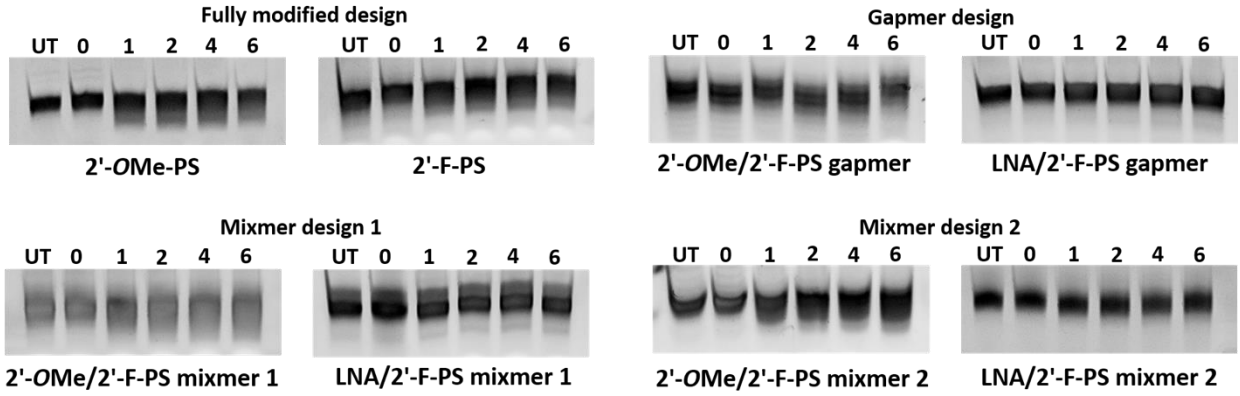

Figure 4.2.2.2.4 Nuclease stability analysis of 2'-F modified AOs.

4.2.2.3 Discussion

The first attempt to study 2'-F modified AOs was reported in 1993 when Kawasaki et al. found that 2'-F modification enhanced the target binding affinity of an AO to their complementary RNA compared, to 2'-OMe modified AOs, and showed excellent nuclease stability [98]. Two decades later, Rigo and colleagues discovered a unique property of the 2'-F modified AO/target pre-mRNA duplex that is able to recruit the ILF2/3 proteins, resulting in exon 7 skipping of *SMN2* mRNA in a SMA model system [99]. Building upon this finding, Aartsma-Rus and coworkers compared the exon skipping capability of the fully 2'-F-PS and fully 2'-OMe-PS AOs in targeting *DMD*, and showed that 2'-F-PS AO induced higher human

exon 53 and mouse exon 23 skipping *in vitro* [53, 54]. This finding was not surprising, as 2'-F modification has many advantages, proven by Kawasaki et al. and Rigo et al. [98, 99], however, the 2'-F-PS AO was less efficient than 2'-OMe-PS *in vivo* and induced toxicity in mice [54]. Thus, their results did not support clinical use of 2'-F-PS AOs [54].

In an attempt to improve the therapeutic potential of 2'-F modified AOs, we incorporated 2'-OMe-PS and LNA-PS nucleotides into an 18-mer 2'-F-PS AO sequence that contained either four 2'-OMe or LNA nucleotides in the sequence designed to target *Dmd* exon 23 in *mdx* mouse H2K myotubes (**Table 4.2**). The efficacies of the AOs were first evaluated at higher (12.5 nM, 25 nM, 50 nM), and then lower concentrations (2.5 nM, 5 nM, 12.5 nM); in addition to performing cytotoxicity and nuclease stability analysis.

Fully modified 2'-F-PS AO induced higher exon 23 skipping than the fully modified 2'-OMe-PS control at 12.5 nM, and both of them indicated similar exon 23 skipping efficiency on higher concentrations (25 nM, 50 nM), in line with the Aartsma-Rus et al. finding that 2'-F-PS AO induced minimal increases in exon 23 skipping when compared to 2'-OMe-PS AO *in vitro* [100]. In general, chimeric 2'-F-PS AOs induced efficient exon 23 skipping. Each of the LNA/2'-F-PS chimeras achieved higher or comparable exon 23 skipping relative to their corresponding 2'-OMe/2'-F-PS counterparts (LNA/2'-F-PS gapmer > 2'-OMe/2'-F-PS gapmer, LNA/2'-F-PS mixmer 1 $\geqslant$ 2'-OMe/2'-F-PS mixmer 1, LNA/2'-F-PS mixmer 2 > 2'-OMe/2'-F-PS mixmer 2), indicating that LNA modification may possess better exon 23 skipping capability than 2'-OMe AO on a 2'-F-PS platform. Notably, at 50 nM, LNA/2'-F-PS mixmer 2 achieved the highest exon 23 skipping over other AOs, and, 2'-OMe/2'-F-PS gapmer induced the least exon 23 skipping compared to the other compounds at 12.5, 25, and 50 nM, suggesting that the positioning of LNA or 2'-OMe analogues also affects exon skipping efficiency. Interestingly, at 12.5 and 25 nM concentrations, the LNA/2'-F mixmers induced less of the unwanted exon 22/23 dual skipping product than their corresponding 2'-OMe/2'-F

mixmers, suggesting that LNA/2'-F mixmers may be a better tool for exon skipping application than 2'-OMe/2'-F mixmers.

At lower concentrations (2.5 nM, 5 nM, 12.5 nM), all 2'-OMe/2'-F mixmer AOs showed higher exon 23 skipping than their gapmer counterpart at all three concentrations, while LNA/2'-F gapmer AO showed higher or comparable exon 23 skipping in comparison to its mixmer counterparts. This further suggests that the positioning of 2'-OMe or LNA nucleotides on a 2'-F-PS platform affects exon skipping efficiency. On the other hand, each of the LNA/2'-F-PS chimeras achieved higher or comparable exon 23 skipping compared with their corresponding 2'-OMe/2'-F-PS counterparts at 5 nM and 12.5 nM (LNA/2'-F-PS gapmer > 2'-OMe/2'-F-PS gapmer, LNA/2'-F-PS mixmer 1 > 2'-OMe/2'-F-PS mixmer 1, LNA/2'-F-PS mixmer 2 > 2'-OMe/2'-F-PS mixmer 2). This is consistent with previous experiments, and confirmed that LNA modification can result in higher exon 23 skipping than 2'-OMe on a 2'-F-PS platform. Furthermore, similar to the observation at higher concentrations (12.5 nM, 25 nM, 50 nM), the LNA/2'-F mixmers induced less of the exon 22/23 dual skipping than its corresponding 2'-OMe/2'-F mixmers at all concentrations, which further confirmed that LNA/2'-F mixmers may be preferable to 2'-OMe/2'-F mixmers for exon skipping application.

In addition, cell viability assay performed to assess the cytotoxicity of the AOs showed that all 2'-F modified chimeric AOs achieved comparable cytotoxicity profiles in comparison to their fully 2'-OMe-PS control and the fully modified 2'-F-PS AO. Notably, the LNA/2'-F-PS chimeras showed better safety profiles than the 2'-OMe/2'-F-PS chimeras, and the 2'-OMe/2'-F-PS mixmer 2 appeared to be the most toxic AO of those studies. This suggests that nucleotide positioning can be important in optimizing AO toxicity, although further evaluation in *in vivo* models are required. Nuclease stability assay demonstrated that fully 2'-F-PS AO and 2'-OMe/2'-F-PS chimeras possess similar stability to the fully 2'-OMe-PS

control *in vitro*. Not surprisingly, LNA/2'-F-PS chimeras were more stable than the other AOs without LNA modification. In addition, LNA/2'-F-PS gamper showed higher nuclease resistance than the corresponding mixmer chimeras. This phenomenon highlights a better protection effect of gapmer design than other mixmer designs. In fact, gapmer design has been regularly used to protect AOs from nuclease attack, for example, 5-10-5 MOE gapmer design has been predominantly used by Ionis pharmaceuticals. Moreover, the company has developed 5-10-5 LNA gapmer AOs for targeting different disease-causing genes as well. The principles underlying this phenomenon (gapmer design possesses higher nuclease protection that mixmer design) is that nuclease attacks AO sequence from its 5' end instead of other positions in the sequence.

4.2.2.4 Conclusion

In conclusion, 2'-F-PS modified AOs induce higher *Dmd* exon 23 skipping efficiency than fully 2'-OMe-PS AO. Introduction of LNA nucleotides into the 2'-F-PS sequence further improved exon 23 skipping efficiencies, while not compromising cell viability and nuclease stability, in comparison to the 2'-OMe/2'-F-PS chimeras. In addition, mixmer designs of 2'-OMe/2'-F chimeras achieved higher efficiency of exon 23 skipping than their gapmer counterparts, while the gapmer design of LNA/2'-F chimeras achieved higher efficiency of exon 23 skipping than their mixmer counterparts. Collectively, our findings expand the scope of utilizing 2'-F modified AOs in splice modulation applications by constructing 2'-OMe and LNA-modified 2'-F-PS chimeras. Specifically, we suggest that development of LNA modified 2'-F-PS mixmer or gapmer chimeric AOs may present a promising therapeutic strategy for DMD.

4.3 Overall discussions and conclusions

This chapter presents the work on design, synthesis and evaluation of chimeric AOs containing novel nucleotide analogues for inducing splice modulation in *H2K mdx* myogenic

cells, using DMD as a disease model. The 2'-OMe, MNA, 2'-F, and LNA analogues were utilized as building blocks for chimeric AO construction. The capability of inducing exon skipping, cytotoxicity, and/or nuclease stability, and/or thermal stability of different chemically modified AO mixmers were tested *in vitro,* compared with their fully modified 2'-OMe-PS counterparts as a control. In conclusion, the findings in this chapter expand the scope of utilizing nucleic acid analogues in splice modulation applications by constructing AO chimeras, and demonstrates the feasibility of using these analogues for the purpose of AO optimization, in terms of improved splice modulating efficacy, safety, and stability. Further, evaluation of chimeric AOs in animal models should be conducted in the future in order to gain additional insights into their *in vivo* performance and pharmacokinetics.

Chapter three references

1. Dominski, Z., Kole, R. Restoration of correct splicing in thalassemic pre-mRNA by antisense oligonucleotides. *Proc Natl Acad Sci USA* 90, 8673-8677 (1993).
2. Syed, Y.Y. Eteplirsen: first global approval. *Drugs* 76, 1699-1704 (2016).
3. Aartsma-Rus, A., Krieg, A.M. FDA approves eteplirsen for Duchenne muscular dystrophy: the next chapter in the eteplirsen saga. *Nucleic Acid Ther* 27, 1-3 (2017).
4. Heo, Y. Golodirsen: first approval. *Drugs* 80, 329-333 (2020).
5. Emery, A.E. Population frequency of inherited neuromuscular diseases – a world survey. *Neuromuscul Disord* 1, 19-29 (1991).
6. Emery, A.E. Clinical and molecular studies in Duchenne muscular dystrophy. *Prog Clin Biol Res* 306, 15-28 (1989).
7. Emery, A.E. The muscular dystrophies. *Lancet* 359, 687-695 (2002).
8. Prior, T.W., Bridgeman, S.J. Experience and strategy for the molecular testing of Duchenne muscular dystrophy. *J Mol Diagn* 7, 317-326 (2005).
9. Davies, K.E., Smith, T.J., Bundey, S., et al. Mild and severe muscular dystrophy associated with deletions in Xp21 of the human X chromosome. *J Med Genet* 25, 9-13 (1988).
10. Govoni, A., Magri, F., Brajkovic, S., et al. Ongoing therapeutic trials and outcome measures for Duchenne muscular dystrophy. *Cell Mol Life Sci* 70, 4585-4602 (2013).
11. Koenig, M., Hoffman, E.P., Bertelson, C.J., et al. Complete cloning of the Duchenne muscular dystrophy (DMD) cDNA and preliminary genomic organization of the DMD gene in normal and affected individuals. *Cell* 50, 509-517 (1987).
12. Mitrpant, C., Fletcher, S., Wilton, S. Personalised genetic intervention for Duchenne muscular dystrophy: antisense oligomers and exon skipping. *Curr Mol Pharmacol* 2, 110-121 (2009).

13. Cohn, R.D., Campbell, K.P. Molecular basis of muscular dystrophies. *Muscle Nerve* 23, 1456-1471 (2000).

14. De Palma, C., Clementi, E. Nitric oxide in myogenesis and therapeutic muscle repair. *Mol Neurobiol* 46, 682-692 (2012).

15. Straub, V., Campbell, K.P. Muscular dystrophies and the dystrophin-glycoprotein complex. *Curr Opin Neurol* 10, 168-175 (1997).

16. Fairclough, R.J., Wood, M.J., Davies, K.E. Therapy for Duchenne muscular dystrophy: renewed optimism from genetic approaches. *Nat Rev Genet* 14, 373-378 (2013).

17. Magri, F., Govoni, A., D'Angelo, M.G., et al. Genotype and phenotype characterization in a large dystrophinopathic cohort with extended follow-up. *J Neurol* 258, 1610-1623 (2011).

18. Muntoni, F., Torelli, S., Ferlini, A. Dystrophin and mutations: one gene, several proteins, multiple phenotypes. *Lancet Neurol* 2, 731–740 (2003).

19. Birnkrant, D.J., Bushby, K., Bann, C.M., et al. Diagnosis and management of Duchenne muscular dystrophy, part 2: respiratory, cardiac, bone health, and orthopaedic management. *Lancet Neurol* 17, 347–361 (2018).

20. Bushby, K., Finkel, R., Birnkrant, D.J., et al. Diagnosis and management of Duchenne muscular dystrophy, part 1: diagnosis, and pharmacological and psychosocial management. *Lancet Neurol* 9, 77–93 (2010).

21. Nakamura, A., Takeda, S. Exon-skipping therapy for Duchenne muscular dystrophy. *Neuropathology* 29,494–501 (2009).

22. Mendell, J.R., Rodino-Klapac, L., Sahenk, Z., et al. Gene therapy for muscular dystrophy: lessons earned and path forward. *Neurosci Lett* 527, 90–99 (2012).

23. Pichavant, C., Aartsma-Rus, A., Clemens, P.R., et al. Current status of pharmaceutical and genetic therapeutic approaches to treat DMD. *Mol Ther* 19, 830–840 (2011).

24. Kinter, J., Sinnreich, M. Molecular targets to treat muscular dystrophies. *Swiss Med Wkly* 144, w13916 (2014).

25. Odom, G.L., Gregorevic, P., Chamberlain, J.S. Viral-mediated gene therapy for the muscular dystrophies: successes, limitations and recent advances. *Biochim Biophys Acta* 1772, 243–262 (2007).

26. Koppanati, B.M., Li, J., Reay, D.P., et al. Improvement of the *mdx* mouse dystrophic phenotype by systemic in utero AAV8 delivery of a minidystrophin gene. *Gene Ther* 17, 1355–1362 (2010).

27. Bowles, D.E., McPhee, S.W., Li, C., et al. Phase 1 gene therapy for Duchenne muscular dystrophy using a translational optimized AAV vector. *Mol Ther* 20, 443–455 (2012).

28. Kodippili, K., Hakim, C. H., Pan, X. Dual AAV Gene therapy for Duchenne muscular dystrophy with a 7-kb mini-dystrophin gene in the canine model. *Hum Gene Ther* 29, 299-311 (2018).

29. Duan, D. Systemic AAV micro-dystrophin gene therapy for Duchenne muscular dystrophy. *Mol Ther* 26, 2337-2356 (2018).

30. Singh, R.N., Singh, N.N. Mechanism of splicing regulation of spinal muscular atrophy genes. *Adv Neurobiol* 20, 31–61 (2018).

31. Sardone, V., Zhou, H., Muntoni, F., et al. Antisense oligonucleotide-based therapy for neuromuscular disease. *Molecules* 22, 563 (2017).

32. McNally, E.M., Wyatt, E.J. Mutation-based therapy for Duchenne muscular dystrophy: antisense treatment arrives in the clinic. *Circulation* 136, 979-981 (2017).

33. Niks, E.H., Aartsma-Rus, A. Exon skipping: a first in class strategy for Duchenne muscular dystrophy. *Expert Opin Biol Ther* 17, 225-236 (2017).

34. Aartsma-Rus, A., Straub, V., Hemmings, R., et al. Development of exon skipping therapies for Duchenne muscular dystrophy: a critical review and a perspective on the outstanding issues. *Nucleic Acid Ther* 27, 251-259 (2017).

35. Echevarria, L., Aupy, P., Goyenvalle, A. Exon-skipping advances for Duchenne muscular dystrophy. *Hum Mol Genet* 27, R163-R172 (2018).

36. Aartsma-Rus, A. Antisense-mediated modulation of splicing: therapeutic implications for Duchenne muscular dystrophy. *RNA Biol* 7, 453-461 (2010).

37. Takeshima, Y., Nishio, H., Sakamoto, H., et al. Modulation of *in vitro* splicing of the upstream intron by modifying an intra-exon sequence which is deleted from the dystrophin gene in dystrophin Kobe. *J Clini Invest* 95, 515-520 (1995).

38. Pramono, Z.A.D., Takeshima, Y., Alimsardjono, H., et al. Induction of exon skipping of the dystrophin transcript in lymphoblastoid cells by transfecting an antisense oligodeoxynucleotide complementary to an exon recognition sequence. *Biochem Bioph Res Co* 226, 445-449 (1996).

39. Takeshima, Y., Wada, H., Yagi, M., et al. Oligonucleotides against a splicing enhancer sequence led to dystrophin production in muscle cells from a Duchenne muscular dystrophy patient. *Brain Dev* 23, 788-790 (2001).

40. Gebski, B.L., Errington, S.J., Johnsen, R.D., et al. Terminal antisense oligonucleotide modifications can enhance induced exon skipping. *Neuromuscul Disord* 15, 622-629 (2005).

41. Yagi, M., Takeshima, Y., Surono, A., et al. Chimeric RNA and 2′-O, 4′-C-ethylene-bridged nucleic acids have stronger activity than phosphorothioate

oligodeoxynucleotides in induction of exon 19 skipping in dystrophin mRNA. *Oligonucleotides* 14, 33-40 (2004).

42. Errington, S.J., Mann, C.J., Fletcher, S., et al. Target selection for antisense oligonucleotide induced exon skipping in the dystrophin gene. *J Gene Med* 5, 518-527 (2003).

43. Van Deutekom, J.C.T., Bremmer-Bout, M., Janson, A.A.M., et al. Antisense-induced exon skipping restores dystrophin expression in DMD patient derived muscle cells. *Hum Mol Genet* 10, 1547-1554 (2001).

44. Takagi, M., Yagi, M., Ishibashi, K., et al. Design of 2′-O-Me RNA/ENA^{TM} chimera oligonucleotides to induce exon skipping in dystrophin pre-mRNA. *Nucleic Acid Symp Ser (Oxf)* 48, 297-298 (2004).

45. Aartsma-Rus, A., Kaman, W.E., Bremmer-Bout, M., et al. Comparative analysis of antisense oligonucleotide analogs for targeted DMD exon 46 skipping in muscle cells. *Gene Ther* 11, 1391-1398 (2004).

46. Aartsma-Rus, A., Janson, A.A.M., Kaman, W.E., et al. Therapeutic antisense-induced exon skipping in cultured muscle cells from six different DMD patients. *Hum Mol Genet* 12, 907-914 (2003).

47. Aartsma-Rus, A., Janson, A.A.M., Kaman, W.E., et al. Antisense-induced multiexon skipping for Duchenne muscular dystrophy makes more sense. *Am J Hum Genet* 74, 83-92 (2004).

48. Wilton, S.D., Fall, A.M., Harding, P.L., et al. Antisense oligonucleotide-induced exon skipping across the human dystrophin gene transcript. *Mol Ther* 15, 1288-1296 (2007).

49. Fletcher, S., Adams, A.M., Johnsen, R.D., et al. Dystrophin isoform induction in vivo by antisense-mediated alternative splicing. *Mol Ther* 18, 1218-1223 (2010).

50. Heemskerk, H.A., De Winter, C.L., De Kimpe, S.J., et al. In vivo comparison of 2'-O-methyl phosphorothioate and morpholino antisense oligonucleotides for Duchenne muscular dystrophy exon skipping. *J Gene Med* 11, 257-266 (2009).

51. Shimo, T., Tachibana, K., Saito, K., et al. Design and evaluation of locked nucleic acid-based splice-switching oligonucleotides in vitro. *Nucleic Acid Res* 42, 8174-8187 (2014).

52. Pires, V.B., Simoes, R., Mamchaoui, K., et al. Short (16-mer) locked nucleic acid splice-swiching oligonucleotides restore dystrophin production in Duchenne muscular dystrophy myotubes. *PLoS One* 12, e0181065 (2017).

53. Jirka, S.M.G., Vander Meulen, J.W., Tanganyika-de Winter, C.L., et al. Evaluation of exon skipping activity of 2′-deoxy-2′-fluoro antisense oligonucleotides for Duchenne muscular dystrophy. *Abstract/Neuromuscul Disord* 24, 791-924. G.P.109 (2014).

54. Jirka, S.M.G., Tanganyika-de Winter, C.L., Boertje-vander Meulen, J.W., et al. Evaluation of 2′-deoxy-2′-fluoro antisense oligonucleotides for exon skipping in Duchenne muscular dystrophy. *Mol Ther Nucleic Acids* 4, e265 (2015).

55. Watanabe, N., Nagata, T., Satou, Y., et al. NS-065/NCNP-01: an antisense oligonucleotide for potential treatment of exon 53 skipping in Duchenne muscular dystrophy. *Mol Ther Nucleic Acids* 13, 442-449 (2018).

56. Lee, J., Echigoya, Y., Duddy, W., et al. Antisense PMO cocktails effectively skip dystrophin exons 45-55 in myotubes transdifferentiated from DMD patient fibroblasts. *PLoS One* 13, e01977084 (2018).

57. Dunckley, M.G., Manoharan, M., Villiet, P., et al. Modification of splicing in the dystrophin gene in cultured *mdx* muscle cells by antisense oligoribonucleotides. *Hum Mol Genet* 5, 1083-1090 (1995).

58. Wilton, S.D., Lloyd, F., Carville, K., et al. Specific removal of the nonsense mutation from the *mdx* dystrophin mRNA using antisense oligonucleotides. *Neuromuscul Disord* 9, 330-338 (1999).

59. Mann, C.J., Honeyman, K., Cheng, A.J., et al. Antisense-induced exon skipping and synthesis of dystriphin in the *mdx* mouse. *Proc Natl Acad Sci USA* 98, 42-47 (2001).

60. Mann, C.J., Honeyman, K., McClorey, Graham., et al. Improved antisense oligonucleotide induced exon skipping in the *mdx* mouse model of muscular dystrophy. *J Gene Med* 4, 644-654 (2002).

61. Lu, L.Q., Rabinowitz, A., Chen, Y.C., et al. Systemic delivery of antisense oligonucleotide restores dystrophin expression in body-wide skeletal muscles. *Proc Natl Acad Sci USA* 102, 198-203 (2005).

62. Gebski, B.L., Mann, C.J., Fletcher, S., et al. Morpholino antisense oligonucleotide induced dystrophin exon 23 skipping in *mdx* mouse muscle. *Hum Mol Genet* 12, 1801-1811 (2003).

63. Fletcher, S., Honeyman, K., Fall, A.M., et al. Dystrophin expression in the *mdx* mouse after localised and systemic administration of a morpholino antisense oligonucleotide. *J Gene Med* 8, 207-216 (2006).

64. Alter, J., Lou, F., Rabinowitz, A., et al. Systemic delevery of morpholino oligonucleotide restores dystrophin expression bodywide and improves dystrophin pathology. *Nat Med* 12, 175-177 (2006).

65. Yin, H., Lu, Q., Wood, M. Effective exon skipping and resoration of dystrophin expression by peptide nucleic acid antisense oligonucleotides in *mdx* mice. *Mol Ther* 16, 38-45 (2008).

66. Gao, X., Shen, X., Dong, X., et al. Peptide nucleic acid promotes systemic dystrophin expression and functional rescue in dystrophin-deficient mdx mice. *Mol Ther Nucleic Acids* 4, e225 (2015).

67. Le, B.T., Murayama, K., Shabanpoor, F., et al. Antisense oligonucleotide modified with serinol nucleic acid (SNA) induces exon skipping in *mdx* myotubes. *RSC Adv* 7, 34049-34052 (2017).

68. Goyenvalle, A., Griffith, G., Babbs, A., et al. Functional correction in mouse models of muscular dystrophy using exon-skipping tricyclo-DNA oligomers. *Nat Med* 21, 270-275 (2015).

69. Relizani, K., Griffith, G., Echevarria, L., et al. Efficacy and safety profile of tricyclo-DNA antisense oligonucleotides in Duchenne muscular dystrophy mouse model. *Mol Ther Nucleic Acids* 8, 144-157 (2017).

70. Le, B.T., Chen, S., Abramov, M., et al. Evaluation of anhydrohexitol nucleic acid, cyclohexenyl nucleic acid and D-altritol nucleic acid-modified 2′-*O*-methyl RNA mixmer antisense oligonucleotides for exon skipping *in vitro*. *Chem Commun* 52, 13467-13470 (2016).

71. Le, B.T., Hornum, M., Sharma, P.K., et al. Nucleobase-modified antisense oligonucleotides containing 5-(phenyltriazol)-2′-deoxyuridine nucleotides induce exon-skipping *in vitro*. *RSC Adv* 7, 54542-54545 (2017).

72. Le, B.T., Adams, A.M., Fletcher, S., et al. Rational design of short locked nucleic acid-modified 2′-O-methyl antisense oligonucleotides for efficient exon-skipping *in vitro*. *Mol Ther Nucleic Acids* 9, 155-161 (2017).

73. Howell, J.M., Flectcher, S., Kakulas, B.A., et al. Use of the dog model for Duchenne muscular dystrophy in gene therapy trials. *Neuromuscul Disord* 7, 325-328 (1997).

74. McClorey, G., Moulton, H.M., Iversen, P.L., et al. Antisense oligonucleotide-induced exon skipping restores dystrophin expression in vitro in a canine model of DMD. *Gene Ther* 13, 1373-1381 (2006).

75. Yokota, T., Lu, Q., Partridge, T., et al. Efficacy of systemic morpholino exon-skipping in Duchenne dystrophy dogs. *Ann Neurol* 65, 667-676 (2009).

76. Saito, Takashi., Nakamura, A., Aoki, Y., et al. Antisense PMO found in dystrophic dog model was effective in cells from exon 7-deleted DMD patient. *PLoS One* 5, e12239 (2010).

77. Aartsma-Rus, A., Fokkema, I., Verschuuren, J., et al. Theoretic applicability of antisense-mediated exon skipping for Duchenne muscular dystrophy mutations. *Hum Mutat* 30, 293-299 (2009).

78. McNally, E.M., Wyatt, E.J., Mutation-based therapy for Duchenne muscular dystrophy. *Circulation* 136, 979-981 (2017).

79. Aartsma-Rus, A., Straub, V., Hemmings, R., et al. Development of exon skipping therapies for Duchenne muscular dystrophy: a critical review and a perspective on the outstanding issues. *Nucleic Acid Ther* 27, 251-259 (2017).

80. Mendell, J.R., Sahenk, Z., Rodino-Klapac, R. Clinical trials of exon skipping in Duchenne muscular dystrophy. *Expert Opin Orphan D* 5, 683-690.

81. Echevarria, L., Aupy, P., Goyenvalle, A. Exon-skipping advances for Duchenne muscular dystrophy. *Hum Mol Genet* 27, 163-172 (2018).

82. Kinali, M., Arechavala-Gomeza, V., Feng, L., et al. Local restoration of dystrophin expression with the morpholino oligomer AVI-4658 in Duchenne muscular dystrophy: a single-blind, placebo-controlled, dose-escalation, proof-of-concept study. *Lancet Neurol* 8, 918–928 (2009).

83. Van Deutekom, J.C., Janson, A.A., Ginjaar, I.B., et al. Local dystrophin restoration with antisense oligonucleotide PRO051. *N Engl J Med* 357, 2677–2686 (2007).

84. Scully, M.A., Pandya, S., Moxley, R.T. Review of phase II and phase III clinical trials for Duchenne muscular dystrophy. *Expert Opin Orphan D* 1, 33–46 (2013).

85. Voit, T., Topaloglu, H., Straub, V., et al. Safety and efficacy of drisapersen for the treatment of Duchenne muscular dystrophy (DEMAND II): an exploratory, randomised, placebo-controlled phase 2 study. *Lancet Neurol* 13, 987–996 (2014).

86. Goemans, N.M., Tulinius, M., van den Akker, J.T., et al. Systemic administration of PRO051 in Duchenne's muscular dystrophy. *N Engl J Med* 364, 1513–1522 (2011).

87. Wilton, S.D., Veedu, R.N., Fletcher, S. The emperor's new dystrophin: finding sense in the noise. *Trends Mol Med* 21, 417–426 (2015).

88. Goemans, N., Mercuri, E., Belousova, E., et al. A randomized placebo-controled phase 3 trial of an antisense oligonucleotide, drisapersen, in Duchenne muscular dystropgy. *Neuromuscul Disord* 28, 4-15 (2018).

89. Mendell, J.R., Rodino-Klapac, L.R., Sahenk, Z., et al. Eteplirsen for the treatment of Duchenne muscular dystrophy. *Ann Neurol* 74, 637–647 (2013).

90. Le, B.T., Veedu, R.N., Fletcher, S., et al. Antisense oligonucleotide development for the treatment of muscular dystrophies. *Expert Opin Orphan D* 4, 139–152 (2015).

91. Bulfield, G., Siller, W.G., Wight, P.A., Moore, K.J. X chromosome-linked muscular dystrophy (*mdx*) in the mouse. *Proc Natl Acad Sci USA* 81, 1189-1192 (1984).

92. Rando, T.A., Blau, H.M. Primary mouse myoblast purification, characterization, and transplantation for cell-mediated gene therapy. *J Cell Biol* 125, 1275-1287 (1994).

93. Mann, C.J., Honeyman, K., Cheng, A.J., et al. Antisense-induced exon skipping and synthesis of dystrophin in the mdx mouse. *Proc Natl Acad Sci USA* 98, 42–47 (2001).

94. Schneider, C.A., Rasband, W.S., Eliceiri, K.W. NIH Image to ImageJ: 25 years of image analysis. *Nat Methods* 9, 671-675 (2012).

95. Lundin, K.E., Gissberg, O., Smith, C.I. Oligonucleotide therapies: the past and the present. *Hum Gene Ther* 26, 475-485 (2015).

96. Eckstein, F. Phosphorothioate oligodeoxynucleotides: what is their origin and what is unique about them? *Nucleic Acid Drug Dev* 10, 117-121 (2000).

97. Majlessi, M., Nelson, N.C., Becker, M.M. Advantages of 2'-O-methyl oligoribonucleotide probes for detecting RNA targets. *Nucleic Acids Res* 26, 2224-2229 (1998).

98. Kawasaki, A.M., Casper, M.D., Freier, S.M. et al. Uniformly modified 2'-deoxy-2'-fluoro-phosphorothioate oligonucleotides as nuclease-resistant antisense compounds with high affinity and specificity for RNA targets. *J Med Chem* 36, 831-841 (1993).

99. Rigo, F., Hua, Y., Chun, S.J. et al. Synthetic oligonucleotides recruit ILF2/3 to RNA transcripts to modulate splicing. *Nat Chem Biol* 8, 555-561 (2012).

100. Geary, R.S., Watanabe, T.A., Truong, L. et al. Pharmacokinetic properties of 2'-O-(2-methoxyethyl)-modified oligonucleotide analogs in rats. *J Pharmacol Exp Ther* 296, 890-897 (2001).

101. Summerton, J., Weller, D. Morpholino antisense oligomers: design, preparation, and properties. *Antisense Nucleic Acid Drug Dev* 7, 187-195 (1997).

102. Veedu, R.N., Wengel, J. Locked nucleic acids: promising nucleic acid analogs for therapeutic applications. *Chem Biodivers* 7, 536-542 (2010).

103. Veedu, R.N., Wengel, J. Locked nucleic acid as a novel class of therapeutic agents. *RNA Biol* 6, 321-323 (2009).

104. Langkjaer, N., Pasternak, A., Wengel, J. UNA (unlocked nucleic acid): a flexible RNA mimic that allows engineering of nucleic acid duplex stability. *Bioorg Med Chem* 17, 5420-5425 (2009).

105. Hyrup, B., Nielsen, P.E. Peptide nucleic acids (PNA): synthesis, properties and potential applications. *Bioorg Med Chem* 4, 5-23 (1996).

106. Renneberg, D., Leumann, C.J. Watson-crick base-pairing properties of tricyclo-DNA. *J Am Chem Soc* 124, 5993-6002 (2002).

107. Le, B.T., Filichev, V.V., Veedu, R.N. Investigation of twisted intercalating nucleic acid (TINA)-modified antisense oligonucleotides for splice modulation by induced exon-skipping *in vitro*. *RSC Adv* 6, 95169-95172 (2016).

108. Le, B.T., Hornum, M., Sharma, P.K., et al. Nucleobase-modified antisense oligonucleotides containing 5-(phenyltriazol)-2'-deoxyuridine nucleotides induce exon-skipping *in vitro*. *RSC Adv* 7, 54542-54545 (2017).

109. Mitrpant, C., Fletcher, S., Wilton, S.D. Personalised genetic intervention for Duchenne muscular dystrophy: antisense oligomers and exon skipping. *Curr Mol Pharmacol* 2, 110-121 (2009).

110. Kole, R., Krieg, A.M. Exon skipping therapy for Duchenne muscular dystrophy. *Adv Drug Deliv Rev* 87, 104-107 (2015).

111. Fletcher, S., Bellgard, M.I., Price, L. et al. Translational development of splice-modifying antisense oligomers. *Expert Opin Biol Ther* 17, 15-30 (2017).

112. Fletcher, S., Adkin, C.F., Meloni, P. et al. Targeted exon skipping to address “leaky” mutations in the dystrophin gene. *Mol Ther Nucleic Acids* 1, e48 (2012).

113. Miceli, M.C., Nelson, S.F. The case for eteplirsen: paving the way for precision medicine. *Mol Genet Metab* 118, 70-71 (2016).

114. GSK and Prosensa Announce Primary Endpoint Not Met in Phase III Study of Drisapersen in Patients With Duchenne Muscular Dystrophy. Available online: https://globenewswire.com/news-release/2013/09/20/574726/10049265/en/GSK-and-

Prosensa-Announce-Primary-Endpoint-Not-Met-in-Phase-III-Study-of-Drisapersen-in-Patients-With-Duchenne-MuscularDystrophy.html (accessed on 20 July 2018).

115. Morgan, J.E., Beauchamp, J.R., Pagel, C.N., et al. Myogenic cell lines derived from transgenic mice carrying a thermolabile t antigen: A model system for the derivation of tissue-specific and mutation-specific cell lines. *Dev Biol* 162, 486-498 (1994).

Appendix A: Supplementary data for Chapter 2

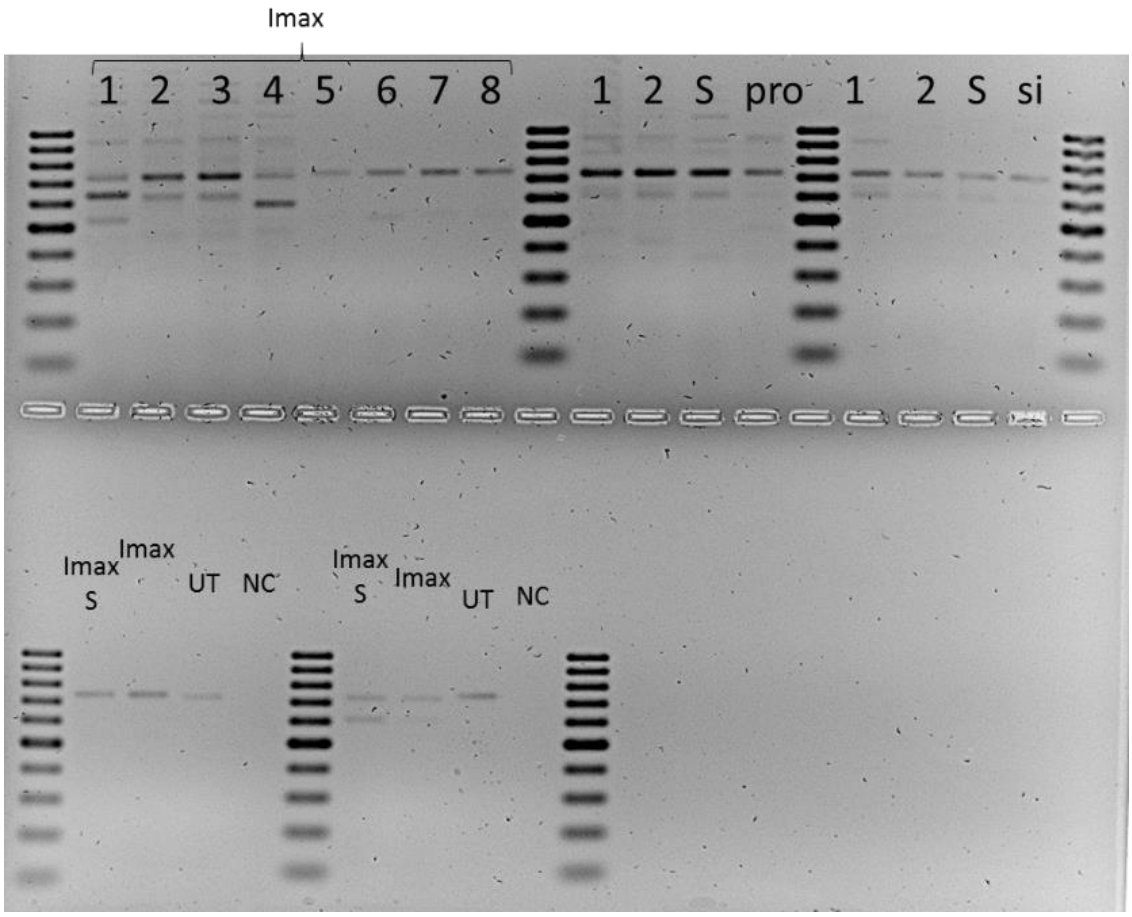

Supplementary figure 4.3.1.1 Screening of AO1-8 in Huh-7 cell line at 400 nanomolar concentration. S: scrambled sequence, UT: untreated, NC: negative control, Imax: RNAiMAX, pro: Metafectene® PRO, si: Metafectene® SI+.

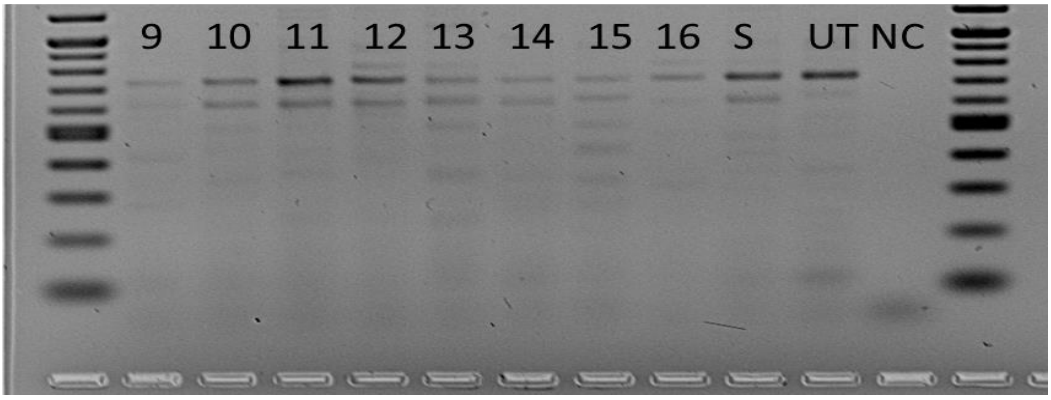

Supplementary figure 4.3.1.2 Screening of AO9-16 in Huh-7 cell line using RNAiMAX reagent in Huh-7 cell line at 400 nanomolar concentration. S: scrambled sequence, UT: untreated, NC: negative control.

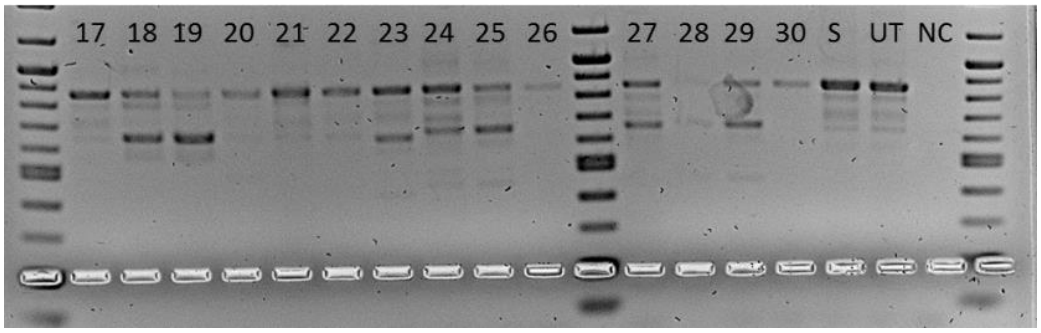

Supplementary figure 4.3.1.3 Screening of AO17-30 in Huh-7 cell line using RNAiMAX reagent in Huh-7 cell line at 400 nanomolar concentration. S: scrambled sequence, UT: untreated, NC: negative control.

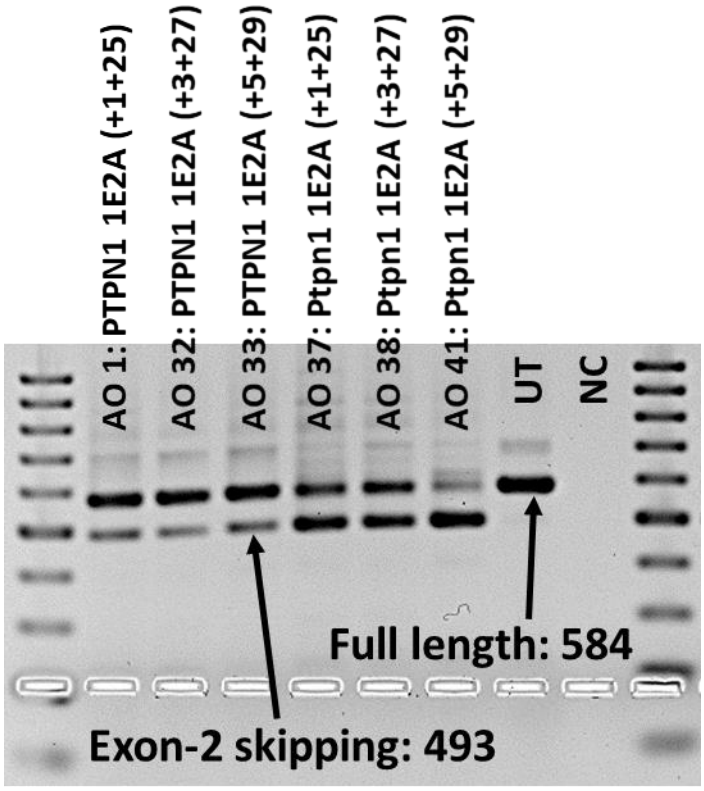

Supplementary figure 4.3.3.1 Comparison of exon-2 skipping efficiency between mouse *Ptpn1* targeting AOs and human *PTPN1* targeting AOs in mouse AML-12 cells at 400 nM concentration.

UT: untreated, NC: negative control.

Appendix B: Publications

First Author and co-author publications (up to 28th May 2020).

Publications from this thesis are listed in chronological order.

The first page of each publications is shown.

RNA BIOLOGY
2016, VOL. 0, NO. 0, 1–14
http://dx.doi.org/10.1080/15476286.2016.1236173

Taylor & Francis
Taylor & Francis Group

REVIEW

In vitro evolution of chemically-modified nucleic acid aptamers: Pros and cons, and comprehensive selection strategies

Farhana Lipi[a], Suxiang Chen[a,b], Madhuri Chakravarthy[a,b], Shilpa Rakesh[a], and Rakesh N. Veedu[a,b]

[a]Western Australian Neuroscience Research Institute, Perth, Australia; [b]Centre for Comparative Genomics, Murdoch University, Perth, Australia

ABSTRACT

Nucleic acid aptamers are single-stranded DNA or RNA oligonucleotide sequences that bind to a specific target molecule with high affinity and specificity through their ability to adopt 3-dimensional structure in solution. Aptamers have huge potential as targeted therapeutics, diagnostics, delivery agents and as biosensors. However, aptamers composed of natural nucleotide monomers are quickly degraded *in vivo* and show poor pharmacodynamic properties. To overcome this, chemically-modified nucleic acid aptamers are developed by incorporating modified nucleotides after or during the selection process by Systematic Evolution of Ligands by EXponential enrichment (SELEX). This review will discuss the development of chemically-modified aptamers and provide the pros and cons, and new insights on *in vitro* aptamer selection strategies by using chemically-modified nucleic acid libraries.

Abbreviations: SELEX, Systematic Evolution of Ligands by EXponential enrichment; US FDA, United States Food and Drug Administration; AMD, Age-related macular degeneration; VEGF, Vascular endothelial growth factor protein, 2′-NH_2, 2′-Amino; 2′-OH, 2′-Hydroxyl; K_d, Equilibrium dissociation constant; 2′-OMe, 2′-O-Methyl; Bfgf, Basic fibroblast growth factor; 2′-F, 2′-Fluoro; PSMA, Prostate specific membrane antigen; IFN-γ, Interferon-gamma; KGF, Keratinocyte growth factor; 4′-S, 4′-Thio; 2′-FANA, 2′-Fluroarabino nudeic acid; HNA, 1,5-Anhydro hexitol nudeic acid; TAR, transactivation responsive element; TNA, Threose nucleic acid; LNA, Locked nudeic acid; SOMAmers, Slow Off-rate Modified Aptamers

ARTICLE HISTORY
Received 29 July 2016
Revised 6 September 2016
Accepted 7 September 2016

KEYWORDS
Aptamers; chemical antibodies; chemically-modified aptamers; *in vitro* selection; modified nucleotides; nucleic acid ligands; SELEX

Introduction

Nucleic acid aptamer technology has attracted considerable attention in recent years in light of their widespread applications in therapeutic development, targeted drug delivery, biosensing and accurate molecular imaging. Aptamers are short single-stranded DNA or RNA oligonucleotides with unique 3-dimensional shape that can bind to their specific target with very high affinity and specificity.[1-5] Aptamers are generally developed from a large pool of oligonucleotide libraries containing approximately 10^{14} members by a reiterative process referred to as SELEX which involves selection, separation and enrichment steps (Fig. 1).[6,7] Till now, antibodies have been widely used for target specific molecular recognition.[8] However, compared to antibody-based technologies, aptamers may possess a number of advantages including easy laboratory production *in vitro* effectively eliminating the use of live animals, no batch to batch variation, low or no immunogenicity, freedom to introduce multiple chemistries during synthesis without losing the affinity and specificity, small size that allows faster tissue penetration, ability to reverse target binding interactions using its complementary antidote sequence, significantly longer shelf-life and low cost. In 2004, an aptamer drug Macugen (Pegaptanib Sodium) was approved by United States Food and Drug Administration (US FDA) for the treatment of neovascular age-related macular degeneration (AMD) by targeting vascular endothelial growth factor protein 165 ($VEGF_{165}$).[9,10] Currently, a number of aptamer-based therapeutic candidates are in preclinical development and in different stages of clinical trials.[11]

Typically, aptamers are developed with naturally occurring nucleotides. However, aptamers composed of natural nucleotide monomers are not suitable for theranostic applications as they possess very poor resistance to enzymatic degradation and show decreased binding affinity, rendering poor pharmacokinetic properties. To circumvent these shortcomings, aptamers containing chemically-modified nucleotide analogs with high stability against nucleases are normally used. Early examples of modified aptamers were primarily produced by post-SELEX-based approach. In this process, the aptamers were first isolated using natural RNA or DNA random sequences by SELEX method and then modified as per demand on affinity, stability and functionality. For this purpose, appropriate chemically-modified nucleotides are systematically incorporated into an existing DNA/RNA aptamer during solid-phase oligonucleotide synthesis. Generally, a web-based secondary structure prediction algorithm (e.g. mfold,[12] RNAfold[13]) is used as a tool to assist with the positioning of chemically-modified nucleotides and to truncate the overall size of the selected aptamers during chemical synthesis. Such chemically-fabricated

CONTACT Rakesh N. Veedu r.veedu@murdoch.edu.au Centre for Comparative Genomics, Murdoch University, Perth, WA, Australia-6149

ChemComm

COMMUNICATION

View Article Online
View Journal

Evaluation of anhydrohexitol nucleic acid, cyclohexenyl nucleic acid and D-altritol nucleic acid-modified 2′-*O*-methyl RNA mixmer antisense oligonucleotides for exon skipping *in vitro*†

Cite this: DOI: 10.1039/c6cc07447b

Received 12th September 2016,
Accepted 20th October 2016

DOI: 10.1039/c6cc07447b

www.rsc.org/chemcomm

Bao T. Le,[ab] Suxiang Chen,[ab] Mikhail Abramov,[c] Piet Herdewijn[c] and Rakesh N. Veedu*[ab]

Antisense oligonucleotide (AO) mediated exon skipping has been widely explored as a therapeutic strategy for several diseases, in particular, for rare genetic disorders such as Duchenne muscular dystrophy (DMD). To date, the potential of anhydrohexitol nucleic acid (HNA), cyclohexenyl nucleic acid (CeNA) and altritol nucleic acid (ANA) has not been explored in exon skipping. For the first time, in this study we designed and synthesised HNA, CeNA and ANA-modified 2′-*O*-methyl (2′-OMe) mixmer AOs on a phosphorothioate (PS) backbone, and evaluated their potential to induce exon 23 skipping in *mdx* mouse myotubes, as a model system. Our results clearly showed that all three AO candidates modified with HNA, CeNA and ANA could efficiently induce *Dmd* exon 23 skipping *in vitro* in parallel to the fully modified 2′-OMePS AO with reduced dual exon 22/23 skipping. In addition, they showed high nuclease resistance and no cytotoxicity compared to the 2′-OMePS AO, demonstrating the applicability of HNA, CeNA and ANA nucleotide-modified AOs in exon skipping.

Synthetic nucleic acid-based therapy has attracted considerable attention in recent years and offers great potential as therapeutics to various diseases.[1] To date, three compounds have been approved by US Food and Drug Administration (FDA) for clinical use including Vitravene, a 21mer phosphorothioate-modified antisense oligonucleotide (AO) against cytomegalovirus retinitis; Macugen, a 27mer aptamer oligonucleotide modified with 2′-*O*-methyl (2′-OMe) and 2′-fluoro-DNA nucleotides for the treatment of age-related macular degeneration; and Kynamro, another AO modified with 2′-*O*-methoxyethyl-RNA chimera against familial hypercholesterolemia.[1,2] However, naturally occurring nucleic acid nucleotide-based oligonucleotides are rapidly degraded *in vivo* and possess poor binding affinity. Therefore, the introduction of chemically modified monomers is widely used for improving the binding affinity, stability against nuclease degradation, and also for limiting the immune-stimulatory properties. Towards this, Herdewijn and colleagues reported the development of anhydrohexitol nucleic acid (HNA),[3] cyclohexenyl nucleic acid (CeNA)[4,5] and altritol nucleic acid (ANA)[6] (Fig. 1). HNA forms stable duplexes with complementary DNA and RNA oligonucleotides in a sequence selective manner with a ΔT_m of +1.3 °C per base pair with DNA and a ΔT_m of +3 °C per base pair with RNA.[3] In addition, HNA monomers show complete stability towards 3′-exonucleases. CeNA is considered to be a DNA mimic with a six-membered cyclohexene ring.[4,5] The introduction of CeNA nucleotide into the DNA strand of a DNA/RNA hybrid increases the thermal stability of the duplex,[4,5] and CeNA-modified oligos are very stable against nuclease degradation.[5] ANA is another unique nucleic acid analogue with very high hybridisation affinity for complementary RNA oligonucleotides adopting an A-type duplex similar to natural RNA, and is very stable in human serum.[6]

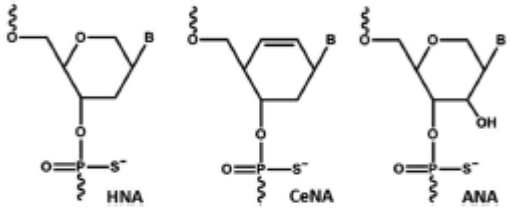

Fig. 1 Structural representations of HNA, CeNA and ANA nucleotide monomers used in this study.

Antisense oligonucleotide (AO) mediated exon skipping has been widely explored as a therapeutic strategy for several diseases, in particular, Duchenne muscular dystrophy (DMD).[7] DMD is a muscle wasting, invariably fatal genetic disease mainly affecting boys, which leads to death in early adulthood.[8] Individuals with DMD lack the protein dystrophin, which is required to strengthen

[a] Centre for Comparative Genomics, Murdoch University, Perth – 6150, Australia. Email: R.Veedu@murdoch.edu.au
[b] Western Australian Neuroscience Research Institute, Perth – 6150, Australia
[c] Laboratory for Medicinal Chemistry, Rega Institute for Medical Research, Katholieke Universiteit Leuven, Minderbroedersstraat 10, 3000 Leuven, Belgium
† Electronic supplementary information (ESI) available. Materials, detailed experimental protocol for cell culture, RNA isolation and RT-PCR, cytotoxicity analysis, and stability analysis by phosphodiesterase. See DOI: 10.1039/c6cc07447b

molecules

MDPI

Article

Synthesis of a Morpholino Nucleic Acid (MNA)-Uridine Phosphoramidite, and Exon Skipping Using MNA/2′-*O*-Methyl Mixmer Antisense Oligonucleotide

Suxiang Chen [1,2], Bao T. Le [1,2], Kamal Rahimizadeh [1], Khalil Shaikh [3], Narinder Mohal [3] and Rakesh N. Veedu [1,2,*]

1 Centre for Comparative Genomics, Murdoch University, Perth 6150, Australia; S.Chen@murdoch.edu.au (S.C.); T.Le2@murdoch.edu.au (B.T.L.); rahimizadeh.kamal@gmail.com (K.R.)
2 Western Australian Neuroscience Research Institute, Perth 6150, Australia
3 GMK Research Laboratories Pvt. Ltd., Mallapur, Hyderabad 500 076, India; khalil.shaikh@gmkresearch.com (K.S.); narinder.mohal@gmkresearch.com (N.M.)
* Correspondence: rveedu@ccg.murdoch.edu.au; Tel.: +61-8-9360-2803

Academic Editor: Derek J. McPhee
Received: 21 September 2016; Accepted: 16 November 2016; Published: 22 November 2016

Abstract: In this study, we synthesised a morpholino nucleoside-uridine (MNA-U) phosphoramidite and evaluated the potential of a MNA-modified antisense oligonucleotide (AO) sequences to induce exon 23 skipping in *mdx* mouse myotubes in vitro towards extending the applicability of morpholino chemistry with other nucleotide monomers. We designed, synthesised, and compared exon skipping efficiencies of 20 mer MNA-modified 2′-*O*-methyl RNA mixmer AO on a phosphorothioate backbone (MNA/2′-OMePS) to the corresponding fully modified 2′-*O*-methyl RNA AO (2′-OMePS) as a control. Our results showed that the MNA/2′-OMePS efficiently induced exon 23 skipping. As expected, the 2′-OMePS AO control yielded efficient exon 23 skipping. Under the applied conditions, both the AOs showed minor products corresponding to exon 22/23 dual exon skipping in low yield. As these are very preliminary data, more detailed studies are necessary; however, based on the preliminary results, MNA nucleotides might be useful in constructing antisense oligonucleotides.

Keywords: morpholino nucleotide; PMO; exon skipping; antisense oligonucleotide

1. Introduction

Nucleic acid-based technologies [1] have attracted significant interest in recent years for targeting the molecular pathogenesis of various diseases. Antisense oligonucleotides (AOs), an important therapeutic molecule of this class, can efficiently regulate the expression of cellular RNAs by selectively cleaving, blocking, or repairing pathogenic messenger RNAs [1]. AOs bind to complementary target RNA sequences through hydrogen bonding. High affinity RNA targeting, better mis-match recognition, and a high degree of nuclease resistance are key factors in developing successful AO-based therapeutics. AOs composed of naturally occurring nucleotides show low target binding affinity and substantially poor resistance to nucleases, and consequently are unsuitable for therapeutic development. Chemically modified nucleotide analogues are generally incorporated into AOs to overcome these limitations and improve the pharmacokinetic profile of nucleic acid-based drugs. A number of chemically modified nucleotides have been developed in recent years. Some examples of the prominent chemistries utilised in AOs are 2′-*O*-methyl (2′-OMe) [2], 2′-*O*-methoxyethyl (2′-*O*-MOE) [3], phosphorodiamidate morpholino (PMO) [4], locked nucleic acid (LNA) [5,6], peptide nucleic acid (PNA) [7], tricyclo-DNA (tcDNA) [8], and unlocked nucleic acid (UNA) [9]. As the internucleotide linkages are vulnerable to

IVYSPRING INTERNATIONAL PUBLISHER

Theranostics

2017; 7(16): 3933-3947. doi: 10.7150/thno.21529

Review

Nucleic Acid-Based Theranostics for Tackling Alzheimer's Disease

Madhuri Chakravarthy[1, 2], Suxiang Chen[1, 2], Peter R. Dodd[3], Rakesh N. Veedu[1, 2, 3]✉

1. Centre for Comparative Genomics, Murdoch University, Murdoch, Perth, Australia 6150;
2. Perron Institute for Neurological and Translational Science, QEII Medical Centre, Nedlands, Perth, Australia 6005;
3. School of Chemistry and Molecular Biosciences, The University of Queensland, St Lucia, Brisbane, Australia 4072.

✉ Corresponding author: Rakesh N. Veedu, PhD. Centre for Comparative Genomics, Murdoch University, Building 390 Discovery Drive, Perth, Western Australia, Australia 6150. Email: R.Veedu@murdoch.edu.au

Received: 2017.06.20; Accepted: 2017.07.28; Published: 2017.09.05

Abstract

Nucleic acid-based technologies have received significant interest in recent years as novel theranostic strategies for various diseases. The approval by the United States Food and Drug Administration (FDA) of Nusinersen, an antisense oligonucleotide drug, for the treatment of spinal muscular dystrophy highlights the potential of nucleic acids to treat neurological diseases, including Alzheimer's disease (AD). AD is a devastating neurodegenerative disease characterized by progressive impairment of cognitive function and behavior. It is the most common form of dementia; it affects more than 20% of people over 65 years of age and leads to death 7–15 years after diagnosis. Intervention with novel agents addressing the underlying molecular causes is critical. Here we provide a comprehensive review on recent developments in nucleic acid-based theranostic strategies to diagnose and treat AD.

Key words: nucleic acids; Alzheimer's disease; amyloid beta peptides; tau peptide; chemically modified oligonucleotides; nucleic acid therapeutics.

Introduction

Nucleic acid-based technologies typically use synthetic oligonucleotides ~8–50 nucleotides in length, most of which bind to RNA through Watson-Crick base pairing to alter the expression of the targeted RNA and protein. Novel chemical modifications and conjugation strategies have been developed to improve pharmacokinetics and tissue-specific delivery. Vitravene, Kynamro, Nusinersen and Eteplirsen are antisense oligonucleotides (AOs) approved by the FDA to treat cytomegalovirus retinitis, familial hypercholesterolemia, spinal muscular atrophy, and Duchenne muscular dystrophy respectively [1-3]. The nucleic acid aptamer drug Macugen was approved for age-related macular degeneration [4]. These successful clinical translations demonstrate the potential of nucleic acid-based technologies and provide scope for developing novel therapeutics for AD. AD is the most common form of dementia; it accounts for 70% of cases with that diagnosis. Globally there are ~47 million current cases; 7.7 million new cases are added each year [5]. AD is characterized by a progressive loss of memory and cognitive function [6]. Patients eventually need 24-hour care that places emotional and economic burdens on the community. There is no cure for AD, nor any treatment that addresses its underlying molecular cause [5]. Current treatments use cholinesterase inhibitors [7] and *N*-methyl-D-aspartate receptor (NMDA) antagonists [8] that improve cognitive function and reduce symptoms temporarily but do not stop the progression of the disease. The current approach to diagnosis relies on a combination of cognitive and clinical assessment, genetic profiling, and magnetic resonance imaging to measure anatomical changes in the brain [9], but confirmation relies on post-mortem neuropathological assessment

ChemComm

COMMUNICATION

View Article Online
View Journal | View Issue

Cite this: Chem. Commun., 2018, 54, 4593

Received 21st March 2018,
Accepted 10th April 2018

DOI: 10.1039/c8cc02256a

rsc.li/chemcomm

Development of DNA aptamers targeting low-molecular-weight amyloid-β peptide aggregates *in vitro*†

Madhuri Chakravarthy,[ab] Hadi AlShamaileh,[ac] He Huang,[c] Rudi K. Tannenberg,[c] Suxiang Chen,[abc] Simon Worrall,[c] Peter R. Dodd[c] and Rakesh N. Veedu*[abc]

We have developed a novel functional nucleic acid aptamer to amyloid-β peptide 1–40 ($A\beta_{1-40}$) and investigated its potential to detect Aβ peptide fragments in neuropathologically confirmed Alzheimer brain hippocampus tissues samples. Our results demonstrate that the aptamer candidate RNV95 could detect tetrameric/pentameric low-molecular-weight Aβ aggregates in autopsy hippocampal tissue from two neuropathologically confirmed Alzheimer disease cases. Although these are preliminary observations, detailed investigations are under way. This is the first demonstration of aptamer-Aβ binding in Alzheimer brain tissues.

Synthetic functional nucleic acids have attracted considerable attention in recent years; they show great potential as therapeutics for various diseases.[1] Aptamers are prominent class of synthetic short single-stranded DNA or RNA oligonucleotide sequences that can bind to their targets with very high affinity and specificity because of their ability to adopt three-dimensional structures in solution.[2–7] Aptamers are normally developed from a large pool ($\sim 10^{15}$ members) of randomised oligonucleotide sequences by an *in vitro* reiterative selection process called Systematic Evolution of Ligands by EXponential enrichment (SELEX).[8,9] We recently reported a rapid one-step selection methodology for developing nucleic acid aptamers.[10] Aptamers (often termed 'chemical antibodies') are ideal for applications in drug delivery[11] and therapeutics development (*e.g.*, blocking target receptors; mediating delivery of a therapeutic agent), biosensing (*e.g.*, labelling and detection) and nanotechnology (*e.g.*, anchoring and nano-sensors). An aptamer-based drug, Macugen (Pegaptanib Sodium), has been approved by the United States Food and Drug Association for clinical use in the treatment of age-related macular degeneration.[12]

Aptamers can potentially target the pathogenic components of Alzheimer's disease (AD).[6,13–16] AD is characterised by progressive impairment of cognitive function and behaviour. It affects more than 20% of people aged 65 or older and leads to death on average nine years after diagnosis.[17] The neuropathological hallmarks of AD are extracellular amyloid-β (Aβ) plaques[18] and intracellular neurofibrillary tangles (NFTs)[19] that accumulate in specific brain areas. Amyloid plaques are mainly composed of aggregates of Aβ peptide 40 to 42 amino acids in length ($A\beta_{1-40}$ and $A\beta_{1-42}$). Previous reports on aptamers developed against the $A\beta_{1-40}$ peptide showed that it is difficult to select peptide-specific aptamers against monomeric $A\beta_{1-40}$ due to its high tendency to form Aβ aggregates in solution, even under strict experimental conditions that aim to limit the aggregation.[20–22] Herein, for the first time, we describe the development of novel nucleic acid aptamers that can detect low-molecular-weight aggregates in brain tissues from confirmed AD cases.

First, we conducted *in vitro* selection (Fig. 1) experiments to isolate novel DNA aptamers targeting $A\beta_{1-40}$ (see ESI† for detailed experimental protocols). An 81mer DNA oligonucleotide library containing 40mer randomised regions flanked by 20 and 21 nucleotide primer-binding regions was used in magnetic bead-based affinity selection protocols. Biotinylated $A\beta_{1-40}$ peptide monomers were immobilised onto streptavidin-coated magnetic beads (Dynabeads®). Prior to immobilisation, $A\beta_{1-40}$ peptide was dissolved in 1,1,1,3,3,3-hexafluoro-2-propanol (HFIP) and sonicated to prevent rapid aggregation. Ten rounds of selection consisted of incubating the ssDNA library with bead-immobilized $A\beta_{1-40}$ peptides, separation of the bound aptamer candidate sequences from the unbound, and amplification and regeneration of the target-bound aptamer candidates. Before target incubation, the library was denatured at 95 °C in selection buffer and slowly cooled to enhance folding to adopt the most stable structure. In the first round of selection, 1 nmol of the library was used; which was then reduced to 100 pmol in

[a] Centre for Comparative Genomics, Murdoch University, Perth, 6150, Australia. Email: R.Veedu@murdoch.edu.au
[b] Perron Institute for Neurological and Translational Science, Perth, 6150, Australia
[c] School of Chemistry and Molecular Biosciences, The University of Queensland, Brisbane, 4072, Australia

† Electronic supplementary information (ESI) available: Materials, detailed experimental protocol for aptamer selection, and protocols for western blot analysis for aptamer binding of amyloid beta peptide binding in Alzheimer brain tissues. See DOI: 10.1039/c8cc02256a

pharmaceuticals

MDPI

Review

Radiolabeling of Nucleic Acid Aptamers for Highly Sensitive Disease-Specific Molecular Imaging

Leila Hassanzadeh [1,2], Suxiang Chen [2,3] and Rakesh N. Veedu [2,3,*]

[1] Department of Nuclear Medicine, School of Medicine, Rajaie Cardiovascular, Medical and Research Center & Department of Medicinal Chemistry, School of Pharmacy-International Campus, Iran University of Medical Sciences, Tehran 1449614535, Iran; hassanzadeh.l@iums.ac.ir

[2] Centre for Comparative Genomics, Murdoch University, Perth 6150, Australia; S.Chen@murdoch.edu.au

[3] Perron Institute for Neurological and Translational Science, Perth 6009, Australia

[*] Correspondence: R.Veedu@murdoch.edu.au; Tel.: +61-89-360-2803

Received: 22 August 2018; Accepted: 10 October 2018; Published: 15 October 2018

Abstract: Aptamers are short single-stranded DNA or RNA oligonucleotide ligand molecules with a unique three-dimensional shape, capable of binding to a defined molecular target with high affinity and specificity. Since their discovery, aptamers have been developed for various applications, including molecular imaging, particularly nuclear imaging that holds the highest potential for the clinical translation of aptamer-based molecular imaging probes. Their easy laboratory production without any batch-to-batch variations, their high stability, their small size with no immunogenicity and toxicity, and their flexibility to incorporate various functionalities without compromising the target binding affinity and specificity make aptamers an attractive class of targeted-imaging agents. Aptamer technology has been utilized in nuclear medicine imaging techniques, such as single photon emission computed tomography (SPECT) and positron emission tomography (PET), as highly sensitive and accurate biomedical imaging modalities towards clinical diagnostic applications. However, for aptamer-targeted PET and SPECT imaging, conjugation of appropriate radionuclides to aptamers is crucial. This review summarizes various strategies to link the radionuclides to chemically modified aptamers to accomplish aptamer-targeted PET and SPECT imaging.

Keywords: aptamers; aptamer-targeted imaging; molecular imaging; aptamer-radiolabeling

1. Introduction

Molecular imaging technologies employ labeled molecules to explore biological targets in living subjects for disease detection and monitoring treatment progress in real time. The nuclear imaging technique is a powerful approach to achieve highly sensitive imaging. The two most current approaches, that is, positron emission tomography and single photon emission computed tomography, use radionuclides to label specific therapeutic and/or diagnostic (theranostic) molecules for diagnosis and prognosis of many diseases [1,2]. Clinical molecular imaging using these techniques facilitates characterization of biological processes in vivo on a molecular and cellular level [3]. In modern nuclear medicine, approximately 95% of radiopharmaceuticals are used for diagnostic purposes [4]. In addition to small chemical structures, radiopharmaceuticals may consist of bigger biomolecules, such as antibodies, antibody fragments, proteins, peptides, and nucleic acids that are usually more specific [5].

Aptamers are oligomers composed of deoxyribonucleotides (DNA aptamers) or ribonucleotides (RNA aptamers), which are promising targeting biomolecules in nuclear medicine. Various three-dimensional structures of aptamers via intramolecular interactions, such as hydrogen bonds, hydrophobic effects, Vander Waals forces, and so on, enable them to bind the target binding domain

SCIENTIFIC REPORTS

Corrected: Author Correction

OPEN

Systematic evaluation of 2′-Fluoro modified chimeric antisense oligonucleotide-mediated exon skipping *in vitro*

Received: 7 January 2019
Accepted: 2 April 2019
Published online: 15 April 2019

Suxiang Chen[1,2], Bao T. Le[1,2], Madhuri Chakravarthy[1,2], Tamer R. Kosbar[1] & Rakesh N. Veedu[1,2]

Antisense oligonucleotide (AO)-mediated splice modulation has been established as a therapeutic approach for tackling genetic diseases. Recently, Exondys51, a drug that aims to correct splicing defects in the dystrophin gene was approved by the US Food and Drug Administration (FDA) for the treatment of Duchenne muscular dystrophy (DMD). However, Exondys51 has relied on phosphorodiamidate morpholino oligomer (PMO) chemistry which poses challenges in the cost of production and compatibility with conventional oligonucleotide synthesis procedures. One approach to overcome this problem is to construct the AO with alternative nucleic acid chemistries using solid-phase oligonucleotide synthesis via standard phosphoramidite chemistry. 2′-Fluoro (2′-F) is a potent RNA analogue that possesses high RNA binding affinity and resistance to nuclease degradation with good safety profile, and an approved drug Macugen containing 2′-F-modified pyrimidines was approved for the treatment of age-related macular degeneration (AMD). In the present study, we investigated the scope of 2′-F nucleotides to construct mixmer and gapmer exon skipping AOs with either 2′-*O*-methyl (2′-*O*Me) or locked nucleic acid (LNA) nucleotides on a phosphorothioate (PS) backbone, and evaluated their efficacy in inducing exon-skipping in *mdx* mouse myotubes *in vitro*. Our results showed that all AOs containing 2′-F nucleotides induced efficient exon-23 skipping, with LNA/2′-F chimeras achieving better efficiency than the AOs without LNA modification. In addition, LNA/2′-F chimeric AOs demonstrated higher exonuclease stability and lower cytotoxicity than the 2′-*O*Me/2′-F chimeras. Overall, our findings certainly expand the scope of constructing 2′-F modified AOs in splice modulation by incorporating 2′-*O*Me and LNA modifications.

Nucleic acid therapeutics has attracted tremendous attention in recent years with a number of successful clinical translations for various diseases[1]. To date, the US Food and Drug Administration (FDA) has approved six oligonucleotide-based therapeutic molecules including one aptamer (Macugen) for the treatment of age-related macular degeneration (AMD), four antisense oligonucleotides (AOs) (Vitravene, Kynamro, Exondys51, and Spinraza) for the treatment of cytomegalovirus retinitis, familial hypercholesterolemia, Duchenne muscular dystrophy (DMD), and spinal muscular atrophy (SMA), respectively[2–4] and one siRNA drug (Onpattro) for the treatment of amyloidosis. Unlike other protein-targeting therapeutic approaches, AOs can alter the pathological hallmark of the disease at the RNA level via different intracellular mechanisms (RNase-H-mediated degradation, imposing steric block to block translation or to modulate splicing)[1,5]. However, oligonucleotides composed of naturally occurring nucleotide monomers (deoxyribonucleotide or ribonucleotide) are easily degraded by nucleases and possess poor target binding affinity[5], thus, they are not suitable for drug development. To overcome these limitations, chemically-modified nucleic acid analogues, mainly of sugar and phosphate backbone modifications, have been utilized in developing therapeutic oligonucleotides. So far, prominent chemical modifications that have been granted approval for clinical usage include phosphorothioate (PS)[6], used in Vitravene, Kynamro, and Spinraza; 2′-*O*-methyl (2′-*O*Me)[7–11], used in Macugen and Onpattro; 2′-Fluoro (2′-F)[7–11], used in Macugen;

[1]Centre for Molecular Medicine and Innovative Therapeutics, Murdoch University, Perth, 6150, Australia. [2]Perron Institute for Neurological and Translational Science, Perth, 6150, Australia. Correspondence and requests for materials should be addressed to R.N.V. (email: R.Veedu@murdoch.edu.au)

Reports

BioTechniques

For reprint orders, please contact: reprints@future-science-group.com

A systematic investigation of key factors of nucleic acid precipitation toward optimized DNA/RNA isolation

Yalin Li[‡,1], Suxiang Chen[‡,2,3], Nan Liu[4], Lixia Ma[5], Tao Wang[*,6], Rakesh N Veedu[2,3], Tao Li[1], Fengqiu Zhang[**,3], Huiyue Zhou[6], Xiang Cheng[6] & Xumiao Jing[1]

ABSTRACT

Nucleic acid precipitation is important for virtually all molecular biology investigations. However, despite its crucial role, a systematic study of the influence factors of nucleic acid precipitation has not been reported. In the present work, via rational experimental design, key factors of nucleic acid precipitation, including the type of nucleic acid, temperature and time of incubation, speed and time of centrifugation, volume ratio of ethanol/isopropanol to nucleic acid solution, type of cation-containing salt solution and type of coprecipitator, were comprehensively evaluated in an attempt to maximize the efficiency of nucleic acid precipitation. Our results indicate that the optimal conditions of each influence factor of nucleic acid precipitation may vary in accordance with the chemistry, structure and length of nucleic acids.

METHOD SUMMARY

To maximize the efficiency of nucleic acid precipitation, the key factors, including incubation and centrifugation conditions, and the volume ratio of polar solvents, cation-containing salts and coprecipitators, were systematically evaluated. To gain more practical information, four types of commonly used nucleic acids were tested. The results indicate that the optimal conditions vary greatly in accordance with the type of nucleic acids under study.

KEYWORDS

ethanol • isopropanol • linear polyacrylamide • nucleic acid precipitation

[1]Henan Key Laboratory of Ion-beam Bioengineering, School of Physics, Zhengzhou University, Zhengzhou 450000, China; [2]Centre for Molecular Medicine & Innovative Therapeutics, Murdoch University, Perth 6150, Australia; [3]Perron Institute for Neurological & Translational Science, Perth 6150, Australia; [4]School of Public Health, Guangzhou Medical University, Guangzhou 510000, China; [5]School of Statistics, Henan University of Economics & Law, Zhengzhou 450000, China; [6]School of Nursing, Zhengzhou University, Zhengzhou 450000, China; *Author for correspondence: wangtaomary@zzu.edu.cn; **Author for correspondence: zhangfengqiu@zzu.edu.cn; ‡Authors contributed equally

BioTechniques 68: 00-00 (April 2020) 10.2144/btn-2019-0109

GRAPHICAL ABSTRACT

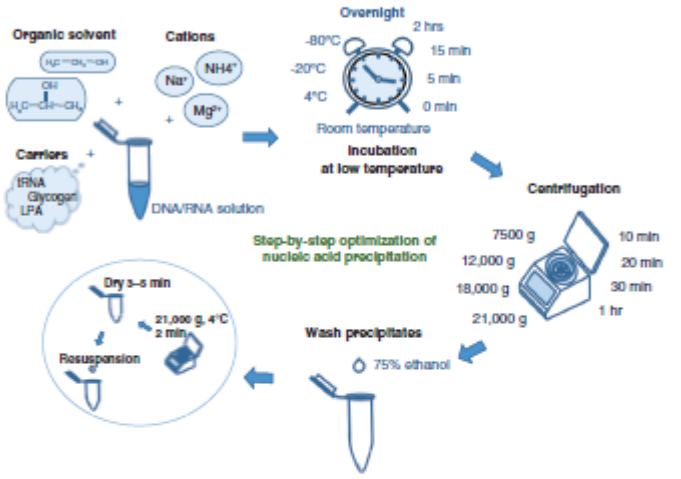

Nucleic acid precipitation is an elementary technique to de-salt and concentrate nucleic acids (DNA or RNA) from their aqueous solutions, and it is involved in virtually all molecular biology investigations, such as cloning [1], sequencing [2], hybridization [3], restriction enzyme analysis [4] and transformation [5]. To date, several different procedures for nucleic acid precipitation have been published [5–7]. The principle of this technique is straightforward. Nucleic acids are hydrophilic polar molecules because they carry negatively charged phosphate residues [8]. In aqueous solutions, the phosphate residues attract water molecules and form hydrated retia surrounding DNA/RNA. The large dielectric constant of water can hinder cations from binding to the phosphate residues [9]. However, the dielectric constant of some polar organic solvents, such as ethanol, is much lower than water, therefore allowing cations to neutralize anionic phosphate groups in ethanol [10,11]. Therefore, with the addition of ethanol and salts (e.g., sodium acetate [NaAc]) that contain cations to nucleic acid solution, the repulsive forces among the polynucleotide chains weaken, resulting in the disturbance of hydrated retia and polymerization of nucleic acids, eventually causing the precipitation of nucleic acids [12]. According to our test, negligible nucleic acids were recovered via adding either alcohol alone or NaAc alone (Supplementary Table 1), indicating both polar organic solvents and salts are essential for nucleic acid precipitation. In general, nucleic acid precipitation is composed of three steps. First, cations and polar organic solvents are added to the DNA/RNA solution, followed by incubation at low temperature to promote the precipitation of nucleic acids. Second, centrifugation is performed to pellet the insoluble DNA/RNA. Third, precipitates are washed with ethanol to remove the impurities (e.g., salts and proteins) [5,6,13–15].

IVYSPRING INTERNATIONAL PUBLISHER

Theranostics

2020; 10(8): 3684-3707. doi: 10.7150/thno.41580

Review

Progress, opportunity, and perspective on exosome isolation – efforts for efficient exosome-based theranostics

Dongbin Yang[1#], Weihong Zhang[2#], Huanyun Zhang[1], Fengqiu Zhang[3], Lanmei Chen[4], Lixia Ma[5], Leon M Larcher[6], Suxiang Chen[6], Nan Liu[7], Qingxia Zhao[8], Phuong H.L. Tran[9], Changying Chen[10]✉, Rakesh N Veedu[6,11]✉, Tao Wang[2,6,11]✉

1. Department of Neurosurgery of Hebi People's Hospital; Hebi Neuroanatomical Laboratory, Hebi, 458030, China.
2. School of Nursing, Zhengzhou University, Zhengzhou, 450001, China.
3. Henan Key Laboratory of Ion-beam Bioengineering, Zhengzhou University, Zhengzhou, China, 450000.
4. Guangdong Key Laboratory for Research and Development of Nature Drugs, School of Pharmacy, Guangdong Medical University, Zhanjiang 524023, China.
5. School of Statistics, Henan University of Economics and Law, Zhengzhou 450046, China.
6. Centre for Molecular Medicine and Innovative Therapeutics, Murdoch University, Perth 6150, Australia.
7. General Practice Centre, Nanhai Hospital, Southern Medical University, 528244, Foshan, China.
8. School of Medicine, Wake Forest University, Winston Salem, NC 27101, USA.
9. School of Medicine, and Centre for Molecular and Medical Research, Deakin University, 3216, Australia.
10. The First Affiliated Hospital of Zheng Zhou University, Zhengzhou 450001, China.
11. Perron Institute for Neurological and Translational Science, Perth 6009, Australia

#These authors contribute equally to this work.

✉ Corresponding author: Tao Wang, wangtaomary@zzu.edu.cn; Rakesh N Veedu, R.Veedu@murdoch.edu.au; Changying Chen, changying@zzu.edu.cn.

Received: 2019.10.29; Accepted: 2020.02.08; Published: 2020.02.19

Abstract

Exosomes are small extracellular vesicles with diameters of 30–150 nm. In both physiological and pathological conditions, nearly all types of cells can release exosomes, which play important roles in cell communication and epigenetic regulation by transporting crucial protein and genetic materials such as miRNA, mRNA, and DNA. Consequently, exosome-based disease diagnosis and therapeutic methods have been intensively investigated. However, as in any natural science field, the in-depth investigation of exosomes relies heavily on technological advances. Historically, the two main technical hindrances that have restricted the basic and applied researches of exosomes include, first, how to simplify the extraction and improve the yield of exosomes and, second, how to effectively distinguish exosomes from other extracellular vesicles, especially functional microvesicles. Over the past few decades, although a standardized exosome isolation method has still not become available, a number of techniques have been established through exploration of the biochemical and physicochemical features of exosomes. In this work, by comprehensively analyzing the progresses in exosome separation strategies, we provide a panoramic view of current exosome isolation techniques, providing perspectives toward the development of novel approaches for high-efficient exosome isolation from various types of biological matrices. In addition, from the perspective of exosome-based diagnosis and therapeutics, we emphasize the issue of quantitative exosome and microvesicle separation.

Key words: Exosome, microvesicle, extracellular vesicle, microfluidic, diagnosis, separation

www.nature.com/scientificreports

SCIENTIFIC REPORTS
natureresearch

OPEN

Author Correction: Systematic evaluation of 2′-Fluoro modified chimeric antisense oligonucleotide-mediated exon skipping *in vitro*

Published online: 16 April 2020

Suxiang Chen, Bao T. Le, Madhuri Chakravarthy, Tamer R. Kosbar & Rakesh N. Veedu

Correction to: *Scientific Reports* https://doi.org/10.1038/s41598-019-42523-0, published online 15 April 2019

The original version of this Article contained errors.

The author Tamer R Kosbar was incorrectly affiliated with "Perron Institute for Neurological and Translational Science, Perth, 6150, Australia". The correct affiliation is listed below.

Centre for Molecular Medicine and Innovative Therapeutics, Murdoch University, Perth, 6150, Australia.

There was also an error in Figure 3C, where the x-axis labels "LNA/2'-F mixmer 1" and "LNA/2'-F mixmer 2" were incorrectly given as "2-'OMe/2'-F mixmer 1" and "2-'OMe/2'-F mixmer 2" respectively.

The Acknowledgements section contained a typographical error where,

"The authors thank Prof. Steve Wilton and Prof. Sue Fletcher for kindly providing H2K cells, Prithi Raguraman for assistance towards experiments, Yanying An and Jessica Cale for help towards figure preparation and Kristin West for informative discussion."

was incorrectly given as:

"The authors thank Prithi Raguraman for assistance towards experiments, Yanying An and Jessica Cale for help towards figure preparation and Kristin West for informative discussion."

In addition, the Supplementary Information file contained an error in Supplementary Figure S3, where the labels of gel C2 were shifted slightly to the right.

These errors have now been corrected in the PDF and HTML versions of the Article, as well as in the accompanying Supplementary Information file.